REPORT 36

ARCHAEAN MAFIC AND ULTRAMAFIC VOLCANIC ROCKS, MENZIES TO NORSEMAN, WESTERN AUSTRALIA

by P.A. Morris

GEOLOGICAL SURVEY OF WESTERN AUSTRALIA

DEPARTMENT OF MINERALS AND ENERGY

GEOLOGICAL SURVEY OF WESTERN AUSTRALIA

REPORT 36

ARCHAEAN MAFIC AND ULTRAMAFIC VOLCANIC ROCKS, MENZIES TO NORSEMAN, WESTERN AUSTRALIA

by
P. A. Morris

Perth 1993

14233—1

Copy editor: **I. R. Nowak**

Morris, P. A. (Paul Andrew), 1952-
Archaean mafic and ultramafic volcanic rocks, Menzies to Norseman, Western Australia

Bibliography.
ISBN 0 7309 4458 1

1. Basalt — Western Australia — Yilgarn Block.
2. Volcanic ash, tuff, etc. — Western Australia — Yilgarn Block.
3. Rocks, Ultrabasic — Western Australia — Yilgarn Block.
4. Geochemistry — Western Australia — Yilgarn Block.
5. Geology, Stratigraphic — Archaean.
6. Cratons — Western Australia
7. Yilgarn Block (W.A.).

I. Geological Survey of Western Australia.
II. Title. (Series: Report (Geological Survey of Western Australia); no. 36).

552.26099416

ISSN 0508–4741

Cover photograph:
Pillowed tholeiitic basalt of the Woolyeenyer Formation, western shore of Lake Cowan, Norseman Terrane (lens cap is 50 mm diameter)

Contents

Part 3 Geochemistry

Part 4 Tectonic setting

Appendices

Figures

Tables

Acknowledgements

The following companies provided access to diamond drillcore and company data: Western Mining Corporation (WMC), Central Norseman Gold Corporation (CNGC), Coolgardie Gold NL (CG), BHP Gold (now Newcrest), Julia Mines NL. Many people from these companies offered advice and help, in particular, David Roberts, Mick Elias, Steve McDonald, Neil Godden (WMC), David Miller (CNGC and WMC), Kevin Johnson and Stuart Murphy (CNGC), Nelleke Swager (CG), and Mick Roche (BHP Gold). Drafts were kindly read by Richard Davy and Alec Trendall (GSWA), John Clout (WMC), David Miller (CNGC and WMC) and Kevin Johnson (CNGC). Hiroo Kagami (Institute for Study of the Earth's Interior, Misasa, Japan) kindly carried out $^{143}Nd/^{144}Nd$ determinations. Thin sections of consistently high quality were provided by staff of the Geological Survey of Western Australia Carlisle Laboratory.

Archaean mafic and ultramafic volcanic rocks, Menzies to Norseman, Western Australia

Abstract

Archaean mafic and ultramafic volcanic rocks between Menzies and Norseman in the eastern Yilgarn Craton have been examined in terms of physical volcanology and geochemistry, using well-established structural and stratigraphic subdivisions (terranes and domains). To maintain stratigraphic control and minimize sample alteration, the study has concentrated on diamond drillcore. Components of a tripartite stratigraphic subdivision (informally termed lower basalt unit, komatiite unit, and upper basalt unit) are recognized in four of the six domains in the well-studied Kalgoorlie Terrane. Basalts comprise massive and pillowed flows which result from the subaqueous eruption of fluid magma in deep water. Flow units are rarely thicker than 10 m, and are laterally discontinuous. Logging of closely spaced holes and rare well-exposed sequences indicates a gradation from massive central parts of flows to pillowed margins. Komatiite units, which comprise both stacked cumulate units and cumulate plus spinifex-textured units, show a wide range in thickness from less than 1 m to more than 10 m.

There are two broad groupings in terms of basalt geochemistry. Members of the lower basalt unit (excluding those in parts of the Ora Banda and Coolgardie Domains) and basalt units from the Norseman and Menzies Terranes have Ti/Zr about 100, Zr/Y about 3, Al_2O_3/TiO_2 about 20, $(La/Yb)_{CN}$ near 1, La 10x chondrite, and ε_{Nd} greater than 0. These are referred to as the lower basalt group. Most within-domain variations for this group can be explained by low-pressure fractional crystallization. Members of the upper basalt unit and the upper basaltic part of the komatiite unit (but excluding the upper basalt unit of the Ora Banda Domain, and including some samples of the lower basalt units from the Ora Banda and Coolgardie Domains) have Ti/Zr about 65, Zr/Y about 2, Al_2O_3/TiO_2 less than 20, $(La/Yb)_{CN}$ greater than or equal to 1, and ε_{Nd} both greater than 0 and less than 0. These are referred to as the upper basalt group. Apart from the Ora Banda Domain, komatiite units have similar Al_2O_3/TiO_2 and Ti/Zr ratios to those of the upper basalt unit.

The lower basalt group has a chemistry consistent with derivation from a depleted mantle source where garnet was not a residual phase (cf. MORB). In contrast, the upper basalt group results from contamination of a komatiite unit by granitoid material, and subsequent fractional crystallization.

The linear distribution of these deep-water volcanic rocks, proximity of arc-derived volcanic rocks, and the chemistry of basalts, indicates eruption in an elongate rift near an active arc, but there is no evidence to suggest that the rift and the arc are genetically related (i.e. the rift is a back-arc basin). The preferred model attempts to reconcile the occurrence of both basalt groups at various stratigraphic levels within the Kalgoorlie Terrane. The model involves the opening of a fan-shaped, north-westerly trending ?intra-continental rift, with rising komatiite magma either melting the asthenospheric mantle (lower basalt group), or being variably contaminated and fractionated (upper basalt group), or being erupted directly (komatiite unit). The type of magma erupted, and the site of eruption is explained by differential rates of opening and closure of the rift.

KEYWORDS: Komatiite, basalt, geochemistry, volcanology, tectonic setting, Yilgarn Craton, Western Australia

Part 1

Introduction

Aims of study

Granitoids and supracrustal greenstones in the eastern part of the Archaean Yilgarn Craton (Fig. 1A) have been divided into five tectono-stratigraphic terranes (Swager et al., 1990). The Kalgoorlie Terrane is the best understood and has been subdivided into six tectono-stratigraphic domains. It is bounded to the west by late Archaean granitoids and gneisses, and to the east by a fault, separating it from mafic and felsic volcanic rocks (Williams, 1975; Barley and Groves, 1990; Barley et al., 1989) termed the Kurnalpi Terrane by Swager et al. (1990). The four other terranes (Norseman, Menzies, Kurnalpi, and Callion) are provisionally identified on the basis of differing stratigraphy, structure and, probably, age (Fig. 1).

Greenstones between Norseman and Menzies (Fig. 1B) are predominantly derived from mafic and ultramafic volcanic flows with minor (probably comagmatic) hypabyssal intrusives, felsic volcanic rocks, and interflow sedimentary rocks. Sensitive High Resolution Ion Microprobe (SHRIMP) U–Pb, single-zircon dating (Compston et al., 1986; Claoué-Long et al., 1988; Campbell and Hill, 1988) indicates that these rocks are approximately 2700 Ma old. The sequence has been deformed and metamorphosed, and is cut by Proterozoic dykes (Hallberg, 1987).

This volcanological and geochemical study complements regional mapping, either completed or in progress, by the Geological Survey of Western Australia (Griffin, 1990; Swager et al., 1990; Witt, 1990), and studies of structural and geochemical controls on nickel and gold mineralization (Dupré and Arndt, 1990; Lesher and Arndt, 1990; Boulter et al., 1987; Phillips et al., 1987; Clark et al., 1988; Witt, 1993). Despite the intensive study of this area prompted by rich nickel and gold mineralization, and the increased knowledge of stratigraphy and structure, only a few studies have addressed regional aspects of volcanology and geochemistry. Komatiite volcanology is one of the principal controls on the locus of nickel mineralization (Gresham and Loftus-Hills, 1981; Lesher and Arndt, 1990); and, although volcanology and geochemistry do not directly control gold mineralization, they can provide information on tectonic setting, which impinges on mineralization models. The volcanology section of this study aims to document variations in flow thickness, flow direction, the number, location, and nature of eruption sites (vents), and the distance and direction that volcanic flows travelled. In a later part, comparisons are made between the geochemistry of stratigraphically equivalent units within and between domains. Comparisons are also drawn between basalts of the Kalgoorlie Terrane and adjacent terranes. Geochemical data are also assessed in terms of petrogenesis, and likely tectonic settings are examined in conjunction with volcanological interpretations. Axiomatic to this study is the assumption that the greenstone stratigraphy preserved in the constituent domains of the Kalgoorlie Terrane is coeval.

As regional correlations are hampered by poor and discontinuous exposure, a deep weathering profile and variable modification of textures by metamorphism, the volcanological study, and geochemical sampling has relied almost entirely on the logging of in excess of 10 km of diamond drillcore. Not all domains and terranes are discussed (Table 1), because diamond drillcore through representative parts of the stratigraphy was not always available, or there was poor stratigraphic control.

Despite a metamorphic overprint, igneous textures are sufficiently well preserved in most mafic and ultramafic volcanic rocks that the prefix 'meta-' can be omitted.

A geochemical classification is used in the second part of this study, but field nomenclature is used in the volcanology section. 'Basalts' are fine-grained, sometimes porphyritic, mafic volcanic rocks. 'Dolerite' consists of interlocking grains of amphibole and plagioclase that are discernible with the naked eye. The development of 'doleritic texture' in pillow lava is due, in some cases, to metamorphic recrystallization (P. J. McGoldrick, pers. comm., 1989). 'Gabbro' has a similar texture to dolerite, but grain size is in the region of 3 mm. The term 'basaltic komatiite' is used for mafic volcanic rocks comprising randomly oriented acicular pyroxene (now amphibole). The term 'basaltic komatiite' is synonymous with 'high-Mg basalt' of other studies. 'Komatiite' is used for both extrusive rocks with olivine spinifex texture, and olivine cumulate rocks genetically associated with such spinifex-textured rocks, such as the cumulate base to komatiite flows.

Introduction to the Kalgoorlie Terrane

Stratigraphy

Within the Kalgoorlie Terrane, the Kambalda and Ora Banda Domains (Table 1) contain a complete sequence of lower basalt unit, komatiite unit, and upper basalt unit. In both domains, a basaltic upper part to the komatiite unit

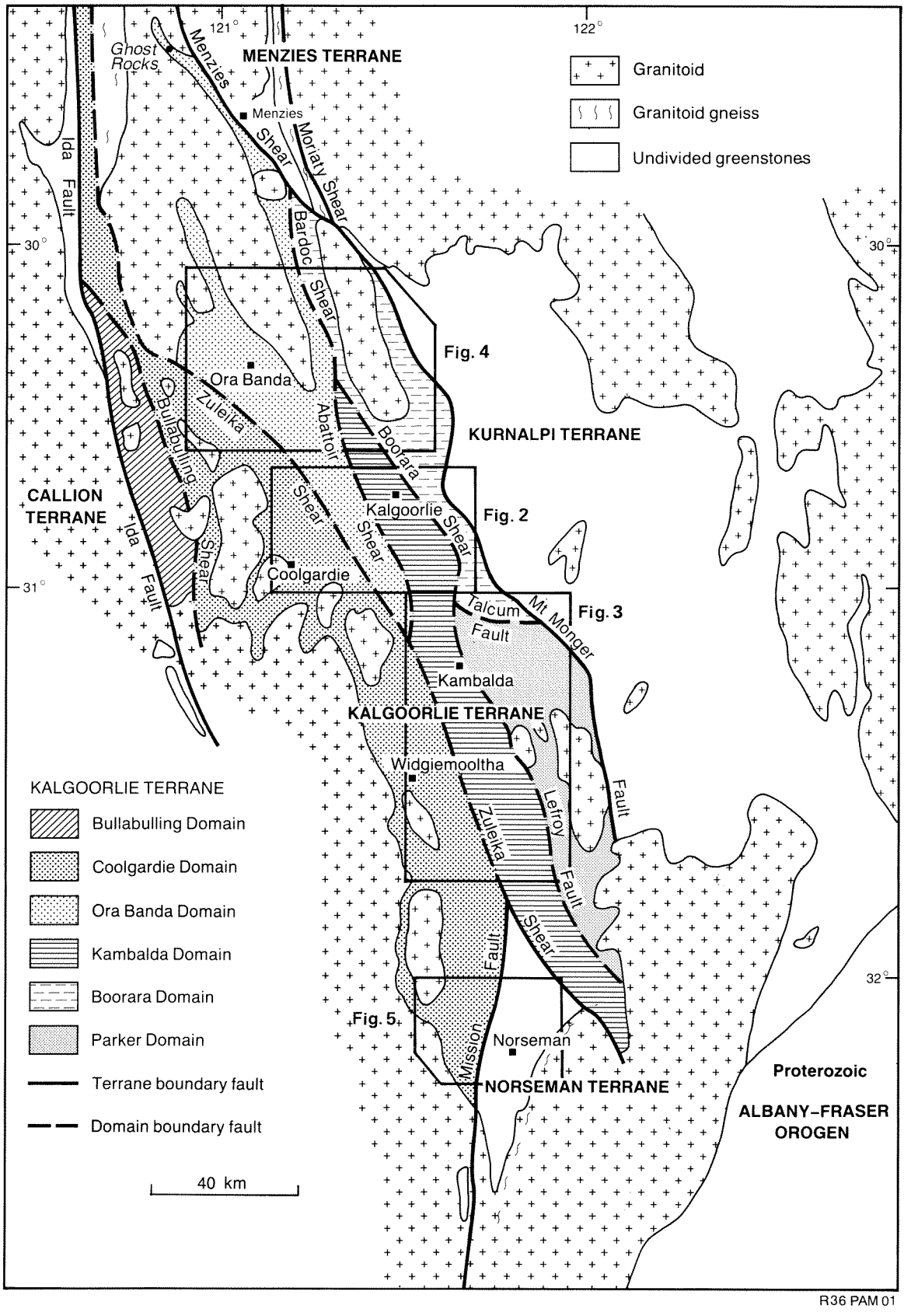

Figure 1A. Terrane map of the Kalgoorlie region, emphasizing the Kalgoorlie Terrane and its six tectono-stratigraphic domains. Locations of Figures 2–5 also shown. From Swager et al. (1990)

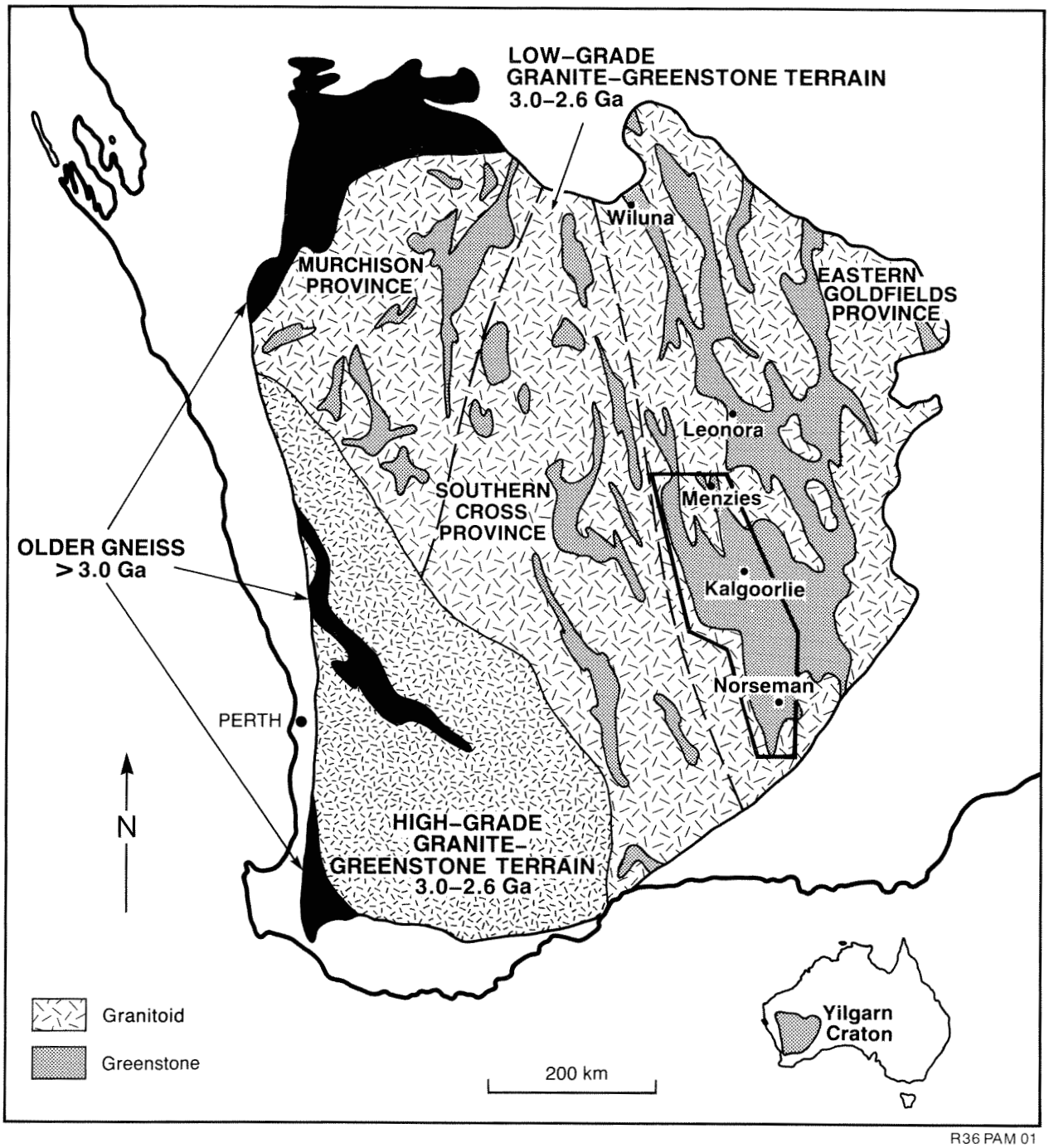

Figure 1B. Regional setting

is well developed. The Coolgardie and Boorara Domains lack the upper basalt unit, and only the Boorara Domain has the upper basaltic part to the komatiite. The stratigraphy of the Bullabulling Domain is not well understood because of poor exposure.

Structure

Four phases of deformation are recognized (Archibald, 1979; Swager, 1989a; Keats, 1987; Swager et al., 1990; Swager and Griffin, 1990): regional-scale thrusting and recumbent folding which caused stratigraphic repetition (D_1); regional upright folding along north-northwesterly trending fold axes (D_2); combined regional northeast–southwest shortening and wrench faulting (D_3); and well-developed north-northeasterly oriented dextral faults (D_4), which offset all earlier structures. Within the Kambalda Domain, Swager and Griffin (1990) have shown that the Kalgoorlie, Foster, Tramways, and Bluebush–Republican successions are thrust-repeated slices of the Kambalda stratigraphy (e.g. see Foster, Tramways, and Republican Faults on Figure 3).

Table 1. Stratigraphic correlation for greenstones of the Kalgoorlie Terrane discussed in this study

Stratigraphic succession	*Ora Banda Domain*	*Kambalda Domain*		*Coolgardie Domain*	*Boorara Domain*
		Kalgoorlie	*Kambalda*	*Coolgardie*	
Upper basalt unit	Victorious Basalt (a,b)	Paringa Basalt (a,b)	Paringa Basalt (a,b)		
			(Defiance Dolerite)		
	Bent Tree Basalt	Kapai	Slate		
Basaltic upper part of komatiite unit	Big Dick Basalt (a,b)	Devon Consols Basalt	Devon Consols Basalt (a,b)		(Harper Lagoon)
Komatiite unit	Siberia Komatiite (a,b)	Hannans Lake Serpentinite (a,b)	Kambalda Komatiite (a,b)	Hampton Formation (a,b)	Highway Ultramafics (a,b)
	Walter Williams Formation (b)				
	Missouri Basalt (b)		Lunnon Basalt (a,b)	Burbanks Formation (a,b)	Scotia Basalt (a,b)
Lower basalt unit	Wongi Basalt (b)				
Reference	Witt (1990)	Woodall (1965)	Woodall (1965)	Hunter (1993)	Christie (1975)
			Roberts (1988)		Witt (1990)
			Langsford (1989)		

Note: (a) examined for volcanology; (b) examined for geochemistry

Metamorphism

The Kalgoorlie Terrane has undergone pervasive regional metamorphism, including both static and dynamic styles, ranging from prehnite–pumpellyite to amphibolite facies (Binns et al., 1976). Peak metamorphic conditions of approximately 400 kPa and between 500 and 600°C were synchronous with D_3 granitoid emplacement. The greenstone sequence has been variably altered by hydrothermal metamorphism. The resultant mafic rock assemblages are actinolite–chlorite–albite–epidote–quartz–zoisite, whereas the ultramafic rock assemblages are tremolite–talc–chlorite–opaques, with the addition of talc–carbonate at high X_{CO_2}.

Geochronology

SHRIMP (Sensitive High Resolution Ion Microprobe) U–Pb single-zircon ion microprobe dating, unlike other systems (e.g. Rb/Sr and Sm/Nd) which are susceptible to weathering, metamorphism, and magma contamination (Claoué-Long et al., 1984; Chauvel et al., 1985), provides accurate and precise age control on greenstones.

Published U–Pb SHRIMP ages relevant to the mafic and ultramafic volcanic sequence in the Kalgoorlie Terrane are shown in Table 2. Ages of zircons from a sedimentary unit (interpreted as airfall tuff) on the lowest flow in the komatiite unit and the Kapai Slate offer constraints on the age of the komatiite unit. The relatively imprecise age for the Victory Dolerite (base of the Devon Consols Basalt) of 2693 ± 50 Ma agrees with that of the Kapai Slate (top of the Devon Consols Basalt), but zircons from the same sample also give younger more precise ages of 2669 ± 11 Ma, which Claoué-Long et al. (1988) interpret as reflecting a later event. This latter age is almost the same as that of the post-D_2 to syn-D_3 Kambalda Granodiorite (2662 ± 4 Ma: Hill and Compston, 1987), which offers some age constraint on the end of tectonism. An age of 2676 ± 4 Ma for felsic volcanic rocks at the base of the Black Flag Group (overlying the upper basalt) has been cited by J. Claoué-Long (pers. comm., 1990).

Unpublished SHRIMP ages for tuffs within the lower basalt unit at Kambalda are considerably greater than the 2702 ± 4 Ma age from the lower basalt unit–komatiite unit interface (Claoué-Long, pers. comm., 1990). Age data for the Bluebush–Republican sequence are not available, but it is assumed that this succession is the same age as Kambalda.

There is less SHRIMP age control for rocks away from the Kambalda area. Hill and Campbell (1989) reported an age of 2593 ± 10 Ma for the Liberty Granodiorite in the Ora Banda Domain, which is significantly younger than other late-tectonic granitoids from Kambalda or the Norseman Terrane reported by Hill et al.(1989).

Table 2. Sensitive high resolution ion microprobe (SHRIMP) single-zircon ages from the Kalgoorlie Terrane.

	Date	*Lithology*	*Interpretation*	*Data*
Kambalda Domain –Kambalda	(a) 2702 ± 4	Sedimentary unit on top of lowest komatiite flow	Magmatic	1
	(a) 2692 ± 4	Kapai Slate	Magmatic	1
	(b) 2693 ± 50	Victory Dolerite	?Magmatic	2
	(b) 2669 ± 11	Victory Dolerite	?Post-magmatic	2
	(b) 3100–3400	Victory Dolerite	Basement	2
	(c) 2662 ± 4	Kambalda Granodiorite	Intrusion	2
Ora Banda Domain	(d) 2593 ± 10	Liberty Granodiorite	?Intrusion	4
	(e) 2675 ± 23	Liberty Ganodiorite	?Intrusion	5
Coolgardie Domain	(c) 2610	Mungari Granite	Intrusion	3
	(d) 2687 ± 7	Felsic ?volcanic Mt Kirk Formation	Magmatic	4

Source: (a) Claoué-Long et al., 1988; (b) Compston et al., 1986; (c) Hill and Compston, 1987; (d) Hill and Campbell, 1989; (e) McNaughton and Cassidy, 1990

McNaughton and Cassidy (1990) offered an alternative interpretation of Hill and Campbell's (1989) age and carried out Pb–Pb mineral and whole-rock analyses, reporting an age of 2675 ± 23 Ma, similar to that of the Kambalda Granodiorite. A U–Pb zircon age for the Mungari Granite in the Coolgardie Domain (Hill and Compston, 1987) of 2610 Ma is significantly younger than other dated granitoids. Zircons from the base of the Mt Kirk Formation (previously a part of the Norseman Terrane, but now included in the Coolgardie Domain) give an age of 2689 ± 7 Ma (Campbell and Hill, 1988).

Kalgoorlie Terrane — domain stratigraphy relevant to this study

Kambalda Domain

Kalgoorlie

Komatiite unit

The komatiite unit in the Kalgoorlie area (Hannans Lake Serpentinite) is a 300–900 m thick unit with a faulted base. The unit largely consists of serpentinized ultramafic rocks. The best exposures show an easterly dip of 60–85°, (Travis et al., 1971; Clout et al., 1990). Keats (1987) described 1–10 m thick, laterally extensive volcanic flows at Serpentine Bay (Hannan Lake), which had well-developed basal cumulate zones and spinifex-textured tops. In the top 200 m of the unit, drilling has exposed a 30 m thick sequence of ultramafic and mafic fragmental rocks and some feldspar-phyric basalts. The top grades into the Devon Consols Basalt.

Upper basalt unit

The 400–700 m thick upper basalt unit (Paringa Basalt) consists largely of tholeiitic basalt, with local intercalations of basaltic komatiite (occasionally pillowed) and interflow sedimentary rocks (Clout et al., 1990). The unit is best exposed at Mt Hunt (Fig. 2), where 200 m of basalt is overlain by 2–20 m of cherty sedimentary rock, 150–250 m of coarser-grained basalt, thin layers of chert, and 250 m of pillowed and variolitic basalt. At Feysville, Keats (1987) recorded approximately 1500 m of basalt (presumed to be Paringa Basalt), with an upper section consisting of basalt with rare feldspar megacrysts (comparable to 'cat rock' occurrences at Coolgardie and Ora Banda).

Kambalda–St Ives–Tramways

Lower basalt unit

The lower basalt unit (Lunnon Basalt) consists of massive and pillowed basalt flows with some interflow sedimentary rocks, dolerite, and gabbro (Fig. 3). The deepest drill hole (KD1029) terminated still in basalt at approximately 2 km depth; thus, the true stratigraphic thickness is unknown. A series of concordant dolerites and gabbros, and a thin sedimentary rock horizon divide the unit into a lower, more Mg-rich flow sequence and an upper less Mg-rich assemblage (Gresham and Loftus-Hills, 1981).

Komatiite unit

The komatiite unit (Kambalda Komatiite of Cowden and Archibald, in prep.) shows an east–west variation in thickness, lensing out northwest of Foster, but exceeding 1000 m north and east of Kambalda Dome (Gresham and Loftus-Hills, 1981). Two members are recognized

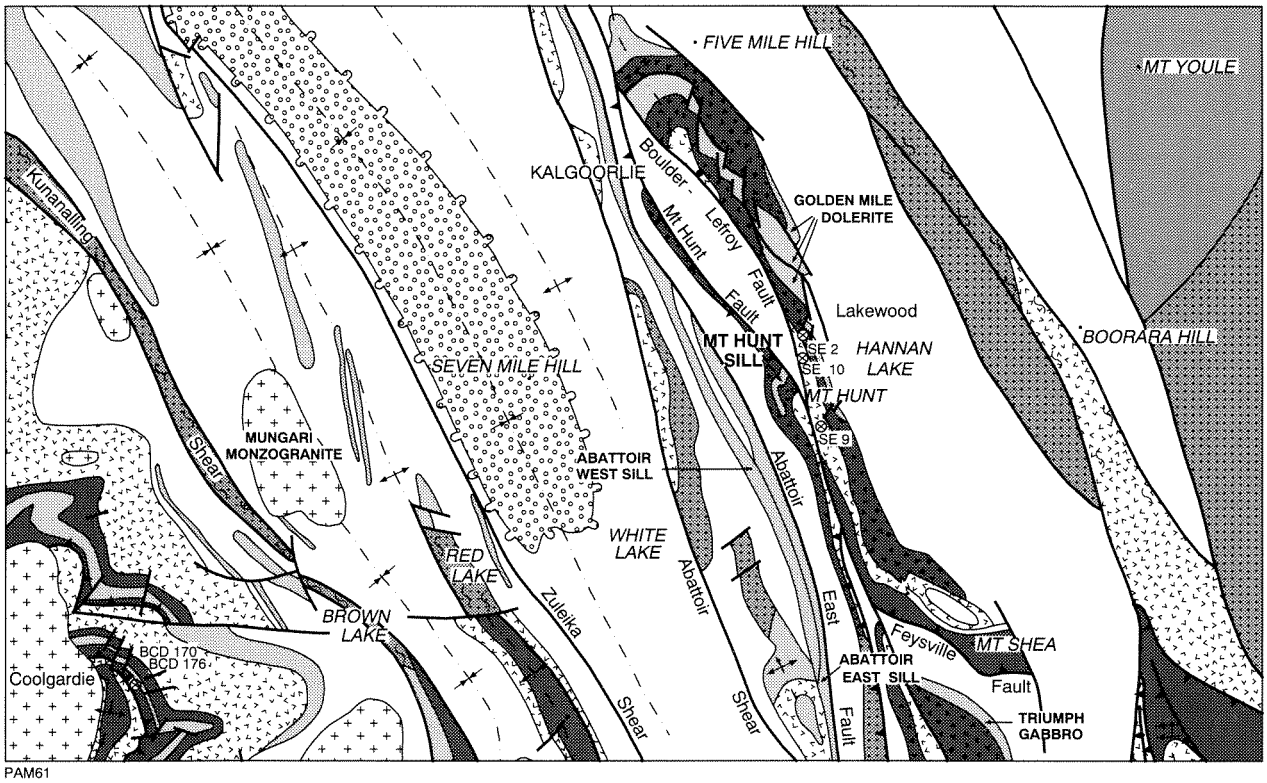

PAM61

LEGEND

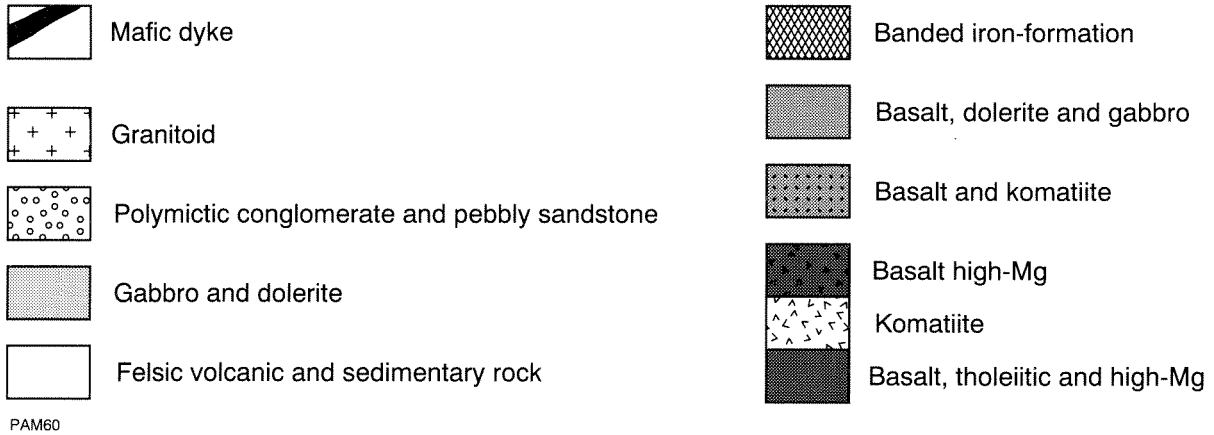

PAM60

Figure 2. Geology of part of the Kambalda and Coolgardie Domains of the Kalgoorlie Terrane. See Figure 1 for map location. From Swager et al. (1990)

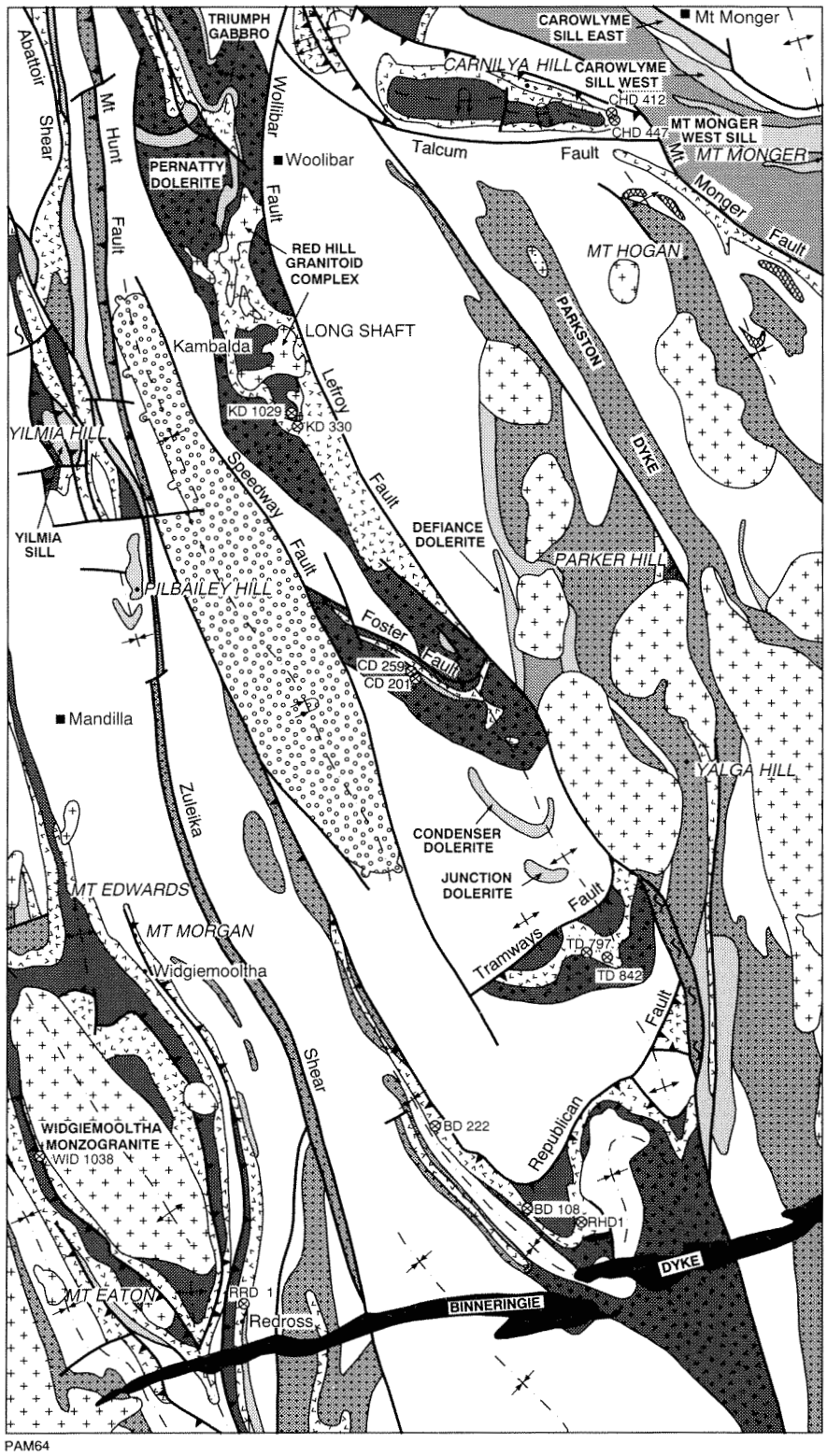

PAM64

Figure 3. Geology of part of the Kambalda, Coolgardie, and Boorara Domains of the Kalgoorlie Terrane. See Figure 1 for location, Figure 2 for legend. From Swager et al. (1990)

(Cowden and Archibald, in prep.). The lower one-third (Silver Lake Peridotite) consists of thick (25–100 m) high-MgO (greater than 36 wt% anhydrous) komatiite flows with occasional thin (2–10 m) spinifex-textured tops, and abundant sulfidic sedimentary rocks (Gresham and Loftus-Hills, 1981). At Lunnon shoot is a 25 m thick zone of spinifex at the top of this unit. The upper unit (Tripod Hill Komatiite) is a sequence of thinner (1–10 m thick) less MgO-rich komatiite flows, with well-developed spinifex texture, rare pillow lava and varioles, and a few interflow sedimentary rocks (Gresham and Loftus-Hills, 1981).

Upper basaltic part of the komatiite unit

At Kambalda Dome, there is a sharp break between the Tripod Hill Komatiite and the overlying upper basaltic part of the komatiite unit (Devon Consols Basalt), but further south at St Ives and Tramways, the contact is gradational. The Devon Consols Basalt is mainly pillowed basalt and some dolerite and interflow sedimentary horizons, according to Gresham and Loftus-Hills (1981). The unit reaches 200 m thickness at Victory, where the top is marked by the regionally extensive Kapai Slate, which Gresham and Loftus-Hills (1981) describe as a 40 m thick zone of sedimentary and intrusive rocks. At Victory, the lowermost part of the Devon Consols Basalt is a layered dolerite (Victory Dolerite), whereas a 30 m thick dolerite (Trafalgar Dolerite) occurs towards the top (Roberts and Elias, 1990).

Upper basalt unit

The upper basalt unit (Paringa Basalt), comprising basalt, rare dolerite and interflow sedimentary rocks exceeds 1000 m in thickness and includes the Defiance Dolerite, the locus of significant gold mineralization (Roberts and Elias, 1990). On the basis of texture and mineralogy, Cowden (unpublished data, 1986) recognized five zones within the Defiance Dolerite. Detailed mapping has shown the unit is locally transgressive (D. Roberts, pers. comm., 1989), although there is some conjecture (J. M. F. Clout, pers. comm., 1991).

Bluebush–Republican

Mapping by Griffin (1990) has shown that the Bluebush and Republican stratigraphies are equivalent (Fig. 3). Swager and Griffin (1990) interpreted that the Bluebush–Republican sequence (Levy, 1975; McDonald, 1976) to be a thinner, overturned, and thrust-repeated slice of the Kambalda stratigraphy, consisting of upper basalt unit and komatiite unit.

Ora Banda Domain

Witt and Harrison (1989) noted strong similarities between the Ora Banda, Kalgoorlie (Travis et al., 1971; Clout et al., 1990), and Kambalda stratigraphies (Gresham and Loftus-Hills, 1981; Roberts, 1988; Cowden and Archibald, in press); thus, Swager et al. (1990) have included Ora Banda in the Kalgoorlie Terrane (Fig. 1; Fig. 4; Table 1). This domain is separated by faults from the adjacent Coolgardie, Boorara, and Kambalda Domains.

Greenstones are weakly deformed and mildly metamorphosed in the Ora Banda area (Witt, 1987; Witt and Harrison, 1989; Witt, 1990)(Fig. 4). They extend south and then north around the closure of the south-plunging Goongarrie–Mt Pleasant Anticline to the Bardoc–Broad Arrow area, where they are more intensely deformed. The sequence can be traced to Ghost Rocks, northwest of Menzies (C. P. Swager, pers. comm., 1989)(Fig. 1).

Lower basalt unit

The lower basalt unit in the Ora Banda domain (Table 1) is divided into the Wongi Basalt and Missouri Basalt. The Wongi Basalt contains few pillows and abundant pyroxene, spinifex- and variolitic-textured basalts, whereas the overlying Missouri Basalt is commonly pillowed, texturally more monotonous, and conspicuously more felsic. Vesicles and plagioclase phenocrysts are more common at the top of the Missouri Basalt.

Komatiite unit

Hill et al. (1988) estimated a thickness of 600–900 m for the lower part of the komatiite unit (Walter Williams Formation), which consists of a basal orthocumlate succeeded by mesocumulate, adcumulate, olivine harrisite, and a thin orthocumulate, all overlain by an upper sedimentary horizon. The sequence is interpreted as an olivine adcumulate derived by olivine accumulation from continuously erupting komatiite magma (Hill et al., 1988). The overlying Siberia Komatiite (greater than 2.5 km thick at Ora Banda) is a series of massive, and olivine and pyroxene spinifex-textured ultramafic flow units, with minor gabbro. The upper part of the komatiite unit is a 500 m thick sequence of variolitic, pillowed basalt (Big Dick Basalt) capped by a thin, discontinuous sedimentary horizon.

Upper basalt unit

The upper basalt unit (Bent Tree Basalt and Victorious Basalt) consists of mafic volcanic flows intruded by layered ultramafic to mafic sills. The Bent Tree Basalt (maximum 3 km thick) is both massive and pillowed aphyric basalt. Dolerite and gabbro make up 50% of the formation in some areas (e.g. Mt Ellis). At Ora Banda, a thin black slate unit separates this formation from the overlying Victorious Basalt, which is a 2 km thick, massive to pillowed unit with conspicuous, well-developed plagioclase megacrysts and coarser grained doleritic horizons.

Coolgardie Domain

Widgiemooltha and Redross

The lower part of the Widgiemooltha sequence consists of mafic and ultramafic volcanic flows with a few interflow

Figure 4. Geology of part of the Ora Banda, Coolgardie, Kambalda, and Boorara Domains of the Kalgoorlie Terrane. See Figure 1 for location, Figure 2 for legend. From Swager et al. (1990)

sedimentary rocks, whereas the upper part is largely felsic volcaniclastics and associated sedimentary horizons (Archibald, 1979). At Redross (approximately 60 km south of Kambalda) a 60–120 m thick sequence of strongly talc-carbonated ultramafic volcanic rocks with occasional flow-tops and spinifex texture, are sandwiched between pillowed and amygdaloidal tholeiitic basalts (Marston, 1984; Barrett et al., 1977).

Lower basalt unit

Fifty to sixty percent of the 340–430 m thick lower basalt unit contains locally vesicular, pillowed, tholeiitic basalt (some basaltic komatiite); the remainder consists of dolerite. In most cases it is unclear whether or not the dolerites are intrusive, but in a dolerite near the contact with the overlying komatiite unit, Hayward (1988) recorded features consistent with an extrusive origin. Pyroxenites, which occur rarely, could be either flow bases or sills. Archibald (1979) interpreted layered gabbros in this unit as residuals of high-level magma chambers.

Komatiite unit

Archibald (1979) recognized two parts to the komatiite unit at Widgiemooltha, a lower peridotite, grading into an upper, thinner, less Mg-rich flow sequence with clear extrusive characteristics and abundant interflow sedimentary rocks. Hayward (1988) recorded flows between 30 and 60 m thick, of which one dunite unit traceable for 8 km.

Coolgardie

Hunter (1993) maintained that the greenstone sequence at Coolgardie (Fig. 2) involved tectonic repetition of a simple stratigraphy and that a series of open, gently plunging folds had, in places, thickened or thinned a series of basalt, komatiite, sedimentary rocks, dolerite, gabbro and acid porphyry. In contrast, Swager et al. (1990) argued for regional D_1 thrust repetition and D_2 folding, facing away from the Bali Monzogranite.

Lower basalt unit

Based on the widespread occurrence of varioles and plumose amphibole, Hunter (1993) assumed a high-Mg composition for the lower basalt unit (Burbanks Formation).

The upper part of this basalt sequence contained a 150–200 m thick unit of feldspar-phyric basalt with

feldspar phenocrysts from 1.5–2 cm, usually agglomerated, similar to other 'cat rock' occurrences at Ora Banda and south of Kalgoorlie (Keats, 1987). Although the unit was in part pillowed and usually concordant, Hunter (1993) favoured an intrusive origin for this unit, with basalt being forcibly pushed into wet sediment. The top of the Burbanks Formation is marked by a thin, grey phyllite horizon.

Komatiite unit

The komatiite unit (Hampton Formation) is 600 m thick and consists of komatiite flows. To the north of Coolgardie, flows lack spinifex texture and have well-developed peridotitic cumulates. Laterally continuous, 1–5 m thick interflow sedimentary horizons make good regional markers.

Towards the top of the komatiite unit is a 100–150 m thick, laterally continuous basalt unit with a sharp upper but a gradational lower contact.

Boorara Domain

Carnilya Hill

The Carnilya Hill area (Fig. 3) consists of an easterly to southeasterly striking sequence of mafic and ultramafic volcanic rocks (Griffin and Hickman, 1988). At Carnilya Hill, Heath and Arndt (1976) identified a combined anticline and syncline on the south-dipping limb of the Bulong anticline. Although spinifex texture and changes in MgO indicate a north younging, the sequence is south facing and is thus overturned.

The greenstone stratigraphy at Carnilya Hill is a structurally repeated sequence of lower basalt unit (Scotia Basalt) and komatiite unit (Highway Ultramafics). Although there are no published ages, inclusion in the Kalgoorlie Terrane implies it is of similar age to greenstones at Kambalda and Ora Banda.

Harper Lagoon

A well-exposed, approximately 0.1 km^2, ultramafic–basalt sequence crops out in a cliff section and on several small islands at Harper Lagoon (Fig. 4), approximately 27 km northeast of Kalgoorlie (A .L. Ahmat, *in* Swager et al., 1990, Fig. III.32; Ahmat, 1991). At this locality, a southeasterly dipping sequence of cumulate and spinifex-textured ultramafic extrusives (komatiite unit) is overlain by pillowed, variolitic and vesicular basalts, and associated pillow breccias (upper basaltic part of the komatiite). The contact between the ultramafic and mafic volcanic rocks is marked by a gabbro–pyroxenite which is possibly intrusive, although Ahmat (pers. comm., 1990) has interpreted this unit as a differentiated part of the ultramafic flow. The sequence is cut by an east-trending acid porphyry dike.

Regional mapping (Ahmat, 1991) places the rocks at Harper Lagoon in a sequence of basalt, komatiite, and felsic volcanic and associated sedimentary rocks. The whole stratigraphy has been folded around the closure of the Scotia–Kanowna Anticline. Ahmat (pers. comm., 1989) has tentatively correlated the Harper Lagoon sequence with basal Ora Banda sequence of Witt (1987) west of the Bardoc Deformation Zone. Furthermore, he maintains that duplication of komatiite horizons by structural repetition has occurred.

Bullabulling Domain

Swager et al. (1990) originally included rocks of the Reptile Dam–Bullabulling area with those at Dunnsville as part of the Coolgardie Domain. However, the poor outcrop and complex structural history of these rocks makes it difficult to group them within the Coolgardie Domain and they have been given separate domain status. It is unclear to what part of the regionally recognized stratigraphy they belong. Because of its poor outcrop and small amount of available diamond drillcore, it has not been investigated in terms of volcanology.

Norseman Terrane

Stratigraphy and structure

Archaean rocks at Norseman consist of a thick sequence of mafic and less common felsic volcanic rocks, and intrusive and sedimentary rocks which strike north-northeast and dip approximately 55° westwards. They are surrounded and intruded by granites (Fig. 5), and cross-cut by east-northeast trending basic intrusions of the Widgiemooltha Dike Suite (e.g. Hallberg, 1987). The Norseman Terrane lacks the thick ultramafic sequences of the Kalgoorlie Terrane, has more abundant BIFs, and has an older mixed mafic volcanic and clastic sedimentary unit.

Three stratigraphic units are recognized: the Penneshaw Formation, Noganyer Formation, and Woolyeenyer Formation, (Bekker, 1962; Hall and Bekker, 1965; Doepel, 1973; McGoldrick, in press). The Mt Kirk Formation was originally part of the Norseman stratigraphy, but is now placed in the Kalgoorlie Terrane (Coolgardie Domain) by Swager et al. (1990), as it is separated from the Woolyeenyer Formation by a major fault.

The maximum stratigraphic thickness of the three formations in the Norseman Terrane is approximately 24 km, although the occurrence of strike-parallel shears suggests the sequence may be structurally repeated (McGoldrick, in press).

Spray (1985) recorded four phases of deformation at Norseman: low-angle thrust faulting, tectonically juxtaposing the greenstones with the granitoid gneiss basement (D_1); upright folding (D_2); the development of a steep north–northwest trending metamorphic fabric (D_3); and the development of a steep east-northeast trending fracture cleavage and open cross-folds during D_4. Peak metamorphism coincided with D_3. The deformation history is, thus, similar to that of the Kalgoorlie Terrane.

Figure 5. Geology of part of the Norseman Terrane. See Figure 1 for location, Figure 2 for legend. From Swager et al. (1990)

Metamorphism

Static style regional metamorphism reached amphibolite facies. Basalt, gabbro, and dolerite, consist of actinolite and plagioclase, accessory opaque oxide, and secondary calcite and biotite. Occasional blocky and sieve-textured plagioclase and amphibole are interpreted as relict phenocrysts.

Two samples from diamond drillhole S433, which resemble basaltic komatiites, contain wispy to feathery pale-green to colourless tremolitic amphibole, a smaller amount of modal feldspar than basalts and accessory calcite. A conformable basaltic komatiite flow outcrops on the southwest corner of A Island (Fig. 7A) in Lake Cowan.

Geochronology

SHRIMP dates of zircons from the Norseman Terrane are presented in Campbell and Hill (1988) and Hill et al. (1990). Felsic 'volcanics' (quartz–feldspar–biotite schists) of the Penneshaw Formation give U–Pb SHRIMP ages from approximately 3100 to 2900 Ma, the former interpreted as a depositional age and the latter as remnants from the gneissic basement. As there is some disagreement about the validity of these ages, further SHRIMP dating of felsic volcanic rocks from the Penneshaw Formation is currently being undertaken by D. Nelson (Geological Survey of Western Australia). Two age populations have also been recorded from zircons in chert of the Noganyer Formation (3670–3650 Ma and 2706 ± 5 Ma); the older ages have been interpreted as basement relics, the younger ages as recording a hydrothermal event. However, a cross-cutting biotite granite was dated at 2691 ± 8 Ma. Dating of the Crown Main Dike, which cross-cuts the Woolyeenyer Formation at 2714 Ma (R. I. Hill, pers. comm., 1990), shows the Woolyeenyer Formation is the same age as the Lunnon Basalt at Kambalda.

Menzies Terrane

The highly deformed nature of the rock sequence in the Menzies Terrane and the small amount of diamond drillcore means that there is no clear stratigraphic correlation with the Kalgoorlie Terrane. Several samples have been collected for geochemistry.

Part 2

Physical volcanology

Physical volcanology deduced from diamond drillcore.

Features logged in drillcore

Flow-top breccia

In this study, basalt flow-top breccias are oligomictic, organized, contain angular fragments, and grade into the lower parts of the flow. Petrographic examination (Appendix 1) shows that fragments are glassy and that the grain size, crystal form and content change towards the edges of fragments in a manner consistent with a magmatic origin. These breccias contrast markedly with other types of breccia in terms of restricted lithology and lack of fragment displacement (Table 3).

Flow-top breccias in ultramafic volcanic flows (e.g. Siberia Komatiite of the Ora Banda Domain) are clearly bounded by a lower spinifex-textured zone, and an upper cumulate zone (i.e. succeeding flow) or a thin glassy cap (chilled base of overlying flow). As in basalts, these flow-top breccias are oligomictic, organized, with little or no matrix, and are similar to flow-top breccia described by Arndt et al. (1977) from Munro Township.

The lack of fragment rotation suggests that flow-top breccias formed when the lava was either stationary or moving slowly. Most flow-top breccia fragments are neither bleached nor altered; this indicates insufficient time for alteration or sea-floor metamorphism and is consistent with the rapid and continuous eruption deduced from other evidence (e.g. lack of interflow sedimentary rocks).

Although several studies have separated flow units using flow-top breccias (Hill et al., 1988; Barnes et al., 1974; Barnes et al., 1987). There are few discussions of physical and/or petrographic characteristics. Arndt et al. (1977) described breccia capping komatiite at Munro Township as 'a chilled aphanitic cap rock to flows, cut by joints that break it into 3–20 cm polyhedra.' They noted

Table 3. Characteristics of breccia types logged in drillcore

	Flow-top	*Pillow*	*Hydraulic*	*Mass-flow*
Stratigraphic position	Top of flow unit	Between or adjacent to to pillow lava	Not stratigraphically controlled	Not stratigraphically controlled
Clast features:				
Size	≤5 cm	1–2 cm +	≤5 cm	Variable 20 cm +
Angularity	Angular	Angular–subangular	Angular	Angular
Type	Oligomictic	Usually oligomictic	Usually oligomictic	Polymictic
Organization	Organized	Disorganized	Disorganized	Disorganized
Compositiontal	Glassy (vesicular)	Glassy, crystalline vesicular, variolitic	Variable; not chilled	Variable; not always chilled
Matrix:				
Present	Rare	Yes	Yes	Yes
Type		Clastic sediment, glass spalls (carbonate)	Secondary quartz, carbonate	Clastic sediment
Thickness	Usually 10–25 cm	20–50 cm	10–50 cm	
Relationship to underlying rock	Gradational; sharp in some ultramafic rocks	Sharp (some gradational)	Sharp	Sharp
Origin	Autobreccia and/or chilling on flow tops	Hydroclastic fracture of pillow lava	Post magmatic fracture	Gravity fall
Environment indicated	Brief hiatus in eruption	Flow margins, some sub-marine relief	Tectonism	Steep flow edge; vent

that it superficially resembled a breccia but 'differs from a true rubble breccia in that the polyhedra are not displaced relative to each other.' Barnes et al. (1974, p. 62) recorded flow-top breccias (i.e. A_1 zones of Arndt et al., 1977) in ultramafic flows from Mt Clifford, noting that each is 'usually less than 20 cm thick and consists of a dense blue-black serpentinite with many irregular fractures.' In their figure 38, they note devitrification, vesicles, and spinifex texture in these A_1 zones, with spinifex texture, glass, and occasional phenocrysts in thin section. Barnes et al. (1988) delineated ultramafic flows at Agnew on flow-top breccias, but did not describe their characteristics.

There are few descriptions of flow-top breccias in basalts. Lesher (1983, p. 27) described flow-top breccias in drillcore from the top of the Lunnon Basalt at Kambalda, noting that 'flow-top breccias normally comprise the upper division of compound lava flows and are rarely laterally transitional into the frontal facies of individual flow units...' and that '....the breccias comprise small ellipsoidal pillows, abundant broken pillow fragments and angular lava crusts in a matrix of shard-shaped metahyaloclastite with pseudomorphed web-textured devitrification textures normally replaced by calcite + quartz; readily distinguished from post-formational tectonic or extensional fracture breccias.' Two sections of diamond drillcore containing these breccias described by Lesher (1983) have been re-examined in this study. Logs are shown in Appendix 2.1. It is concluded here that these are pillow rather than flow-top breccias: pillow-margin fragments are abundant, and they are bleached and associated with sediment and pillows, suggesting fragmentation of hot lava, spalling of pillow margins and subsequent reaction of basalt with sea-water, accompanied by sedimentation. Both drillcore intersections are at the top of the Lunnon Basalt, and these rocks represent a period when basaltic volcanism was waning immediately prior to eruption of the Kambalda Komatiite.

Pillow breccia

Pillow breccias occur in, or lie adjacent to, pillow lava and consist of pillow fragments or spalls from pillow margins. A typical pillow breccia association (e.g. western side of Lake Cowan, Norseman Terrane) is a chaotic assortment of angular, fine-grained basalt fragments, hyaloclastite, and pelitic (rarely calcareous) sedimentary rock. Clasts are generally matrix-supported; some are vesicular and variolitic (e.g. Harper Lagoon, Boorara Domain); and breccias lack organization (Table 3).

Hydraulic breccia

The most common type of breccia in ultramafic and mafic volcanic rocks is angular to subangular, disorganized, rarely polymict, and usually supported by a calcite and quartz matrix (Table 3). Cross-cutting of original structures shows the breccia post-dates cooling. These breccias result from post-magmatic shearing accompanying or succeeded by injection of a fluid phase. Some hydraulic breccias result from brecciation and fluid flow along inter-pillow zones.

Mass-flow breccia

Mass-flow breccia comprises large (in the region of 10–20 cm diameter), disorganized, frequently polymictic and angular clasts, which are both matrix and clast supported (Table 3). Such breccia is usually in sharp contact with the surrounding rock; clasts are usually fine-grained, and a few have chilled margins. The multiple lithologies, relationship with enclosing rocks, and lack of magmatic features (e.g. glass spalls), suggests that they are a type of gravity-controlled breccia within the volcanic pile. Likely sites of formation are on the flanks of vents or the edge of thick flows.

Varioles

Varioles are mostly pea-sized spherules, usually composed of plagioclase and amphibole (after pyroxene) as radiating crystals. As plagioclase is greater than pyroxene (unlike plagioclase less than or equal to pyroxene in the host), the varioles appear as light coloured spots. Occasionally, varioles consist of epidote pools, possibly after glass. Varioles are spherical to occasionally elongate and up to 2 cm in diameter, and a few have a diffuse margin.

Variolitic basalts are a common feature in the upper basalt of the Kambalda and Boorara Domains. They are less common in the lower basalt of the Kambalda Domain and the Woolyeenyer Formation of the Norseman Terrane.

Other features

Other features logged in drillcore are the size and distribution of vesicles, pillow intersection widths, pillow rim thicknesses, inter-pillow widths, interflow sedimentary horizon thickness, the thickness of intrusions (identified by chilled upper and lower contacts), and types of inclusions (e.g. xenocrysts, xenoliths).

Examples of features logged in drillcore, and their interpretation, are shown in Appendices 2.2 and 2.3.

Criteria for separating adjacent flow units

The least equivocal features for separating adjacent flow units (single lava eruptions) are interflow sedimentary rocks, but in the Norseman–Menzies area, these are scarce and most are laterally discontinuous (Hallberg, 1972; Gresham and Loftus-Hills, 1981). In a few places, cumulate zones (representing crystal accumulations at flow bases) can be used, but these are not abundant either, and can be confused with high-level intrusions; similarly, pillow lava capping a massive flow unit can be used, but such occurrences are rarely seen, and cannot be used in separating flow units in unpillowed successions. Plagioclase-rich zones mark the top of some flow units in the upper basalt unit at Kalgoorlie.

Flow-top breccia is the main criterion used in this study to separate flow units in both mafic and ultramafic volcanic

sequences. The preservation potential of flow-top breccias is low because of their fragile nature; and as they could have been removed by the mechanical and thermal erosive power of successive flows (Huppert et al., 1984; Gole et al., 1990), thick lava sequences lacking flow-top breccias may not indicate one massive flow, but may result from several flow units where flow-top breccias have either not had sufficient time to develop or have been removed by the succeeding eruption.

In ultramafic volcanic successions where textures are not preserved and flow-top breccias cannot be identified, the change in MgO content can be reflected in a change in metamorphic mineralogy from talc-dominated (flow base) to chlorite-dominated (flow top: D. E. Roberts, pers. comm., 1989).

Physical volcanology in the Kalgoorlie Terrane

Kambalda Domain

Kalgoorlie

The three diamond drillholes examined (SE2, SE9, SE10) were from an early drilling program by Western Mining Corporation at Lakewood, approximately 7 km south-southeast of Kalgoorlie–Boulder (Fig. 2). The holes penetrate the komatiite (Hannans Lake Serpentinite), and two (SE2 and SE10) cut the upper basalt (Paringa Basalt). Although the upper basaltic part of the komatiite (Devon Consols Basalt) is cut by SE10, much core has been lost, and there is little control on this unit.

Komatiite unit

Over 600 m of the Hannans Lake Serpentinite has been logged from drillhole SE9 and, although the core is uniformly serpentinized, some A and B subdivisions of flows (Arndt et al., 1977) can be recognized. A frequency histogram of flow thicknesses (Appendix 2.4A) shows a broad distribution from 50 cm to 10.5 m.

A well-preserved section from 432 to 444 m in SE9, with the interpreted A and B divisions, is shown in Appendix 2.3. Flow units ranging from 1–10 m are present. Flow-top breccias (A_1) contain platy olivine spinifex set in ?devitrified glass; more ordered platy olivine is characteristic of A_2 divisions.

Upper basalt unit

The two diamond drillholes logged through the Paringa Basalt are quite different, in that SE2 contains rare pillowed units, with massive flow units delimited by thin plagioclase segregation at the top of flows and/or flow-top breccia. Breccia units up to 6 m thick, showing characteristics of mass-flow breccias, are well developed throughout (Table 3).

Pillow lava in SE2 has 1 cm thick plagioclase-rich rims, and pillow fragments occur in breccia units. Clasts in these matrix-supported pillow breccias range up to 5 cm diameter. They are angular, oligomictic and some are variolitic. Breccias are gradational with the underlying basalt.

In contrast, two-thirds of the approximately 600 m of basalt logged in SE10 is variolitic. Despite variations in variole distributions, pillow rims are not well preserved and measurement of individual pillows was not possible. Sedimentary horizons are rare in both holes. Frequency histograms for flow-top breccia and flow thicknesses (Appendix 2.4A,D) show that flows range from 0.5 to 2.5 m in thickness.

In SE10, individual varioles are less than 1 cm diameter and may have coalesced to give a bleached appearance to the rock. Varioles are either concentrated in pillow cores or, if the core is variole free, the rim is dotted with varioles. In more massive (non-pillowed) units, varioles are larger (up to 1.5 cm) and have a well-developed 1–2 mm rim.

Kambalda–St Ives (Foster)–Tramways

Six surface diamond drillholes, covering a lateral extent of approximately 40 km, have been logged and sampled in this study, two from Kambalda Dome (KD330, KD1029), two from Tramways (TD797, TD842), and two from Foster (CD259, CD201). In addition, five closely spaced underground holes from the top of the lower basalt into the komatiite at Long Shaft (Kambalda) have been logged.

Basalt sequences

Forty flow-top breccias from the lower basalt unit, basaltic upper part of the komatiite unit, and the upper basalt unit, have been measured (Appendix 2.4E). Most are less than 30 cm thick, although two from CD201 (one from the lower basalt unit and the other from the upper basalt unit) are 70–90 cm thick.

Fifty-nine flow units have been measured (Appendix 2.4B), the majority from the lower basalt unit. Some flows are separated by flow-top breccias, and others have been delimited by changes in grain size, or pillowed tops (e.g. 432–450 m in TD842, Appendix 2.2). The majority of flows are less than 5 m thick, and few exceed 10 m.

Pillow intersections (Appendix 2.4G) range from less than 20 cm to 120 cm, with a mode between 20 and 60 cm. Thicker intersections (140–160 and 180–200 cm) are possibly cross sections through the bulbous toes of pahoehoe-type lava.

Apart from pillow breccias in the Lunnon Basalt immediately below the contact with the Silver Lake Peridotite, other breccia types are uncommon.

Closely spaced diamond drillholes

In order to examine the lateral continuity of volcanic flows, a fan of six underground holes from a common collar on 15 Level, Long Shaft (Fig. 3) have been logged.

The holes are variably inclined (0–31°) up to a maximum 143 m length, collared in the Lunnon Basalt into the overlying Kambalda Komatiite. Drill logs at 1:500 scale are presented in Appendix 2.5. Close to the collar and extending approximately 15 m in four of the six holes (LG 15-1, 15-12, 15-14 and 15-13) the sequence is of pillow lava. A thinner pillowed unit occurs in LG15-15 (disrupted by acid intrusive rocks) and LG15-16, and, generally, the pillow lava unit is thinnest in the three holes showing the steepest inclination (ie LG15-14, 15-15 and 15-16). In hole LG15-1, the pillowed sequence is succeeded by a 2 m thick flow (pillowed top), a 9 m thick flow (pillowed top), and a 6 m thick flow (pillowed and brecciated top). The 9 m thick flow can be recognized in LG15-12 and arguably in LG15-14, but flow units in LG15-12, LG15-14 and LG15-13 are less easily correlated with flow units in other holes. Broadly, the remainder of the succession is dominated by non-pillowed, massive dolerite, with a few flow-top breccias and chill zones indicating a packet of flows in the order of 5–10 m rather than a single flow unit. Sedimentary rock horizons are discontinuous between holes. The best correlations are drawn between holes LG15-1 and LG15-12, both of which have a zero azimuth.

Ultramafic volcanic sequences

Recognition of the two members of the Kambalda Komatiite in any particular drillhole is not always possible, although logging undertaken in this study has shown that the lower parts of the komatiite unit are more massive and less variable; and this is characteristic of the Silver Lake Peridotite rather than the Tripod Hill Komatiite (Cowden and Archibald, in prep.).

Using either A–B pairs, or changes in metamorphic mineralogy, flow units in the 5 holes examined range widely in thickness, from 2 m in KD330 to 42 m in TD842. A plot of thicknesses against downhole height above the Kambalda Komatiite–Lunnon Basalt contact (Appendix 2.6) shows a weak negative correlation (*see* especially Foster holes TD842 and 797), consistent with the Gresham and Loftus-Hills (1981) stratigraphic division and the observations of Groves and Hudson (1981). In CD201, shearing and brecciation, plus the frequency of acid porphyry intrusions and the paucity of spinifex-textured horizons, have meant limited identification of flow units.

Bluebush and Republican

Both logged diamond drillholes at Bluebush (BD108 and BD222) penetrate the komatiite unit and the upper basalt unit. Diamond drillhole RHD1 (Republican) comprises approximately 320 m of upper basalt unit and underlying komatiite unit.

Basalt sequences

BD108 penetrates approximately 25 m of the upper basalt unit, comprising a 12 m weakly brecciated, sporadically variolitic and pillowed lower sequence, with few flow-top breccias. One flow is 2.4 m thick (Appendix 2.4C). The upper half of the unit (about 13 m) is brecciated, and clasts range from 1 to 3 cm diameter, usually matrix supported. Brecciation appears to post-date cooling, and shows other characteristics of hydraulic brecciation (Table 3). The contact with the overlying ultramafic is bleached.

Approximately 100 m of basalt has been logged in BD222. From 260 m to 297 m, some of the basalt is veined and brecciated, and there is a series of well-developed flow-top breccias, delimiting flows between 0.6 and 3 m thick. One flow is 6.4 m thick (Appendix 2.4C). The upper 50 m of the basalt unit is separated from the lower sequence by a 9 m thick, locally brecciated and weakly sulfidic, sedimentary horizon. The basalt is strongly brecciated and matrix-supported. The top 8 m is less brecciated but is, in part, sheared.

Of the 45 m of basalt in RHD1, the lower 10–11 m comprises pillow lava (sometimes variolitic), minor pillow breccia (cf. basalt in BD222), and rare interflow sedimentary rock. A 1 m thick carbonaceous sedimentary unit at about 309 m is succeeded by approximately 20 m of dolerite with a chilled top. As there is no chilling or disruption at the base, the dolerite probably represents a slowly cooled flow. The uppermost 10 m of the basalt unit is enriched in secondary biotite and interbedded with sedimentary units.

Ultramafic sequences

BD108 contains about 400 m of reasonably monotonous, veined and locally foliated, talcose and carbonated ultramafic rocks. Excessive alteration has obliterated many fine-scale features, although rare flow-top breccias and changes in metamorphic mineralogy (i.e. MgO-rich bases to less MgO-rich tops) delineate flows of 1–3 m (Appendix 2.4C); but, as much of the sequence lacks flow-top breccias, massive (tens of metres thick) flows could be present.

BD222 shows a little more variety than BD108 in that it has several flow-top breccias (flows from 0.8 to 3 m, two adjacent flows of 50 and 60 cm respectively); and has sulfidic and carbonaceous sediments in the upper parts.

The lower part of the ultramafic unit in RHD1 is talcose and the upper part serpentinized. Above 210 m, changes in mineralogy could mark flow tops, which would indicate flow thicknesses of between 2 and 5 m (Appendix 2.4C). From approximately 70 to 90 m, spinifex texture is well developed, and flow units are between 0.8 and 2 m (Appendix 2.4). Bands of coarse-grained acicular amphibole (up to 75 mm long) occur between 62 and 68 m.

Ora Banda Domain

Interpretation of volcanology is restricted to drillcore from the komatiite unit (Siberia Komatiite at Vettersburg, diamond drillholes VBD1 and VBD2; Big Dick Basalt at Theil Well, diamond drillholes NMXD14 and 16), and the upper basalt unit (Bent Tree Basalt and Victorious Basalt

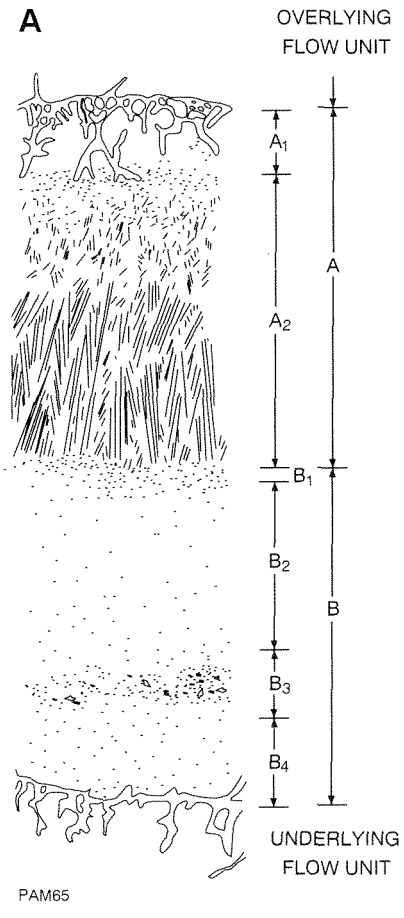

Figure 6. Idealized komatiite flow unit, showing division into B and A zones. A_1 — flow-top breccia; A_2 — spinifex. B — cumulate zone. B_1 — foliated skeletal olivine; B_2 — cumulate olivine; B_3 — knobbly peridotite; B_4 — cumulate olivine. From Arndt et al. (1977)

at Gimlet South, diamond drillholes DDH11 and 12). Diamond drillhole locations are shown on Figure 4.

Komatiite unit (Siberia Komatiite)

Diamond drillholes VBD1 and VBD2 in the Siberia Komatiite at Vettersburg contain carbonated or serpentinized ultramafic rocks with complete or near-complete flow units (Appendix 2.8A).

In most cases B_1–B_4 units of Arndt et al.'s (1977) schematic section through a komatiite flow (Fig. 6) cannot be separated in the Vettersburg core because of textural destruction, and in these cases a 'B' zone only is identified. However, spinifex texture (A_2), and chilled and fractured flow tops (A_1), have been identified in both holes (Appendix 2.7). Characteristics of these 'B' and 'A' zones are discussed below.

B zones contain 1–3 mm olivine euhedra (now carbonate) (e.g. 220 m in VBD2; 189 m in VBD1), showing ortho- and mesocumulate texture. Where identified, rare B_4 zones are thin (up to 30 cm thick) between the cumulate zone and the underlying flow-top breccia. Flow bases are usually sharp and may be erosional. The top of a cumulate zone in VBD1 at about 208 m is bleached, possibly altered prior to burial.

Spinifex texture (A_2) ranges from well-organized plates of (former) olivine (up to 5 cm long in VBD2 at about 207 m) to random or 'patchy' spinifex only a few millimetres long. At 244.5 m in VBD2 there is a decrease in olivine plate size upwards over several centimetres (cf. idealized flow of Arndt et al., 1977). In some sections, sharp breaks occur between B and A zones (possible B_1?). There is a wide range in thicknesses of A_2 zones (Appendix 2.8C), although most group between 10 and 60 cm.

Flow-top breccias (A_1) are usually less than 30 cm thick (Appendix 2.8D). They are organized, oligomictic, and contain angular fragments with little matrix (Table 3), sandwiched between underlying A_2 (either as spinifex, or spinifex succeeded by a zone of finer grained rock (i.e. top of A_2)), and the overlying cumulate base of a flow (B_4). These breccias are noticeably different in morphology from those described from Marshall Pool by Barnes et al. (1974).

In the well-preserved parts of VBD1, four flows contain B, A_2, A_1 (1.3 to 4.7 m thick), seven flows (0.8 to 3.4 m thick) lack the A_2 (spinifex-textured) component, and two flows (1.3 to 3.2 m) consist of B and A_2 (i.e. no flow-top breccia nor chill zone). In VBD2, five flows have B, A_2, A_1 (0.8 to 5.2 m thick), four flows have B and A_1 (both 0.3 m thick) and two flows have B and A_2 (1.1 and 1.8 m thick).

Several consecutive cumulate units in both VBD1 and VBD2 (e.g. VBD1 214–217 m; VBD2 at about 130 m) have no intervening A horizons. These cumulate units range up to 8 m in thickness (Appendix 2.8E).

Upper basaltic part of komatiite unit (Big Dick Basalt)

The lower 90–170 m of diamond drillhole NMXD14 contains pillow lava units (up to 25 m thick) alternating with massive, in part fine-grained, volcanic flows of the Big Dick Basalt. Pillow lava is variolitic (varioles are up to 3 mm diameter and usually coalesced) and, locally, vesicular. A rare interflow sedimentary unit at 126 m is 2 m thick; it has a sheared top and a sulfidic base with minor fuchsite. Massive units in the upper part of the logged sequence may represent either flows or concordant sills. In places, they are plagioclase-phyric, which appear to be late-stage segregations. The lower 16 m of diamond drillhole NMXD16 is massive and occasionally sheared basalt, separated from the remaining approximately 80 m of variolitic and occasionally vesicular pillowed lava (cf. lower part of NMXD14) by a 2 m thick sill or flow.

Pillow intersections, pillow edge and pillow breccia characteristics, are well preserved in both holes. The distribution and mode (20–40 cm) for pillow intersections are similar in both NMXD14 and 16, with intersections

at 160–220 cm, 280–300 cm, and 520–540 cm interpreted as pahoehoe toes transitional to massive flows, although the small number of these anomalous occurrences suggests a sharp transition from pillowed to massive flows (Appendix 2.9A,B). The high frequency of pillow edge zones ranging from 0–10 cm (Appendix 2.9C,D) reflects pillow to pillow contact and little inter-pillow matrix.

In this core, four types of variole distribution are observed in pillow lava:

1. pillows have variole-rich bands parallel to and within a few centimetres of the pillow rim (common);
2. varioles only occur on the upper pillow rim (uncommon);
3. the total intersection comprises coalesced varioles (uncommon); and
4. the total intersection is devoid of varioles (uncommon).

In Appendix 2.9E, total variole thickness (expressed as a percentage of the total pillow intersection thickness) is plotted against the intersection width. All four cases above are represented. Although not totally conclusive, it appears that thicker pillow intersections have fewer varioles.

Upper basalt unit (Bent Tree Basalt and Victorious Basalt)

Two diamond drillholes have been logged. DDH11 comprises approximately 90 m of Victorious Basalt and roughly 40 m of the Ora Banda Sill, whereas DDH12 comprises about 240 m of the Bent Tree Basalt.

The lowest 50 m of Victorious Basalt in DDH11 is dark-grey pillowed basalt, containing sub- to euhedral plagioclase crystals up to 6 cm long. Nineteen pillow intersections measured between 186 m and 150 m (Appendix 2.9F) show a wide range in pillow intersection thickness. Pillows are non-variolitic with well-developed fine-grained (chilled) rims; a 2.32 m ?pahoehoe toe at 184 m has an 18 cm chilled margin, and the adjacent 1.10 m ?toe has a 13 cm thick chilled rim. Hyaloclastite, pillow fragments, and sedimentary rock commonly occupy the interstices between pillows. Breccia units up to 9 m thick have been recorded. The occurrence of secondary calcite and quartz and some hydrothermal alteration indicates that the breccias were conduits for secondary fluids.

The upper 40 m of the Victorious Basalt lacks pillows and is cut by breccias and quartz veins. Much is epidotized and the core is poorly preserved, making flow unit delineation difficult. The contact with the Ora Banda Sill is sheared.

The 230 m of Bent Tree Basalt logged in DDH12 is a series of pillow lava units interlayered with massive dolerite. Histograms of pillow intersections (n is 83) and pillow edge thicknesses (n is 86) are shown in Appendix 2.9G,H). Pillow intersection widths for the Bent Tree Basalt and Victorious Basalt are generally greater than the Big Dick Basalt (Appendix 2.9A,B). The massive units have chilled margins adjacent to pillow edge zones and are more likely to be extrusive than intrusive. In some places, both upper and lower dolerite contacts are chilled indicating intrusion.

Coolgardie Domain

Widgiemooltha and Redross

Diamond drillhole WID1038 penetrates the lower part of the komatiite unit and the top of the lower basalt unit. Diamond drillhole RRD1 (Redross) consists of about 115 m of basalt and ultramafic, stratigraphically equivalent to the lower basalt unit and the komatiite unit.

Lower basalt unit

The 50 m of basalt logged in WID1038 is weakly brecciated and in part veined and pillowed; it has few flow-top breccias and no interflow sedimentary units. There is a sharp contact with the overlying komatiite unit. Of the 60 m of basalt in RRD1, the lower 15 m contains several flow-top breccias and associated flows ranging from 80 cm to 3.6 m thick. Quartz veining is prominent from 90–100 m, and interflow sedimentary rocks occur at 70–76 m. Shearing of basalt and sediment occurs at the contact with the overlying ultramafic unit.

Komatiite unit

The lower 10 m of the komatiite unit in WID1038 contains a distinctive alternation of 80–100 cm thick bands of porphyritic amphibole rock (amphibole grains up to 2 cm long) and finer grained mafic material. This is overlain by approximately 50 m of featureless, fine-grained, serpentinized ultramafic rock, and is in turn succeeded by about 100 m of ultramafic rock containing a few finer grained, mafic zones, possibly flow tops. Within this 100 m section, one 4 m-thick flow has been measured. The uppermost 100 m or so of logged core contains some spinifex-textured ultramafic rocks and a few flow-top breccias. Overall, there appears to be a transition from thicker, peridotitic flow units at the base of the sequence to thinner less Mg-rich units higher up (cf. Kambalda Komatiite: Thomson, 1989a,b; Groves and Hudson, 1981).

The shearing at the top of the lower basalt unit at Redross persists into the ultramafic rock in RRD1. Individual flow units (0.6–1 m thick) can be identified by the presence of massive grey talcose basal units overlain by thinner more chloritic tops.

Coolgardie

Examination of two diamond drillholes from the Bayleys Consols area (BCD170 and BCD176) indicates that the lower basalt unit (Burbanks Formation) contains both pillowed and massive units. Appendix 2.10 shows a broad spread in pillow intersection widths, implying a

gradation from pillowed to pahoehoe-type flows to more massive units. Some massive units have chilled margins consistent with intrusion, and probably represent high-level comagmatic sills, although they are lithologically similar to pillows.

Immediately overlying this succession, a series of basalts containing plumose amphibole have been intruded by porphyry. The remainder of BCD 176 comprises coarse-grained basalt capped by ultramafic rock.

In some well-exposed areas, Hunter (1993) noted that pillowed sequences are traceable over hundreds of metres, suggesting lateral continuity of flows. Individual pillows are 20–100 cm diameter, rarely up to 200 cm, and occur in the upper parts of flows. Varioles (up to 1 cm diameter) occur in pillows and scattered throughout massive flows. Flow-top breccias, which consist of 10–20 cm blocks and interstitial hyaloclastite, are rare and less than 50 cm thick. Interbedded dolerite units are usually variants of individual flows, and occur at the base or middle of flow units.

Komatiite flows in the Hampton Formation are 5–30 m thick according to Hunter (1993). Although outcropping poorly, flows appear to be laterally continuous but vertically variable, and to have well-developed and well-preserved spinifex texture. Some weakly variolitic pillows (10–100 cm diameter) with narrow (2–10 mm) once-glassy rinds are found lower in the sequence.

Boorara Domain

Carnilya Hill

In both logged diamond drillholes (CHD412 and CHD447), there has been good preservation of textures in basalts (Appendix 2.11), but ultramafic volcanic rocks have suffered significant destruction of textures because of metamorphism, carbonation and K-metasomatism, so there are few features, such as flow-top breccias and spinifex-textured horizons, which give any clue to eruptive conditions.

CHD412 contains about 200 m of basalt overlain by approximately 90 m of ultramafic rock that is, in turn, overlain by 60 m of basalt. CHD447 has three basalt units, each overlain by ultramafic rocks, although in the light of regional mapping (Griffin and Hickman, 1988), there is some likelihood of structural repetition.

Lower basalt unit

Pillow basalt is more common than massive flow units in CHD412 (40% of basalt logged), and sedimentary units are more common in the lower part of the core.

A frequency histogram for 55 measured pillow intersections (Appendix 2.12A) shows a strong grouping at 20–60 cm, but a spread to 2 m, implying a gradual transition from pillows to pahoehoe toes and eventually massive flows.

In contrast to the situation in the Kalgoorlie Terrane, pillow breccias are a common feature in basalt units at Carnilya Hill (Appendix 2.12D). They show a limited range of thicknesses, from 5–45 cm, and consist of angular basalt fragments (occasional pillow rims) in a felsic sedimentary matrix.

Most flow-top breccias in basalts are between 10 and 20 cm thick (Appendix 2.12C).

Basalt flows (Appendix 2.12B) are thin (usually less than 2 m), with no relationship between flow thickness and stratigraphic height. However, the average thickness of flows and the variability in flow thickness, as shown by standard deviation (sd), in CHD412 are more than twice that of CHD447 (CHD412 mean thickness 193 cm, sd = 163 cm, n = 6: CHD447 mean thickness 93 cm, sd = 83 cm, n = 15).

Hydraulic breccias show a limited range of thicknesses, with the majority from 10 to 30 cm (Appendix 2.12E).

Komatiite unit

The only flow-top breccia recorded from ultramafic is, at 45 cm, thicker than those in most basalts.

Harper Lagoon

Komatiite unit

The komatiite unit exposed at Harper Lagoon consists of an orthocumulate horizon overlain by well-developed olivine spinifex-textured ultramafic, and a gabbro unit. This is interpreted as a single ultramafic flow which is capped by a differentiated gabbro.

Upper basaltic part of the komatiite unit

Pillow lava in the upper basaltic part of the komatiite unit contrasts markedly with that of the Kalgoorlie Terrane in that individual pillows are highly vesicular and accompanied by significant pillow breccia. Varioles within pillows are both concentric to pillow margins and accumulated in pillow cores.

Physical volcanology in Norseman Terrane

Diamond drillholes have been examined from the Woolyeenyer Formation, a unit in excess of 9500 m thick, although there is a possibility of tectonic thickening (P. J. McGoldrick, pers. comm., 1990). The sequence is dominated by basic submarine lavas and comagmatic intrusives, which may be separated by thin cherty sedimentary units. Four of the holes are from near the base of the unit and one from near the top (Fig. 5).

Massive (non-pillowed) lava constitutes between 17% (S207) and 62% (S169) of the logged core. Most flow-

top breccias are 10–20 cm thick (Appendix 2.13A); they are often seen in the middle and upper parts of the Mararoa Pillow Lava, but are rare in the lower Mararoa Pillow Lava, and only two examples have been recorded from the Desirable Pillow Lavas (C126). It is unclear whether cumulate zones represent lower parts of flows or parts of intrusions; and interflow sedimentary rocks are too infrequent to be useful in the separation of flow units. Only S156 contains a sufficient number of flow-top breccias to get a consistent idea of the thicknesses of flow units, which range from 1.1 m to 7.6 m (Appendix 2.13A).

Pillow thickness, pillow-edge width, and the nature and thickness of inter-pillow material, are shown in Appendix 2.13B–D. Although most pillows are between 20 and 80 cm thick, the apparent thickness of pillows in drillholes S207 to S433 decreases gradually in a stratigraphically upward sense: this suggests that the proportion of pahoehoe toes decreases with stratigraphic height. As discussed below, the thickness of true pillows (vs pahoehoe toes) from the Woolyeenyer Formation on the western shore of Lake Cowan cluster below 100 cm; therefore, intersections greater than 100 cm in drillcore may not be true pillows, but tubes or interconnected pillows.

Frequency histograms for pillow-edge thicknesses (i.e. chill zones) are shown in Appendix 2.13C. There is a broad spread from 2 to 18 cm, but with most intersections are between 2 and 6 cm.

Pillows are closely packed, and there is little inter-pillow breccia or sedimentary material. For pillows not in contact, most inter-pillow distances fall between 5 and 30 cm, with some anomalous values (e.g. 85 cm pillow breccia at 186 m in S207; 1.58 m breccia at 249 m in S433).

Vesiculation is uncommon but occurs in both pillowed and massive flows, locally with variolitic basalt (e.g. 103 m in S156). In S156 at 205 m, weakly vesicular basalt occurs in massive flows associated with flow-top breccias.

Varioles occur throughout the sequence, usually associated with pillow lava, although about 4 m of massive lava with 1 mm diameter varioles occurs at approximately 300 m in S169. Pillow lava occurs stratigraphically close by. Varioles occur as either coalesced masses in the cores of pillows (e.g. 25 cm thick area at the core of a pillow at 62 m in S169), or are randomly distributed near pillow margins (e.g. 4 mm diameter scattered varioles at 79 m in S169).

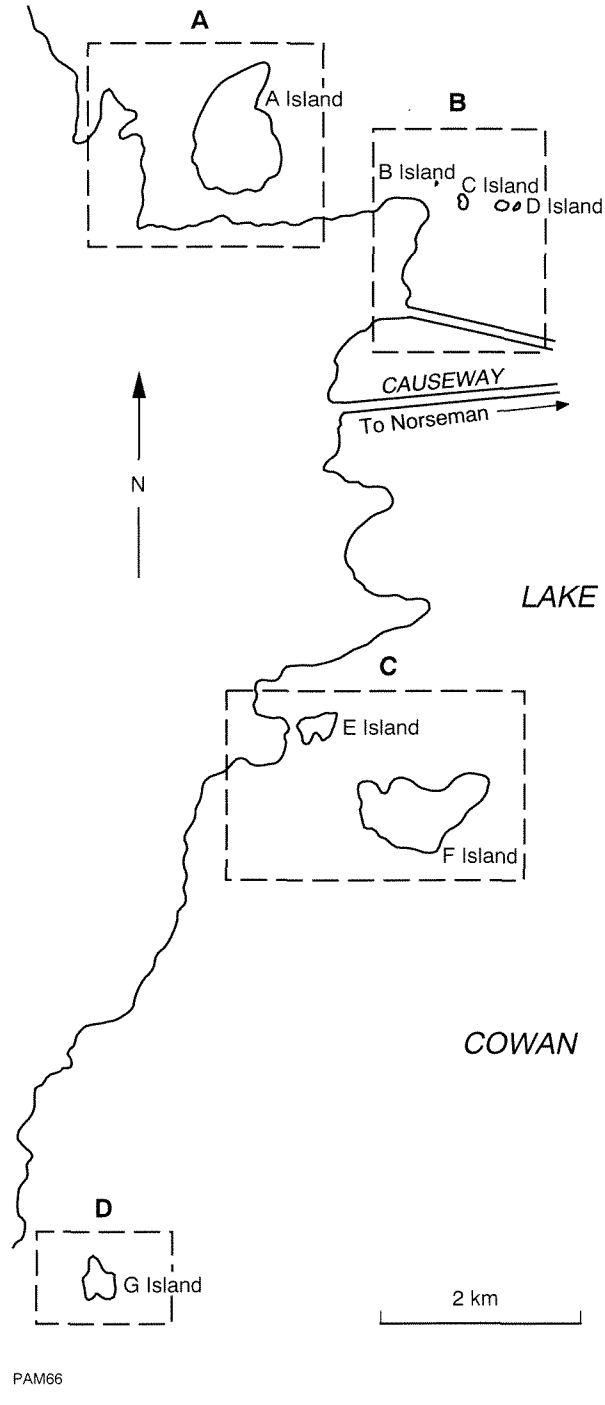

Figure 7. Volcanological features mapped in the Woolyeenyer Formation on the western shore of Lake Cowan, Norseman Terrane (see enlarged insets A–D)

Flow sequences on the western margin of Lake Cowan

Pillowed and massive flows of the Desirable Pillow Lavas form good outcrop along approximately 6 km of the western edge of Lake Cowan and adjacent islands (Fig. 7). Pillow orientation and the attitude of the few interflow sedimentary rocks indicate a constant northerly strike and a 50–60° westerly dip and younging direction.

Although lake-edge outcrop rapidly degenerates into rubble inland, areas of continuous exposure (especially around islands) allow some three-dimensional investigation, even though interflow sedimentary rocks are of limited use in separating flow units, and flow-top breccias have not been identified.

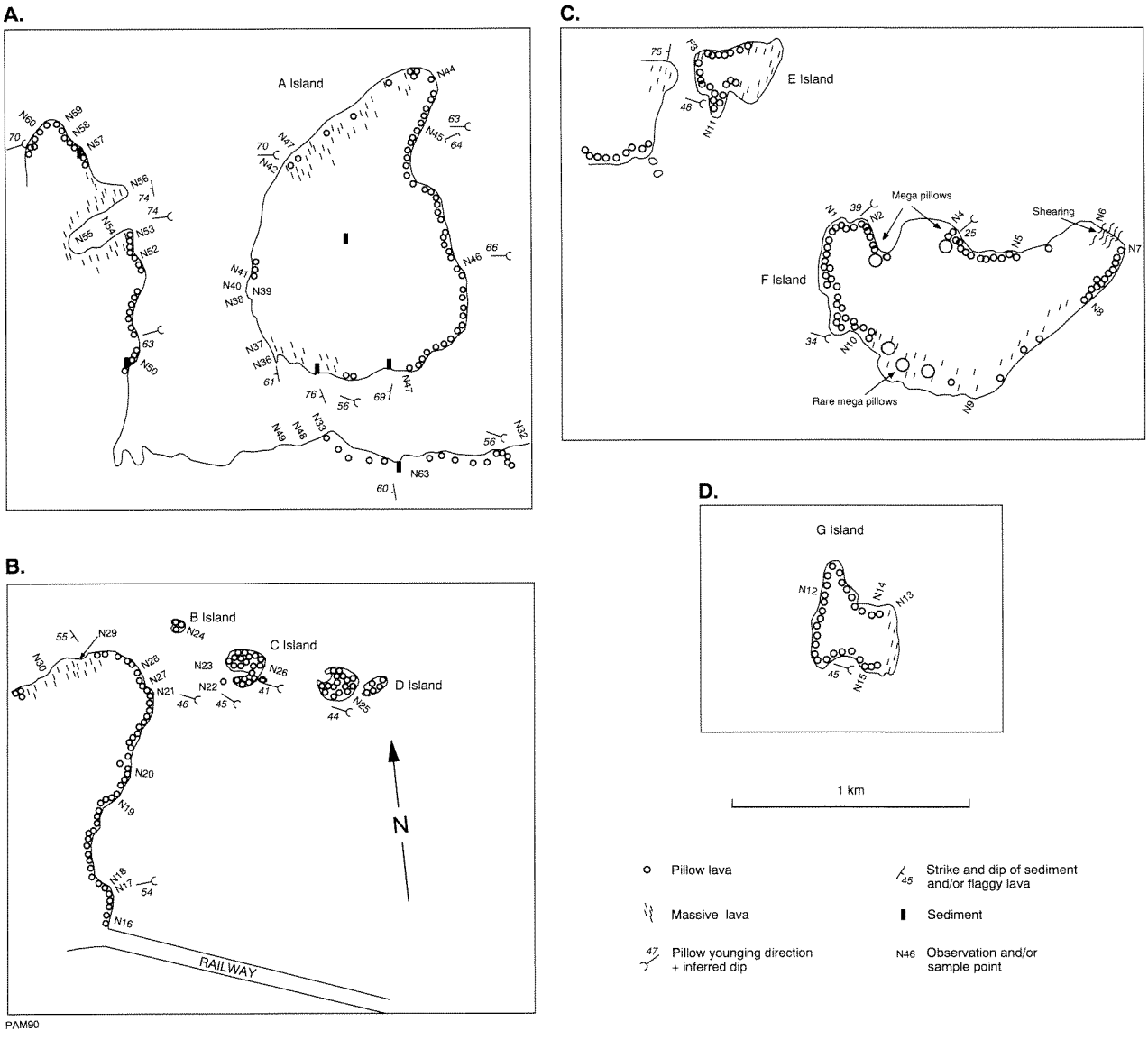

The majority of flows are pillowed but, as exposures are usually only two-dimensional, it is difficult to determine whether pillows are separate entities or represent cross sections through tubes or mattresses. However, at location N21 (Fig. 7B), a three-dimensional outcrop comprises bifurcating lava toes, and at N9 (Fig. 7C), pillow-form lava occurs as tubes 1.5–1.8 m long. A three-dimensional outcrop of pillow-form lava at N26 (Fig. 7B) has lobes between 80 cm and 120 cm long.

On the north side of F Island (Fig. 7C), the pillowed unit at N2 has a 5 m lower and upper zone of larger pillows (1–2 m), gradational to massive lava. A similar transition zone occurs between N14 and N15 on G Island (Fig. 7D).

On F Island (Fig. 7C), pillowed units southeast of N4 give way laterally to weakly pillowed and locally massive units (N9) over approximately 400 m. One interpretation is that the central parts of flows are massive and unpillowed; but give way vertically and laterally to megapillows, then to more regular, smaller pillows.

Pillow dimensions have been measured at 12 locations (Appendix 2.14). As exposures are usually parallel to strike, only two dimensions have been regularly measured. Most pillows are strongly elongated parallel to strike, coincident with a regional shear (e.g. eastern end of F Island at N7, Fig. 7C), indicating that pillow elongation is at least in part tectonic. In areas of low strain, pillow dimensions are closer to 1:1 (e.g. N16: Fig. 7B; N11: Fig. 7C). As more equant pillows have only a weakly developed foliation (P. J. McGoldrick, pers. comm., 1991), those with width to length ratios of less than 1:3 have not been tectonically flattened. Pillow widths group between 10 and 30 cm (Appendix 2.13B), but range up to 1 m, and a variety of pillow sizes at one outcrop (e.g. N16: Fig. 7B) is a feature of pillowed flows.

Individual pillows are fine grained (usually aphanitic), green, occasionally amygdaloidal, and/or strongly variolitic; cores or bands of varioles are concentric and adjacent to the rim. Varioles range up to 5 mm, e.g. N5

(Fig. 7C) and N49, (Fig. 7A). At N22 (Fig. 7B), varioles are concentrated in a 5 cm concentric zone 1 cm in from the pillow margin. In outcrops where both non-variolitic and variolitic pillows occur, the smaller pillows usually contain varioles, whereas the larger ones are variole-free but usually weakly vesicular on the margin. Some pillows have a coarser grain size (cf. dolerite), because of metamorphic recrystallization. Pillow margins consist of a 2–3 cm, brown, fine-grained (originally glassy) rim, which is rarely vesicular, although pipe vesicles (1–2 cm long) occur in the margin of pillows at N24 (Fig. 7B), where they overprint varioles. Concentric bands of vesicles occur in pillows at N10 (Fig. 7C), and concave vesicles are parallel to pillow edges at F3 (Fig. 7C).

Interpillow interstices containing pelitic and carbonate-rich sedimentary material accompanied by angular basalt fragments, probably spalled off pillow margins, are uncommon. Significant inter-pillow breccia (including hyaloclastite) has only been recorded at N23.

Massive lava flows, for example A Island west of N35 (Fig. 7A) and N30 (Fig. 7B), are medium-grained, in part doleritic, jointed, and flaggy. Thicknesses between interflow sedimentary units on A island are about 60 and 90 m respectively. Both flows have doleritic central parts and pillowed margins. Thin, glassy basalt units occur at N42 (Fig. 7A), and on the headland west of E Island; the latter contains some quartz xenocrysts. One unit between N36 and N38 has pyroxene needles (now plumose amphibole), and there are weak pillow structures at N38 (Fig. 7A).

As intrusions are usually concordant, they are difficult to distinguish from massive flows, although vesiculation and pillowing on the margins of massive units supports an extrusive origin. A variolitic flow on the western side of A Island at N36 (Fig. 7A) shows lateral thickness variations on a scale of decimetres.

Strongly vesicular or amygdaloidal flows are rarely seen, although massive flaggy flows at N30 (Fig. 7B) contain conspicuous, aligned, tear-drop shaped vesicles. The majority of bulbous ends are oriented to the north (bearing 345°, 345°, 357°) suggesting a south to north flow direction, although one measurement (bearing 165°) suggests the reverse.

Closely spaced diamond drillholes

In order to examine lateral continuity, diamond drillcore from three closely spaced surface holes from near the base of the Woolyeenyer Formation have been logged, one of which (S207) has been discussed previously (Fig. 5). Two of the holes (S448 and S202) are 80 m apart and the third (S207) is approximately 160 m from them. Holes with a common stratigraphic marker and lacking late-stage intrusions, shearing etc. were preferred. Unfortunately, the 'common datum' in these holes (Venture Slate) occurs at three levels (110 m, 134 m and 142 m) in S202.

Drill logs are summarized in Appendix 2.15. Likely flow packages are represented by 78 m of dolerite (60 m to 138 m) in S207 progressively thinning to 65 m (113 m–178 m) in S202, and 15 m (214 m to 229 m) in S448. Similarly, there is a progressive thinning of dolerite from S448 to S202 to S207 in the lower parts of the logged sequence. In the upper sequence, there are more pillows, flow-top breccias, and sedimentary horizons in S448, whereas in the lower parts of the sequence, the reverse is true: S207 contains significantly more pillow lava (i.e. fewer massive flow units, less-massive flows) than S448.

One interpretation of this sequence is that the axial region of massive, unpillowed lava immediately below the Venture Slate in S207 thins laterally towards the edge of the flow in S202 and eventually S448. Lower in the sequence, the axial region is in S448, thinning laterally to S202 and then S207.

If sedimentary units are used to delimit the flows, they range up to 50 m thick. A minimum estimate for the lateral extent of flows is given by the drillhole spacing: as the direction of flow is unknown, the maximum assumed width must be 2 times (about) 160 m, suggesting flow dimensions of at least 50 by 400 m. This rather crude size estimate compares well with basalts mapped on the western shore of Lake Cowan (discussed previously), where flows are 60–90 m thick and 400–500 m wide. Thickness to width ratios from drillcore range from 0.15 to 0.25, although it should be stressed that these are probably not based on dimensions of flow units, but on dimensions of assemblages or packets of flow units.

Review of volcanological features

Characteristics of pillow lava

Studies of Cretaceous and Tertiary diamond drillcore have shown that the degree of pillow curvature and the range in pillow intersection widths can indicate if pillows were erupted onto a flat or sloping surface (Robinson et al., 1979, 1987). In the core examined in this study, the limited range in intersection widths and the curvature indicates that pillows are equant, consistent with eruption on a flat surface. Thin rims on individual pillows imply rapid chilling and, as most pillows are in contact (little inter-pillow sediment or hyaloclastite) and adjacent pillows are intimately draped, the lava was fluid and erupted rapidly but not violently. Varioles are usually restricted to pillow lava and range from holocrystalline assemblages of plagioclase greater than amphibole (a similar mineralogy but different mode to the host pillow) to plagioclase + amphibole with chlorite pools; the latter, possibly after glass, imply rapid cooling. Smaller pillows usually have a higher variole content, but varioles are uncommon in massive lava flows; this suggests that the slow eruption of lava associated with pillow lava production favours variole development. Varioles are usually distributed in pillows as concentrically zoned bands or coalesced masses in pillow cores. This is well illustrated in pillow lava of the upper basaltic part of the komatiite unit at Harper Lagoon (Boorara Domain). The inferred mechanism responsible for this variole distribution is the progressive cooling from the pillow edge to the centre, until an immiscible fraction reached saturation,

when the immiscible fraction would coalesce as varioles. The remaining liquid would be depleted in the immiscible component and the pillow would be variole-free until the immiscible fraction built up sufficiently to allow varioles to precipitate. In pillows with variole-rich cores, the last liquid fraction would be almost all immiscible component. Overprinting of varioles by vesicles at Harper Lagoon and Norseman indicates that varioles formed prior to magma solidification, and are not metasomatic.

Pillow breccia is associated with a slower rate of submarine eruption than that which produces massive lava, and also with some topographic relief, such as the margins of flows or the sides of vents.

Characteristics of massive lava flows

As massive lava flows in the Norseman–Menzies area are usually fine grained and, as there is no indication of crystal settling as expected with one thick flow unit, it is likely that they are composed of multiple flow units. This is consistent with observations of Hynes and Gee (1986), who noted that 20 m thick flows of the Proterozoic Narracoota Volcanics had developed internal differentiation and cumulate horizons.

Flows range from tens of centimetres to a few metres, but flows greater than 10 m are uncommon and few are vesicular or variolitic. Taking into account flow unit thicknesses measured in drillcore, 'flows' with dimensions of 50 x 400 m (cf. closely spaced holes and western side of Lake Cowan, Norseman Terrane) are more likely to be packets or assemblages of flow units. Clearly, the difficulty in recognizing flow-top breccia in the field is an inhibiting factor in delimiting flow units.

Sills are lithologically similar to flows and are probably high-level intrusive equivalents.

Relationship of pillowed and massive lava

Detailed mapping on the shore of Lake Cowan (Norseman Terrane) shows a gradation from pillowed to massive lava. This relationship is also interpreted from histograms of pillow lava intersections in drillcore where there is usually a gradation in intersections and most pillows less than 1 m. The exception is for some units in the Ora Banda Domain, where there is little gradation between pillowed and massive lava; this implies derivation from separate magma pulses or the channelling of lava flows, resulting in a sharp decrease in lava velocity from the centre to the margin of the flow.

Review of Kalgoorlie and Norseman Terranes

Kalgoorlie Terrane

Lower basalt unit

The lower basalt unit at Kambalda consists of pillowed and massive flows, and high-level, probably comagmatic, intrusions. Individual pillows are usually less than 120 cm diameter, and most less than 80 cm; larger intersections may be cross sections through toes of pahoehoe-type flows ('megapillows'). Of the fifty-nine flow units identified in drillcore, 76% are less than 5 m thick. The thickness and distribution of massive flow units, pillow lava, and flow-top breccia, shows no relationship to stratigraphic height. The proportion of sedimentary rocks associated with flow units can be equated to eruption rates. Throughout most of the sequence, interflow sedimentary rocks are rare, implying rapid eruption. A higher proportion of sedimentary rocks at the very top of the Lunnon Basalt coincides with significant pillow breccia, hylaoclastite, and bleached basalt fragments, and is consistent with the waning of basaltic volcanism.

Pillow breccia and mass-flow breccia are uncommon, implying eruption on a flat surface with few vents. As vesicular and less common non-vesicular lava are locally interbedded, vesicularity is a function of variable magma volatility rather than depth of eruption (Jones, 1969).

Examination of closely spaced diamond drillholes shows that major facies changes occur on a scale of 5–10 m, and few flow units can be correlated between adjacent holes. Thus, it is more realistic to group flow units according to style of eruption (i.e. pillowed or massive), into *flow packets*. However, this approach may cause problems as the change from massive to pillowed lava over a few metres may be due to gradual changes in lava velocity between the centre and margins of a flow unit (cf. Robinson et al., 1979, 1987).

Similar flow characteristics were observed in the lower basalt unit at Widgiemooltha–Redross, where interflow sedimentary units are rare and flows, comprising both pillowed and massive units, are less than 10 m thick.

In contrast to the situation in the Kambalda Domain, the two drillholes logged from the lower basalt unit of the Coolgardie Domain indicate some lateral continuity accompanied by gradual changes from massive central portions of flows to pillowed margins. This circumstance is consistent with Hunter's (1993) observations that lithologic units can be traced laterally for hundreds of metres.

At Carnilya Hill (Boorara Domain), pillow lava intersections indicate a gradation from pillowed into more massive flow units. The consistency of pillow intersection widths throughout the core suggests little variation in conditions of eruption over time. However, spatial variations in conditions of eruption are implied by the range in flow thickness between the two holes. Most flows are thinner (less than 5 m) than those logged in the lower basalt unit of the Kambalda Domain.

Komatiite unit

The lower parts of the komatiite unit at Kambalda, Widgiemooltha, Kalgoorlie, and Ora Banda, comprise thicker more Mg-rich flows than the upper parts.

Flow units within ultramafic volcanic sequences can be identified using flow-top breccia, changes in meta-

morphic mineralogy, and cumulate–spinifex texture pairs. However, massive unstructured ultramafic units could represent flows in which these features failed to form, were removed by erosion or texturally destroyed by metamorphism (Arndt et al., 1977; Thomson, 1989a,b). Measurements of flow thicknesses in ultramafic sequences are, therefore, biased towards successions in which diagnostic textures are well preserved (e.g. parts of the Siberia Komatiite). Within the Siberia Komatiite, sedimentary rocks and breccia are only locally present, flow tops are unaltered: it is asumed, therefore, that lava was rapidly erupted onto a flat surface. Parts of the core lack spinifex texture and flow-top breccia (i.e. A zones). This could indicate either thermal erosion by successive flows (Huppert et al., 1984; Huppert and Sparks, 1985; Barnes et al., 1988) or their non-development (Thomson, 1989a,b). Thin (less than 1 m thick) flow units frequently comprise only a cumulate base and a flow-top breccia (i.e. B–A_1) Flows range from 0.8 to about 6 m thick. As B-only units are thicker than B + A units, it is likely that the core cuts different parts of the flow succession. If this is not the case, then substantial surface relief would be required, producing flows of highly variable thickness. This is inconsistent with other arguments featured above.

Recently published studies on komatiite volcanology at Kambalda (Thomson, 1989a,b) included documentation of approximately 150 flows in a 220–270 m downhole thickness in the lower one-third of the Tripod Hill Komatiite at Hunt shoot, southwest of Kambalda Dome. The Silver Lake Peridotite contained two or three, 10–100 m thick, peridotitic flows separated by cherty sedimentary rocks. Four categories and nine subcategories of komatiite flow, broadly based on the ratio of spinifex texture to cumulate and the closeness of packing of the cumulate zone, were recognized. Thomson (1989a,b) maintained that spinifex texture and closely packed cumulate implied ponding of lava (developed at flow centres), whereas 'immature' profiles involving a high ratio of cumulate to spinifex and loose packing of the cumulate represented moving lava characteristic of flow margins.

In one area Thomson (1989a) recognized 38–43 flows, ranging from 0.06–12.48 m (average 1.67 m), in an 80 m downhole interval. He also recognized three stratigraphic zones, comprising a lower zone (flows with little or no spinifex), a central zone (thick spinifex and close-packed cumulates) and an upper zone, largely devoid of spinifex (i.e. 'immature' units). The sequence was traceable along strike for approximately 500 m, although (significantly) 'correlation of individual flow profiles on section (across strike) is difficult, even between adjacent drillholes' (Thomson, 1989a, p. 258). Identification of flow *packages* was more appropriate rather than separation into individual flow *units*. Lack of sedimentary rocks implies rapid deposition, whereas the lack of breccia units indicates lava accumulation some distance from a vent.

Upper basaltic part of the komatiite

The upper basaltic part of the komatiite is well developed in drillcore examined from the Ora Banda Domain. The Big Dick Basalt shows limited gradation between pillowed and massive flows and suggests that both are derived from separate magma pulses. The narrow range of widths of pillow intersections and the preserved curvature of pillow margins suggest that pillows are equant and, therefore, not erupted on a sloping surface; an observation supported by the lack of significant pillow breccia. Rapid eruption is indicated by the scarcity of interflow sedimentary rocks. As varioles are more common in smaller pillows, either the formation of varioles or the expulsion of an immiscible liquid fraction is related to pillow size. Vesicular lava is sporadically distributed throughout the flow pile, consistent with variable volatile content of magma rather than eruption of lava at variable water depths.

The upper basaltic part of the komatiite unit at Harper Lagoon (Boorara Domain) consists of variolitic and vesicular pillow lava and pillow breccia, but lacks the mass-flow breccia of the Kambalda Domain. The vesicularity of all deposits could either indicate uniformly vesicular lava or more eruption of lava in shallower water compared with the Kambalda and Ora Banda Domains.

Upper basalt unit

Despite a similar magma type, there are notable differences in volcanic facies between the two drillholes logged in the upper basalt unit at Kalgoorlie. In both holes, pillow lava constitutes a large proportion of the core, and indicates that the lava was moving slowly. Mass-flow breccia units are common, consistent with relief at the site of eruption. Their distribution in drillcore indicates several adjacent vents.

Pillow lava is also common in the upper basalt unit at Bluebush–Republican, although compared with Kalgoorlie, there are more interflow sediments and a higher proportion of mass-flow breccias; this implies a slower rate of eruption and more topographic relief.

Volcanological characteristics of the upper basalt unit in the Ora Banda Domain differ markedly from those in the Kambalda Domain: the unit in the Ora Banda Domain has a higher proportion of massive flows and a smaller amount of mass-flow breccia than the unit in the Kambalda Domain. There is little size gradation in pillowed units of the Bent Tree Basalt indicating that pillow lava is not gradational to massive flows but represents discrete eruption events. In contrast, pillowed units in the Victorious Basalt show a size gradation consistent with pillow to megapillow to massive flow transition. This gradation from pillowed to massive lava, plus the fact that pillow breccia is common, argues for eruption of a more viscous lava in an area of detectable submarine relief. The lithologic similarity of intrusions and pillow lava suggests the former are cogenetic, high-level feeders to flows.

Harrison (1984) examined 62 diamond drillhole logs from the upper basalt unit in the Gimlet South area, and suggested that the top 500 m of the Bent Tree Basalt could be divided into six alternating pillowed and massive formations. Gabbro units ranged from 1–40 m thick and, although some could be weakly transgressive, they were interpreted as flows that cooled slowly. He noted that the

paucity of breccias and vesicles supported eruption on a flat surface at depths of less than 2000 m. From isopachs of pillow pinchouts, supported by the form of a lens-shaped gabbro in a massive unit, Harrison(1984) deduced an easterly to southeasterly flow direction. He maintained that there was no gradation from massive to megapillowed to pillowed units (i.e. centre to margin of flow), consistent with interpretation of pillow intersection data discussed here. Instead, he stated that pillowed and massive flows represented slow and fast moving or, alternatively, thin and thicker flows.

Norseman Terrane

Massive lava accounted for between 17 and 62% of basalt logged in diamond drillcore from the Woolyeenyer Formation of the Norseman Terrane, the remainder being pillow lava. Flow units range from 1 to 8 m thick and are usually thinner than those recorded from the Kalgoorlie Terrane. Flow-top breccias range from 13 to 20 cm thick. Individual pillows are 20–80 cm thick, and their curvatures in drillcore suggests they were erupted on a flat surface. Variations in the widths of pillow intersections seems to decrease in proportion to decreasing stratigraphic depth. This implies a less gradual transition from pillowed to massive flows in the latter stages of volcanism, and may indicate that younger flows are thinner and wider. Throughout the succession, inter-pillow material is uncommon, the lava is usually non-vesicular and there is a strong association of varioles with pillow lava. These characteristics are similar to those of the lower basalt unit at Kambalda and indicate the eruption of uniform, low-viscosity magma with a low content of volatiles.

The well-exposed sequence of basaltic eruptives on the western margin of Lake Cowan offers some three-dimensional control and the opportunity to test drillcore interpretation. The association of massive and pillowed lava and fine-grained, water-laid sedimentary units argues for subaqueous eruption. Flow packages either pinch and swell or change character (pillowed to massive) over intervals of 10 to more than 100 m. Flow packages are of the order of 80 x 400 m, as individual flow units logged in drillcore are considerably thinner.

The gradation from pillowed to massive lava (with gradually increasing pillow size) is consistent with, rather than having been formed by, separate magma pulses. Massive flows represent the faster moving, thicker central part of a flow, and pillow lava the slower moving margins.

Individual pillows display delicate re-entrants and draping, a feature that indicates a fluid, low-viscosity lava. Eruption was sufficiently rapid to preclude sedimentation. The equant pillow dimensions and the lack of breccia suggest a lack of submarine topography. Rare three-dimensional exposures show that pillow-form lava was erupted as elongate mattresses as well as pillows. In two-dimensional outcrops, there is a wide range in pillow-form sizes indicating some pillows have budded off from mattresses.

The intimate association of, locally, vesicular and the more common non-vesicular massive and pillowed lava suggests variable volatility of magma rather than variable depth of eruption (cf. Jones, 1969; Gill et al., 1990). Gas-streamed vesicles in one massive lava indicate either a northerly or southerly flow. Vesicles in pillow lava are usually arranged concentric to the pillow edge, near or on the rim, parallel to the cooling front. Pipe vesicles, which overprint varioles, were formed by gas streaming towards the pillow margin; they indicate that varioles formed prior to degassing of the magma. Variolitic and non-variolitic pillows can occur in the same outcrop, but the varioles are usually restricted to smaller pillows: this suggests that larger lava bodies managed to re-equilibrate the immiscible component.

Regional aspects of physical volcanology

Direction of lava flow

Harrison's (1984) work on the upper basalt unit at Ora Banda suggested an east-southeast flow direction. Thomson's (1985) observations on the distribution of nickel ore at Hunt shoot, Kambalda, and the continual deposition of sulfides (i.e. thinner sulfides and decreasing grade towards the southeast), required a paleotopographic reconstruction resulting in lava flow from the north-northwest. However, new drilling has cast some doubt on this (J. M. F. Clout, pers. comm., 1991). A north to south polarity in flow direction is also indicated by vesicle alignment in a massive lava unit at Lake Cowan (Norseman Terrane).

Rate of eruption

Any estimates of eruption rates must be considered in the light of interpreted stacking of greenstone sequences (Swager and Griffin, 1990). Published SHRIMP ages (Table 2) for interflow sedimentary rock on the Lunnon Basalt–Kambalda Komatiite contact (2698–2706 Ma) and the Kapai Slate (2688–2696) give an age range of 2–18 Ma for eruption of the Kambalda Komatiite. Taking a maximum thickness of 1 km for this unit, the eruption rate ranges from 55 to 500 m/million years (m.y.). This result is of little value due to the highly variable thickness of the unit, and the wide range in estimated duration of eruption. There is an obvious need for more SHRIMP data on stratigraphically controlled interflow sedimentary rocks. Furthermore, as the extent of units cannot be accurately gauged, volume–time relationships cannot be estimated. An idea of likely komatiite eruption rates and volumes has been given by Hill et al. (1988), who estimated a rate of 1 km^3/day and volumes of 100 km^3 for komatiites, using data of Huppert and Sparks (1985). Published accounts of eruption rates for Archaean and post-Archaean volcanic successions give some idea of eruption rates, volumes, and flow dimensions. The Hill et al. (1988) rate for komatiites is far in excess of eruption rates estimated for various flood basalt provinces by Yoder (1988, table 1, p. 141), which range from 0.006 to 0.024 km^3/a.

Richards et al. (1989) reviewed $^{40}Ar/^{39}Ar$ dating for the 2000 m thick Western Ghats (Deccan Traps), showing

that volcanism occurred over a period of less than 2 m.y. Considering all data, they estimated Deccan Trap volcanism could have occurred over a mere 0.5 m.y.

Qualitatively, the lack of interflow sedimentary rocks throughout the flow sequence and the lack of alteration of flow-tops argues for consistently rapid outpourings of both mafic and ultramafic lava. Indeed, SHRIMP ages dating eruption, and U–Pb and Ar–Ar ages for metamorphism show that the whole eruption–metamorphism–deformation episode occurred within a span of 130 m.y..

Site of eruption

The intimate association of pillow lava and water-laid sediments argues for submarine eruption. Although vesicularity is not necessarily a reliable indicator of depth, for example Gill et al. (1990), deep-water eruption is supported by the low vesicularity of lava and the fine-grained nature of sedimentary units.

Part 3

Geochemistry

Introduction

Regional geochemical comparisons for mafic and ultramafic volcanic rocks in the Norseman–Menzies area are difficult for several reasons. Published studies have either dealt with specific areas or problems (e.g. petrogenesis of ultramafic volcanics and hangingwall basalts at Kambalda: Arndt and Jenner, 1986; Chauvel et al., 1985; Dupré and Arndt, 1990), consisted of regional surveys using data summaries (e.g. Redman and Keays, 1985; Barley, 1986; Hallberg, 1972), utilized incomplete data (e.g. Roddick (1984), provided major-element data but few trace-element data, lacked stratigraphic control in sampling, or suffered from interlaboratory variations in data quality. This study attempts to rectify the situation by providing a regional geochemical picture of mafic and ultramafic volcanic rocks in the Norseman–Menzies area based on the stratigraphic framework of Swager et al. (1990).

Three hundred and seventy-six XRF major- and trace-element analyses, supplemented by published and unpublished data where necessary, were made. Although the geochemistry of some units has been discussed elsewhere (e.g. Kambalda: Arndt and Jenner, 1986), these units have been analysed in this study to avoid inter-laboratory variation. This discussion of geochemistry aims to determine: if stratigraphically equivalent units in the Kalgoorlie Terrane have similar geochemistry; if there is any geochemical similarity between similar rock types of the Kalgoorlie Terrane and other terranes; and what these data can tell about tectonic setting and petrogenesis.

Analytical strategy

XRF major-element oxide and trace-element analyses and thirty-seven rare-earth element (REE) analyses were presented in Morris et al. (1991), which also discussed sample preparation, analytical techniques, precision, and accuracy. Unpublished data from the Ora Banda Domain were provided by W. K. Witt. Two samples have been analysed for additional trace elements by instrumental neutron activation analysis (INAA) at Becquerel Laboratories (Sydney), and Nd isotope analyses of samples from the Norseman Terrane were made by Hiroo Kagami at the Institute for Study of the Earth's Interior (Misasa, Japan). These data are presented in this report.

Sample selection and element mobility

Element redistribution is a strong possibility for Archaean rocks that have undergone several phases of deformation, greenschist–amphibolite facies metamorphism and, in some cases, metasomatism and surface weathering. In order to minimize surface effects and offer stratigraphic control, most samples have been taken from diamond drillcore, avoiding variolitic units, or those adjacent to felsic intrusions and shear zones.

The degree of textural alteration is taken as a guide to element mobility. Remnant igneous textures in basalts suggest limited element remobilization or mobilization on hand-specimen scale, although more extreme textural modification in ultramafic volcanic rocks (coupled with serpentinization and/or carbonation) implies a greater likelihood of element redistribution.

Published accounts of Archaean geochemistry have examined the mobility of various elements. Redman and Keays (1985) and Hallberg (1972) have argued that consistency in certain element ratios argues for little element remobilization. Redman and Keays (1985) suggested that Sc, Cr, Co, Ni, Zr, and Ti, were largely immobile, that Y and V behaved more erratically, and that Rb, Sr, Cu, and S were mobile. Arndt and Jenner (1986) used coherent geochemical behaviour to suggest that Ti, Al, Fe (total), Zr, V, Ni, Cr, and REE, were immobile, that Si, Ca, Na, K, Rb, Sr, and Ba, were mobile, and that P, Nb, Y, and Sc, were equivocal. Studies of post-Archaean volcanic rocks have cast doubt on the stability of the alkaline-earth elements (e.g. Arculus, 1987), and element coherency has been attributed to coherent mobility as well as immobility. Na, K, Si, Mg, Rb, Sr, Ba, and H_2O are considered mobile (Coish 1977; Seyfried et al., 1978), whereas the high field strength (HFS) elements such as Ti, P, Zr, Y, Cr, and Ni, are more likely to remain unchanged (Saunders et al., 1980; Wood et al., 1976; Pearce, 1982). There is some conflict as to the mobility of the rare-earth elements (REE), as discussed by Hellman et al. (1979) and Bartley (1986).

As a test of likely element mobility, tholeiitic basalts of the Woolyeenyer Formation (Norseman Terrane) analysed in this study are plotted in terms of Ti/Zr (both presumed to be immobile). Igneous textures in this suite are partly preserved, and rocks show little alteration. Both plots should show some degree of coherency if all three

elements are immobile. This plot shows strong coherency of these immobile elements (Fig. 8A). These data are also shown on a MORB (i.e. mid-ocean ridge basalt) normalized spidergram (Fig. 8B), which also demonstrates the consistency of Ti and Zr, along with Y. However, there is considerable spread for other elements (e.g. Rb, Ba, K), which is attributed to immobility. The range in some other elements (e.g. Ce) is due to the fact that concentrations of these elements approach the detection level. Thus, little emphasis is placed on Rb, Ba, K, and Na although they are reported for completeness in Morris et al. (1991). This mobility is unfortunate, as alkaline-earth abundances are useful in identifying magma types, magmatic processes, and tectonic setting (Pearce, 1983; Thompson et al., 1983; Arculus, 1987).

Petrogenetic processes affecting immobile elements

Emphasis is placed on immobile elements which can be accurately and precisely measured by the analytical technique employed: these include Ti, Zr, Y, V, Sc, and, to a lesser extent, Al, Si, and La. Of these elements, Zr, Ti, and La have mineral/melt distribution coefficients (Kd) less than 1 (Table 4) for mantle minerals (olivine, pyroxene, garnet, spinel) or minerals involved in low-pressure fractional crystallization (olivine, pyroxene, plagioclase). Therefore, element concentrations are controlled by either the degree of melting in the mantle and/or the amount of fractional crystallization. More importantly, the ratio of any two elements (e.g. Ti/Zr) is independent of the degree of melting or fractionation and is the same as that of the source from which the melt was derived. To this group of three elements can be added Y if the degree of melting is sufficiently large that garnet is not retained in the mantle source.

Some elements are sensitive to the presence of one mineral phase: for example, the bulk distribution coefficient (D = (mineral proportion x mineral/melt distribution coefficient)) for Sc during low-pressure fractionation is strongly affected by clinopyroxene, so Sc variations would be useful in identifying clinopyroxene vs olivine fractionation. Other elements are relatively insensitive to low-pressure fractionation, in that Kds are greater than 1 for a variety of minerals (e.g. Cr, Ni).

Melt ratios of immobile and incompatible elements such as Ti/Zr and Zr/Y may not directly reflect those of the mantle source if the source is inhomogeneous (metasomatized) or the melt has been contaminated by other melts or crustal material. Assimilation of crust, either during magma rise or flow on the surface, is especially important for komatiites which have estimated eruption temperatures of about 1600°C (Huppert et al., 1984). Metasomatic fluids are enriched in volatiles, LREE, and alkaline-earth elements (Rb, Sr, Ba, Na, K), Zr, Th (Perfit, 1990; Tatsumi et al., 1986), many of which cannot be accurately determined by XRF, are mobile, or also occur in significant proportions in likely contaminants (Pearce, 1983). Radiogenic isotopes such as $^{143}Nd/^{144}Nd$ help in sorting out the relative contributions of source, metasomatism, contamination and fractionation, but many interpretations are inconclusive because of the large number of variables involved.

Classification and nomenclature

Reference should be made to Jensen and Langford (1986) and Basaltic Volcanism Study Project (1981; table 1.2.1.1) for a review of various nomenclatural schemes. Classification and nomenclature based on whole-rock chemistry must use elements that can be accurately determined by the analytical method employed, are minimally affected by post-magmatic redistribution, and categorize the rocks examined both in terms of broad groupings (e.g. komatiite vs tholeiite) and subdivision of individual groups The Jensen Cation Diagram (e.g. Appendix 3.1) satisfies these criteria, and is an approach favoured by Donaldson (1982) and Grunsky et al. (1990). The division of komatiites and tholeiites on this diagram corresponds to approximately 11 wt% (anhydrous) MgO, whereas the ultramafic–basaltic komatiite boundary corresponds to approximately 20 wt% (anhydrous) MgO (cf. recommended value of 18 wt% (anhydrous) MgO for komatiite proposed by Donaldson, 1982). Basalts are divided into high-Fe tholeiitic basalt (HFTB) or high-Mg tholeiitic basalt (HMTB), and divisions are also made within tholeiitic and calc-alkalic fields. The term 'basaltic komatiite' is used here for rocks with between 11 and 20 wt% (anhydrous) MgO. Analogous terms are 'high-MgO basalt' and 'komatiitic basalt'.

Kalgoorlie Terrane

Lower basalt unit

Kambalda Domain

Kambalda

Apart from studies that have contrasted the upper and lower basalt units for petrogenetic or stratigraphic purposes (e.g. Arndt and Jenner, 1986; Redman and Keays, 1985; Kelly and Donaldson, 1982; Redman, 1982), few studies have examined the lower basalt unit (Lunnon Basalt) in detail, and most have concentrated on the Kambalda Dome. Data presented here extend knowledge of the Lunnon Basalt away from Kambalda southeast to Foster and Tramways (Fig. 3).

Gresham and Loftus-Hills (1981) and Redman and Keays (1985) divided the Lunnon Basalt into a lower, MgO-rich part and upper, less MgO-rich unit. Analyses made in this study show a greater spread than these published data (Appendix 3.1A), extending from the HMTB to the HFTB and calc-alkalic basalt fields. Analyses from low in the Lunnon Basalt (lower part of KD1029) plot in the HMTB field, whereas analyses from the upper part (upper part of KD1029; KD330, CD201, CD259), plot as HFTB and calc-alkalic basalts; this result is consistent with the Gresham and Loftus-Hills (1981) and Redman and Keays (1985) observations.

Chemical variations according to stratigraphic height are shown in Figure 9. Where Zr/Y and Mg* (i.e.

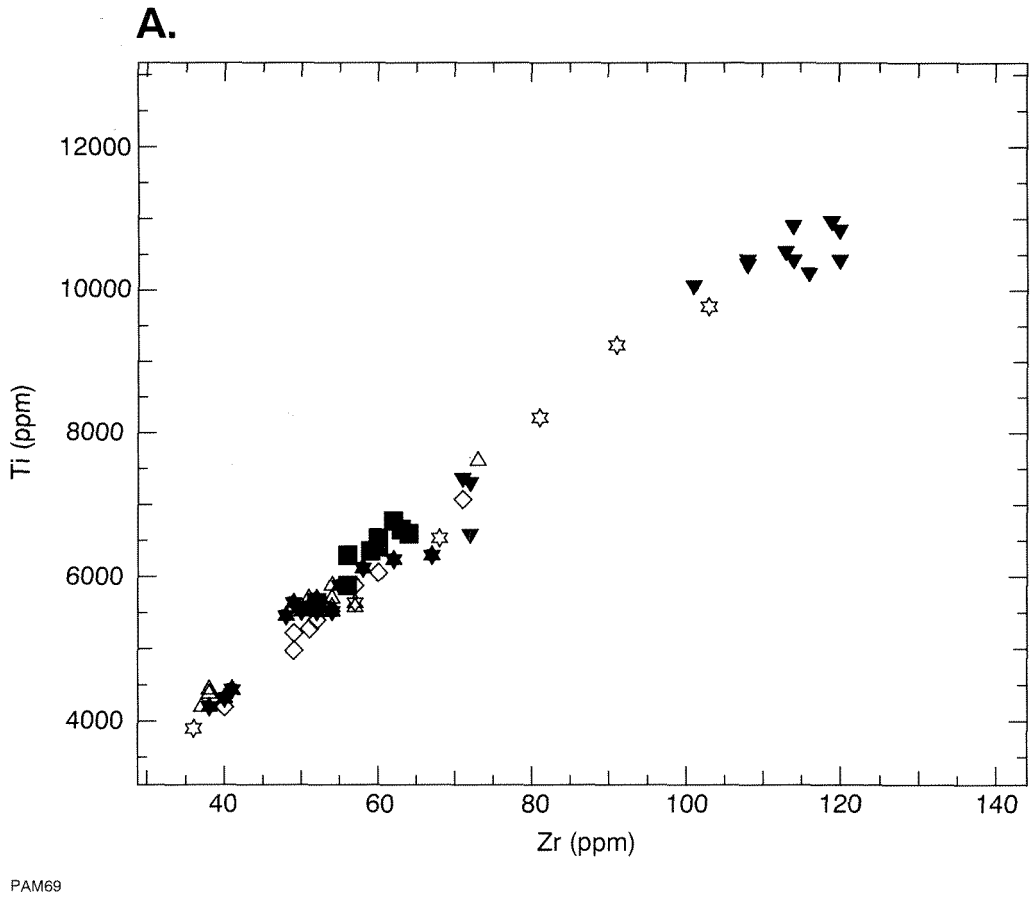

Figure 8A. Ti (ppm) versus Zr (ppm) for samples of drillcore from the Woolyeenyer Formation, Norseman Terrane.

100.MgO/(MgO + FeO)) are constant, there is no antithetic relationship between Mg^* and Zr, and poor agreement between Mg^* and Ni. Redman's (1982) Zr/Y ratios plot at lower values than those of this study; this is interpreted as inter-laboratory variation.

Analyses from the upper Lunnon Basalt form a continuum with the lower Lunnon Basalt to higher Ti and Zr (Appendix 3.2A), in contrast to the clear stratigraphic separation reported by Redman and Keays (1985). Most lower Lunnon Basalt analyses plot close to the chondritic trend (Appendix 3.3A), but analyses from higher in the sequence generally plot as a group at similar Al_2O_3 but higher TiO_2.

Chondrite-normalized REE plots (Appendix 3.4A, B) are flat to slightly LREE-depleted. $(La/Sm)_{CN}$ ranges from 0.8 to 1 (CN = chondrite-normalized, using the normalization values of Nakamura (1974) and Evensen et al. (1978)), and La is about 10x chondrite. One analysis from the lower Lunnon Basalt (99561) is more REE-depleted than upper Lunnon Basalt analyses.

Available Nd isotope data (Chauvel et al., 1985; Claoué-Long et al., 1984; McCulloch and Compston, 1981a, b) are summarized in Appendix 3.5B. All ε_{Nd} show a limited range of between 2 and 4.

Ora Banda Domain

Both the lower (Wongi Basalt) and upper (Missouri Basalt) parts of the lower basalt unit in the Ora Banda Domain have been examined. Samples have been collected from the Ora Banda area and from a stratigraphically equivalent sequence at Ghost Rocks about 20 km northwest of Menzies (Figs 1 and 4).

Analyses of the Wongi Basalt span both tholeiite and basaltic komatiite fields (Appendix 3.1B), whereas Missouri Basalt analyses plot in the HFTB field. Analyses from Ghost Rocks overlap the Ora Banda analyses, apart from gabbro (100134), which plots in the ultramafic komatiite field.

Missouri Basalt analyses plot on an extension of the Lunnon Basalt trend (Appendix 3.2B), whereas Wongi Basalt analyses show a broad spread, generally plotting at lower Ti/Zr. Basaltic andesite 100113 (Wongi Basalt) and vesicular basalt 100109 (Missouri Basalt) plot separately at higher Zr.

The Lunnon Basalt and Missouri Basalt have similar Zr/Y, but samples of the Wongi Basalt have higher Zr/Y, Cr, Ni, and MgO. Basaltic andesite 100113 and vesicular flow 100109 have lowest Cr and highest Zr and are clearly fractionated.

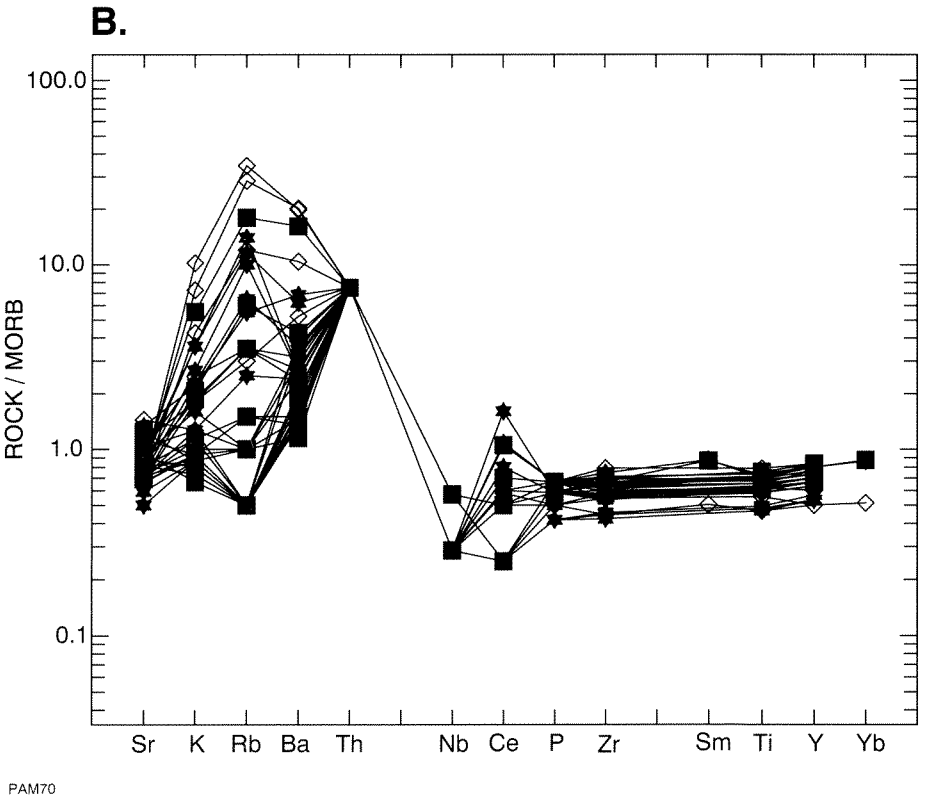

Figure 8B. Mid-ocean-ridge basalt (MORB)-normalized spidergram for representative samples of drillcore from the Woolyeenyer Formation of the Norseman Terrane. Normalizing factors cited in Pearce (1983)

Most Wongi Basalt analyses lie close to a chondritic trend for Al_2O_3/TiO_2 (Appendix 3.3B), whereas Missouri Basalt analyses have a zero slope. All REE are flat (Appendix 3.4C, D), with $(La/Yb)_{CN}$ near 1, but Wongi Basalt analyses from Ora Banda have lower total REE. The two REE analyses from Ghost Rocks have similar REE concentrations. Basaltic andesite 100113 is significantly LREE-enriched (La approximately 60x chondrite).

Coolgardie Domain

Widgiemooltha and Redross

Most lower basalt unit analyses from Widgiemooltha and Redross form a tight cluster in the HMTB field of Appendix 3.1C. Ti and Zr are well correlated (Appendix 3.2C), and similar to the Lunnon Basalt. Analyses from Widgiemooltha cluster on the edge of the Lunnon Basalt field (Appendix 3.3C), whereas Redross analyses plot at higher Al_2O_3. Chondrite-normalized REE patterns (Appendix 3.4F) are flat to slightly LREE-depleted ($(La/Sm)_{CN}$ and $(La/Yb)_{CN}$ about 0.9) and La is approximately 10x chondrite.

Coolgardie

The lower basalt unit at Coolgardie is divided into an upper and lower part by a regionally extensive sedimentary unit (N. Swager, pers. comm., 1989). Analyses from below this unit plot in the Lunnon Basalt field (Appendices 3.1C, 3.2C) with analyses from Widgiemooltha–Redross, whereas analyses from above the unit are tholeiite and basaltic komatiite and generally have lower Ti and Zr than stratigraphically lower samples. These stratigraphically higher samples plot at lower Al_2O_3 and TiO_2 and to the right of the chondritic line (Appendix 3.3C).

The three chondrite-normalized REE patterns are from samples located below the sedimentary unit. They have similar $(La/Yb)_{CN}$ (near 1), and La is between 10x and 13x chondrite (Appendix 3.4E).

Dunnsville

The six samples from the Dunnsville area span the tholeiite and basaltic komatiite fields (Appendix 3.1C). The Ti/Zr trend (Appendix 3.2C) is oblique to that of the Lunnon Basalt, and analyses show a broad spread with a near zero slope in terms of Al_2O_3/TiO_2 (Appendix 3.3C). The one REE analysis (Appendix 3.4F) is flat ($(La/Yb)_{CN}$ = 1.2) with La near 10x chondrite. Specimen 99978 is variolitic and has high La (62ppm).

Boorara Domain

Carnilya Hill

Most samples of Scotia Basalt from diamond drillholes CHD412 and CHD447 at Carnilya Hill cluster in the calc-

Table 4. Mineral/melt distribution coefficients used in this study

	Ol	*Opx*	*Cpx*	*Gar*	*Plag*	*Sp*
Zr [a]	0.01	0.03	0.1	0.3	0.1	[e] 0.07
Y	[b] 0.002	[b] 0.009	[b] 0.2	[b] 1.4	[a] 0.03	[f] <1
Sc [b]	0.25	[b] 1.1	[b] 3.1	[b] 6.5	[c] 0.065	[e] 00.05
Ti [a]	0.02	0.1	0.3	0.3	0.04	[e] 00.15
La [d]	0.0005	0.0005	0.02	0.001	-	0.0006
Cr [e]	2.0	8.0	2.0	-	-	200.0
Ni [e]	11.0	3.5	3.0	-	-	10.0

Source: (a) quoted in Redman and Keays, 1985, p. 134, Table VI; (b) quoted in Frey et al., 1978, p. 512, Table A-2; (c) quoted in Irving, 1978; (d) quoted in Frey et al. 1978, p. 511, Table A-1, set 1; (e) Keleman et al. 1990, p. 522, Table 1; (f) estimated

alkalic basalt and andesite fields (Appendix 3.1D). Ti and Zr (Appendix 3.2D) are highly correlated (r = 0.91), with analyses plotting at higher Ti/Zr and with a flatter slope (67) than the Lunnon Basalt (114).

Analyses are highly correlated for Al_2O_3/TiO_2 (Appendix 3.3D) (slope about 14) on the edge of the Lunnon Basalt field. REE are depleted ($(La/Yb)_{CN}$ near 0.9: Appendix 3.4G, H), with La approximately 10x chondrite. ε_{Nd} ranges from 2 to 5 (Appendix 3.5E).

Bullabulling Domain

The stratigraphic positions of greenstones in the Bullabulling Domain are poorly understood (C. P. Swager, pers. comm., 1991). All the rocks analysed are tholeiite–calc-alkalic basalts (Appendix 3.1C), which lie on a Ti/Zr trend similar to that of samples from Dunnsville (Appendix 3.2C), and are thus on an oblique trend to the Lunnon Basalt. Ti and Zr contents of Bullabulling Domain rocks are higher than those from Dunnsville. Analyses Al_2O_3/TiO_2 plot parallel to the X axis (Appendix 3.3C).

Discussion

All Lunnon Basalt samples of this study have similar Ti/Zr; this is consistent with derivation from a single mantle source. The flat to LRE-depleted REE patterns and limited range in ε_{Nd} (greater than 0) suggest that this source was homogeneous, and depleted in garnet. Element trends in the lower part of the Lunnon Basalt indicate multiple episodes of melting and variable fractionation rather than fractionation of one magma batch. Overall, the lower part of the Lunnon Basalt is less fractionated than the upper part, but there is no clear geochemical separation. As Sc is strongly partitioned into clino-pyroxene relative to Ti and Zr (Table 4), a plot of Ti/Sc vs Zr should be sensitive to clinopyroxene fractionation. The near-zero slope shown by analyses of the lower Lunnon Basalt (Fig. 10) is consistent with olivine fractionation, whereas clino-pyroxene fractionation is shown by higher Ti/Sc at a given Zr for analyses of the upper Lunnon Basalt.

Unpublished SHRIMP ages for sedimentary units within the lower Lunnon Basalt (J. Claoué-Long, pers. comm., 1990) are significantly older than the published age of 2702 ± 4 Ma from the lower basalt–komatiite contact (Claoué-Long et al., 1988). Thus, although a uniform mantle source is likely for the Lunnon Basalt, the lower and upper parts may not be genetically related.

The lower basalt unit of the Ora Banda Domain comprises two distinct units. The Ti/Zr trend obtained from the Wongi Basalt, which contains both basaltic komatiite and tholeiite, is oblique to that of the overlying Missouri Basalt, which follows the trend of the Lunnon Basalt, but is more fractionated. REE patterns for the Wongi Basalt show that some samples with high MgO also have high LREE. Small negative Eu anomalies in the Missouri Basalt are consistent with some plagioclase fractionation.

The composition of the lower basalt unit at Widgiemooltha and Redross resembles that of the lower basalt unit of the Kambalda Domain, as it does the composition of the lower basalt unit from below the sedimentary marker horizon at Coolgardie. However, samples from the lower basalt unit from above the sedimentary marker horizon at Coolgardie are compositionally more varied and encompass both tholeiite and basaltic komatiite. Basalt analysed from Dunnsville (Coolgardie Domain), and the Bullabulling Domain have similar Ti/Zr and Al_2O_3/TiO_2 trends, and may be cogenetic. The Ti/Zr trend is oblique to that of the Lunnon Basalt and implies a different magma lineage.

Most analyses of the lower basalt unit in the Boorara Domain plot in the calc-alkaline field and are quite separate from analyses of other lower basalt units. Both Ti and Zr and Al_2O_3 and TiO_2 are well correlated, but the Ti/Zr and Al_2O_3/TiO_2 slopes are lower (65 and 14) than in the case of the Lunnon Basalt at Kambalda (114 and 20).

Komatiite unit

Kambalda Domain

Kambalda and Kalgoorlie

Samples from the Kambalda Komatiite and the Hannans Lake Serpentinite are shown in Appendix 3.6A;

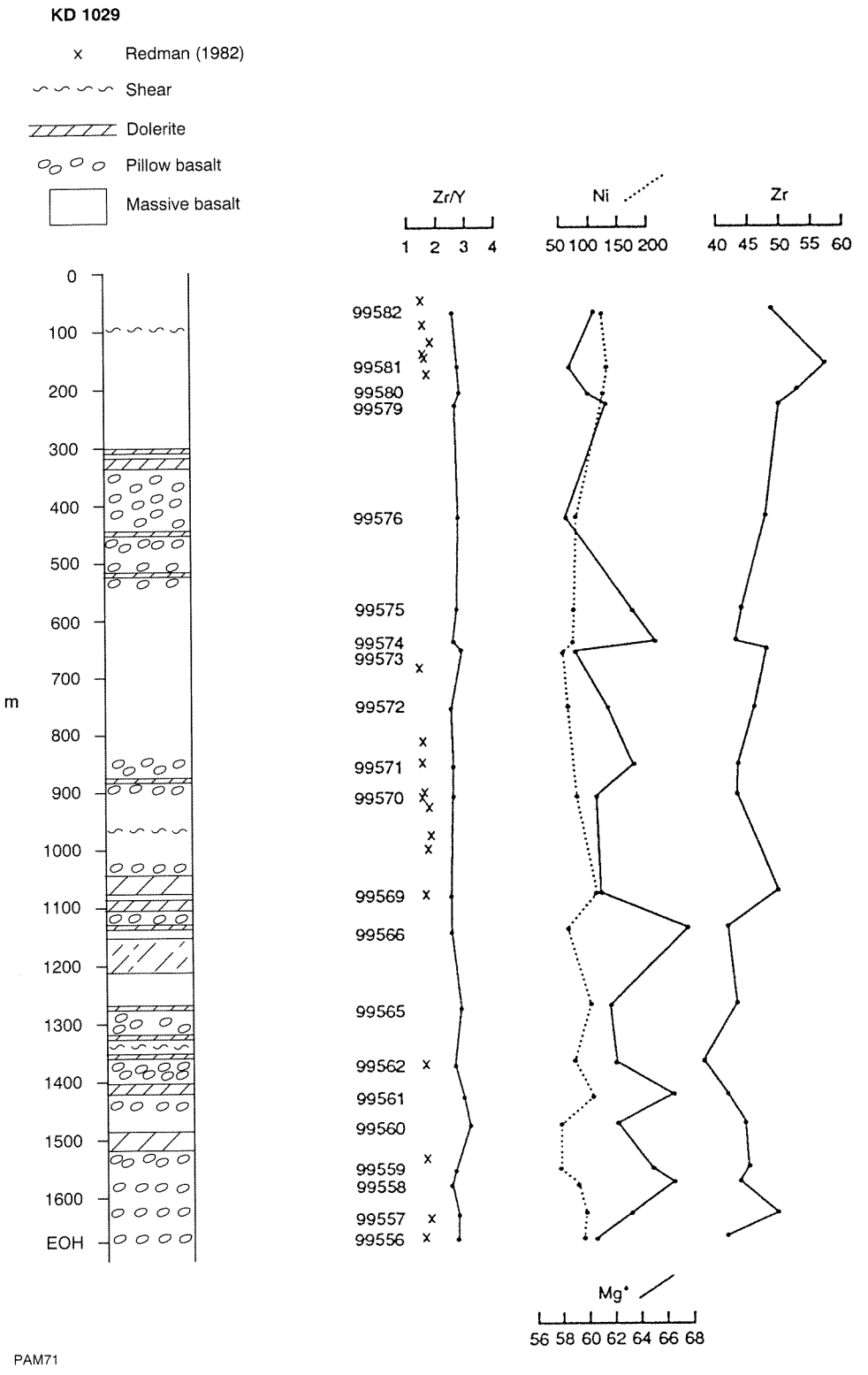

Figure 9. **Compositional variations according to stratigraphic height in the lower basalt unit in diamond drillhole KD1029 (Kambalda). Location of samples shown by closed circle and relevant GSWA number (e.g. 99579). Also shown as crosses are Zr:Y ratios from this drillcore from Redman (1982). See text for discussion. Units — Zr, Ni (ppm). Mg* is MgO/(MgO + (FeO + Fe_2O_3))**

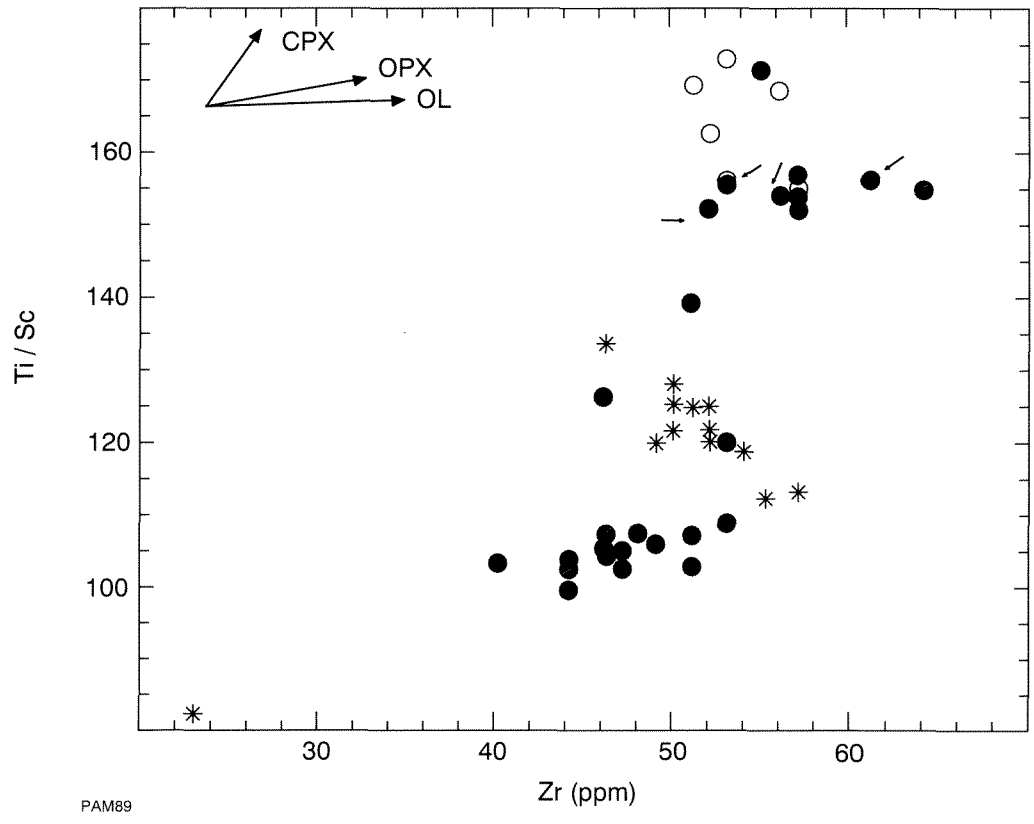

Figure 10. ***Ti:Sc versus Zr (ppm) for lower basalt unit samples from Kambalda, Foster, and Tramways.*** **Arrowed analyses are from stratigraphically higher parts KD1029. Fractionation vectors for clinopyroxene (cpx), orthopyroxene (opx), and olivine (ol) are shown, calculated using distribution coefficients of Table 4. Symbols: closed circles — KD1029, KD330 (Kambalda); asterisk — Tramways; open circle — Foster**

the latter cluster in the middle of the Kambalda Komatiite range. Most of these ultramafic volcanic rocks have CaO/Al_2O_3 less than 1 (Fig. 11), and although CaO loss during alteration could account for lowering of ratios, this is unlikely as CaO/Al_2O_3 is poorly correlated with volatile content.

Kambalda Komatiite and Hannans Lake Serpentinite analyses are well correlated for Ti/Zr (r = 0.84; slope = 65; Appendix 3.7A) and group slightly above a chondritic slope of 20 for Al_2O_3/TiO_2 (Appendix 3.8A).

REE analyses of komatiites from Kambalda (Arndt and Jenner, 1986) are LREE depleted ($(La/Sm)_{CN}$ 0.6–1) with La 1.5–2.5x chondrite (Appendix 3.9). Published Nd isotope data (Appendix 3.5D) show a wide range in ε_{Nd}, from -2 to +8.

Bluebush–Republican

Ultramafic rocks analysed in this study occur both within and below the upper basalt unit. It is unclear whether this is due to tectonic interleaving or to comagmatism of mafic and ultramafic volcanic rocks.

Samples span both basaltic and ultramafic komatiite units (Appendix 3.6B). CaO/Al_2O_3 decreases with increasing MgO (Fig. 11), but CaO/Al_2O_3 values are greater than 1 in contrast to less than 1 for the komatiite unit at Kambalda. Bluebush–Republican analyses plot with those from the Hannans Lake Serpentinite and Kambalda Komatiite in terms of Ti/Zr (Appendix 3.7B) and Al_2O_3/TiO_2 (Appendix 3.8B).

Ora Banda Domain

The single analysis of the Walter Williams Formation plots as ultramafic komatiite, whereas most of the thirteen Siberia Komatiite analyses are basaltic komatiite (Appendix 3.6E). Samples of both the Kambalda Komatiite and Siberia Komatiite lie on parallel Ti/Zr trends (65 and 58 respectively). The analyses of the Siberia Komatiite plot at higher Ti than those of the Kambalda Komatiite, and a few analyses lie in the Lunnon Basalt field (Appendix 3.7C). Analyses lie on the low Al_2O_3 side of the chondritic ratio (Appendix 3.8C).

CaO/Al_2O_3 for the Siberia Komatiite is consistently near 1 (Fig. 11), whereas CaO/Al_2O_3 for the sole analysis of the Walter Williams Formation is less than 1, and resembles those of the Kambalda Komatiite.

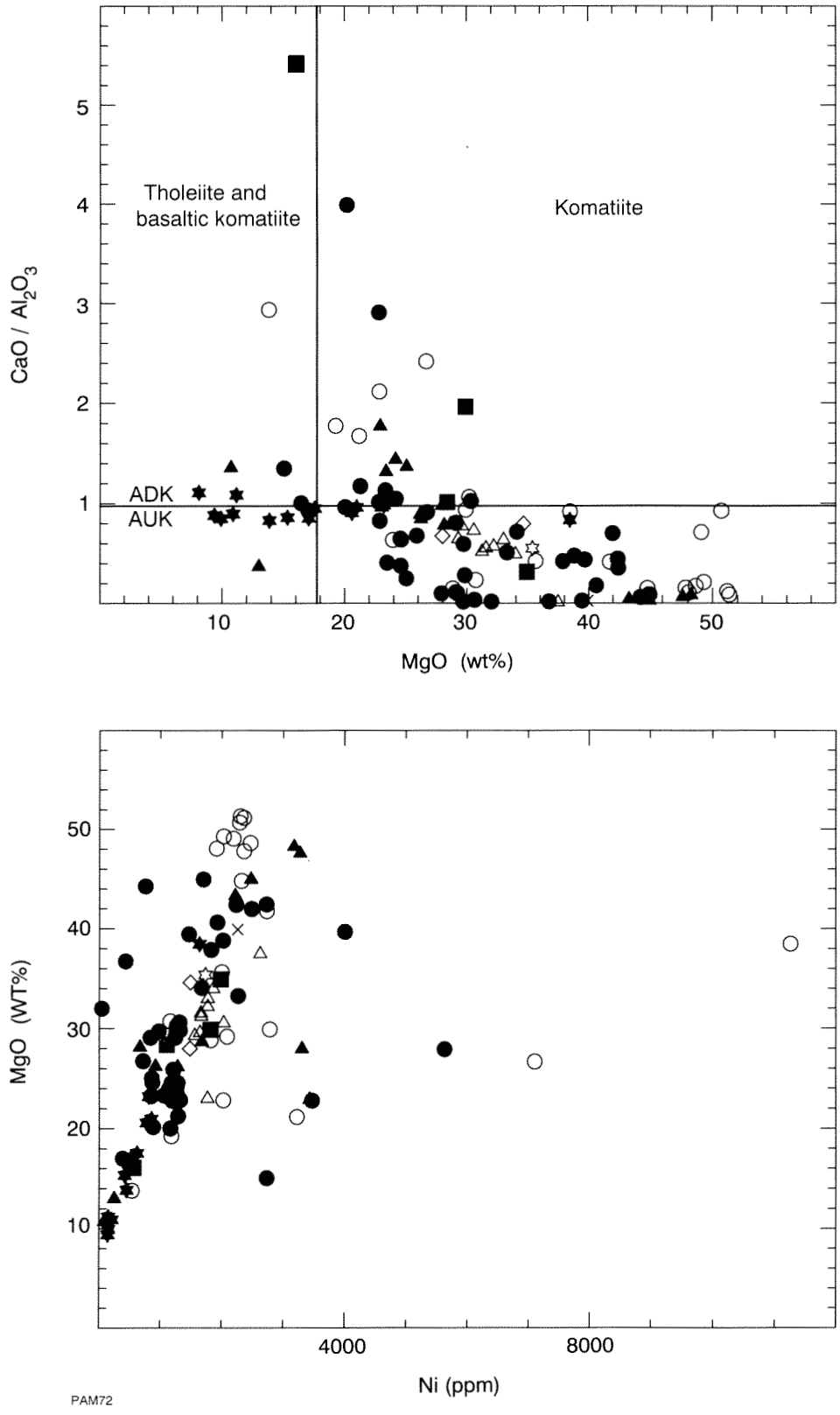

Figure 11 (Top). **$CaO:Al_2O_3$ versus MgO (wt% anhydrous) for all komatiite unit samples. Line at $CaO:Al_2O_3$ = 1 separates aluminium undepleted komatiite (AUK) and aluminium depleted komatiite (ADK); see text for discussion. Line at MgO = 18 separates komatiites from basaltic komatiites and tholeiites. Symbols. Kambalda Domain: closed circles — Kambalda; open circles — Bluebush–Republican; open triangles — Kalgoorlie. Coolgardie Domain: open diamonds — Coolgardie. Ora Banda Domain: cross — Walter Williams Formation; closed star — Siberia Komatiite. Boorara Domain: closed square — Carnilya Hill; open star — Harper Lagoon**

Figure 12. **MgO (wt% anhydrous) versus Ni (ppm) for samples of the komatiite unit. Symbols as on Figure 11**

Boorara Domain

The four samples of the Highway Ultramafics from Carnilya Hill and one sample from Harper Lagoon plot in or close to the ultramafic komatiite field (Appendix 3.6D). CaO/Al_2O_3, Ti/Zr and Al_2O_3/TiO_2 are similar to those of the Kambalda Komatiite (Fig. 11; Appendices 3.7E, 3.8E), but two Carnilya Hill samples have CaO/Al_2O_3 greater than 1. ε_{Nd} is 7 for the komatiite unit at Harper Lagoon (Appendix 3.5E).

Discussion

Ultramafic volcanic rocks of the Hannans Lake Serpentinite and Kambalda Komatiite exhibit overlapping chemical trends, with Ti/Zr near 65 and CaO/Al_2O_3 less than 1 (i.e. Al-undepleted komatiites of Nesbitt et al., 1979). Al_2O_3/TiO_2 is close to the chondritic ratio (20). ε_{Nd} shows wide range (-2 to +8): this is consistent with Dupré and Arndt's (1990) and Arndt and Jochum's (1990) observations that many komatiites have probably been contaminated, either during their rise to the surface, or through incorporating other lithologies following extrusion.

Ti/Zr and Al_2O_3/TiO_2 of komatiite unit samples from Bluebush–Republican resemble those of the Kambalda Komatiite and Hannans Lake Serpentinite, but have higher CaO/Al_2O_3. For the Kambalda Komatiite and Hannans Lake Serpentinite, MgO increases at approximately the same rate as Ni; this indicates some olivine control (Fig. 12).

Al_2O_3/TiO_2 is lower and CaO/Al_2O_3 higher for the Siberia Komatiite (Ora Banda Domain) than the Kambalda Komatiite, yet both have similar Ti/Zr trends. One interpretation is that the source for the Siberia Komatiite is depleted in Al, possibly through removal of garnet prior to melting. The higher Ti and Zr of the Siberia Komatiite is consistent with fractionation, supported by the agreement of MgO and Ni (Fig. 12). Hill et al. (1988) maintained that the Walter Williams Formation underlying the Siberia Komatiite resulted from accumulation of olivine from voluminous komatiite lava flows. It is possible that the Siberia Komatiite crystallized from the residual liquid.

Ti/Zr, CaO/Al_2O_3 and Al_2O_3/TiO_2 of Widgiemooltha and Redross ultramafic volcanic rocks are similar to those of the Kambalda Komatiite. Compared with the Kambalda Komatiite, Al_2O_3/TiO_2 of komatiites in the Burbanks Formation at Coolgardie are lower and similar to the Siberia Komatiite, but analyses from Dunnsville plot above the chondritic ratio. Ti/Zr for Dunnsville and Coolgardie analyses (Appendix 3.7D) are similar to those from Widgiemooltha and Redross.

The Highway Ultramafics and the ultramafic unit from Harper Lagoon show a similar chemistry to the Kambalda Komatiite. MgO/Ni relationships (Fig. 12) indicate some olivine control.

Upper basaltic part of the komatiite unit

The basalt unit at the top of the ultramafic (Table 1) is only well developed in the Kambalda and Ora Banda Domains, where it is separated from the overlying upper basalt unit by regionally extensive sedimentary units: the Kapai Slate in the Kambalda Domain, and an unnamed unit in the Ora Banda Domain. It forms a thin unit above the komatiite unit at Harper Lagoon in the Boorara Domain.

Kambalda Domain

Analyses of the Devon Consols Basalt plot as tholeiite and calc-alkalic basalt (Appendix 3.10A), although analyses from Arndt and Jenner (1986) extend the range into the basaltic komatiite field. This discrepancy is attributed to the exclusion of variolitic samples in this study, which Arndt and Jenner (1986) noted had high-MgO affinities. In terms of Ti/Zr, both Arndt and Jenner's (1986) analyses and data of this study are well correlated, plotting above analyses from the lower basalt unit at Kambalda, and below the envelope of the upper basalt unit (Appendix 3.11A). Analyses plot at higher Al_2O_3/TiO_2 (slope = 19) — cf. Lunnon Basalt (Appendix 3.12A).

REE analyses from Arndt and Jenner (1986) are divided into types A and B (Appendix 3.13A), the former having higher SiO_2 and lower MgO and FeO. Both show similar LREE/HREE enrichment ($(La/Yb)_{CN}$ 1.3–1.4) and La about 12x chondrite.

Ora Banda Domain

Samples of the Big Dick Basalt samples plot in the basaltic komatiite field (Appendix 3.10A), and the trends for Ti/Zr and Al_2O_3/TiO_2 are similar to those of the Devon Consols Basalt (Appendices 3.11A and 3.12A).

Boorara Domain

The one available analysis plots in the basaltic komatiite field (Appendix 3.10A), but resembles the analyses of the Bent Tree Basalt and the Victorious Basalt in terms of Ti/Zr (Appendix 3.11D). In terms of Al_2O_3/TiO_2 the sample plots well to the right of the chondritic line (Appendix 3.12A). Despite the high MgO, Cr, and Ni, the sample is LREE-enriched, La is roughly 30x chondrite, and $(La/Yb)_{CN}$ about 2.5 (Appendix 3.13C).

Discussion

In terms of incompatible element ratios, the basaltic upper part of the komatiite unit lies on oblique trends to the lower basalt unit, which indicates the two units are not genetically related. Ti/Zr is similar for the Siberia Komatiite and the Bent Tree Basalt (Ora Banda Domain), and they may be genetically related.

The one sample analysed from Harper Lagoon is a LREE-enriched basaltic komatiite whose Ti/Zr is similar

to that of other samples from the basaltic upper part of the komatiite unit, yet has high Al_2O_3 relative to TiO_2.

Upper basalt unit

Kambalda Domain

Kalgoorlie and Kambalda

The upper basalt unit at Kambalda and Kalgoorlie (Paringa Basalt) comprises basalts and dolerites (Table 1), which span the tholeiite and basaltic komatiite fields (Appendix 3.10B). Analyses of the upper basalt unit plot below the Lunnon Basalt field and show only a weak overlap with the Devon Consols Basalt field for Ti/Zr (Appendix 3.11B); the slope is 65 (r = 0.98; excluding 99531 and 99534; Kambalda only).

Of the four analyses which plot away from the chondritic Al_2O_3/TiO_2 trend (Appendix 3.12B), three are basalts, with variable TiO_2 for the same Al_2O_3 and relatively low MgO, Cr, and Ni. The remaining sample is from the Defiance Dolerite.

REE plots of upper basalt unit samples (Appendix 3.13B) from Arndt and Jenner (1986) all show LREE enrichment, with increasing degree of enrichment in some cases being accompanied by decreasing MgO and Ni, but two samples have greater than 15 wt% MgO and are LREE enriched. ε_{Nd} shows a wide spread from +4 to -3 (Appendix 3.5C).

Bluebush–Republican

Twelve analyses of the upper basalt unit at Bluebush–Republican are tholeiites (Appendix 3.10C), but form two groups based on their Zr content (Appendix 3.11C). One group of five analyses (99681, 99682, 99683, 99699, 99998) plot with upper basalt unit analyses from Kambalda and Kalgoorlie, and have higher La and possibly Nb than the remaining seven analyses. This latter group has similar Ti/Zr to the Lunnon Basalt (Appendix 3.11B). Both groups have similar MgO but the high La group also has high Ni and Cr, and all analyses show some overlap in terms of Al_2O_3/TiO_2 (Appendix 3.12C). The LREE-enrichment of the high-Zr group is shown in Appendix 3.13D.

Ora Banda Domain

The upper basalt unit at Ora Banda consists of two lithologically distinct units, the Bent Tree Basalt and Victorious Basalt. Analyses of the Bent Tree Basalt plot as tholeiites (Appendix 3.10D), whereas samples from the Victorious Basalt plot as calc-alkalic andesite. Appendix 3.11D shows that most analyses of the Bent Tree Basalt and Victorious Basalt lie on or close to the Lunnon Basalt trend rather than on the Kambalda Domain upper basalt unit trend. The near-zero slope for Al_2O_3/TiO_2 (Appendix 3.12D) and low Cr and Ni of the Victorious Basalt is consistent with fractionation of olivine and plagioclase.

Discussion

Basalt and dolerite of the upper basalt at both Kalgoorlie and Kambalda cannot be separated on geochemistry, but four samples at Kambalda (three basalts and one dolerite) have relatively lower MgO, Cr, and Ni, and near-zero slope for Al_2O_3/TiO_2 and are clearly fractionated. In some cases, the LREE-enrichment can be attributed to fractionation, but other samples have high MgO and Ni as well as LREE: this is inconsistent with fractionation.

Bluebush–Republican analyses fall into two groups, one overlapping with the Lunnon Basalt and the other plotting with Kambalda–Kalgoorlie upper basalt unit analyses. This latter group has members that are LREE-enriched as well as having high MgO and Ni. The two groups have different Ti/Zr, and are, therefore, not related by variable degrees of partial melting or fractionation. It is unclear whether the two groups are comagmatic or tectonically interleaved.

The Ti/Zr trend for the upper basalt unit in the Ora Banda Domain is similar to the lower basalt unit of the Kambalda Domain. Al_2O_3/TiO_2 variations indicate fractionation of the uppermost unit (Victorious Basalt).

Norseman Terrane

Seventy-two analyses from the 9 km-thick Woolyeenyer Formation (Morris et al., 1991) represents 66 samples of drillcore from four holes near the base of the sequence (Fig. 5) and six surface samples. All but three samples that show basaltic komatiite chemistry (99542, a surface sample from south of Norseman; 99934 and 99938, dykes cross-cutting the Woolyeenyer Formation in diamond drillhole S433) are tholeiites (Appendix 3.14A). For simplicity, these three samples are referred to as basaltic komatiite, even though the term should strictly be applied to extrusive rocks only.

All analyses are well correlated in terms of Ti/Zr (Appendix 3.15A), plotting on the upper edge of the Lunnon Basalt field. The line of best fit has a slope of 81 (r = 0.99) compared with 114 for the Lunnon Basalt. Basaltic komatiites 99934 and 99938 lie slightly off the main trend. Compared with other tholeiites, most samples from drillhole S207 have higher Zr, Ti (Fig. 3.15A) and Y, and have lower MgO, Ni and Cr. Most basalts show little variation in Al_2O_3 (Appendix 3.16A), but basaltic komatiites plot at lower Al_2O_3.

Four of the five tholeiitic basalts analysed for REE have similar LREE/HREE enrichment (Appendix 3.17A, B), but variable REE contents (8–15x chondrite). Sample 99944 has a steeper REE pattern (La/Yb_{CN} = 2.4) and is more LREE enriched (La near 22x chondrite). Basaltic komatiites 99934 and 99938 are strongly LREE enriched (La 70–90x chondrite) with steep $(La/Yb)_{CN}$ of 9–10 (Appendix 3.17C). In addition, both samples have high Nb, P, Ti, As, Th, Hf, and Zr (Appendix 3.18) relative to other basaltic komatiites (e.g. Sun et al., 1989).

New Nd isotope data are presented in Appendix 3.18 and Appendix 3.5A. ε_{Nd} for tholeiites and basaltic komatiite 99542 is greater than 0, whereas basaltic komatiites 99934 and 99938 have ε_{Nd} of -1.96 and -1.29 respectively.

Discussion

The high correlation of Ti and Zr, the limited range in ε_{Nd}, and the flat REE patterns of most Woolyeenyer tholeiites, are consistent with a homogeneous, depleted mantle source and minimal post-melting contamination. Samples with high Ti, Zr, and Y also have relatively low MgO, and Cr and Ni decreases with increasing Zr, indicating the major control on basalt composition is fractional crystallization. The 'cloud' of data for most tholeiites at lower Zr contents implies fractionation of several magma batches derived from a compositionally homogeneous source (Appendix 3.15A). This is also supported by the interleaving of variably fractionated flows (e.g. S207) within the flow pile.

Basaltic komatiites 99934 and 99938 have steep LREE/HREE, ε_{Nd} less than 0, and are enriched in REE, Zr, Ti, P, Nb, As, and Hf relative to published analyses of other basaltic komatiites.

Menzies Terrane

Because of the poor outcrop and severe deformation, little is known about stratigraphic relations in the Menzies Terrane. All analysed samples are tholeiite–calc-alkalic basalts (Appendix 3.14B) apart from 99991 (Mararoa West) which plots on the edge of the basaltic komatiite field. The Ti/Zr relationship (Appendix 3.15B) is similar to the Lunnon Basalt, and Al_2O_3 shows little variation with increasing TiO_2(Appendix 3.16B).

All these samples show similar characteristics to the lower basalt unit at Kambalda or the upper basalt unit of the Ora Banda Domain.

Summary of basalt geochemistry

Samples from the Kalgoorlie Terrane (lower basalt unit, basaltic upper part of the komatiite unit, upper basalt unit) and analyses from the Norseman and Menzies Terranes follow two trends in terms of Ti/Zr. One — consisting of samples from the lower basalt unit of the Kalgoorlie Terrane (excluding the Wongi Basalt, Ora Banda Domain and five samples from Bluebush–Republican), the upper basalt unit from the Ora Banda Domain (i.e. Bent Tree Basalt and Victorious Basalt), the Woolyeenyer Formation (Norseman Terrane), Menzies Terrane, Bullabulling Terrane — has a steep Ti/Zr trend. The other has a flatter trend for Ti/Zr. It consists of samples from the basaltic upper part of the komatiite unit, the upper basalt unit (excluding the Victorious Basalt and Bent Tree Basalt at Ora Banda), the Wongi Basalt (lower basalt unit of the Ora Banda Domain), and five lower basalt unit analyses from Bluebush–Republican, all of which are from within the Kalgoorlie Terrane. The groups are informally termed 'lower basalt group' (first trend) and 'upper basalt group' (second trend). Characteristics of each group are summarized in Table 5.

Table 5. Summary of chemical characteristics of the two main basalt units of this study, with available data for primitive mantle (from Sun and McDonough, 1989)

	Basalt unit		*Mantle*
	Lower	*Upper*	
Ti/Zr	100	70	116
Zr/Y	1.9	3.0	2.5
Al_2O_3/TiO_2	20	>20	?20
ε_{Nd}	>0	>0 and <0	?0
$(La/Yb)_{CN}$	≈1	≥1	0.94

Lower basalt unit: Lower basalt of the Kalgoorlie Terrane (excluding Wongi Basalt, Ora Banda Domain), Woolyeenyer Formation (Norseman Terrane), Menzies Terrane

Upper basalt unit: Basaltic upper part of the komatiite, upper basalt (excluding Victorious and Bent Tree Basalts, Ora Banda Domain; several analyses from Bluebush–Republican, Kambalda Domain)

The lower basalt group has limited ε_{Nd}, $(La/Yb)_{CN}$ close to 1, La about 10x chondrite, and Ti/Zr between 80 (Woolyeenyer Formation, Norseman Terrane) and 106 (lower basalt unit at Kambalda). These are similar characteristics to basalts derived from a depleted, homogeneous mantle source in which garnet was not a residual phase; for example, N-MORB (Sun and McDonough, 1989). Calc-alkaline basalts from Carnilya Hill (Boorara Domain) have lower Ti/Zr (65) and Al_2O_3/TiO_2 (14), and flat REE patterns, and are loosely assigned to the lower basalt group. Chemical variations within the lower basalt group are largely controlled by low-pressure fractional crystallization of clinopyroxene and, occasionally, olivine and/or plagioclase.

Compared with the lower basalt group, the upper basalt group is more diverse, both in terms of lithology and chemistry. The group comprises both basaltic komatiite and tholeiite with variable REE contents and LREE enrichment ($(La/Yb)_{CN} \geq 1$), a wider range in ε_{Nd} (both greater than and less than 0), higher Zr/Y (3) and lower Ti/Zr (65). Apart from the few Bluebush–Republican analyses, associations of rocks in the upper basalt group always contain basaltic komatiite as well as tholeiite. This, and the coherency of element trends for this group, suggest that basaltic komatiite and tholeiite are genetically related. Furthermore, the disparity of element trends and variation in ε_{Nd} between the lower and upper basalt groups means that they are not related by common processes such as variable degrees of partial melting or fractionation. Although some members of the upper basalt group are fractionated, the Ti/Zr trend is oblique to fractionation vectors, and fractional crystallization cannot explain the high Zr and LREE contents of some basaltic komatiites.

Basaltic komatiites with high LREE and incompatible element contents — i.e. the siliceous high-Mg series

basalts (SHMSB) of Redman and Keays (1985) — lie on upper basalt unit element trends (e.g. Ti/Zr). The close spatial relationship of komatiite and basaltic komatiite, and the dissimilarity of these rock types to tholeiites is compelling evidence for a genetic relationship between komatiite and basaltic komatiite. Several studies have concluded that contamination of a komatiite magma by continental crust, followed by fractional crystallization, is the most likely explanation for SHMSB chemistry (Arndt and Jenner, 1986; Barley, 1986; Sun et al., 1989). Arndt and Jenner (1986) showed that the composition of certain Kambalda hangingwall basalt (i.e. basaltic upper part of the komatiite unit, and upper basalt units of this study) could be explained by assimilation of about 24% of modern upper crust by komatiite, followed by the fractional crystallization of about 60% of the ensuing magma. Notably, Archaean crust could not produce the required LREE enrichment.

In this study, assimilation and fractional crystallization (AFC) modelling (DePaolo, 1981) of a komatiite parent and felsic contaminant is simulated using TRACE.FOR, a computer program that models both major- and trace-element behaviour (Nielsen, 1988). The required inputs for AFC modelling are: the compositions of the parent liquid and the contaminant; and the ratio of assimilant added to crystals extracted. For a given liquid composition, the program calculates mineral compositions, proportions, and equilibrium temperatures, selecting the appropriate liquidus phase. Following removal of an increment of this liquidus phase, the program loops to calculate a new mineral composition, temperature, etc. for the new composition. For each step, the amount and type of each mineral, and the equilibrium temperature are calculated. Although TRACE.FOR has not been tested for ultramafic compositions, the calculated magma temperatures, and the type and amount of fractionating phases (Table 6), are quite credible, and the approach is, therefore, taken to be a valid one.

Two contaminants are considered, an Archaean greywacke (Taylor and McLennan, 1985) and a calc-alkaline granitoid (Cassidy et al., 1991). Samples of the Wongi Basalt are taken as representative of the upper basalt unit. To estimate the type and amount of contaminant that is most likely, MORB-normalized spidergrams for selected trace elements are used (Figs 13A and 13B). The elements selected are those that are relatively easily measured by XRF, and have a variety of bulk distribution coefficients: broadly, Cr and Ni have D»1, Ti and Sc have D less than 1, and Sr, La, and Zr, have D«1. Thus, Cr and Ni are sensitive to the most likely fractionating phases (olivine and spinel), whereas Sr, La, and Zr, are more common in the contaminants than the komatiite.

Results are summarized in Figure 13A,B, and Table 6. Although contamination by both the greywacke and the granitoid produced patterns for Ti and V that resembled those of the Wongi Basalt, only the granitoid produced the required enrichment in Sr and La. To produce the appropriate levels of Sr and La using the greywacke required about 40% fractional crystallization, but this resulted in Cr and Ni values below many Wongi Basalt samples (Fig. 13A). The most appropriate model is 20–30% fractional crystallization (i.e. 10–15% assimilation), using the granitoid contaminant (Fig. 13B). The crystal extract is dominantly olivine, but small amounts of spinel are present, and the calculated eruption temperatures range from about 1400°C to 1500°C (Table 6).

Table 6. Results of assimilation/fractional crystallization (AFC) modelling, using the computer program TRACE.FOR (Nielsen, 1988)

	Contaminant								
	Archaean greywacke (a)				*Calc-alkaline granitoid (b)*				
	Kom (c)	*G'wacke (a)*	*20% (b)*	*30% (b)*	*Kom (c)*	*Gran (b)*	*20% (b)*	*30% (b)*	*40% (b)*
Sr	5	93	14	21	5	596	60	100	145
La	0.79	17	2.43	3.62	0.79	46	5.06	8.20	11.68
Ti	2 158	3 117	2 638	2 938	2 158	2 158	2 578	2 818	3 057
Zr	25	113	38	47	25	154	42	53	66
Y	11	12	13	15	11	10	13	14	16
V	164	72	171	173	–	NM	NM	NM	–
Sc	27	16	29	30	27	–	–	–	–
Cr	3 516	110	1 924	1 099	3 516	30	1 814	1 068	437
Ni	1 323	95	632	294	1 323	17	624	281	29
T°C (d)	1 591	–	1 478	1 397	1 591	–	1 480	1 398	1 277
XF (e)	–	–	Ol(20)	Ol(30)	–	–	Ol(20)	Ol(30)	Ol(40)
XF (e)	–	–	Sp(tr)	Sp(tr)	–	–	Sp(tr)	Sp(tr)	Sp(tr)
% Assim.	–	–	10	15	–	–	10	15	20

Source: (a) Taylor and McLennan, 1985; (b) Cassidy et al., 1991; (c) Komatiite, Kambalda, Sun et al. (1989); (d) calculated eruption temperature; (e) calculated crystallizing phases

Ol = olivine as percent; Sp = spinel; tr = trace; % Assim = percentage assimilant; NM = not measured

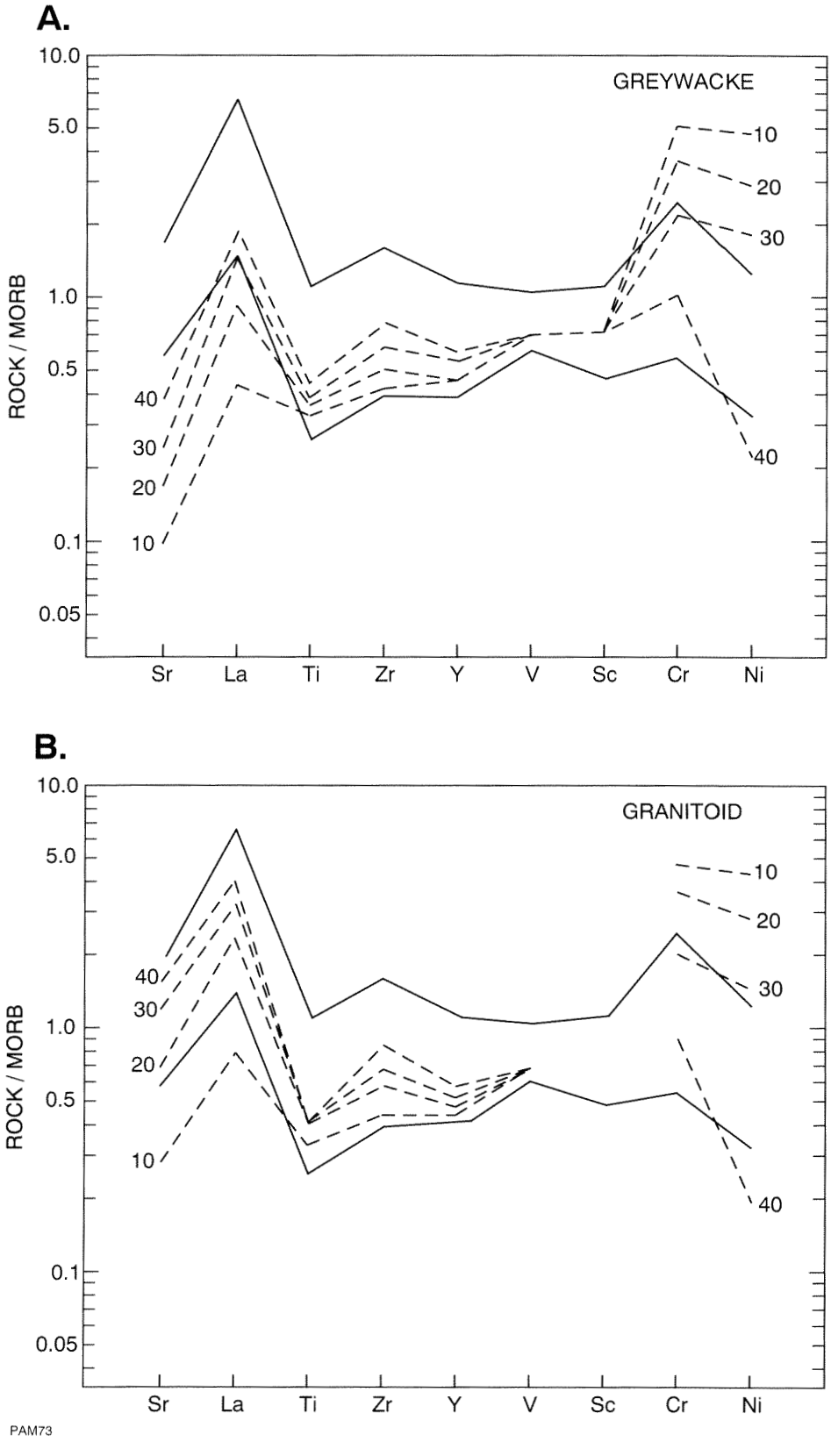

Figure 13. Mid-ocean-ridge basalt (MORB) normalized spidergram for samples of the Wongi Basalt (lower basalt unit, Ora Banda Domain) shown as solid lines on Figures A and B. n = 14. Normalization values (Sun and McDonough, 1989; Schilling et al., 1983) are Sr = 90; La = 2.5; Ti = 7600; Zr = 74; Y = 28; V = 262; Sc = 40; Cr = 528; Ni = 214. A — Calculated patterns (broken lines) from TRACE.FOR for 10–40% fractional crystallization of a komatiite, contaminated by Archaean greywacke. See Table 6 for data. B — Calculated patterns (broken lines) from TRACE.FOR for 10–40% fractional crystallization of a komatiite, contaminated by calc-alkaline granitoid. See Table 6 for data

Fluid is another type of contaminant capable of producing LREE enrichments. Investigations of boninite genesis by Tatsumi et al. (1986) involved simulating the metasomatic alteration of the mantle wedge overlying a subducting lithospheric plate by experimental dehydration of serpentinite (i.e. descending lithospheric plate). The resultant enrichment of LREE in the mantle wedge (La about 15% and Sm about 9%) was not accompanied by an increase in Nb. This result seems to conform to the compositional differences between basaltic komatiites and SHMSB. The effect of fluid metasomatism on $^{144}Nd/^{143}Nd$ is presently unknown (Perfit, 1990).

Basaltic komatiites 99934 and 99938 (Norseman Terrane) show an enrichment of LREE and Zr that is similar to that of some members of the upper basalt unit. They are also enriched in P, Nb, Ti, As, Th, and Hf, but concentrations of Sc, V, MgO, Ni, and Cr approximate those of other basaltic komatiites. Morris et al. (in press) have suggested that these rocks are the first recorded Archaean occurrence of mafic rocks derived from an OIB-type mantle source.

Komatiite genesis

Restriction of komatiite magma to the Archaean, and the rarity of other magma types (e.g. ocean island basalt) in Archaean terrains, implies atypical conditions for magma genesis. Early work on komatiite genesis maintained that lavas with 25–30 wt% MgO and estimated eruption temperatures near 1600°C required extensive melting (greater than 50%) at high temperatures, only possible if melting occurred at depths in excess of 400 km with elevated geothermal gradients (Nesbitt and Sun, 1976; Sun and Nesbitt, 1978; Nesbitt et al., 1979). With the increased amount of analytical data, two types of komatiite were recognized (Nesbitt et al., 1979): an aluminium-undepleted type (AUK, with CaO/Al_2O_3 less than 1); and an aluminium-depleted type (ADK, with CaO/Al_2O_3 greater than 1). The former is more common in young (c. 2.7 Ga) deposits; the latter, characteristic of the early Archaean (3.5 Ga). According to the results of experimental work (Ohtani et al., 1989; Ohtani, 1990), there are two hypotheses to explain various degrees of Al depletion of komatiites. One, that ADK results from the melting of an ascending mantle diapir at 200–650 km, whereas AUK results from a higher degree of partial melting of a shallower primitive mantle (less than 450 km). The latter cannot be generated by low degrees of partial melting at any depth. Alternatively, if the Archean mantle was variably enriched in Al (by extraction of melts or crystallization of majorite garnet), melts of variable Al enrichment would result. Homogenization of the mantle by the late Archaean would result in the characteristic AUK (cf. this study). A possible problem with the mantle-stratification model is Hf isotope data, which indicates a chondritic Archaean mantle for Lu and Hf, whereas majorite fractionation should produce non-chondritic Lu/Hf ratios. These are not observed, so variable depths and degrees of partial melting may be more acceptable.

Experimental work of Herzberg and Ohtani (1988) has suggested derivation of komatiites by pseudoinvariant melting at variable depth, with MgO content reflecting not the degree but the depth of melting. They suggested that komatiites with 20–28 wt% MgO were derived at 130–260 km, whereas early Archaean komatiites were derived from near the core mantle boundary.

Although experimental work may cast new light on komatiite genesis, rheological (Huppert et al., 1984), isotope (Dupré and Arndt, 1990), and trace-element studies (Arndt and Jenner, 1986; Sun et al., 1989) have shown that komatiites are sufficiently hot to thermally erode wall rocks or surface rocks. Thus, their compositions may not accurately reflect either the nature of their source or the process of melting. Komatiites examined in this study have near chondritic Al_2O_3/TiO_2, CaO/Al_2O_3 less than 1 (i.e. AUK), and flat to LREE-depleted REE patterns. By analogy with experimental work discussed above, they were derived from a chondritic mantle at depths of less than 300 km. Small variations in Al_2O_3/TiO_2 ratios in komatiites from the Ora Banda domain argue for small variations in source composition or locus of melting.

Part 4

Tectonic setting

Although geochemical data are routinely used to determine the tectonic setting of basaltic rocks (Pearce and Cann, 1973; Pearce, 1975; Holm, 1982), several studies have cautioned against the use of this approach without support from other geological information, especially if the rocks in question are removed from their site of eruption (Duncan, 1987; Arculus, 1987; Pearce, 1987; Hall and Plant, 1991). The choice of geochemical approach is limited by several factors: element mobility (e.g. TiO_2–K_2O–P_2O_5 diagram of Pearce et al., 1977); the insensitivity of the analytical technique for accurate low-level analysis (Hf/3–Th–Ta: Wood et al., 1979; various diagrams in Pearce et al., 1977; Winchester and Floyd, 1976); poor resolution for certain tectonic settings (e.g. Ti/100–Zr–3Y diagram of Pearce and Cann, 1973); the reliance on one element for discrimination (e.g. Cr–Y: Pearce, 1975).

Regional-scale non-geochemical constraints on tectonic setting

Interflow sedimentary rocks within the mafic–ultramafic volcanic succession have chemical and textural characteristics of airfall rhyolitic ash (Bavinton, 1981). Some zircons in these sedimentary units and mafic volcanic rocks have U–Pb SHRIMP ages greater than 3000 Ma. These are interpreted as zircons inherited from older crustal material (Compston et al., 1986). Published studies of isotopic and trace-element modelling (Arndt and Jenner, 1986; Sun et al., 1989; Barley, 1986), and modelling of the upper basalt unit discussed above, have shown that continental crust is a possible contaminant of some magma.

Intermediate and acid volcanic rocks and volcanic-derived sedimentary rocks are common in the Kurnalpi Terrane (Barley et al., 1989; Swager, in prep.; Morris, in prep.; Ahmat, 1991), and a few intermediate to acid volcanic rocks are interbedded with mafic volcanic rocks in the Kalgoorlie Terrane. Thick sequences of acid volcanic rocks and associated sedimentary rocks overly the greenstone succession in the Kalgoorlie Terrane (e.g. Black Flag Group), and acid volcanic rocks with calc-alkaline chemistry intrude the volcanic pile throughout the Kalgoorlie Terrane.

Banded iron-formation (BIF) is not an important constituent of Kambalda and Ora Banda Domains, but does outcrop in areas marginal to these domains, such as the Norseman Terrane and parts of the Boorara and Coolgardie Domains. Komatiites are volumetrically more important in the Kalgoorlie Terrane than the Norseman Terrane, where thinner sequences are found.

These variations in the proportions of banded iron-formation and mafic to ultramafic volcanic rocks between the Norseman–Menzies region and regions to the east and west have been interpreted in terms of a rift environment (Kalgoorlie Terrane), bordered by a shallower water platform sequence (Gee et al., 1981; Groves and Batt, 1984).

The rapid and voluminous outpouring of mafic and ultramafic lava, the fine-grained nature of sediments, the abundance of pillow lava, the low volatility of magma, and the northwest to southeast polarity of lava flow, are consistent with rapid rifting and eruption in a deep ocean basin. The greater lateral continuity of flow units on the margin of the basin indicates a smoother topography. SHRIMP dating and magma contamination indicate flooring of the greenstone pile by continental crust.

Hill et al. (1990) maintained that the thinning of komatiite flow sequences from north to south in the Kalgoorlie Terrane reflects eruption of komatiite magma to the north and flow to the south.

Terrane-scale variations in volcanology and geochemistry

Kalgoorlie, Kambalda, parts of the structurally repeated Bluebush–Republican succession (Kambalda Domain), and the Widgiemooltha–Redross succession (Coolgardie Domain) show consistent volcanological and chemical characteristics between stratigraphically equivalent units. However, the lower basalt unit in the Coolgardie area (Coolgardie Domain) is more diverse (tholeiite and basaltic komatiite) and flows show more lateral consistency. Further within-terrane variability is shown on the eastern margin of the Kalgoorlie Terrane, where the lower basalt unit at Carnilya Hill (Boorara Domain) is calc-alkaline rather than tholeiitic and has different Ti/Zr and Al_2O_3/TiO_2 to most other lower basalt unit samples. The most significant differences in volcanology and chemistry occur between stratigraphically equivalent units of the Ora Banda Domain and other domains of the Kalgoorlie Terrane. Although all domains have the 'basalt–komatiite–basalt' succession, the lower basalt unit of the Ora Banda Domain has basaltic komatiite and tholeiite with similar chemistry to the upper basalt unit of the Kambalda Domain, whereas the Ora Banda Domain upper basalt unit has element trends that are similar to

those of the lower basalt unit in the Kambalda Domain. In summary, the most marked chemical variations in the Kalgoorlie Terrane occur on a north–south axis, but there are variations along an east–west axis that must also be accounted for in any tectonic model.

Samples from the Bullabulling Terrane and from Dunnsville (Coolgardie Domain) are chemically similar, and their element trends are oblique to the element trends from the lower basalt of other areas. Although the amount of data is limited, the element trends bear some similarity to the basaltic upper part of the komatiite unit. The basalts of the Menzies Terrane are compositionally similar to the lower basalt unit of the Kambalda Domain. In both the Bullabulling and Menzies terranes, there is a need for more chemistry when the stratigraphies are better understood.

Mafic volcanic rocks of the Woolyeenyer Formation (Norseman Terrane) are a similar age and broadly resemble the lower basalt unit of the Kambalda Domain in terms of volcanology and chemistry. The Woolyeenyer Formation basalts have lower Ti/Zr (81) than the Kambalda Domain lower basalt unit (106), but similar flat REE patterns and similar ε_{Nd}.

Tectonic models for the eastern Yilgarn Craton

Plume model

Using laboratory studies, and by analogy with continental flood-basalt provinces (Hooper, 1990; Richards et al., 1989; Peate et al., 1990; White and McKenzie, 1989; Campbell and Griffiths, 1990), Campbell and Griffiths (1990), Griffiths and Campbell (1990), Campbell et al. (1989) and Campbell and Hill (1988) propose a mantle-plume model to explain the basalt–komatiite volcanic sequence, the rapid onset and short duration of volcanism, the uplift, and the origin of post-tectonic granitoids. A 600–800 km diameter komatiite plume initiated at the core–mantle boundary, ascended through thermal buoyancy. Mantle was entrained into the plume head, which was constantly fed by komatiite magma of the plume axis. On reaching the lithospheric mantle, the plume head flattened and attained a diameter of approximately 2000 km.

The first erupted magma, corresponding to the plume head, had tholeiite chemistry and corresponded to the Lunnon Basalt at Kambalda (lower basalt unit). This was followed by the eruption of komatiite magma comprising the plume axis (Kambalda Komatiite). Contamination of the axis could not occur until the plume head was deflected by plate motion, a situation appropriate to producing contaminated komatiite magma, such as the upper basalt unit. The absence of komatiite in the Norseman Terrane indicates that the plume axis was centred to the north (R. I. Hill, pers. comm., 1990), presumably at least 300–400 km distant. By analogy with continental flood-basalt provinces, the plume model explains the rapid onset and short duration of volcanism in the Eastern Yilgarn Craton.

Using mathematical modelling Campbell and Hill (1988) predicted that granite plutonism would commence about 15 Ma after the end of plume volcanism; this is borne out by currently available age data for intrusive rocks.

Although the plume model explains the eruption, first of basalt then komatiite, in the Kambalda area, it does not account for the compositional diversity of the lower basalt unit in the Kalgoorlie Terrane, in that komatiite is a member of the lower basalt unit in the Ora Banda and Coolgardie Domains. Moreover, although the plume model may explain the chemistry of the upper basalt unit of the Kambalda Domain by contamination of a single komatiite plume, it is inconsistent with lack of komatiite in the upper basalt unit of the Ora Banda Domain. The plume model also fails to address the widespread occurrence of felsic volcanic rocks and associated sedimentary rocks that are coeval and, in parts, interbedded with mafic and ultramafic volcanic rocks, or the northwest–southeast polarity of the greenstone sequence.

Convergent plate-margin model

A convergent plate–margin model for the Eastern Yilgarn Craton has been proposed by Barley et al. (1989) and Barley and Groves (1990). They delineate two tectono-stratigraphic associations in the Norseman–Wiluna area: a tholeiite + calc-alkaline volcanic association with felsic sedimentary rocks to the east (Kurnalpi Terrane of this study); and a tholeiite + komatiite assemblage with fine-grained siliceous sedimentary rocks to the west (includes all terranes discussed in this study). Barley and co-workers maintain that the eastern association corresponds to a volcanic arc succession, whereas the western association represents a marginal basin (back-arc) sequence.

Two well-documented arc–back-arc associations are now reviewed. The Jurassic–Cretaceous 'rocas verdes' of South America (Tarney et al., 1981) is a marginal basin sandwiched between continental crust and a volcanic arc. Mafic igneous rocks rest on the continental margin. The basin was synformal and parallel to the continental margin. Metamorphism was low grade, and sulfide mineralization, pillow lava, and chert were common. The greenstones were derived from a depleted mantle source. The amount of arc-derived sedimentary rocks (predominantly of andesitic composition) was controlled by the timing of basin closure and the uplift rate. In a more recent study, Alabaster and Storey (1990) interpreted chemical and isotopic data for a displaced part of the 'rocas verdes' in southern Chile in terms of oblique slip rather than subduction.

The Miocene back-arc of the Sea of Japan opened by about 57° clockwise rotation from the Asian mainland at about 15 Ma, following initiation of west-dipping subduction at 40 Ma (Matsuda, 1979). Opening was completed in less than 1 m.y. (Otofuji and Matsuda, 1984; Otofuji et al., 1985). Several lines of evidence suggest that the Japan Sea is at least in part ensialic: continental crust occurs in the eastern Japan Sea, and 2000 Ma gneiss and gravel derived from this gneiss have been recorded

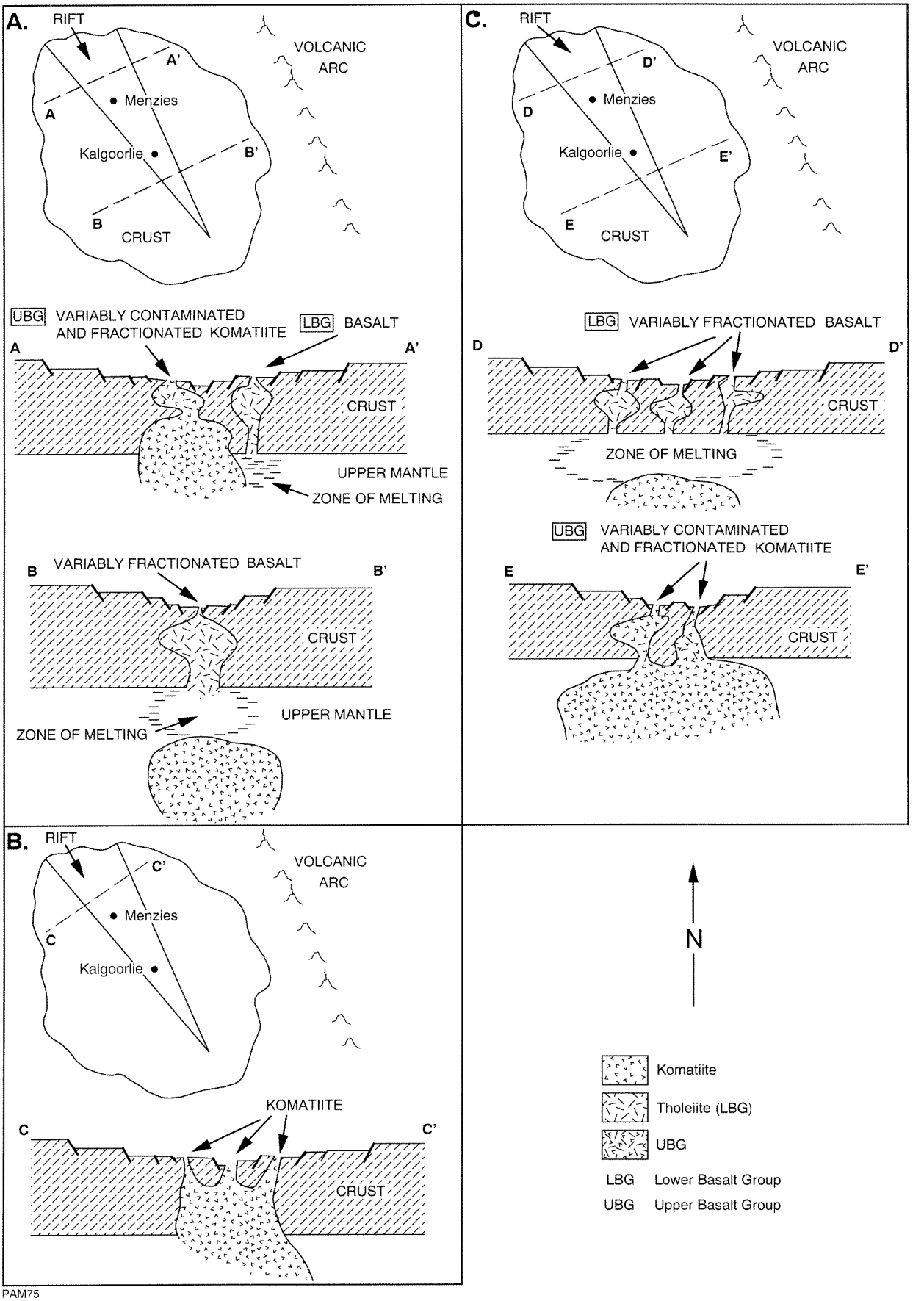

PAM75

Figure 14. Cartoon illustrating volcanic and chemical evolution of the Kalgoorlie Terrane. Position of descending plate is inferred, and is not an intrinsic part of the model. See text for discussion

from southwestern Japan. A chemical and isotopic study of volcanism since the opening of the Japan Sea (Morris and Kagami, 1989) has been linked with detailed K/Ar dating (Morris et al., 1990). Effusive volcanism coinciding with the opening of the back-arc basin involved eruption of tholeiitic magma. The next phase of volcanism resulted from the melting of the metasomatically altered mantle wedge overlying the subducting plate. Alkaline basalts were erupted further to the west, whereas calc-alkaline volcanic rocks were erupted closer to the arc.

Clearly, there are strong analogies between the 'rocas verdes', Sea of Japan, and the Eastern Yilgarn Craton, in terms of volcanology, the spatial relationship of volcanic and sedimentary rocks, and the chemistry of the volcanic rocks. Unlike the plume model, a convergent margin can explain both mafic–ultramafic and calc-alkaline volcanic rocks. However, Barley et al.'s (1989) eastern (arc) association also contains komatiite (Ahmat, 1991; Swager, in prep.; Morris, in prep.), and it is clear from experimental work discussed above that komatiite is generated at depths beyond the locus of arc volcanism.

This study

The preferred tectonic model is summarized in cartoon form in Figure 14. A northwest–southeast oriented continental rift (proto-Kalgoorlie, Norseman, and Menzies Terranes) developed in ?continental crust. The rift was paralleled to the east by a volcanic arc. The downgoing plate dipped to the west. It is unclear if the rift and arc were genetically related (i.e. the rift was a back-arc basin), or if the downgoing slab underlay the rift. The volcanic products in the rift are consistent with deep-water eruption, i.e. pillow lava and fine-grained sedimentary rocks, and some of the latter represent ash fall-out from the volcanic arc.

The rift opened in a fan-shaped fashion, at a greater rate to the north (Fig. 14A). Concomitant with this rifting, komatiite magma rose to the surface, but it is unclear whether rifting promoted volcanism or vice versa. Prior to eruption, some of the komatiite was contaminated by, and fractionated within, the continental crust, i.e. Wongi Basalt of the Ora Banda Domain (Fig. 14A, section A–A'), whereas further south, the komatiite acted as a heat source to melt the asthenospheric mantle producing tholeiitic basalt that was variably fractionated in crustal magma chambers prior to eruption (i.e. lower basalt unit of the Kambalda Domain and most of the Coolgardie Domain (Fig. 14A, section B–B').

Accelerated rifting (still at a greater rate to the north) resulted in crustal thinning and eruption of uncontaminated and variably fractionated komatiite (Fig. 14B). The lava flowed from north to south, broadly parallel to the rift.

The abatement of komatiite volcanism coincided with the closure of the rift, faster in the north than the south. This resulted in komatiite becoming a source of heat for the melting of the mantle to the north of the rift, i.e. Ora Banda Domain (Fig. 14C, D–D'), and the eruption of variably contaminated and fractionated komatiite to the south, i.e. Kambalda Domain (Fig. 14C, E–E').

Further compression of the rift resulted in the closure of magma conduits, and this, in turn, caused the komatiite to melt the continental crust and to produce dacitic and rhyolitic volcanic rocks and associated sedimentary rocks characteristic of the overlying Black Flag Group.

Assuming the same broad geographic relationship of the Norseman and Kalgoorlie Terranes now as in the Archaean, this model is consistent with voluminous outpourings of tholeiitic magma in the south of the Kalgoorlie Terrane and in the Norseman Terrane during the early stages of rifting. The model also explains the attenuation of the greenstones on the margins of the rift, which have undergone less faulting during rifting (i.e. Coolgardie and Boorara Domains).

As both tholeiitic and komatiitic volcanic rocks outcrop in the Kurnalpi Terrane, it is tentatively included with the rift sequence; the higher proportion of felsic volcanic rocks and related sedimentary rocks in this terrane is consistent with its proximity to the eastern volcanic arc.

References

AHMAT, A. L., 1991, Kanowna, Western Australia: Western Australia Geological Survey, 1:100 000 Geological Series Map.

ALABASTER, T., and STOREY, B. C., 1990, Modified Gulf of California model for South Georgia, North Scotia Ridge, and implications for the Rocas Verdes back-arc basin, southern Andes: Geology, v. 18, p. 497–500.

ARCHIBALD, N. J., 1979, Tectonic-metamorphic evolution of an Archaean terrain — A study of the Norseman–Widgiemooltha granitoid–greenstone belt, Eastern Goldfields Province, Western Australia: University of Western Australia, Ph. D. thesis (unpublished), 270p.

ARCULUS, R. J., 1987, The significance of source versus process in the tectonic controls on magma genesis: Journal of Volcanology and Geothermal Research, v. 32, p. 1–12.

ARNDT, N. T., FRANCIS, D., and HYNES, A. J., 1979, The field characteristics and petrology of Archaean and Proterozoic komatiites: Canadian Mineralogist v. 17, p. 147–163.

ARNDT, N. T., and JENNER, G. A., 1986, Crustally contaminated komatiites and basalts from Kambalda, Western Australia: Chemical Geology, v. 56, p. 229–255.

ARNDT, N. T., and JOCHUM, K-P., 1990, Komatiites — Unreliable witnesses of the Archaean mantle: International Archaean Symposium, 3rd, Extended Abstracts, Geoconferences (Western Australia) Perth, p. 147–148.

ARNDT, N. T., NALDRETT, A. J., and PYKE, D. R., 1977, Komatiitic and iron-rich tholeiitic lavas of Munro Township, northeast Ontario: Journal of Petrology, v. 18, p. 319–369.

BARLEY, M. E., 1986, Incompatible-element enrichment in Archaean basalts — A consequence of contamination by older sialic crust rather than mantle heterogeneity: Geology, v. 14, p. 947–950.

BARLEY, M. E., EISENLOHR, B. N., GROVES, D. I., PERRING, C. S., and VEARNCOMBE, J. R., 1989, Late Archaean convergent margin tectonics and gold mineralization — A new look at the Norseman–Wiluna Belt, Western Australia: Geology, v. 17, p. 826–829.

BARLEY, M. E., and GROVES, D. I., 1990, Deciphering the tectonic evolution of Archaean greenstone belts — The importance of contrasting histories to the distribution of mineralization in the Yilgarn Craton, Western Australia: Precambrian Research, v. 46, p. 3–20.

BARNES, R. G., LEWIS, J. D., and GEE, R. D., 1974, Archaean ultramafic lavas from Mt Clifford: Western Australia Geological Survey, Annual Report 1973, p. 59–70.

BARNES, S. J., GOLE, M. J., and HILL, R. E. T., 1987, The Agnew nickel deposit, Western Australia — Stratigraphy, structure, geochemistry and origin: Western Australia Mining and Petroleum Research Institute, Report 32, 187p.

BARNES, S. J., HILL, R. E. T., and GOLE, M. J., 1988, The Perseverance Ultramafic Complex, Western Australia — The product of a komatiite lava river: Journal of Petrology, v. 29, p. 305–331.

BARRETT, F. M., BINNS, R. A., GROVES, D. I., MARSTON, R. J., and McQUEEN, K. G., 1977, Structural history and metamorphic modification of Archaean volcanic-type nickel deposits, Yilgarn Block, Western Australia: Economic Geology, v. 72, p. 1195–1223.

BARTLEY, J. M., 1986, Evaluation of REE mobility in low-grade metabasalts using mass-balance calculations: Norsk Geologisk Tidsskrift, v. 66, p. 145–152.

BASALTIC VOLCANISM STUDY PROJECT, 1981, Basaltic volcanism on the terrestrial planets; New York, Pergammon Press Inc., 1286p.

BAVINTON, O. A., 1981, The nature of sulfidic metasediments at Kambalda and their broad relationship with associated ultramafic rocks and nickel ores: Economic Geology, v. 76, p. 1606–1628.

BEKKER, C., 1962, The 'greenstones' of the Norseman district: University of Western Australia, M.Sc. thesis (unpublished).

BINNS, R. A., GUNTHORPE, R. J., and GROVES, D. I., 1976, Metamorphic patterns and development of greenstone belts in the Eastern Yilgarn Block, Western Australia, *in* The early history of the earth *edited by* B. F. WINDLEY: New York, John Wiley and Sons, p. 303–313.

BOULTER, C. A., FOTIOS, M. G., and PHILLIPS, G. N., 1987, The Golden Mile, Kalgoorlie — A giant gold deposit localized in ductile shear zones by structurally induced infiltration of an auriferous metamorphic fluid: Economic Geology, v. 82, p. 1661–1678.

CAMPBELL, I. H., and GRIFFITHS, R. W., 1990, Implication of mantle plume structure for the origin of flood basalts: Earth and Planetary Science Letters, v. 99, p. 79–93.

CAMPBELL, I. H., GRIFFITHS, R. W., and HILL, R. I., 1989, Melting in an Archaean mantle plume — Heads it's basalts, tails it's komatiites: Nature, v. 339, p. 697–699.

CAMPBELL, I. H., and HILL, R. I., 1988, A two-stage model for the formation of granite–greenstone terrains of the Kalgoorlie–Norseman area, Western Australia: Earth and Planetary Science Letters, v. 90, p. 11–25.

CASSIDY, K. F., BARLEY, M. E., GROVES, D. I., PERRING, C. S., and HALLBERG, J. A., 1991, An overview of the nature, distribution and inferred tectonic setting of granitoids in the late-Archaean Norseman–Wiluna Belt: Precambrian Research, v. 51, p. 51–83.

CHAUVEL, C., DUPRÉ, B., and JENNER, G. A., 1985, The Sm–Nd age of Kambalda volcanics is 500 Ma too old! Earth and Planetary Science Letters, v. 74, p. 315–324.

CHRISTIE. D., 1975, Scotia nickel sulfide deposits, *in* Economic geology of Australia and Papua New Guinea, Volume 1, Metals *edited by* C. L. KNIGHT: Australasian Institute of Mining and Metallurgy, Monograph 5, p. 121–124.

CLAOUÉ-LONG, J. C., COMPSTON, W., and COWDEN, A., 1988, The age of the Kambalda greenstones resolved by ion-microprobe — Implications for Archaean dating methods: Earth and Planetary Science Letters, v. 89, p. 239–259.

CLAOUÉ-LONG, J. C., THIRLWALL, M. F., and NESBITT, R., 1984, Revised Sm–Nd systematics of Kambalda greenstones, Western Australia: Nature, v. 307, p. 697–701.

CLARK, M. E., CARMICHAEL, D. M., and HODGSON, C. J., 1988, Metasomatic processes and T–X$_{CO_2}$ conditions of wall-rock alterations, Victory gold mine, Kambalda, Western Australia: Geological Society of Australia: Abstracts 22, Bicentennial Gold 88, Extended Abstracts, Oral Program, p. 230–234.

CLOUT, J. M. F., CLEGHORN, J. H., and EATON, P. C., 1990, Geology of the Kalgoorlie Gold Field, *in* Geology of the mineral deposits of Australia and Papua New Guinea *edited by* F. E. HUGHES: Melbourne, The Australasian Institute of Mining and Metallurgy, p. 411–431.

COISH, R. A., 1977, Ocean floor metamorphism in the Betts Cove Ophiolite, Newfoundland: Contributions to Mineralogy and Petrology, v. 60, p. 255–270.

COMPSTON, W., WILLIAMS, I. S., CAMPBELL, I. H., and GRESHAM, J. J., 1986, Zircon xenocrysts from the Kambalda volcanics — Age constraints and direct evidence for older continental crust below the Kambalda–Norseman greenstones: Earth and Planetary Science Letters, v. 76, p. 299–311.

COWDEN, A., and ARCHIBALD, N. J., in prep., Stratigraphy of the Kambalda–Kalgoorlie Archaean greenstone terrain, Western Australia: Australian Journal of Earth Sciences.

de PAOLO, D. J., 1981, Trace elements and isotopic effects of combined wallrock assimilation and fractional crystallization: Earth and Planetary Science Letters, v. 53, p. 189–202.

DOEPEL, J. J. G., 1973, Explanatory notes on the Norseman 1:250,000 Geological Sheet, Western Australia: Western Australia Geological Survey, Record 1970/9.

DONALDSON, C. H., 1982, Spinifex-textured komatiites — A review of textures, compositions and layering, *in* Komatiites *edited by* N. T. ARNDT and E. G. NISBET: Sydney, George Allen and Unwin, p. 213–244.

DUNCAN, A. R., 1987, The Karoo igneous province — A problem area for inferring tectonic setting from basalt geochemistry, *in* Tectonic controls on magma chemistry *edited by* S. D. WEAVER and R. W. JOHNSON: Journal of Volcanology and Geothermal Research v. 32, p. 13–34.

DUPRE, B., and ARNDT, N. T., 1990, Pb-isotopic compositions of Archaean komatiites and sulfides: Chemical Geology, v. 85, p. 35–56.

EVENSEN, N. M., HAMILTON, P. J., and O'NIONS, R. K., 1978, Rare earth element abundances in chondritic meteorites: Geochimica et Cosmochmica Acta, v. 42, p. 1199–1212.

FREY, F. A., GREEN, D. H., and ROY, S. D., 1978, Integrated models of basalt petrogenesis — A study of quartz tholeiites to olivine melilites from south eastern Australia utilizing geochemical and experimental petrological data: Journal of Petrology v. 19, p. 463–513.

GEE, R. D., BAXTER, J. L., WILDE, S. A., and WILLIAMS, I. R., 1981, Crustal development in the Archaean Yilgarn Block, Western Australia: Geological Society of Australia, Special Paper 7, p. 43–56.

GILL, J., TORSSANDER, P., LAPIERRE, H., TAYLOR, R., KAIHO, K., KOYAMA, M., KUSAKABE, M., AITCHISON, J., CISOWSKI, S., DADEY, K., FUJIOKA, K., KLAUS, A., LOVELL, M., MARSAGLIA, K., PEZARD, P., TAYLOR, B., and TAZAKI, K., 1990, Explosive deep water basalt in the Sumisu backarc rift: Science, v. 248, p. 1214–1217.

GOLE M. J., BARNES S. J., and HILL R. E. T., 1990, Partial melting and recrystallization of Archaean komatiites by residual heat from rapidly accumulated flows: Contributions to Mineralogy and Petrology, v. 105, p. 704–714.

GRESHAM, J. J., and LOFTUS-HILLS, G. D., 1981, The geology of the Kambalda nickel field, Western Australia: Economic Geology, v. 76, p. 1372–1416.

GRIFFIN, T. J., 1990, Geology of the granite–greenstone terrane of the Lake Lefroy and Cowan 1:100 000 sheets, Western Australia: Western Australia Geological Survey, Report 32, 53p.

GRIFFIN, T. J., and HICKMAN, A. H., 1988, Lake Lefroy, Western Australia: Western Australia Geological Survey, 1:100 000 Geological Series.

GRIFFITHS, R. W., and CAMPBELL, I. H., 1990, Stirring and structure in mantle starting plumes: Earth and Planetary Science Letters, v. 99, p. 66–78.

GROVES, D. I., and BATT, W. D., 1984, Spatial and temporal variations of Archaean metallogenic associations in terms of evolution of granitoid–greenstone terrains with particular emphasis on the Western Australian shield, *in* Archaean geochemistry *edited by* A. KRONER, G. N. HANSON, and A. M. GOODWIN: Berlin, Springer Verlag, p. 73–98.

GROVES, D. I., and HUDSON, D. R., 1981, The nature and origin of Archaean stratabound volcanic-associated nickel–iron–copper sulphide deposits, *in* Handbook of stratabound and stratiform ore deposits *edited by* K. H. WOLF: Amsterdam, Elsevier, p. 305–410.

GRUNSKY, E., EASTON, M., THURSTON, P., and JENSEN, L. S.,1990, Statistical classification of Archaean volcanic rocks using major element geochemistry: Australia, Commonwealth Scientific and Industrial Research Organization, Exploration Research News, v. 4, p. 12–15.

HALL, H. I. E., and BEKKER, C., 1965, Gold deposits of Norseman, *in* Geology of Australian Ore Deposits (2nd edition) *edited by* J. McANDREW: Melbourne, 8th Commonwealth Mining and Metallurgical Congress, p. 101–107.

HALL, G. E. M., and PLANT, J. E., 1991, Analytical errors in the determination of high field strength elements and their implications in tectonic interpretation studies: Chemical Geology, v. 95, p. 141–156.

HALLBERG, J. A., 1972, Geochemistry of Archaean volcanic belts in the Eastern Goldfields region of Western Australia: Journal of Petrology, v. 13, p. 45–56.

HALLBERG, J. A., 1987, Postcratonization mafic and ultramafic dykes of the Yilgarn Block: Australian Journal of Earth Sciences, v. 34, p. 135–149.

HARRISON, N., 1984, The influence of volcanic stratigraphy and chemistry on the development of lodes in the basalts and porphyritic basalts at Ora Banda, Western Australia: BHP Minerals Division, Exploration Department Report C4231, 33p.

HAYWARD, B., 1988, Geology of the Widgiemooltha area and exploration progress to February 1988: Western Mining Corporation, Report K/3099, 82p.

HEATH, A. G., and ARNDT, C. D., 1976, Nickel exploration of the Carnilya ultramafic belt, Mt Monger, Western Australia: BHP, Report CR 2025 (unpublished).

HELLMAN, P. L., SMITH, R. E., and HENDERSON, P., 1979, The mobility of the rare earth elements — Evidence and implications from selected terrains affected by burial metamorphism: Contributions to Mineralogy and Petrology, v. 71, p. 23–44.

HERZBERG, C. T., and OHTANI, E., 1988, Origin of komatiite at high pressures: Earth and Planetary Science Letters, v. 88, p. 321–329.

HILL, R. E. T., BARNES, S. J., GOLE, M. J., and DOWLING, S. E., 1990, The physical volcanology of komatiites in the Norseman–Wiluna Belt: Third International Archaean Symposium Excursion Guidebook. p. 362–397.

HILL, R. E. T., GOLE, M. J., and BARNES, S. J., 1988, Physical volcanology of komatiites — A field guide to the komatiites between Kalgoorlie and Wiluna, Eastern Goldfields Province, Western Australia: Geological Society of Australia, Western Australian Division, Excursion Guidebook 1, 74p.

HILL, R. I., and CAMPBELL, I. H., 1989, A post-metamorphic age for gold mineralization at Lady Bountiful, Yilgarn Block, Western Australia: Australian Journal of Earth Sciences, v. 36, p. 313–316.

HILL, R. I., CAMPBELL, I. H., and COMPSTON, W., 1989, Age and origin of granitic rocks in the Kalgoorlie–Norseman region of Western Australia — Implications for the origin of Archaean crust: Geochimica et Cosmochimica Acta, v. 53, p. 1259–1275.

HILL, R. I., CAMPBELL, I. H., and COMPSTON, W., 1990, Crustal growth, crustal reworking, and granite genesis in the southeastern Yilgarn Block, Western Australia: International Archaean Symposium, 3rd, Geoconferences (Western Australia) Perth, Extended Abstracts, p. 473–475.

HILL, R. I., and COMPSTON, W., 1987, Age of granite emplacement, southeastern Yilgarn Block, Western Australia: Australian National University, Research School of Earth Sciences, Annual Report 1986, p. 70–71.

HOLM, P., 1982, Non-recognition of continental tholeiites using the Ti–Zr–Y diagram: Contributions to Mineralogy and Petrology, v. 79, p. 308–310.

HOOPER, P. R., 1990, The timing of crustal extension and the eruption of continental flood basalts: Nature, v. 345, p. 246–249.

HUNTER, W. M., 1993, Geology of the granite–greenstone terrain of the Kalgoorlie and Yilmia 1:100,000 sheets: Western Australia Geological Survey, Report 35.

HUPPERT, H. E., and SPARKS, R. S. J., 1985, Komatiites I — Eruption and flow: Journal of Petrology, v. 26, p. 694–725.

HUPPERT, H. S., SPARKS, R. S. J., TURNER, J. S., and ARNDT, N. T., 1984, The emplacement and cooling of komatiite lavas: Nature, v. 309, p. 19–23.

HYNES, A., and GEE, R. D., 1986, Geological setting and petrochemistry of the Narracoota Volcanics, Capricorn Orogen, Western Australia: Precambrian Research, v. 31, p. 107–132.

IRVING, A. J., 1978, A review of experimental studies of crystal/liquid trace element partitioning: Geochimica et Cosmochimica Acta, v. 42, p. 743–770.

JENSEN, L. S., 1976, A new cation plot for classifying subalkalic volcanic rocks: Ontario Division of Mines, Miscellaneous Paper 66, 22p.

JENSEN, L. S., and LANGFORD, F. F., 1986, Geology and petrogenesis of the Archaean Abitibi belt in the Kirkland Lake area, Ontario: Ontario Geological Survey, Miscellaneous Paper 123.

JONES, V. G., 1969, Pillow lavas as depth indicators: American Journal of Science, v. 267, p. 181–195.

KEATS, W., 1987, Regional geology of the Kalgoorlie–Boulder gold-mining district: Western Australia, Geological Survey, Report 21, 44p.

KELEMAN, P. B., JOHNSON, K. T. M., KINZLER, R. J., and IRVING, A. J., 1990, High-field-strength element depletions in arc basalts due to mantle-magma interaction: Nature, v. 345, p. 521–524.

KELLY, G. R., and DONALDSON, M. J., 1982, Geochemical discrimination between hangingwall and footwall basalts, St. Ives, Western Australia: Western Mining Corporation, Kambalda Nickel Operations report K/2629, 9p.

LANGSFORD, N., 1989, The stratigraphy of Locations 48 and 50 *in* The 1989 Kalgoorlie gold workshops (field volume) *edited by* I. M. GLACKEN: Australian Institute of Mining and Metallurgy and Eastern Goldfields Geological Discussion Group, Kalgoorlie, Western Australia, p. B1–B8.

LESHER, C. M., 1983, Localization and genesis of komatiite-associated Fe–Ni–Cu sulphide mineralization at Kambalda, Western Australia: University of Western Australia, Ph.D. thesis (unpublished).

LESHER, C. M., and ARNDT, N. T., 1990, Geochemistry of komatiite at Kambalda, Western Australia — Assimilation, crystal fractionation and lava replenishment: International Archaean Symposium, Third, Perth, Extended Abstracts, p. 149–151.

LEVY, I. L., 1975, The geology of the Bluebush area, Western Australia: Australian National University, B.Sc. Honours thesis (unpublished).

MARSTON, R. J., 1984, Nickel mineralization in Western Australia: Western Australia Geological Survey, Mineral Resources Bulletin 14.

MATSUDA, T., 1979, Collision of the Izu–Bonin arc with central Honshu — Cenozoic tectonics of the Fossa Magna, Japan, *in* Geodynamics of the Western Pacific *edited by* S. UYEDA, R. W. MURPHY, and K. KOBAYASHI: Japan Scientific Societies Press, Advances in Earth and Planetary Sciences 6, p. 409–421.

McCULLOCH, M. T., and COMPSTON, W., 1981a, Nd isotopic constraints on the age and petrogenesis of the Kambalda volcanics, Yilgarn Block, Western Australia: Australian National University, Research School of Earth Sciences, Annual report 1980, p. 179–180.

McCULLOCH, M. T., and COMPSTON, W., 1981b, Sm–Nd age of Kambalda and Kanowna greenstones and heterogeneity in the Archaean mantle: Nature v. 294, p. 322–327.

McCULLOCH, M. T., and COMPSTON, W., 1981c, Sm–Nd constraints on Kambalda and Kanowna greenstones: Australian Geological Convention, Fifth, Sediments through the ages, Geological Society of Australia, Abstracts 3, p. 82.

McDONALD, I. R., 1976, Terminal report — Exploration in the Paris–St Ives Temporary Reserve, 1965 to September 1975: Western Mining Corporation, Report M349 (unpublished).

McGOLDRICK, P. J., in press, Norseman 1:100 000 geology sheet: Western Australia Geological Survey.

McNAUGHTON, N. J., and CASSIDY, K. F., 1990, A reassessment of the age of the Liberty Granodiorite — Implications for a model of synchronous mesothermal gold mineralization within the Norseman–Wiluna Belt, Western Australia: Australian Journal of Earth Sciences, v. 37, p. 373–376.

MORRIS, P. A., 1990, Archaean volcanics at Norseman, Western Australia — Tholeiitic *and* alkalic magma?: International Archaean Symposium, Third, Perth ,1990, Extended Abstracts, p. 207–208.

MORRIS, P. A., in prep., Mulgabbie, Western Australia: Western Australia Geological Survey, 1:100 000 Geological Series Map.

MORRIS, P. A., ITAYA, T., WATANABE, T., and YAMAUCHI, Y., 1990, Potassium/argon ages of Cenozoic igneous rocks from eastern Shimane Prefecture, Oki Dozen Island, Southwest Japan and the Japan Sea opening: Journal of Southeast Asian Earth Sciences v. 4, p. 125–131.

MORRIS, P. A., and KAGAMI, H., 1989, Nd and Sr isotope systematics of Miocene to Holocene volcanic rocks from Southwest Japan — Volcanism since the opening of the Japan Sea: Earth and Planetary Science Letters, v. 92, p. 335–346.

MORRIS, P. A., McCUAIG, T. C., and KERRICH, R., in press, 2.7 Ga enriched high-MgO tholeiites from Norseman, Western Australia: The product of an enriched OIB-like mantle source: Geochimica et Cosmochimica Acta.

MORRIS, P. A., PESCUD, L., THOMAS, A., GAMBLE, J., TOVEY, E., and MARSH, N., 1991, Major element oxide, trace and rare earth element concentrations in Archaean mafic and ultramafic volcanic rocks from the Eastern Yilgarn Craton, Western Australia: Western Australia Geological Survey, Record, 1991/18, 78p.

NAKAMURA, N., 1974, Determination of REE, Ba, Fe, Mg, Na and K in carbonaceous and ordinary chondrites: Geochimica et Cosmochimica Acta, v. 38, p. 757–775.

NESBITT, R. W., and SUN, S. S., 1976, Geochemistry of Archaean spinifex textured peridotites and magnesian and low magnesian tholeiites: Earth and Planetary Science Letters, v. 31, p. 433–453.

NESBITT, R. W., SUN, S. S., PURVIS, A. C., 1979, Komatiites — Geochemistry and genesis: Canadian Mineralogist, v. 17, p. 165–186.

NIELSEN, R. L., 1988, TRACE.FOR — A program for the calculation of combined major and trace-element liquid lines of descent for natural magmatic systems: Computers and Geosciences, v. 14, p. 15–35.

OHTANI, E., 1990, Majorite fractionation and genesis of komatiite in the deep mantle: Precambrian Research, v. 48, p. 195–202.

OHTANI, E., KAWABE, I., MORIYAMA, J., and NAGATA, Y., 1989, Partitioning of elements between majorite garnet and melt implications for petrogenesis of komatiites: Contributions to Mineralogy and Petrology, v. 103, p. 263–269.

OTOFUJI, Y., and MATSUDA, T., 1984, Timing of rotational motion of southwest Japan inferred from paleomagnetism: Earth and Planetary Science Letters, v. 70, p. 373–382.

OTOFUJI, Y., MATSUDA, T., and NOHDA, S., 1985, Opening mode of the Japan Sea inferred from the paleomagnetism of the Japan Arc: Nature, v. 317, p. 603–604.

PEARCE, J. A., 1975, Basalt geochemistry used to investigate past tectonic environments on Cyprus: Tectonophysics, v. 25, p. 41–67.

PEARCE, J. A., 1982, Trace element characteristics of lavas from destructive plate boundaries, *in* Andesites *edited by* R. S. THORPE: New York, John Wiley and Sons, p. 525–548.

PEARCE, J. A., 1983, Role of the subcontinental lithosphere in magma genesis at active continental margins, *in* Continental basalts and mantle xenoliths *edited by* C. J. HAWKESWORTH and M. J. NORRY: Shiva Geology Series, p. 230–249.

PEARCE, J. A., 1987, An expert system for the characterization of ancient volcanic rocks: Journal of Volcanology and Geothermal Research, v. 32, p. 51–65.

PEARCE, J. A., and CANN, J. R., 1973, Tectonic setting of basic volcanic rocks determined using trace element analyses: Earth and Planetary Science Letters, v. 19, p. 290–300.

PEARCE, T. H., GORMAN, B. E., and BIRKETT, T. C., 1977, The TiO_2–K_2O–P_2O_5 diagram — A method of discriminating between oceanic and non-oceanic basalts: Earth and Planetary Science Letters, v. 24, p. 419–426.

PEATE, D. W., HAWKESWORTH, C. J., MANTOVANI, M. S. M., and SHUKOWSKY, W., 1990, Mantle plumes and flood-basalt stratigraphy in the Parana, South America: Geology, v. 18, p. 1223–1226.

PERFIT, M., 1990, The role of fluids in arc-related magmas in the southwest Pacific — Some news and reviews: Australian Geological Congress, 10th, Abstracts, p. 202–203.

PHILLIPS, G. N., GROVES, D. I., and BROWN, I. J., 1987, Source requirements for the Golden Mile, Kalgoorlie — Significance to the metamorphic replacement model for Archaean gold deposits: Canadian Journal of Earth Sciences, v. 24, p. 1643–1651.

REDMAN, B. A., 1982, Petrography, petrology and geochemistry of Archaean basic volcanism in the Eastern Goldfields Province, Western Australia — Stratigraphic controls on gold mineralisation: Parkville, University of Melbourne, M.Sc. thesis (unpublished).

REDMAN, B. A., and KEAYS, R. R., 1985, Archaean basic volcanism in the Eastern Goldfields Province, Yilgarn Block, Western Australia: Precambrian Research, v. 30, p. 113–152.

RICHARDS, M. A., DUNCAN, R. A., and COURTILLOT, V. E., 1989, Flood basalts and hot spot tracks — Plume heads and tails: Science, v. 240, p. 103–107.

ROBERTS, D. E., 1988, Kambalda–St Ives area and the Victory–Defiance complex, *in* Bicentennial Gold 88, Excursion Guidebook, Western Australian Gold Deposits *edited by* D. I. GROVES, M. E. BARLEY, S. E. HO, and C. M. F. HOPKINS: University of Western Australia, Geology Department and University Extension, Publication 14, p. 109–113.

ROBERTS, D. E., and ELIAS, M., 1990, Gold deposits of the Kambalda–St Ives region, *in* Geology of the Mineral Deposits of Australia and Papua New Guinea *edited by* F. E. HUGHES: Melbourne, The Australasian Institute of Mining and Metallurgy, p. 479–491.

ROBINSON, P. T., FLOWER, M. F. J., SWANSON, D. A., and STAUDIGEL, H., 1979, Lithology and eruption stratigraphy of Cretaceous oceanic crust, western Atlantic Ocean — Initial report of the Deep Sea Drilling Project 51: Washington, U. S. Government Printing Office, p. 1535–1546.

ROBINSON, P. T., GIBSON, I. L., and PANAYIOTOU, A, (editors), 1987, Cyprus crustal project — Initial report, Holes CY-2 and 2a: Canada, Geological Survey, Special Paper 85-29, 381p.

RODDICK, J. C., 1984, Emplacement and metamorphism of Archaean mafic volcanics at Kambalda, Western Australia — Geochemical and isotopic constraints: Geochimica et Cosmochimica Acta, v. 48, p. 1305–1318.

SAUNDERS, A. D., TARNEY, J., MARSH, N. G., and WOOD, D., 1980, Ophiolites as ocean crust or marginal basin — A geochemical approach: International Ophiolite Symposium, Cyprus, 1979 *edited by* A PANAYIOUTU, Republic of Cyprus, Proceedings, p. 193–204.

SEYFRIED, W. E., MOTTL, M. J., and BISCHOFF, J. L., 1978, Seawater/basalt ratio effects on the chemistry and mineralogy of spilites from the ocean floor: Nature v. 275, p. 211–213.

SPRAY, J. G., 1985, Geological setting of Archaean vein-type gold deposits within the Norseman greenstone sequence, Western Australia, *in* Metallogeny of basic and ultrabasic rocks *edited by* M. J. GALLAGHER, R. A. IXER, C. R. NEWRY, and H. M. PRICHARD, Institute of Mining and Metallurgy, London, p. 133–150.

SUN, S. S., 1989, Growth of lithospheric mantle: Nature v. 340, p. 509–510.

SUN, S. S., and McDONOUGH, W. F., 1989, Chemical and isotopic systematics of oceanic basalts — Implications for mantle composition and processes, *in* Magmatism in the ocean basins *edited by* A. D. SAUNDERS and M. J. NORRY: Geological Society, Special Publication 42, p. 313–345.

SUN, S. S., and NESBITT, R. W., 1978, Petrogenesis of Archaean ultrabasic and basic volcanics — Evidence from rare earth elements: Contributions to Mineralogy and Petrology, v. 65, p. 301–325.

SUN, S. S., NESBITT, R. W., and McCULLOCH, M. T., 1989, Geochemistry and petrogenesis of Archaean and early Proterozoic siliceous high-magnesian basalts, *in* Boninites and related rocks *edited by* A. J. CRAWFORD: Allen and Unwin, p. 148–173.

SWAGER, C. P., 1989a, Structure of Kalgoorlie greenstones — Regional deformation history and implications for the structural setting of the Golden Mile gold deposits: Western Australia Geological Survey, Report 25, p. 59–84.

SWAGER, C. P., 1989b, Dunnsville, Western Australia: Western Australia Geological Survey, 1:100 000 Geological Map Series.

SWAGER, C. P., in prep., Kurnalpi, Western Australia: Western Australia Geological Survey, 1:100 000 Geological Map Series.

SWAGER, C. P., and GRIFFIN, T. J., 1990, An early thrust duplex in the Kalgoorlie–Kambalda greenstone belt, Eastern Goldfields Province, Western Australia: Precambrian Research, 48, p. 63–73

SWAGER, C., GRIFFIN, T. J., WITT, W. K., WYCHE, S. W., AHMAT, A. L., HUNTER, W. M., and McGOLDRICK, P. J., 1990, Geology of the Archaean Kalgoorlie Terrane — An explanatory note: Western Australia Geological Survey, Record 1990/12, 54p.

TARNEY, J., DALZIEL, I. W. D., and De WIT, M. J., 1981, Marginal basin 'Rocas Verdes' complex from southern Chile — A model for Archaean greenstone belt formation *in* The early history of the earth *edited by* B. F. WINDLEY: New York, John Wiley and Sons, p. 131–146.

TATSUMI, Y., HAMILTON, D. L., and NESBITT, R. W., 1986, Chemical characteristics of fluid phase released from a subducted lithosphere and origin of arc magmas — Evidence from high-pressure experiments and natural rocks: Journal of Volcanology and Geothermal Research, v. 29, p. 293–309.

TAYLOR, S. R., and McLENNAN, S. M., 1985, The Continental Crust — Its Composition and Evolution: Melbourne, Blackwell Scientific Publications, 312p.

THOMSON, B., 1985, Progress report November 1985, Hunt Shoot: Kambalda Nickel Operations, Report K/2850, 78p.

THOMSON, B., 1989a, B1 subdivisions in thin komatiites at Kambalda, Western Australia: *Geological Magazine*, v. 126, p. 263–270.

THOMSON, B., 1989b, Petrology and stratigraphy of some texturally well preserved thin komatiites from Kambalda, Western Australia: Geological Magazine, v. 126, p. 249–261.

THOMPSON, R. N., MORRISON, M. A., DICKIN, A. P., and HENDRY, G. L., 1983, Continental flood basalts . . . arachnids rule, OK? *in* Continental basalts and mantle xenoliths *edited by* C. J. HAWKESWORTH and M. J. NORRY: Shiva Geology Series, p. 158–185.

TRAVIS, G. A., WOODALL, R., and BARTRAM, G. D., 1971, The geology of the Kalgoorlie Goldfields, *in* Symposium on Archaean Rocks *edited by* J. E. GLOVER: Geological Society of Australia, Special Publication 3, p. 175–190.

WHITE, R. W., and McKENZIE, D., 1989, Magmatism at rift zones — The generation of volcanic continental margins and flood basalts: Journal of Geophysical Research, v. 94, p. 7685–7729.

WILLIAMS, I. R., 1975, Eastern Goldfields Province: Western Australia Geological Survey, Memoir 2, p. 33–54.

WINCHESTER, J. A., and FLOYD, P. A., 1976, Geochemical magma type discrimination — Application to altered and metamorphosed basic igneous rocks: Earth and Planetary Science Letters v. 28, p. 459–469.

WITT, W. K., 1987, Stratigraphy and layered mafic/ultramafic intrusions of the Ora Banda sequence, Bardoc 1:100 000 sheet, Eastern Goldfields — An excursion guide: Eastern Goldfields Geological Field Conference, 2nd, Geological Society of Australia, Western Australian Division, Abstracts and Excursion Guide, p. 69–83.

WITT, W. K., 1990, Geology of the Bardoc 1:100 000 sheet, Western Australia: Western Australia Geological Survey, Record 1990/14, 111p.

WITT, W. K., 1993, Gold mineralization in the Menzies–Kambalda region, Eastern Goldfields, Western Australia: Western Australia Geological Survey, Report 39, 165p.

WITT, W. K., and HARRISON, N., 1989, Volcanic rocks and bounding shear zones of the Ora Banda greenstone sequence, *in* The 1989 Kalgoorlie Gold Workshops *edited by* I. M. GLACKEN: Australasian Institute of Mining and Metallurgy, A2–A7.

WOOD, D. A., GIBSON, I. L, and THOMPSON, R. N., 1976, Elemental mobility during zeolite facies metamorphism of the Tertiary basalts of eastern Iceland: Contributions to Mineralogy and Petrology, v. 55, p. 241–254.

WOOD, D. A., and JORON, J-L., and TREUIL, M., 1979, A re-appraisal of the use of trace elements to classify and discriminate between magma series erupted in different tectonic settings: Earth and Planetary Science Letters, v. 45, p. 326–336.

WOODALL, R. W., 1965, Structure of the Kalgoorlie Goldfield, *in* Geology of Australian Ore Deposits (2nd edition) *edited by* J. McANDREW: Melbourne, Eighth Imperial Mining and Metallurgical Congress, p. 71–79.

YODER, H. S., 1988, The great basaltic 'floods': South African Journal of Geology, v. 91, p. 139–156.

Appendix 1

Representative petrographic descriptions of breccia types, and variolitic basalt

Petrography of flow-top breccias

100189, Vettersburg, Siberia Komatiite (VBD-1, 147.2 m):

Angular fragments up 5 mm across consist of wispy to feathery (occasionally blocky) tremolite and talc, set in a groundmass of chlorite and serpentinite. Fragment edges are slightly finer grained (?chilled) and have a higher proportion of elongate (?quenched) crystallites and ?altered glass. Fragments are separated by a maximum of 0.4 mm matrix.

99577, Kambalda, Lunnon Basalt (KD1029, 410.9 m):

Weakly interlocking 'organized' breccia comprising angular, fine-grained, originally glassy, basalt fragments up to 20 mm in diameter, now with epidote patches. Occasional patches of amphibole and calcite. Amphibole is feathery and acicular (quenched). One patch of quartz, calcite, and felspar is probably of sedimentary origin. Weak cementation of breccia by ?altered glass.

99958, Norseman, Woolyeenyer Formation, (S156, 160.3 m):

Angular fragments of basalt up to 10 mm in diameter. Originally glassy fragments are now matted, feathery, weakly fasicular, green amphibole and enclose sparsely disseminated plagioclase euhedra up to 0.3 mm long. Fragment rims lack plagioclase and are finer grained than cores. Possible weak development of spherules (?after glass pools). Fragment interstices are ?altered glass with scattered feldspar, biotite, and bunches of amphibole. Occasional felsic areas contain clots of epidote. Some areas show clast support.

Appendix 2

Physical volcanology: observed and interpreted features in selected drillcore

KEY TO APPENDICES SHOWING DRILL LOGS

Use this key to interpret drill logs throughout the text. Features are used in combination. Thus:

FG BAS, BI, CC V — is fine grained variolitic basalt with noticeable biotite and calcite veining.

(1) ROCK TYPE

- Medium grained mafic or ultramafic
- Fine grained mafic or ultramafic
- Doleritic (possible sill)
- Felsic porphyry
- Pillow lava
- Pillow curvature

(2) BRECCIA

- Hydraulic breccia
- Mass-flow breccia
- Flow-top breccia
- Minor brecciation

(3) OTHER

- Random spinifex texture
- Platy olivine spinifex texture
- Vein
- Variolitic

(4) CONTACT

- Sharp
- Diffuse

PAM11

ABBREVIATIONS ADJACENT TO COLUMN

- Feature decreases in direction of arrow
- p 45 — Pillow thickness (cm)
- 45 — Flow thickness (cm)
- 100181 — GSWA sample location

(5) GRAIN SIZE AND TEXTURE

FG	Fine-grained
CG	Coarse-grained
GS	Grain-size
CUM	Cumulate texture
ST	Spinifex texture

(6) COLOUR AND HUE

DK	Dark
GN	Green
BN	Brown
GY	Grey

(7) SECONDARY PHASES

CC	Calcite
Q	Quartz
BI	Biotite

(8) ROCK TYPE

BAS	Basalt
DOL	Dolerite
UM	Ultramafic
PB	Pillow basalt

(9) OTHER

SHATTERED	Core shattered
V	Veining
BLEACHED	Core has undergone alteration giving a bleached appearance (usually albitisation).

- Sheared

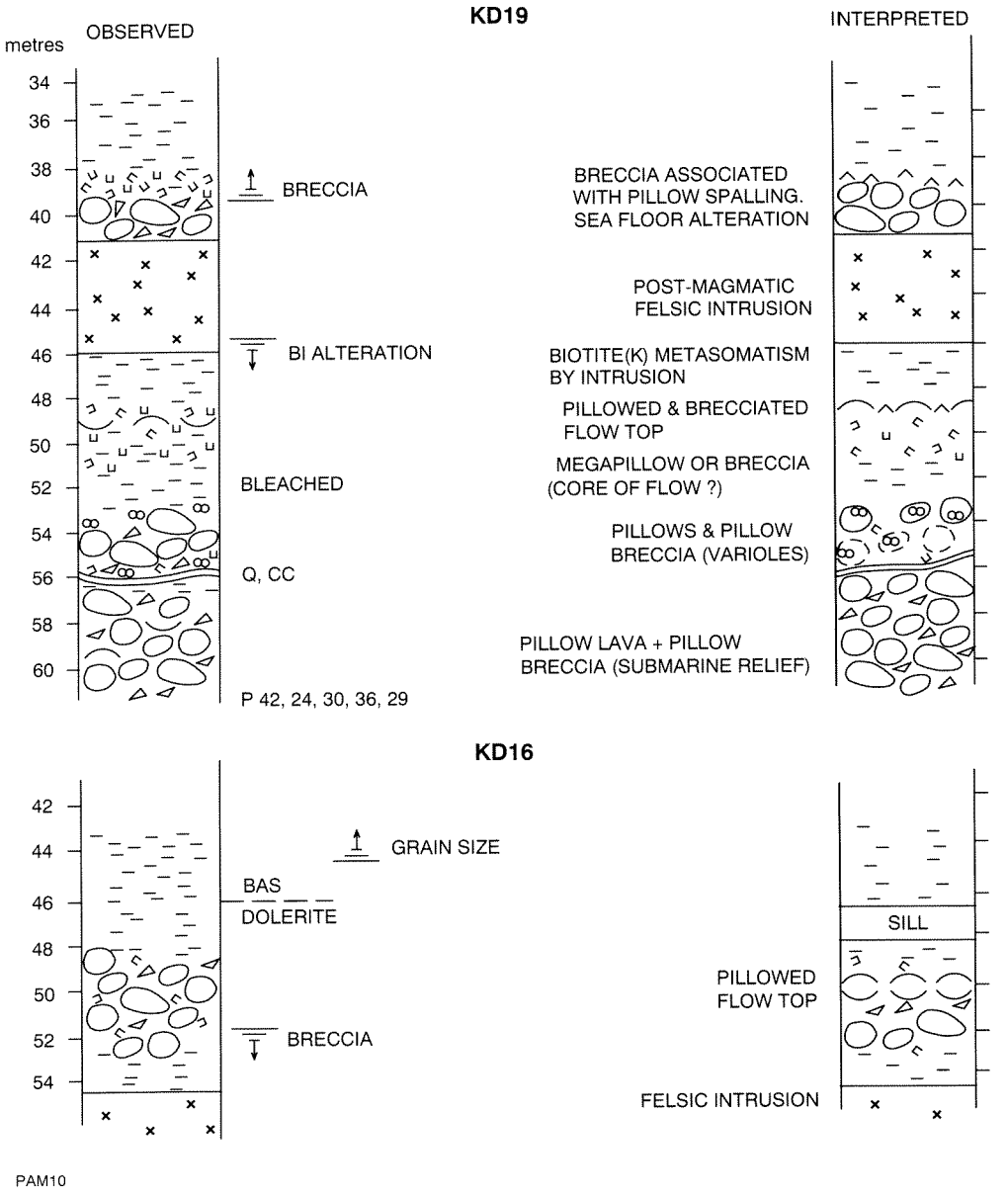

Appendix 2.1 Observed and interpreted features in drillcore through the upper part of the lower basalt unit at Kambalda, drillholes KD19 and KD16.

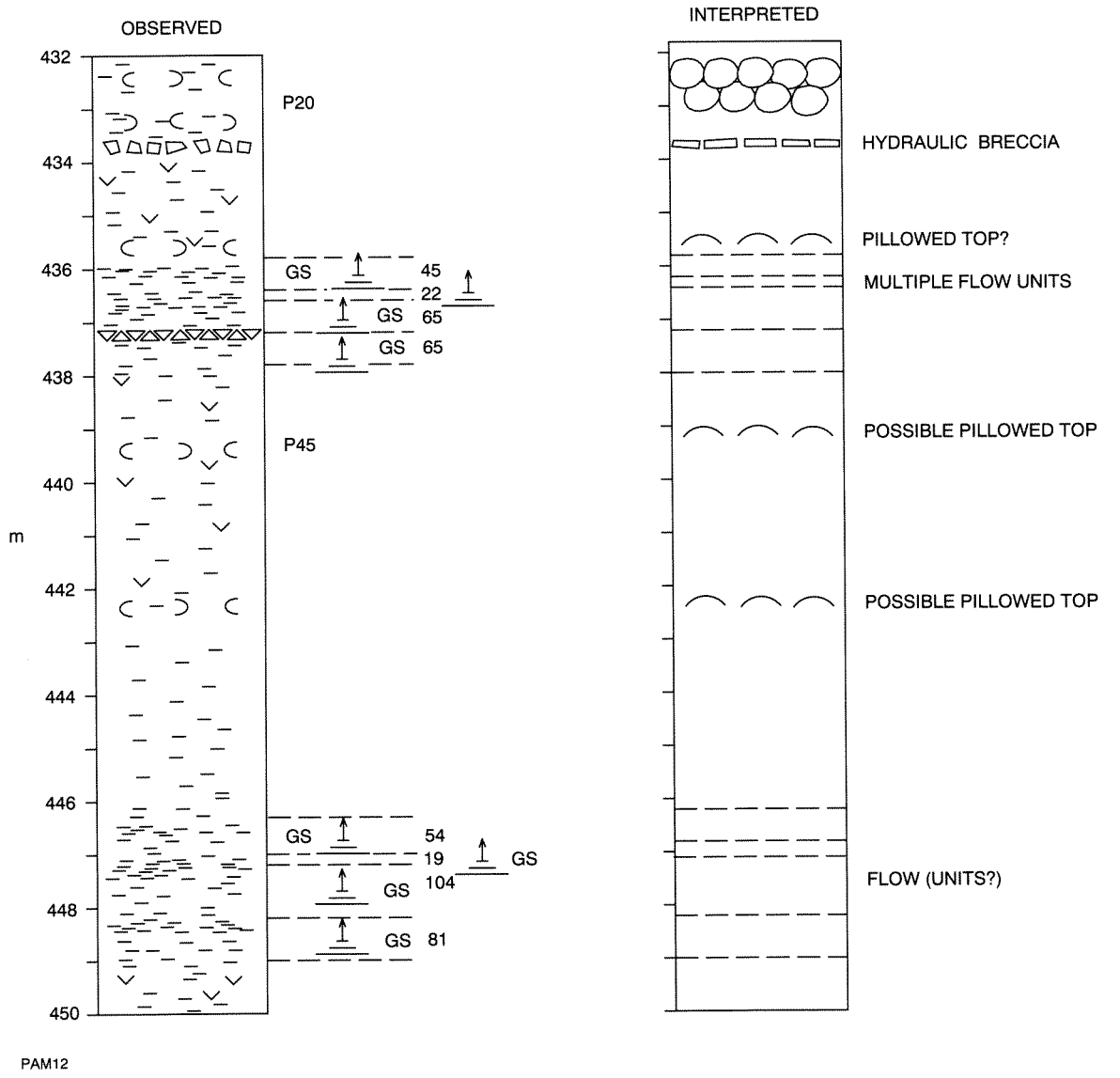

Appendix 2.2 Observed and interpreted features from the lower basalt unit, drillhole TD842, Tramways area, Kambalda Domain. See Appendix 2.1 for explanation of symbols.

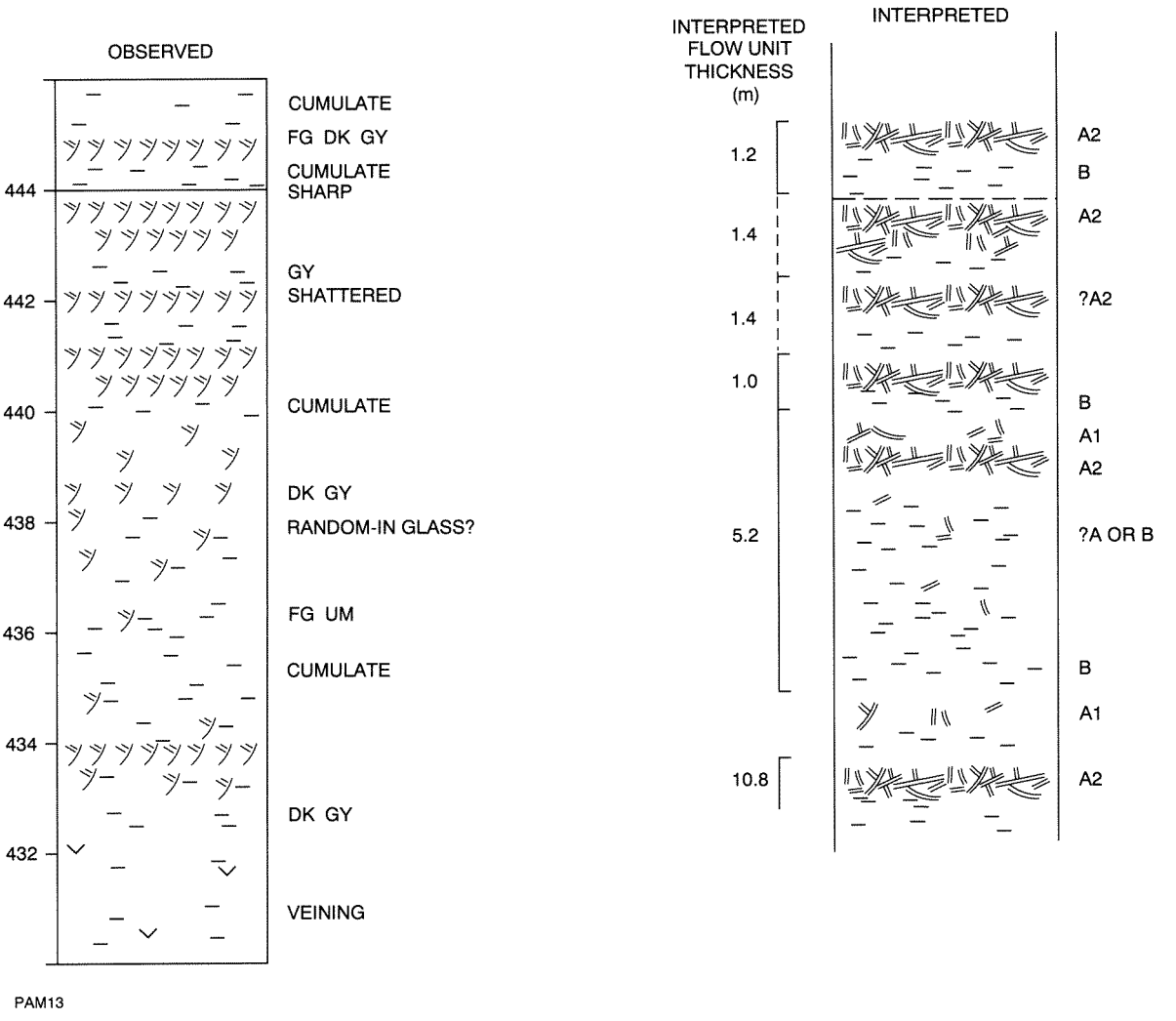

Appendix 2.3 Observed and interpreted features from the komatiite unit, drillhole SE9, Hannan Lake area, Kalgoorlie, Kambalda Domain. See Appendix 2.1 for explanation of symbols.

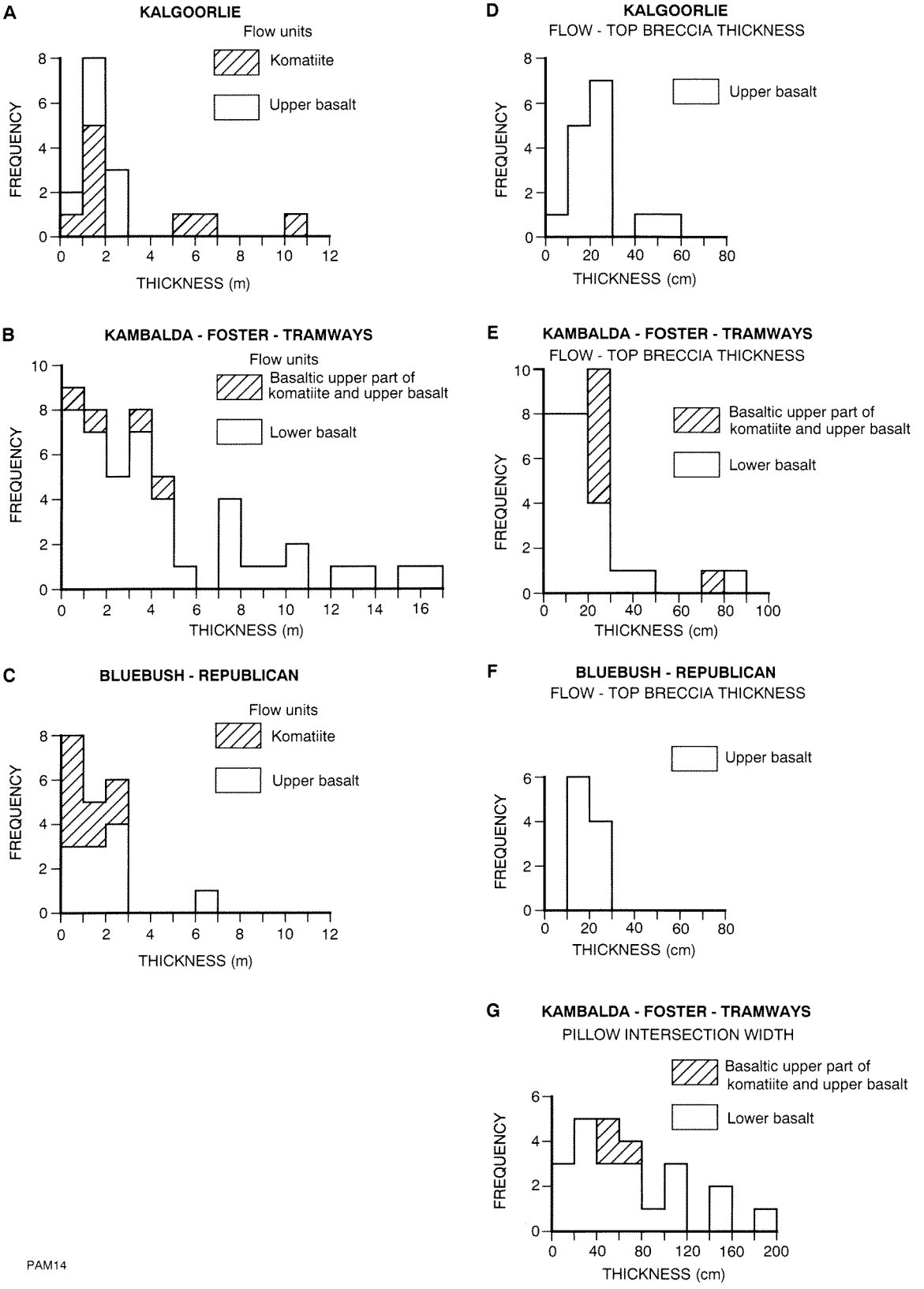

Appendix 2.4 Frequency histograms for the thicknesses (metres) of flow units, flow-top breccias, and pillow intersections, in the Kambalda Domain.

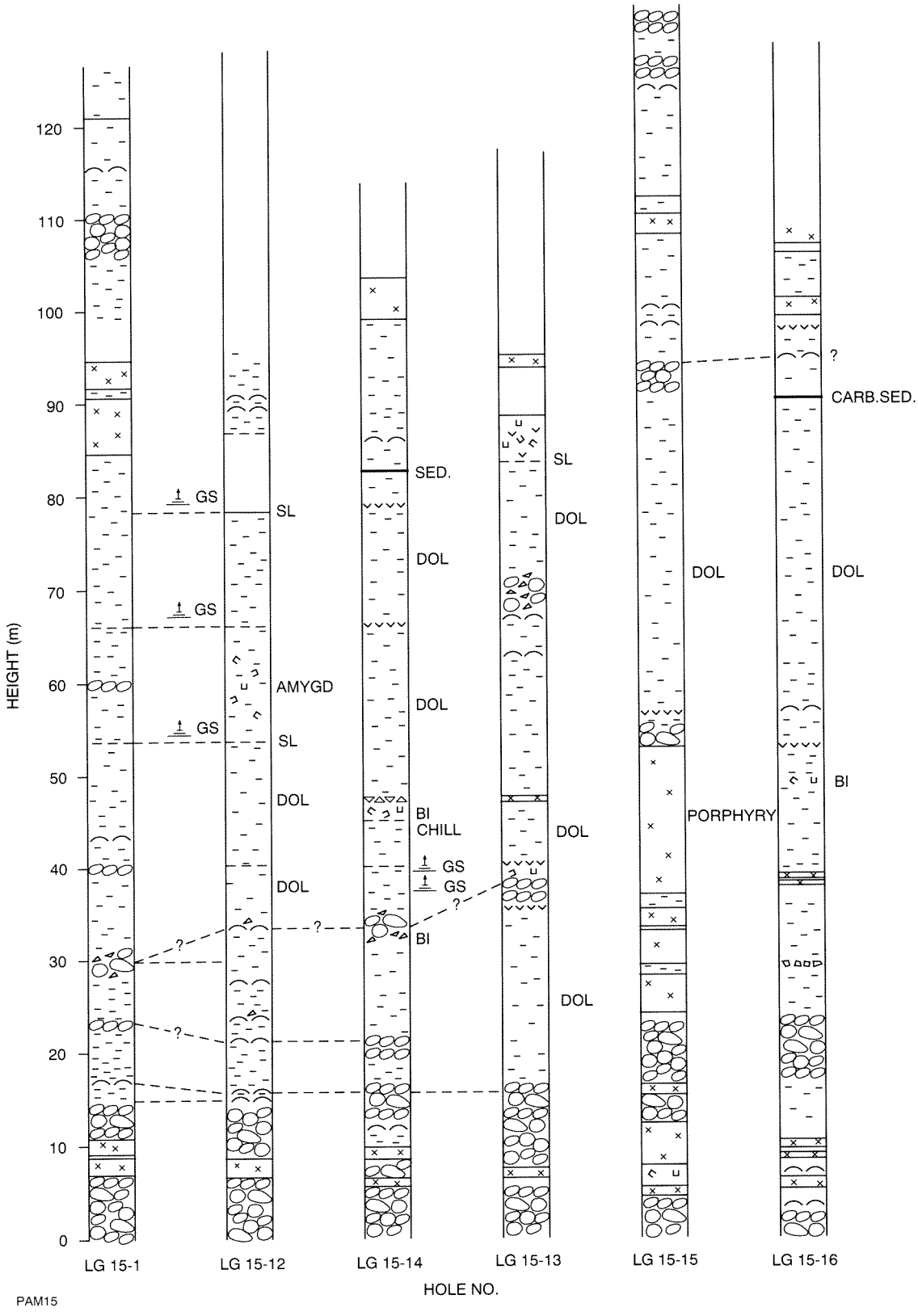

Appendix 2.5 Observed features in 6 diamond drillholes, drilled from a common collar, 15 Level, Long Shaft, Kambalda, Kambalda Domain. See Appendix 2.1 for explanation of symbols. Dotted lines join possible common features.

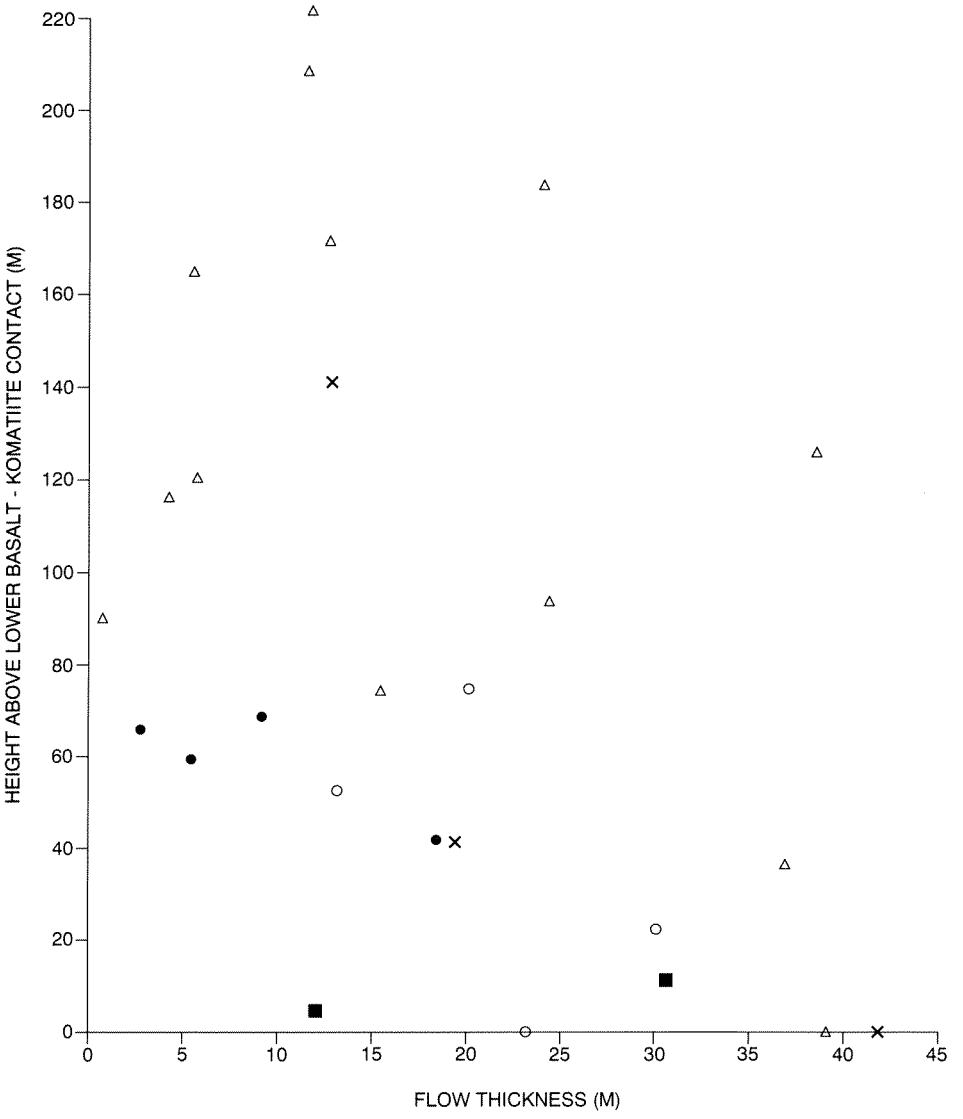

PAM16

Appendix 2.6 **Height above contact between lower basalt unit and komatiite unit (metres) versus flow thickness (metres) in drillcore from Kambalda, Foster and Tramways. Symbols: closed circles — TD842; cross — TD797 (both Tramways); open circle — CD259; closed square — CD201 (both Foster); open diamond — KD330 (Kambalda).**

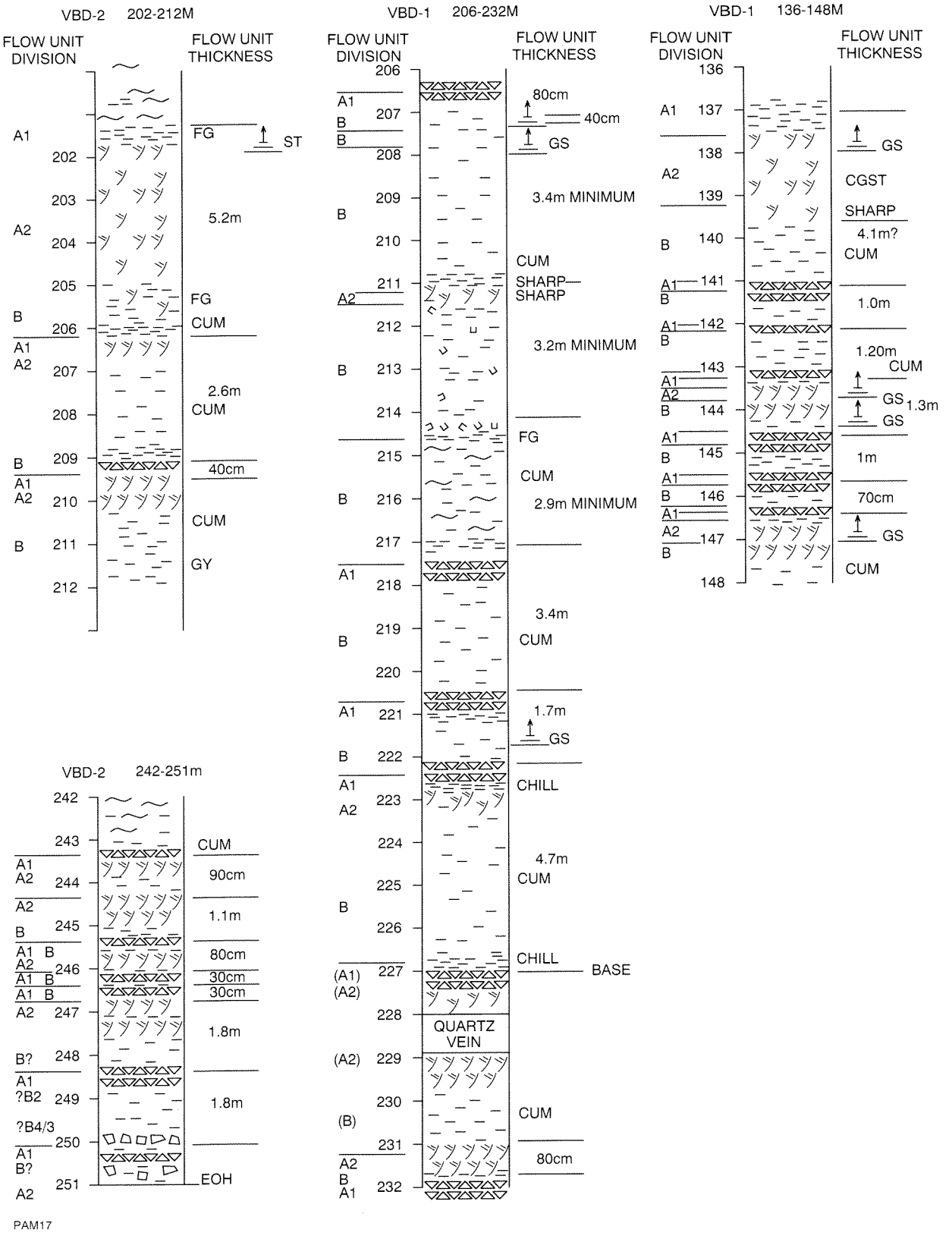

Appendix 2.7 Interpreted division of flow units in komatiite unit from diamond drillcore VBD-1 and VBD-2, Siberia Komatiite at Vettersburg. See Appendix 2.1 for explanation of symbols, and Figure 6 for division of flow unit.

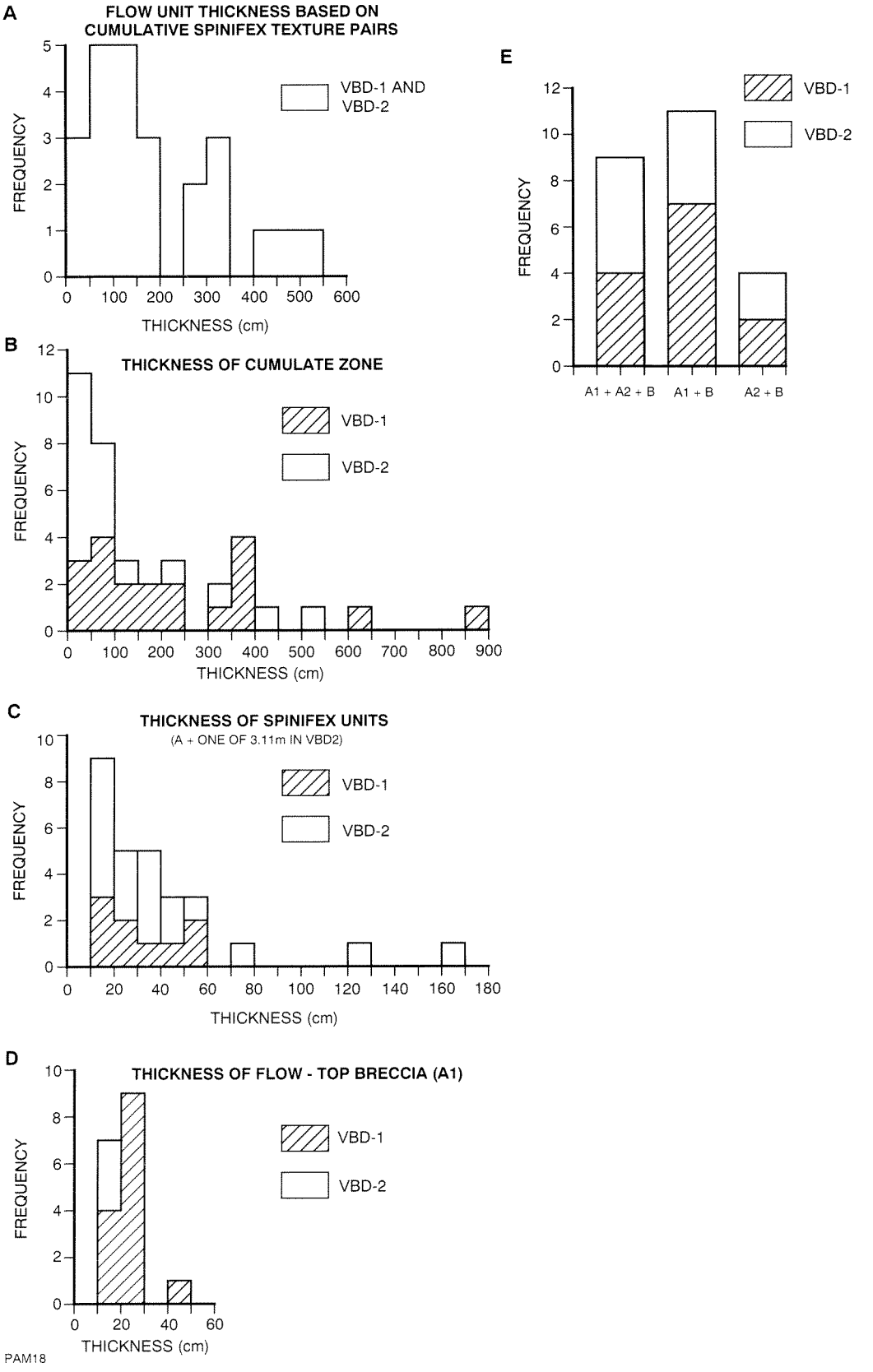

Appendix 2.8 **Frequency histograms for thicknesses of flow units, cumulate zones, spinifex units, flow-top breccias, and A + B associations in komatiite unit of the Siberia Komatiite. Diamond drillholes VBD-1 and VBD-2, Vettersburg.**

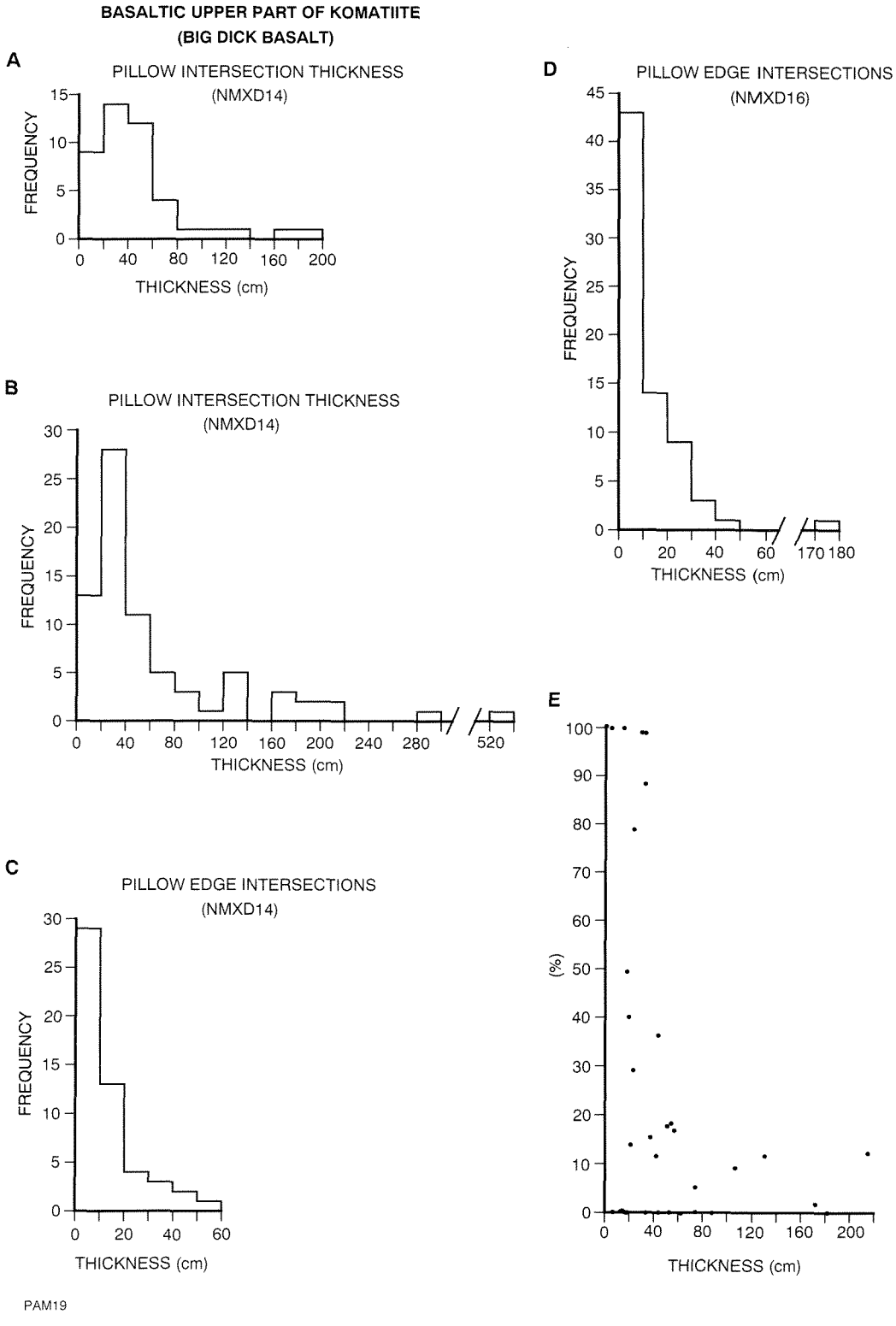

Appendix 2.9 **Frequency histograms for pillow intersection widths (A, B), and pillow edge widths (C, D) for the basaltic upper part of the komatiite unit in drillcore from Theil well (NMXD14 and NMXD16), Ora Banda Domain. E. Variole intersection width (as a percentage of pillow intersection width) versus pillow intersection width in the basaltic upper part of the komatiite unit, drillcore from NMXD14, Theil Well, 96–121 m, Ora Banda Domain. Frequency histograms of pillow intersection widths (F, G), and pillow edge thicknesses (H) for the Upper basalt unit of the Ora Banda Domain (Victorious and Bent Tree Basalts).**

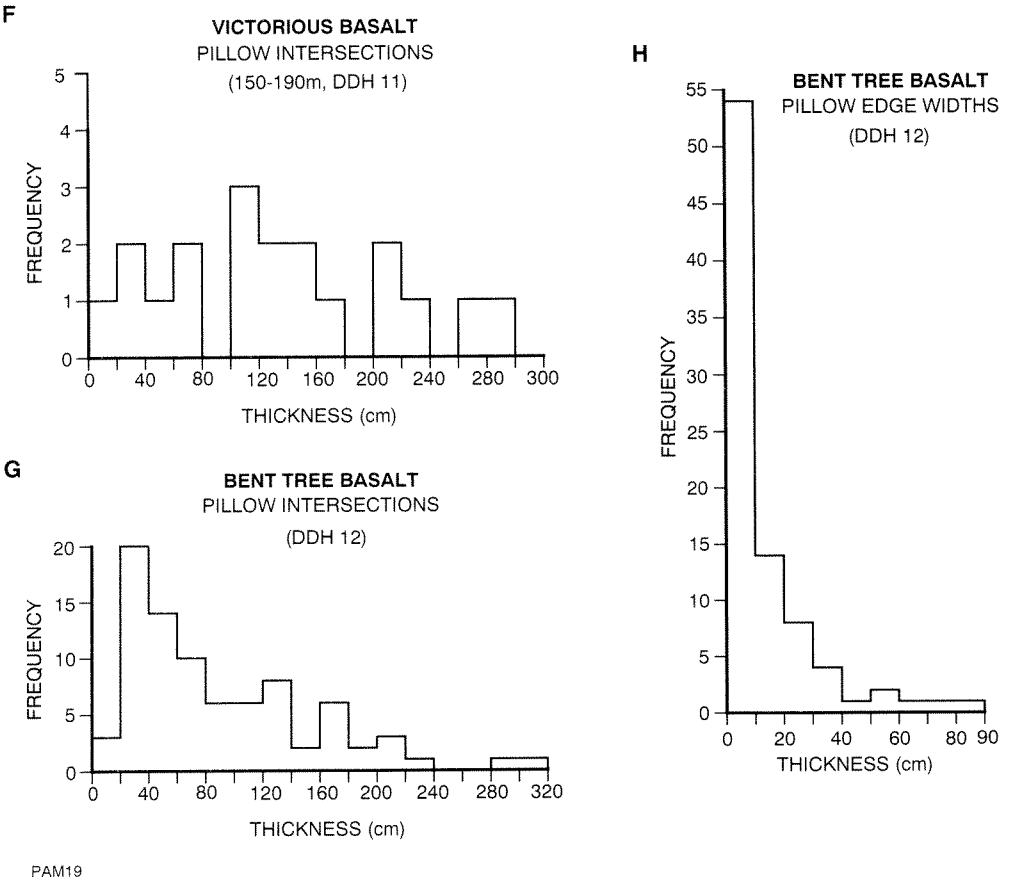

Appendix 2.9 (continued) (see previous page)

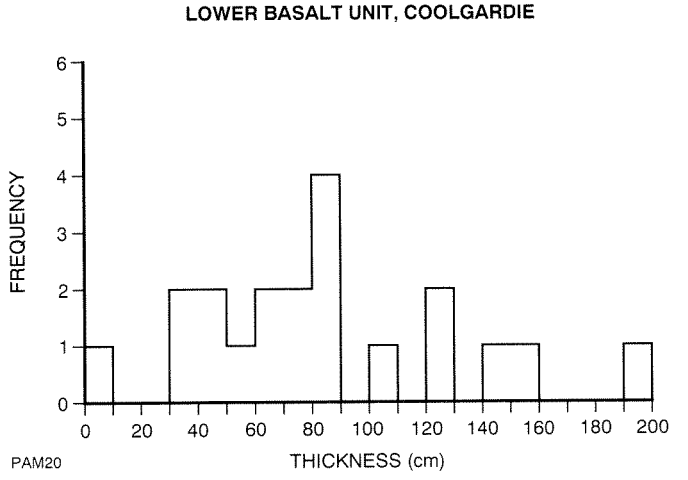

Appendix 2.10 Frequency histogram of pillow intersection thicknesses, drillcore from the lower basalt unit, Coolgardie Domain, Coolgardie.

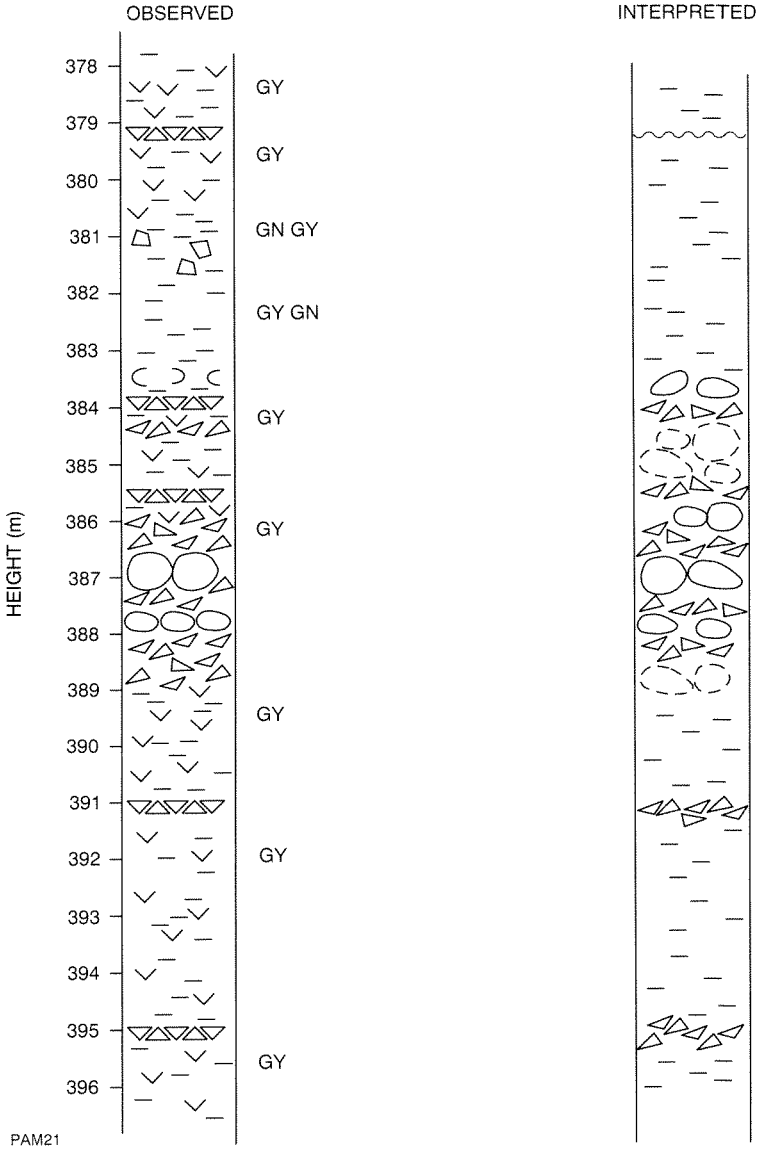

Appendix 2.11 Observed and interpreted features in the lower basalt unit of the Boorara Domain at Carnilya Hill. Drillhole CHD412 between 378 and 396 m.

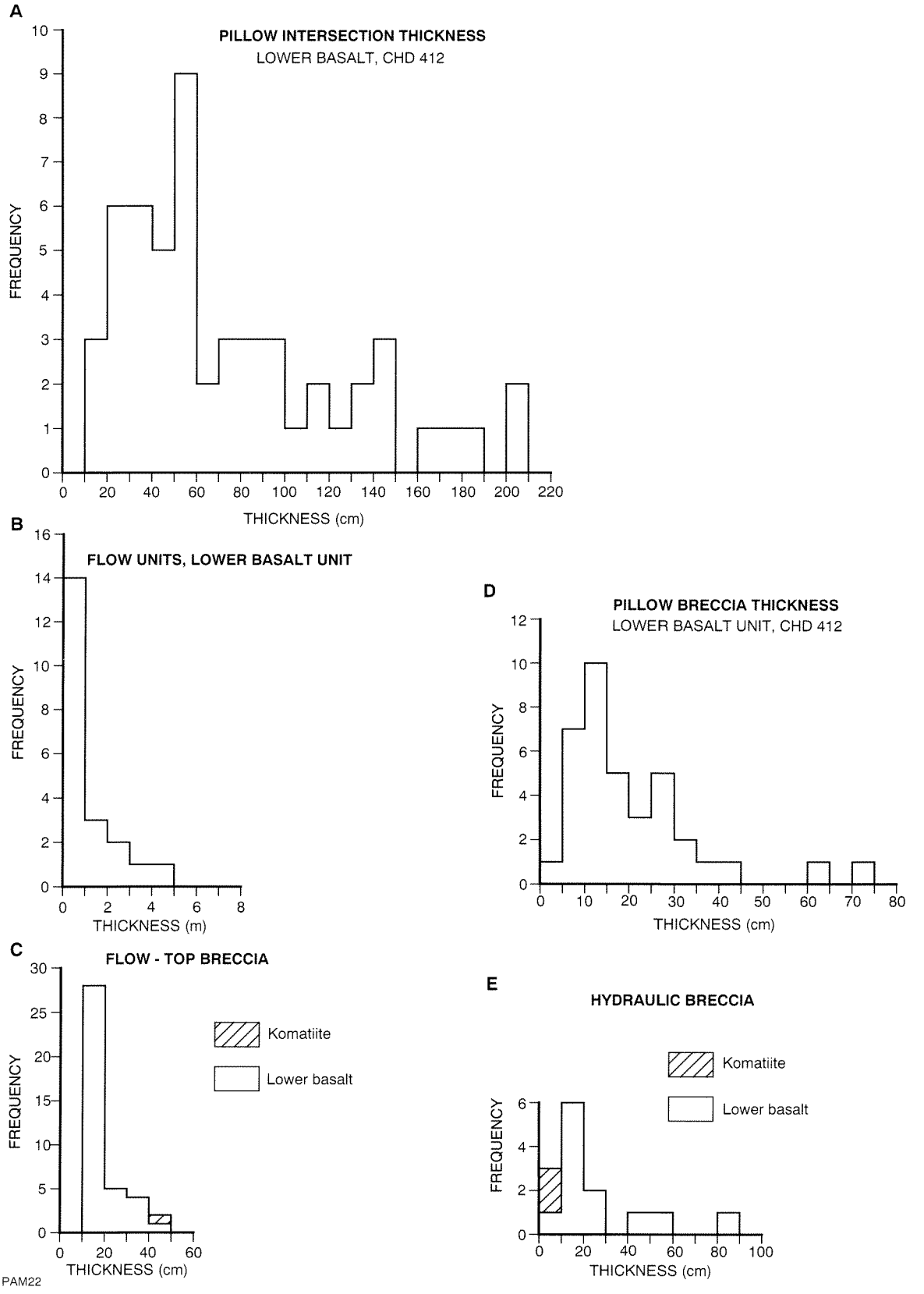

Appendix 2.12 Frequency histograms of pillow intersection thicknesses (A), flow unit (B), flow-top breccia (C), pillow breccia (D), and hydraulic breccia (E) in drillcore from the lower basalt unit of the Boorara Domain at Carnilya Hill.

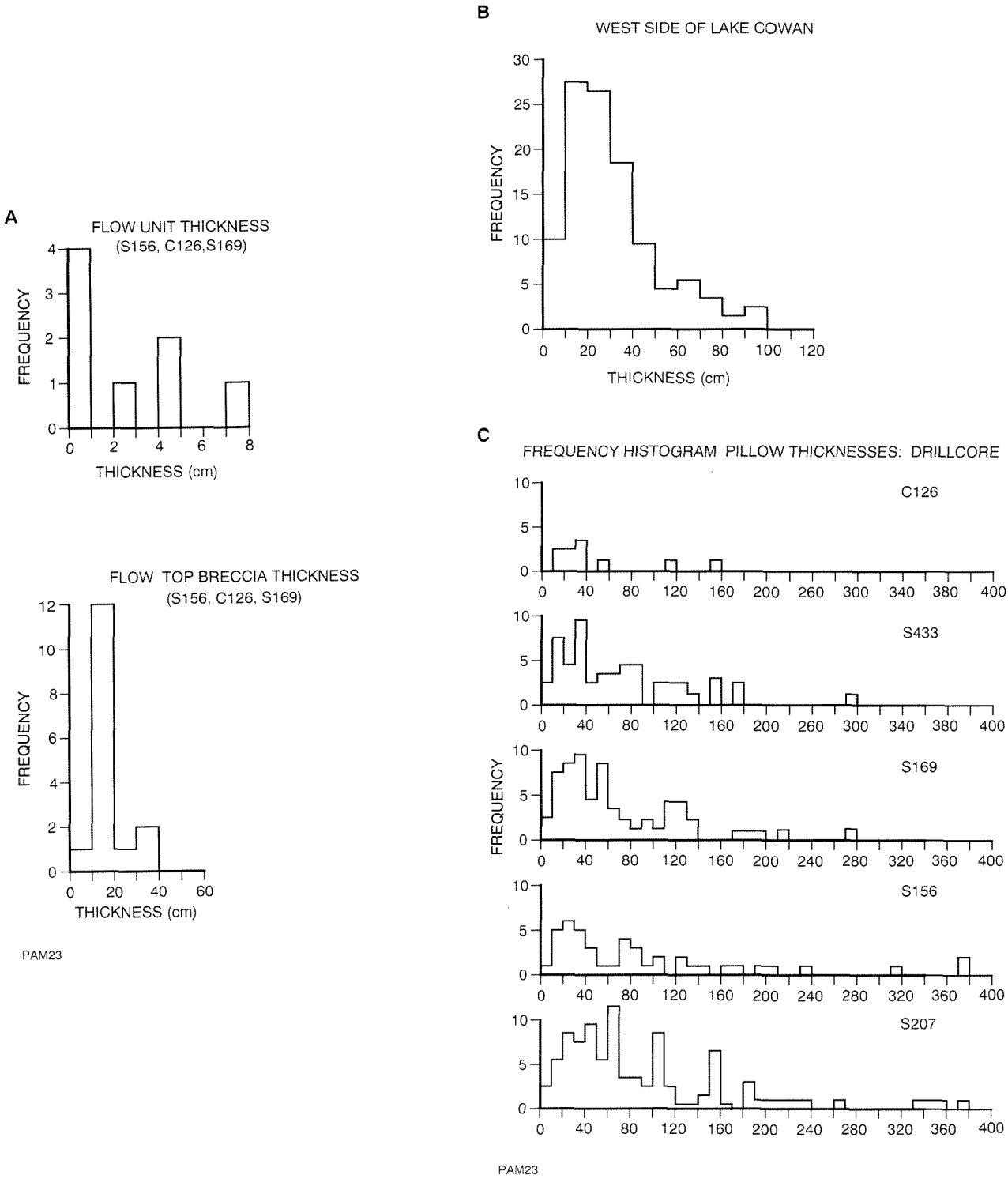

Appendix 2.13 **A. Frequency histograms for thicknesses of flow units, and flow-top breccias in diamond drillholes S156, C126, and S169, Woolyeenyer Formation, Norseman Terrane.**

B. Frequency histograms for pillow intersection thicknesses in drillcore and on the western shore of Lake Cowan.

C. Frequency histograms for pillow thicknesses measured in drillcore, Woolyeenyer Formation, Norseman Terrane.

D. Frequency histograms for interpillow thicknesses measured in drillcore, Woolyeenyer Formation, Norseman Terrane.

E. Frequency histograms for pillow edge thicknesses measured in drillcore, Woolyeenyer Formation, Norseman Terrane.

D FREQUENCY HISTOGRAMS INTER-PILLOW THICKNESS

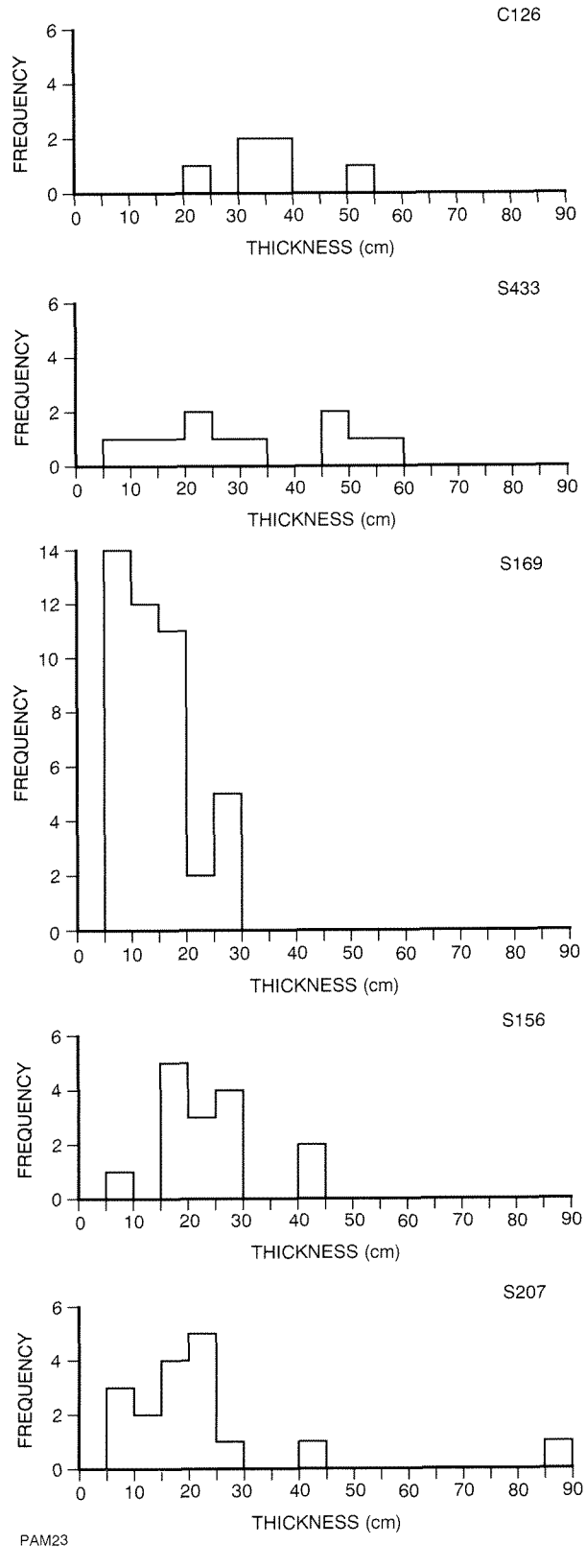

E

FREQUENCY HISTOGRAM PILLOW EDGE THICKNESS

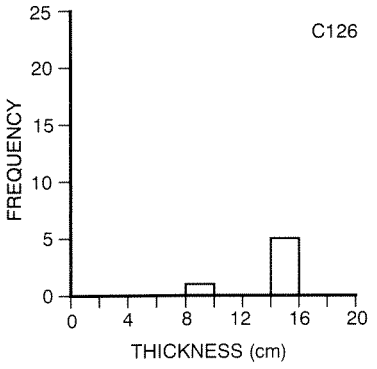

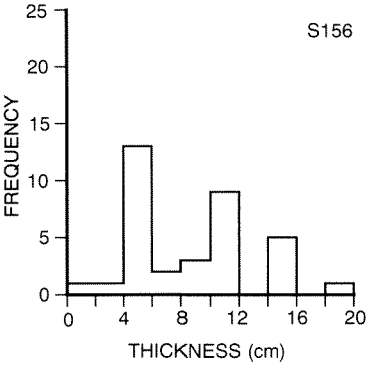

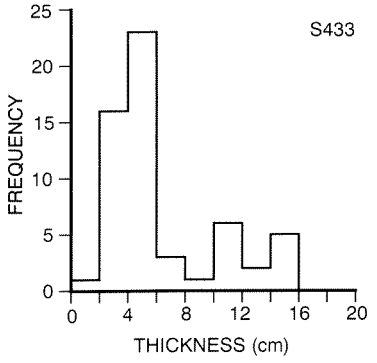

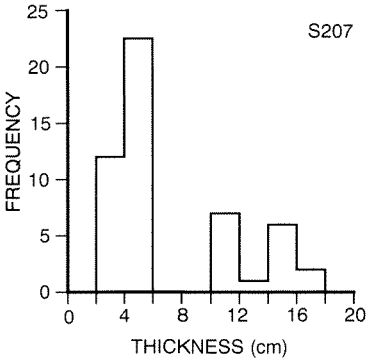

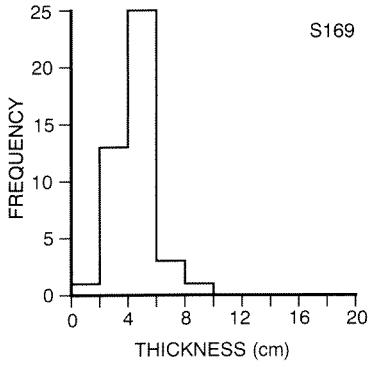

PAM23

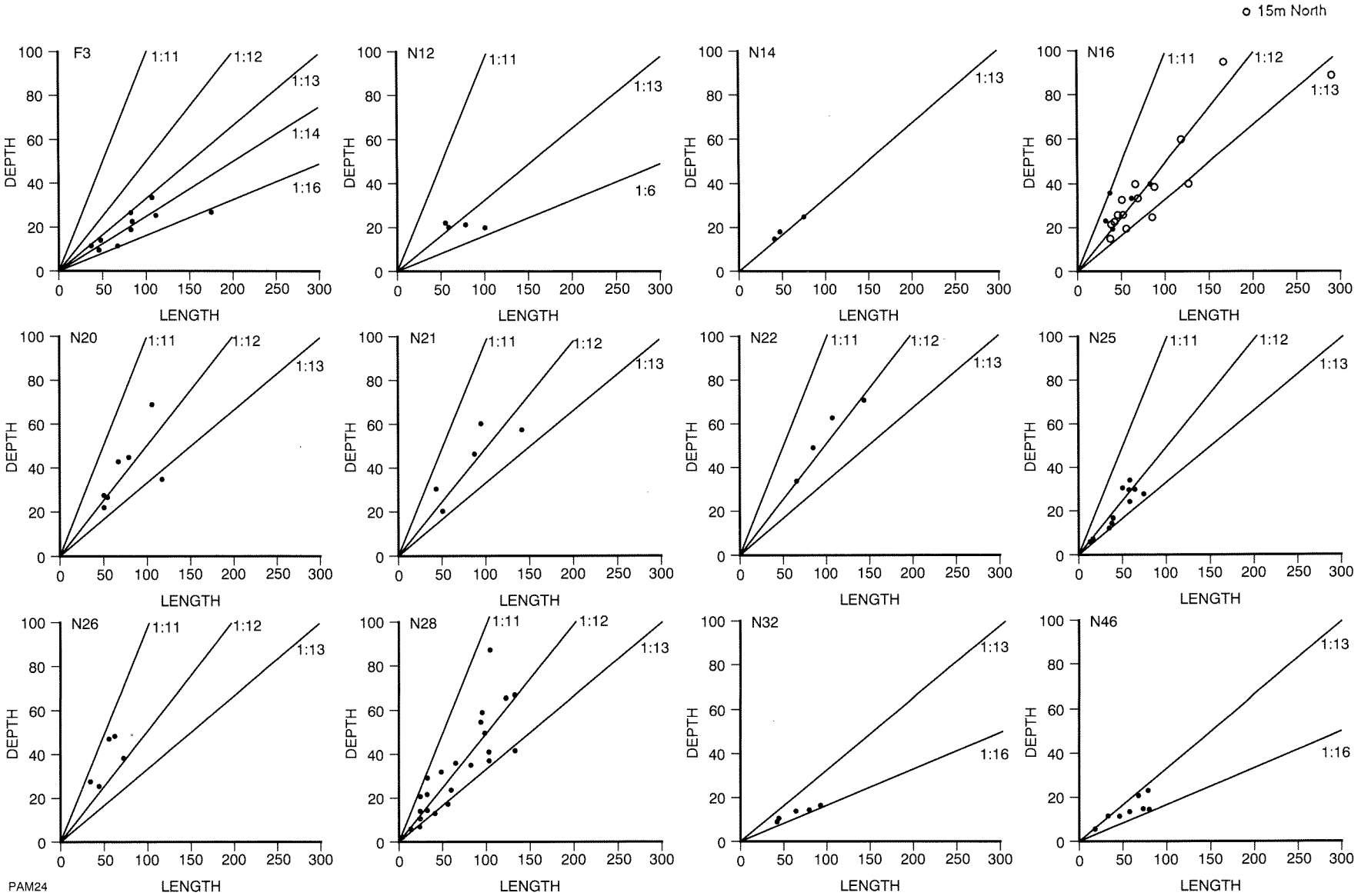

Appendix 2.14 Plots of pillow dimensions (vertical versus horizontal) for outcrops of the Woolyeenyer Formation, on the western shore of Lake Cowan, Norseman Terrane. See Figure 7 for locations.

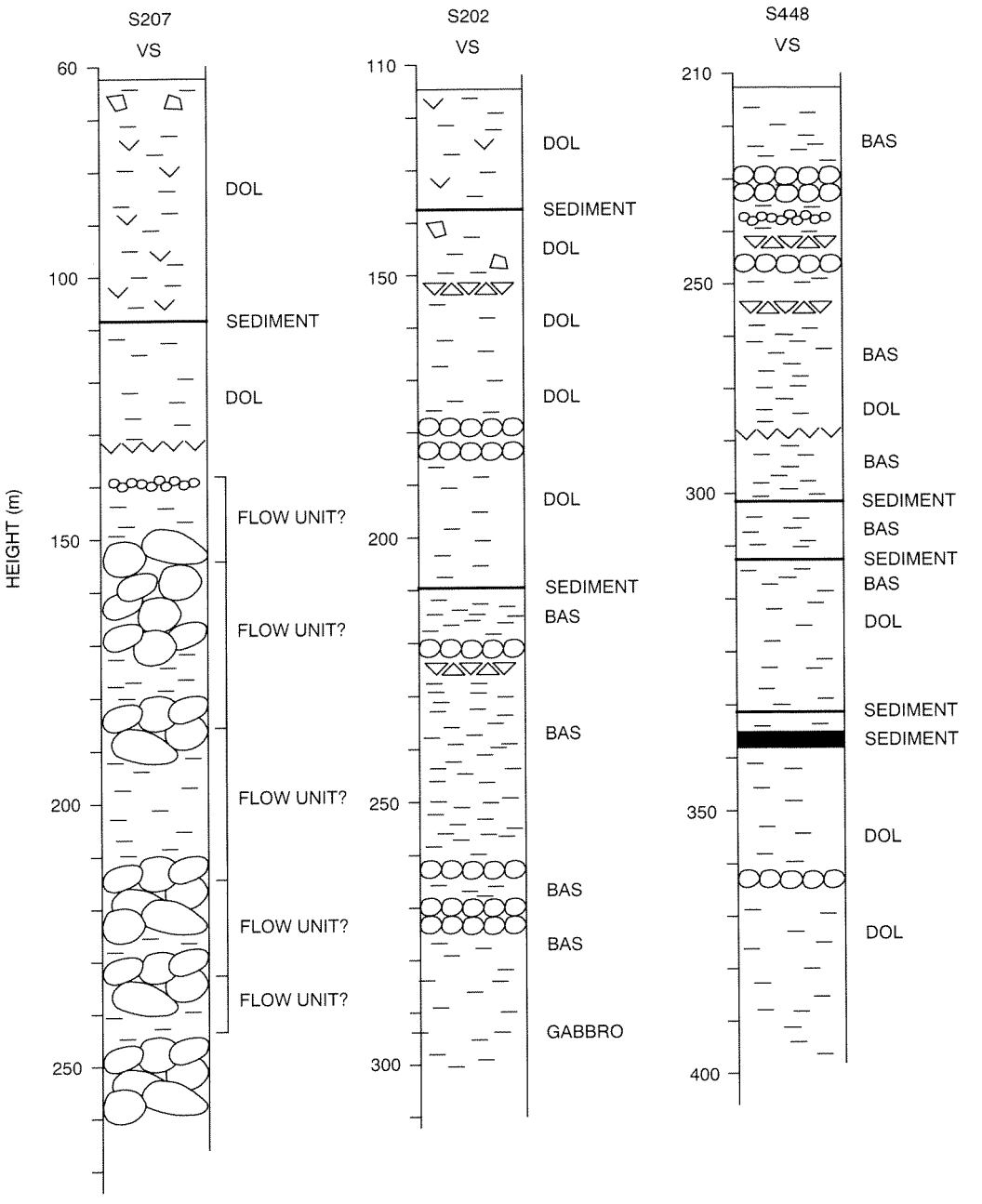

Appendix 2.15 Drill logs through part of the Woolyeenyer Formation, with acommon datum (Agnes Venture Slate). See Appendix 2.1 for explanation of symbols, and text for discussion.

Apppendix 3

Geochemistry

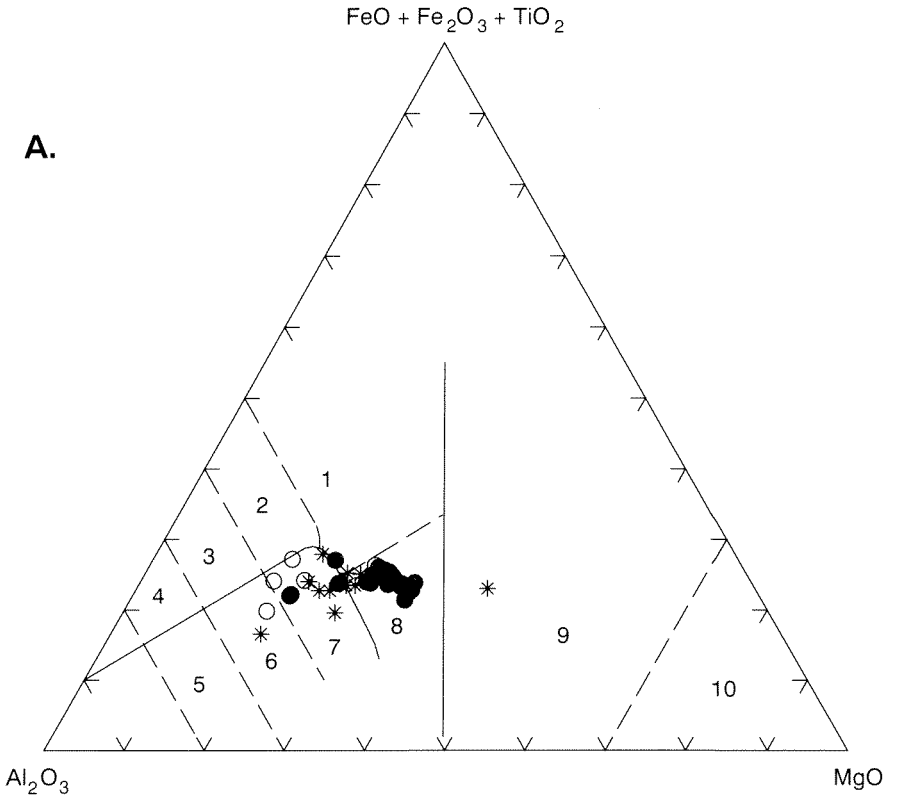

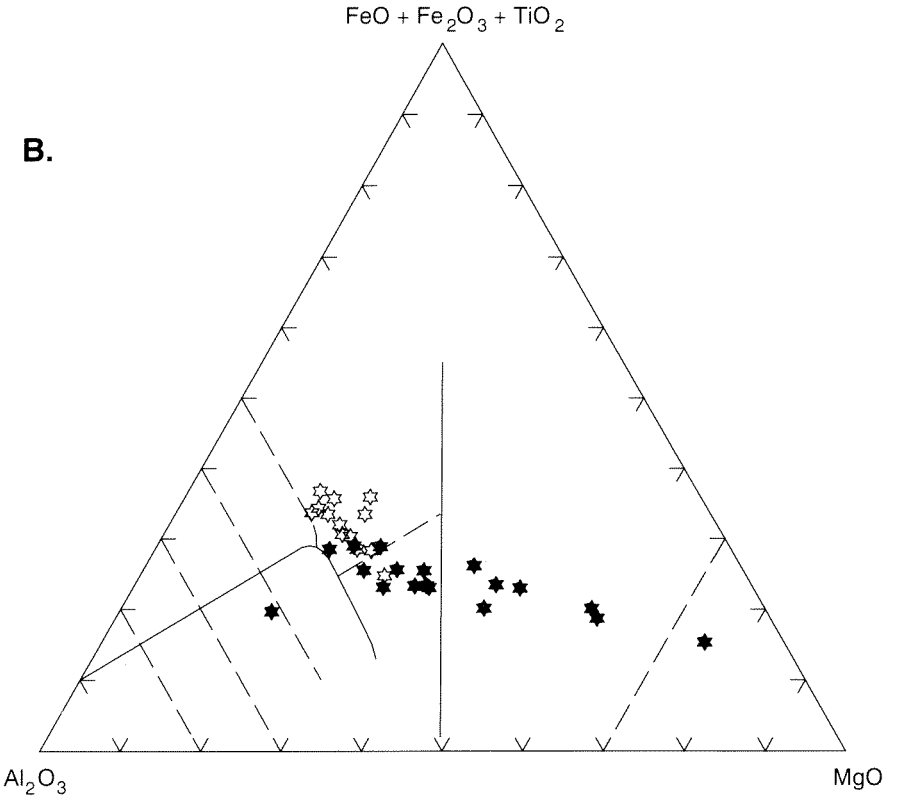

PAM26

Appendix 3.1 Jensen Cation Diagrams (Jensen, 1976). Fields: 1 — high iron tholeiitic basalt (HFTB); 2 — tholeiitic andesite; 3 and 5 — dacite; 4 — rhyolite; 6 — calc-alkalic andesite; 7 — calc-alkalic basalt; 8 — high-magnesium tholeiitic basalt (HMTB); 9 — basaltic komatiite; 10 — ultramafic komatiite.

A. Lower basalt unit, Kambalda Domain. Symbols: closed circles — Kambalda; open circles — Foster; asterisks — Tramways.

B. Lower basalt unit, Ora Banda Domain. Symbols: closed stars — Wongi Basalt; open stars — Missouri Basalt.

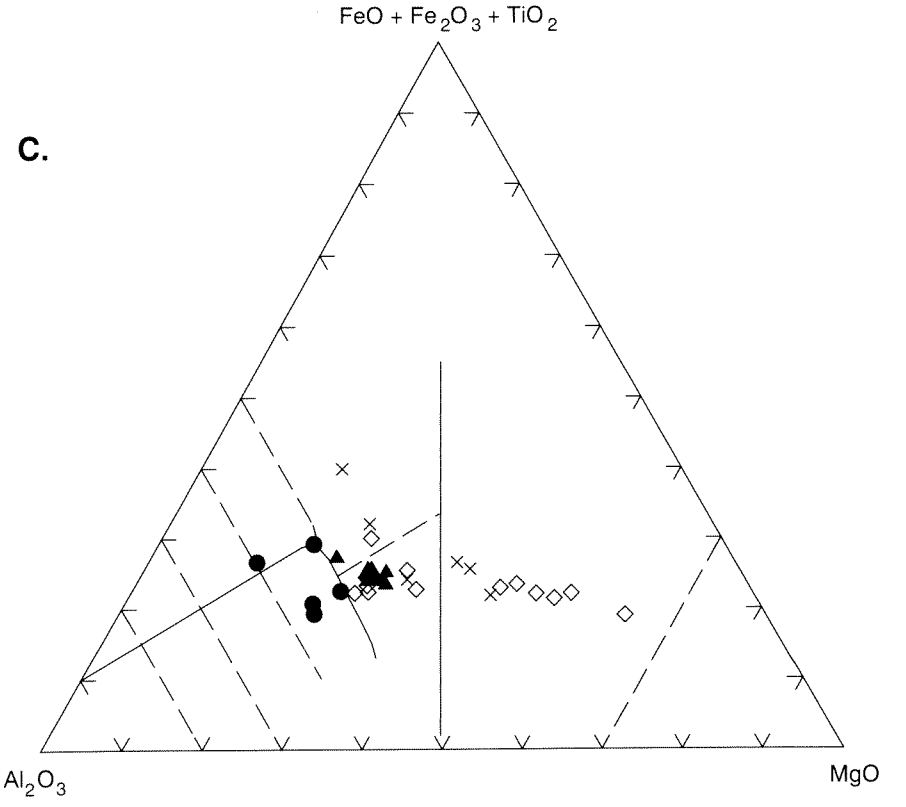

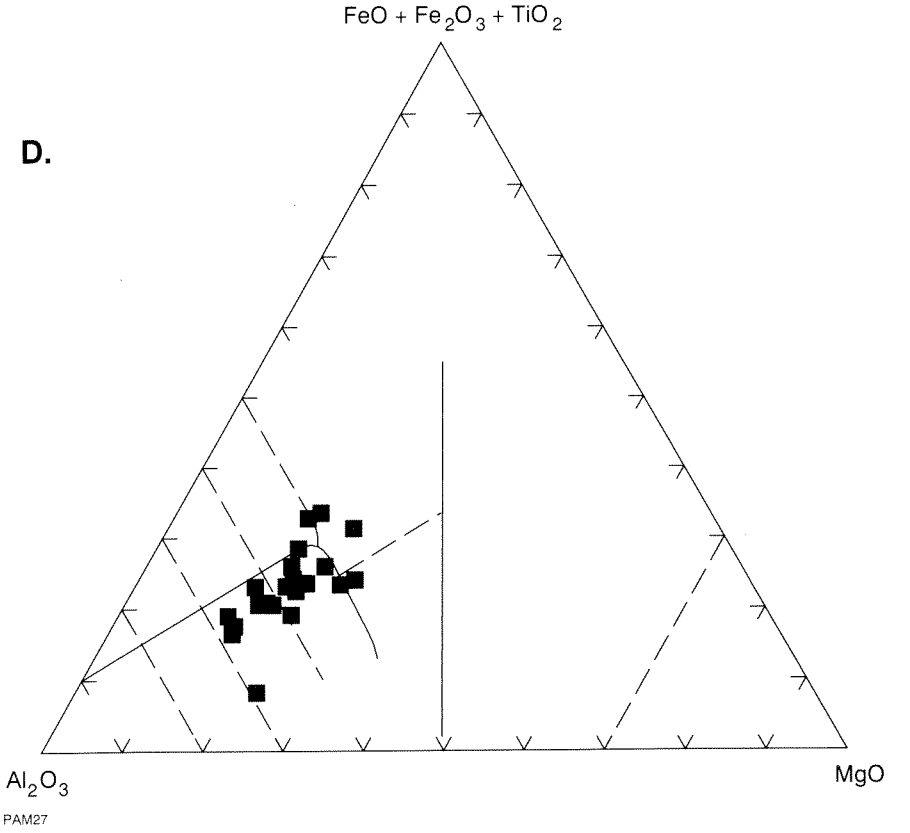

C. Lower basalt unit, Coolgardie and Bullabulling Domains. Symbols (Coolgardie Domain): closed triangles — Widgiemooltha–Redross; open diamonds — Coolgardie; crosses — Dunnsville. Closed circles — Bullabulling Domain.

D. Lower basalt unit, Boorara Domain (Carnilya Hill).

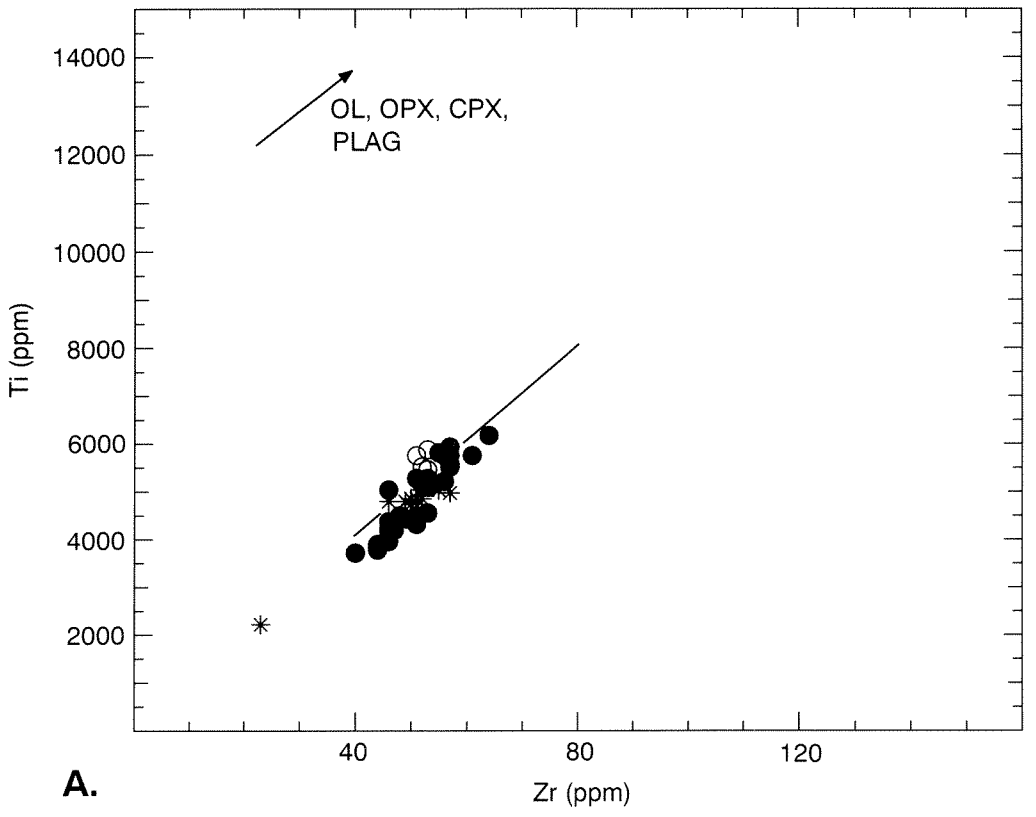

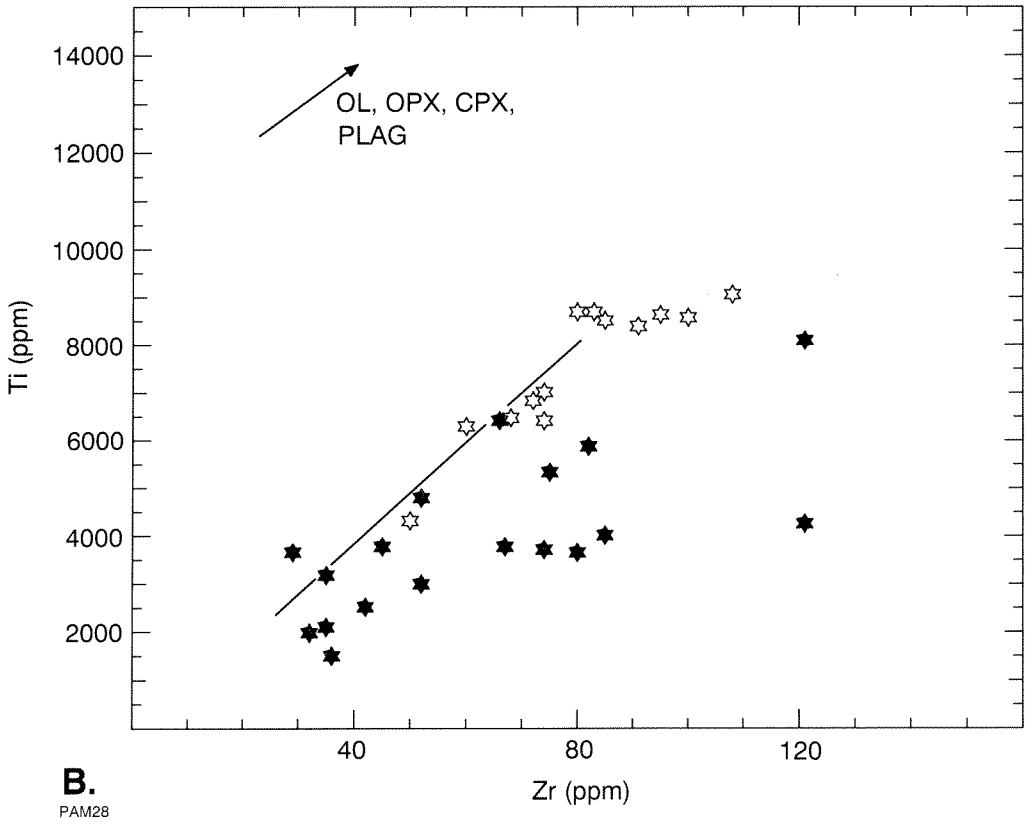

Appendix 3.2 **Ti (converted to ppm from wt% TiO_2, anhydrous) versus Zr (ppm) for the lower basalt unit. Fractionation vectors for olivine (ol), orthopyroxene (opx), clinopyroxene (cpx), and plagioclase (plag) also shown. Line of best fit for Kambalda data also shown; slope = 106, intercept = -529, r = 0.89, n = 46.**

A. Kambalda Domain. Symbols as for Appendix 3.1.
B. Ora Banda Domain. Symbols as for Appendix 3.1.

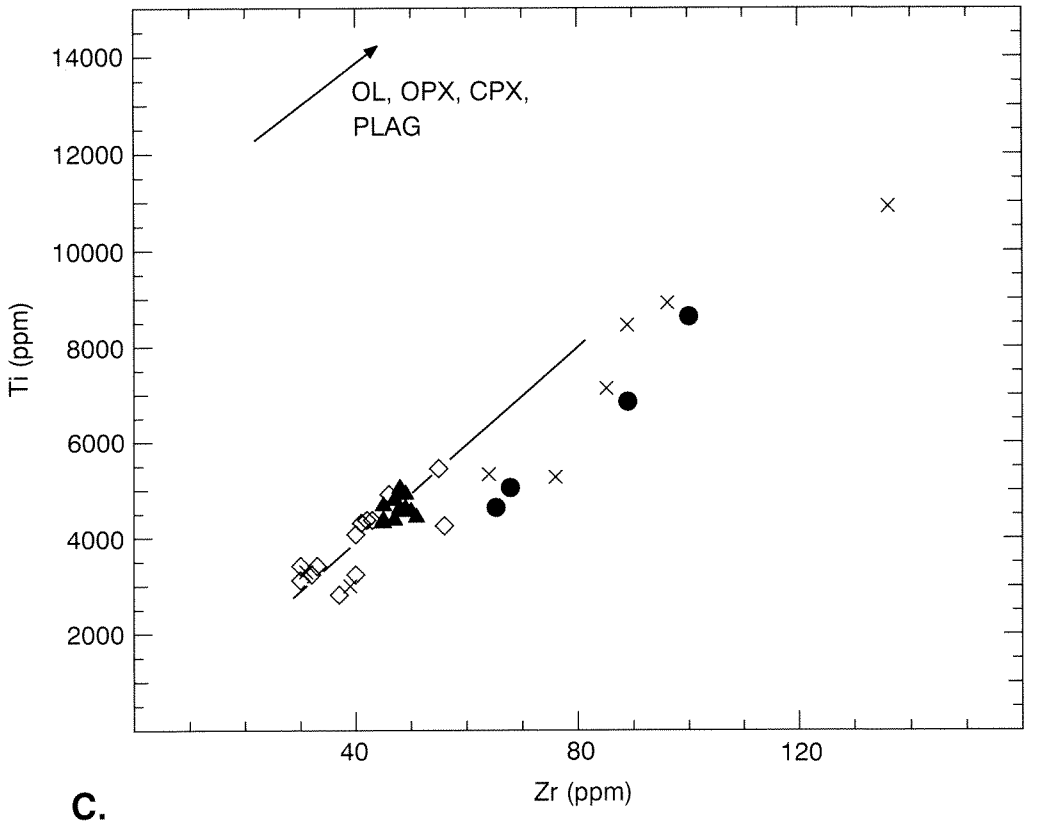

C.

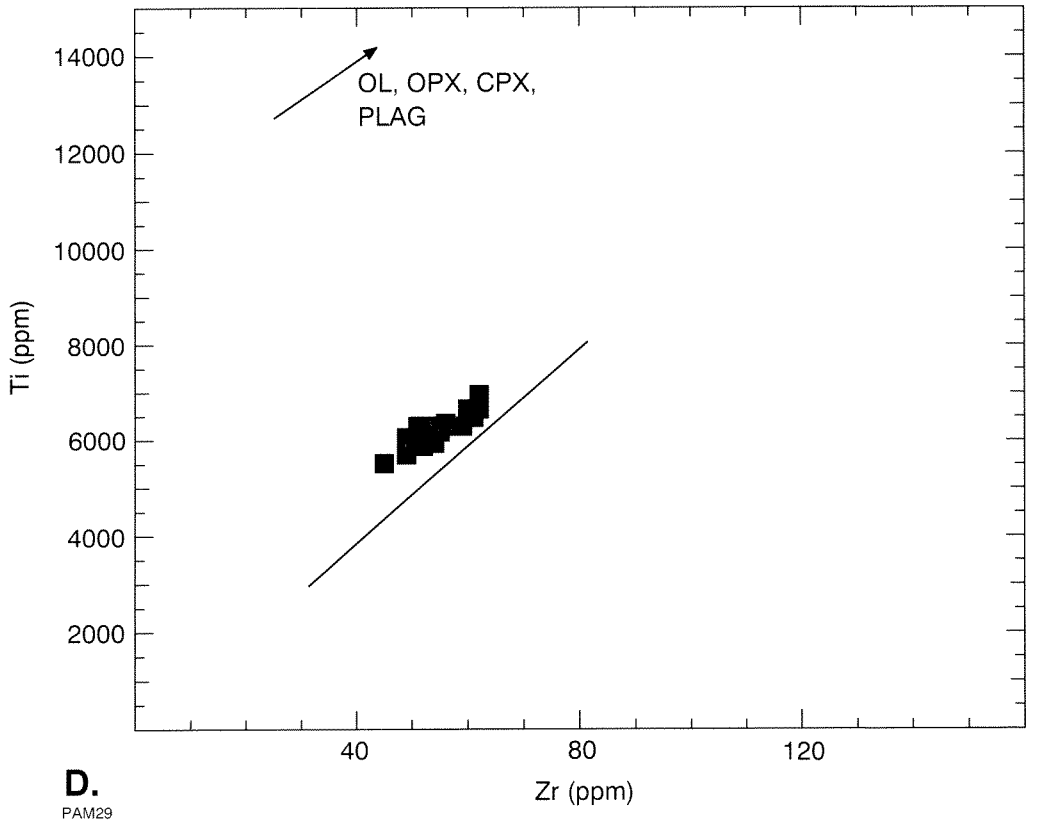

D.

PAM29

C. Coolgardie and Bullabulling Domains. Symbols as for Appendix 3.1.
D. Boorara Domain (Carnilya Hill). Symbols as for Appendix 3.1.

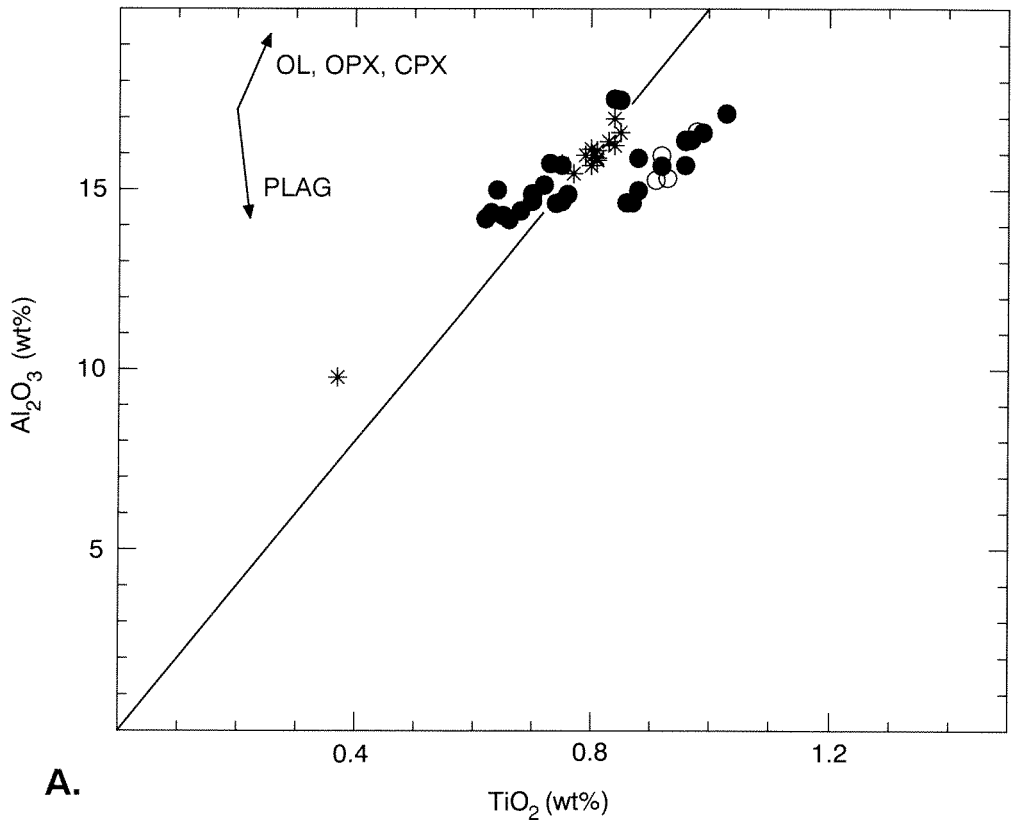

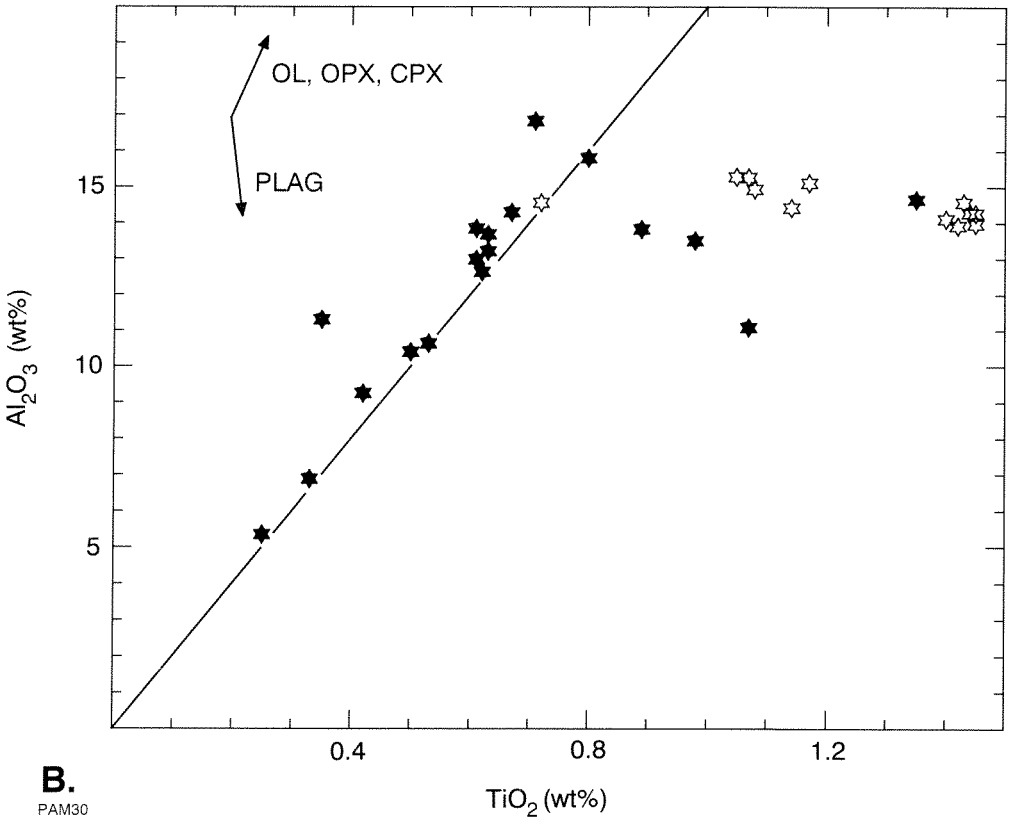

Appendix 3.3 Al_2O_3 vs TiO_2 (wt% anhydrous) for the lower basalt unit. Fractionation vectors for olivine (ol), orthopyroxene (opx), clinopyroxene (cpx) and plagioclase (plag) shown. Line is chondritic ratio of 20 drawn through the origin.

A. Kambalda Domain. Symbols as for Appendix 3.1.
B. Ora Banda Domain. Symbols as for Appendix 3.1.

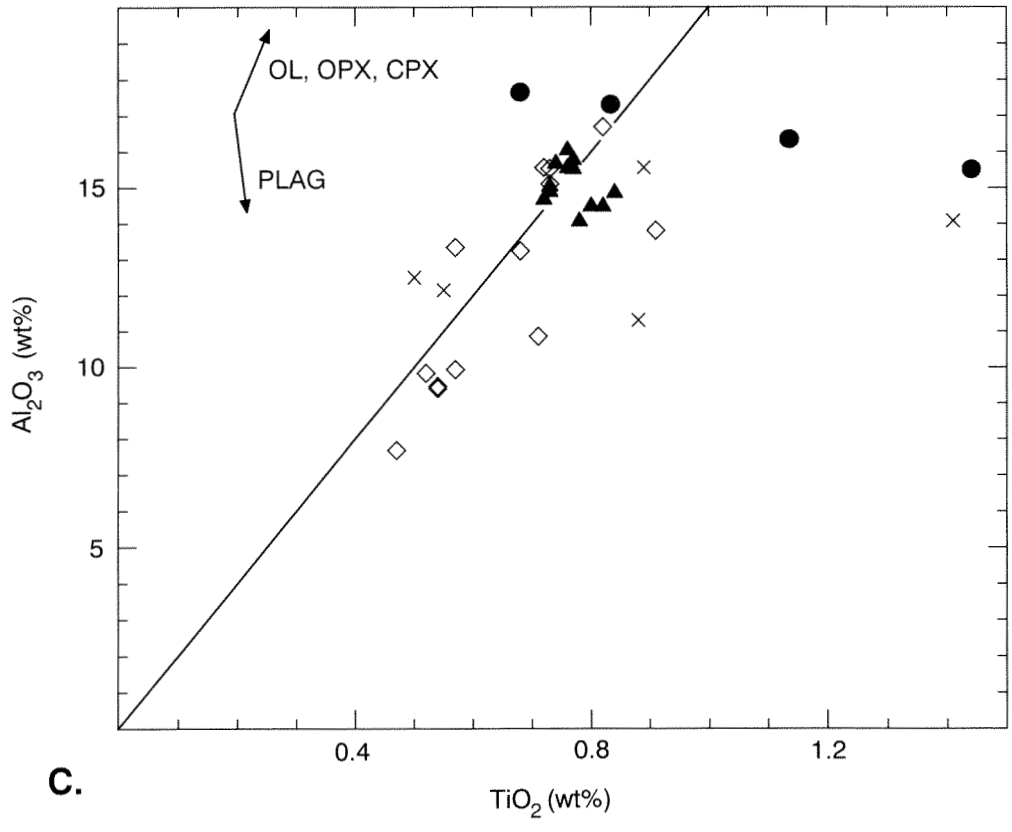

C.

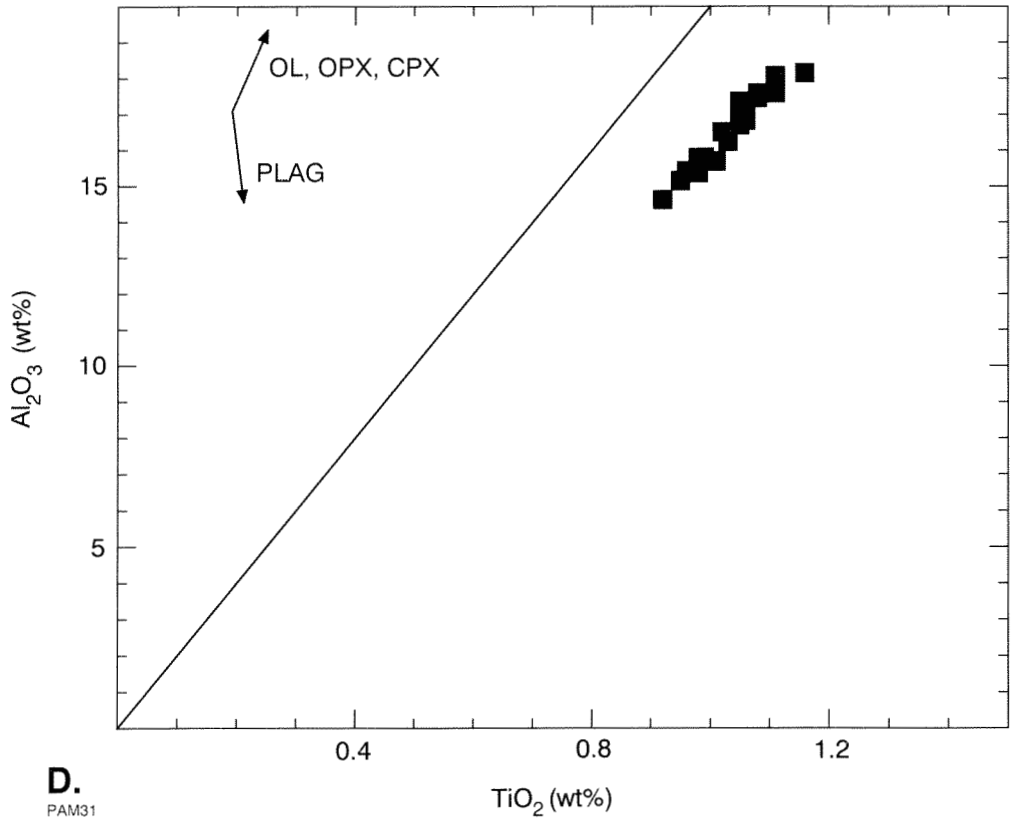

D.

PAM31

C. Coolgardie and Bullabulling Domains. Symbols as for Appendix 3.1.
D. Boorara Domain (Carnilya Hill). Symbols as for Appendix 3.1.

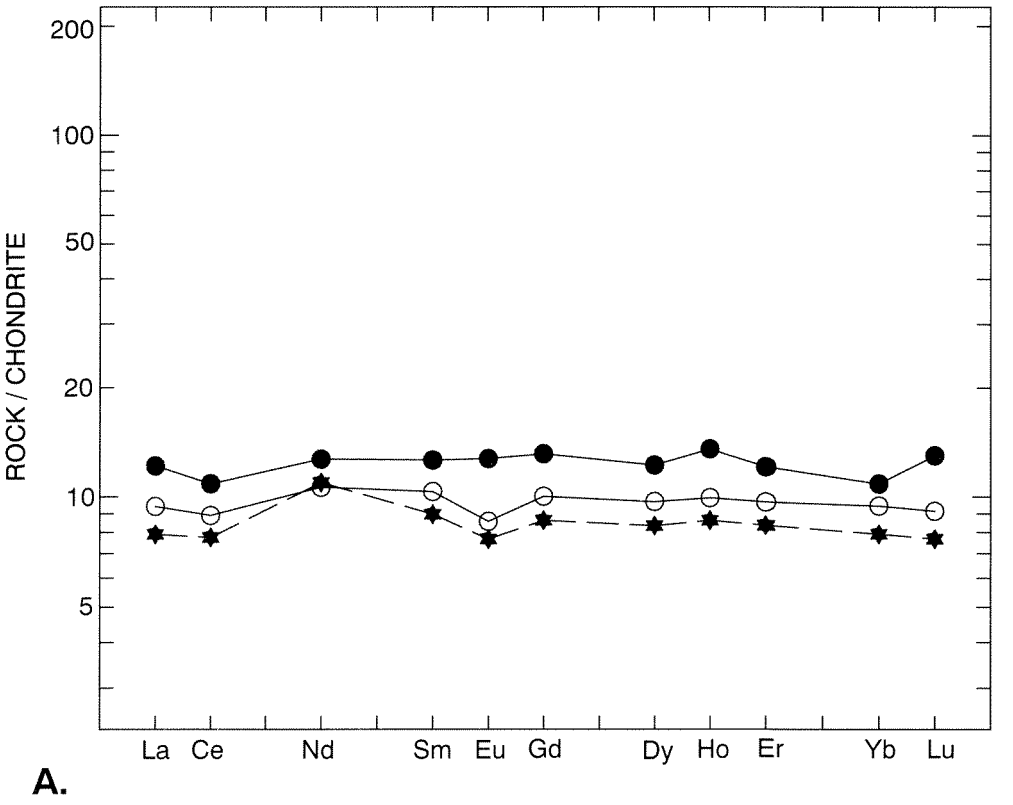

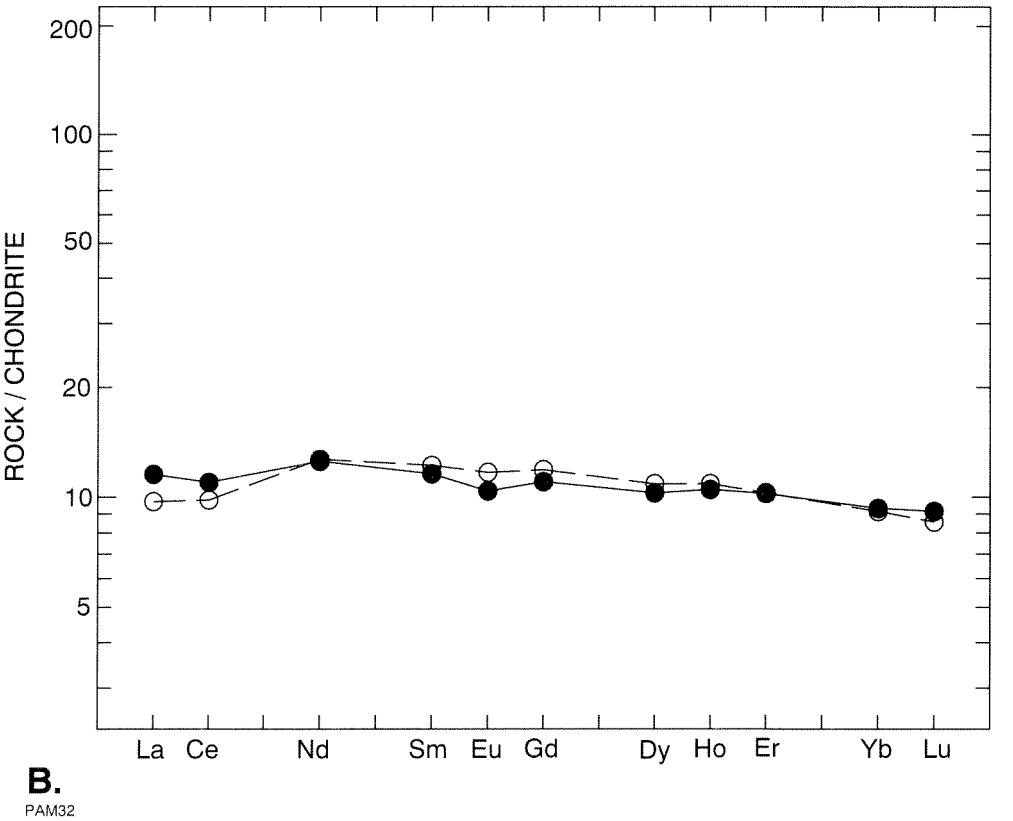

Appendix 3.4 **Chondrite normalized rare-earth-element (REE) patterns for the lower basalt unit. Normalization factors from Nakamura (1974) and Evensen et al. (1984).**

A. Lower basalt unit, Kambalda Domain, Kambalda. Closed circle — 99516; open circle — 99559; closed star — 99561.

B. Lower basalt unit, Kambalda Domain, Foster — Tramways. Closed circle — 99624; open circle — 99604.

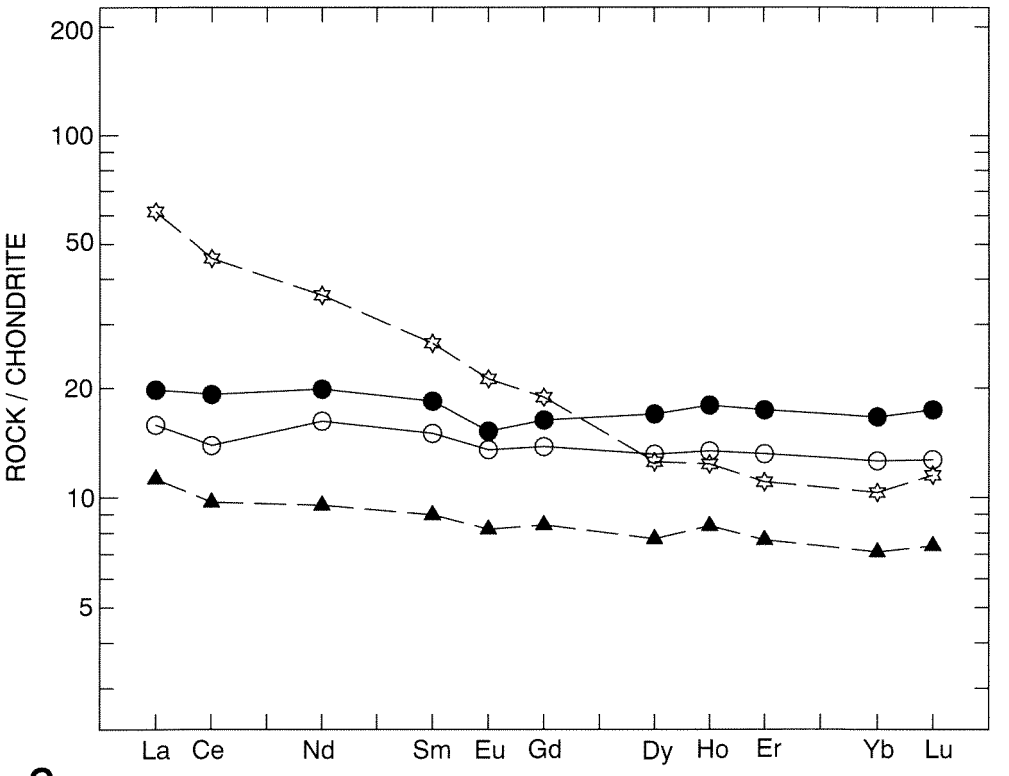

C.

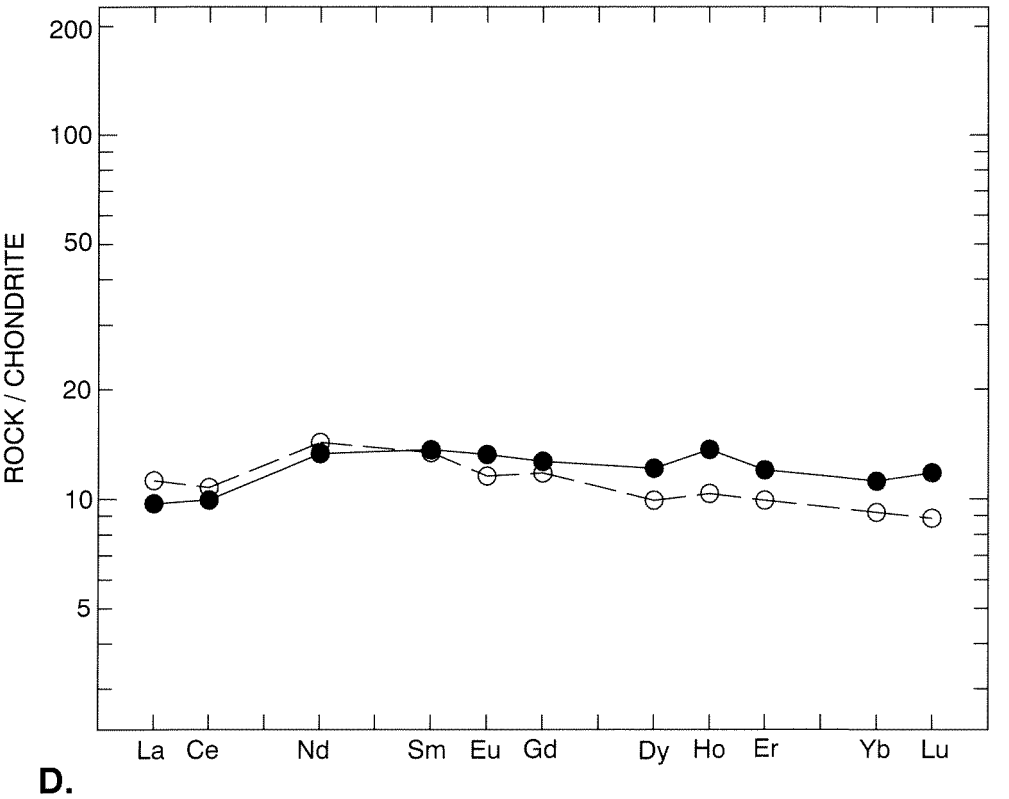

D.

PAM33

C. Lower basalt unit, Ora Banda Domain. Closed circle — 100115; open circle — 100114; open star — 100113; closed triangle — 100108.

D. Lower basalt unit, Ora Banda Domain, Ghost Rocks. Closed circle — 100128; open circle — 100125.

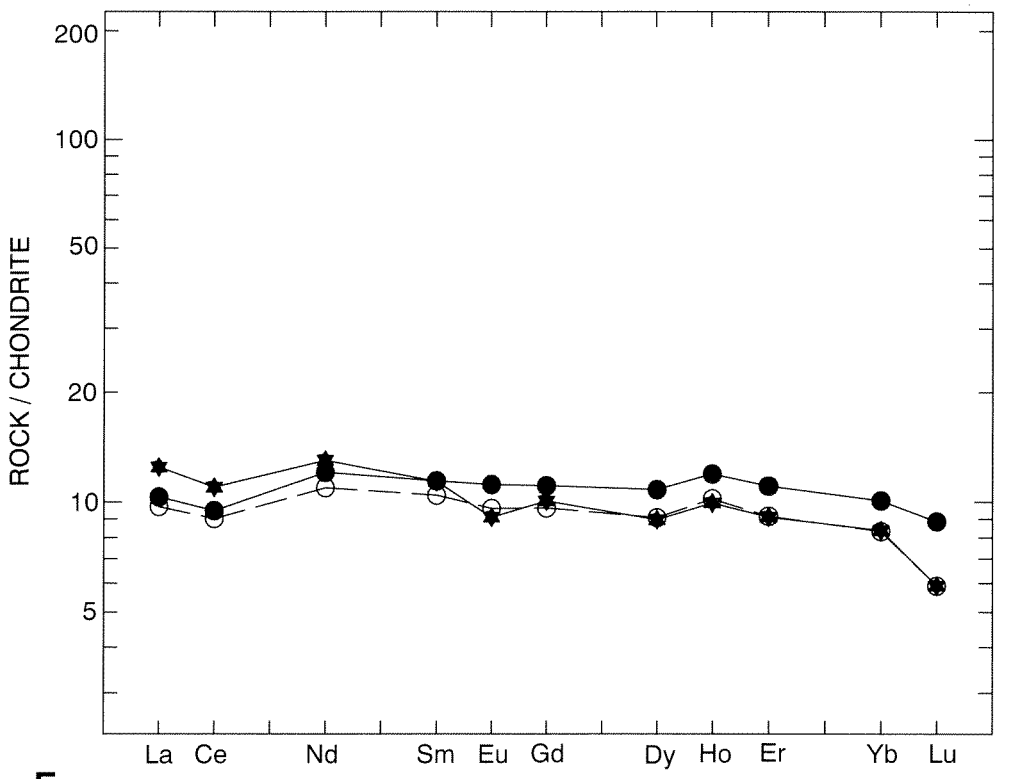

E.

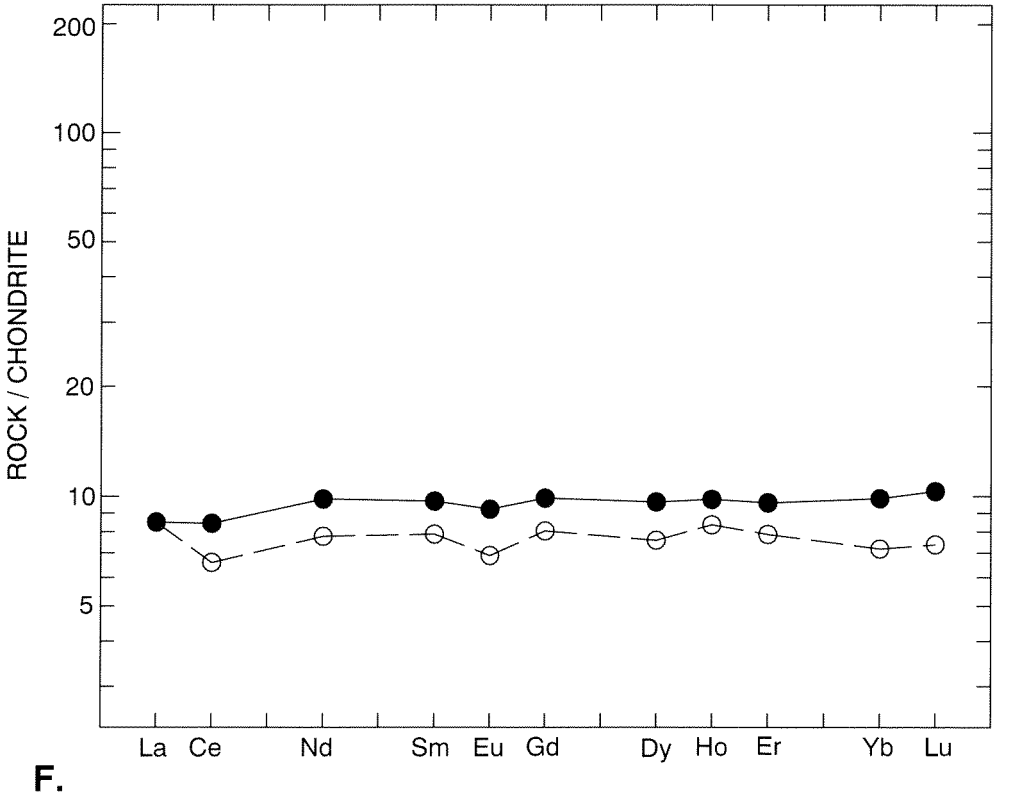

F.

PAM34

E. Lower basalt unit, Coolgardie Domain, Coolgardie. Closed circle — 100141; open circle — 100179; closed star — 100177.

F. Lower basalt unit, Coolgardie Domain, Dunnsville. Closed circle — 99767; open circle — 99979.

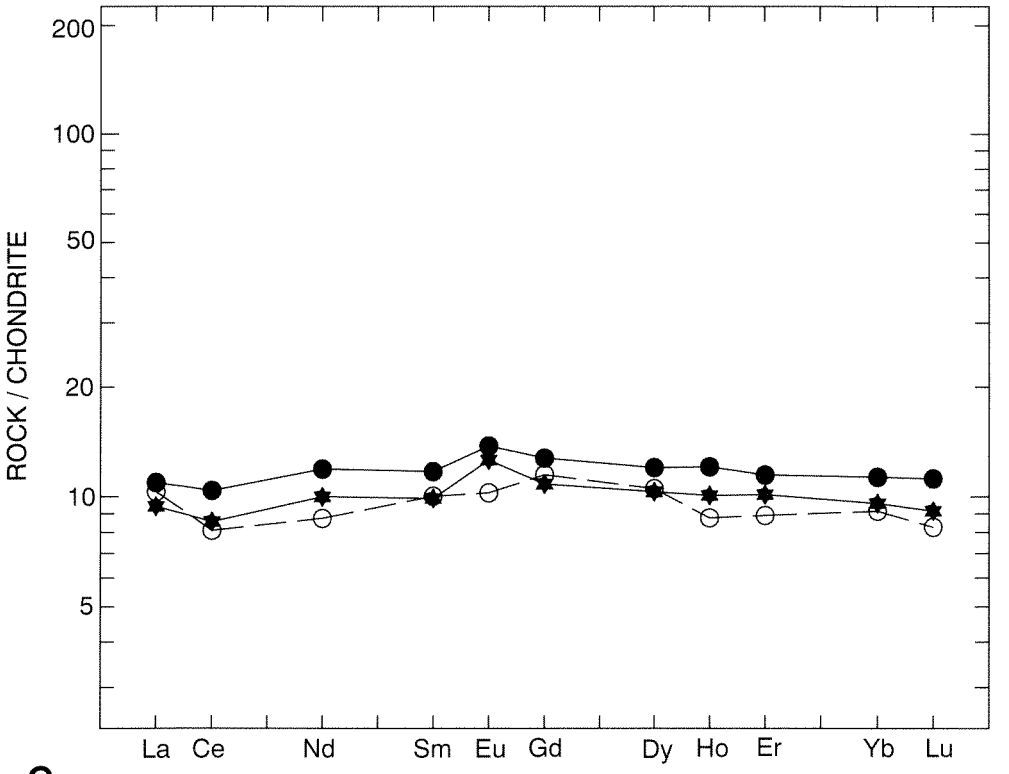

G.

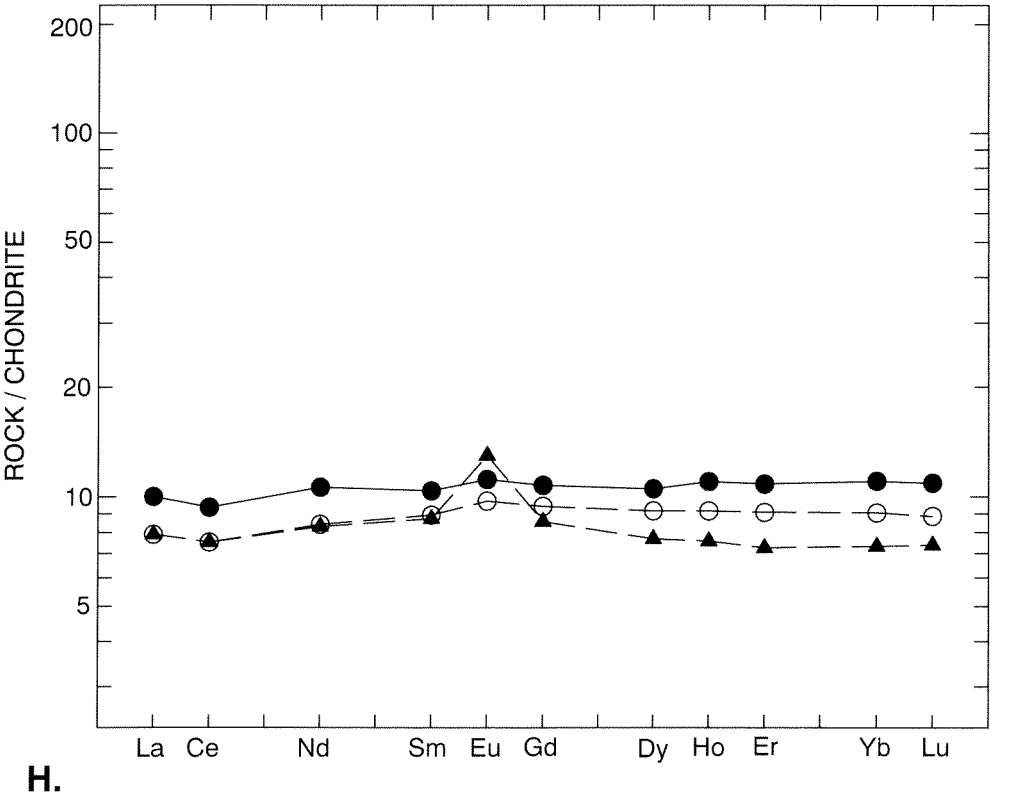

H.

PAM35

G. Lower basalt unit, Boorara Domain, Carnilya Hill. Closed circle — 99726; open circle — 99721; closed star — 99732.

H. Lower basalt unit, Boorara Domain, Carnilya Hill. Closed circle — 99734; open circle — 99755; closed triangle— 99761.

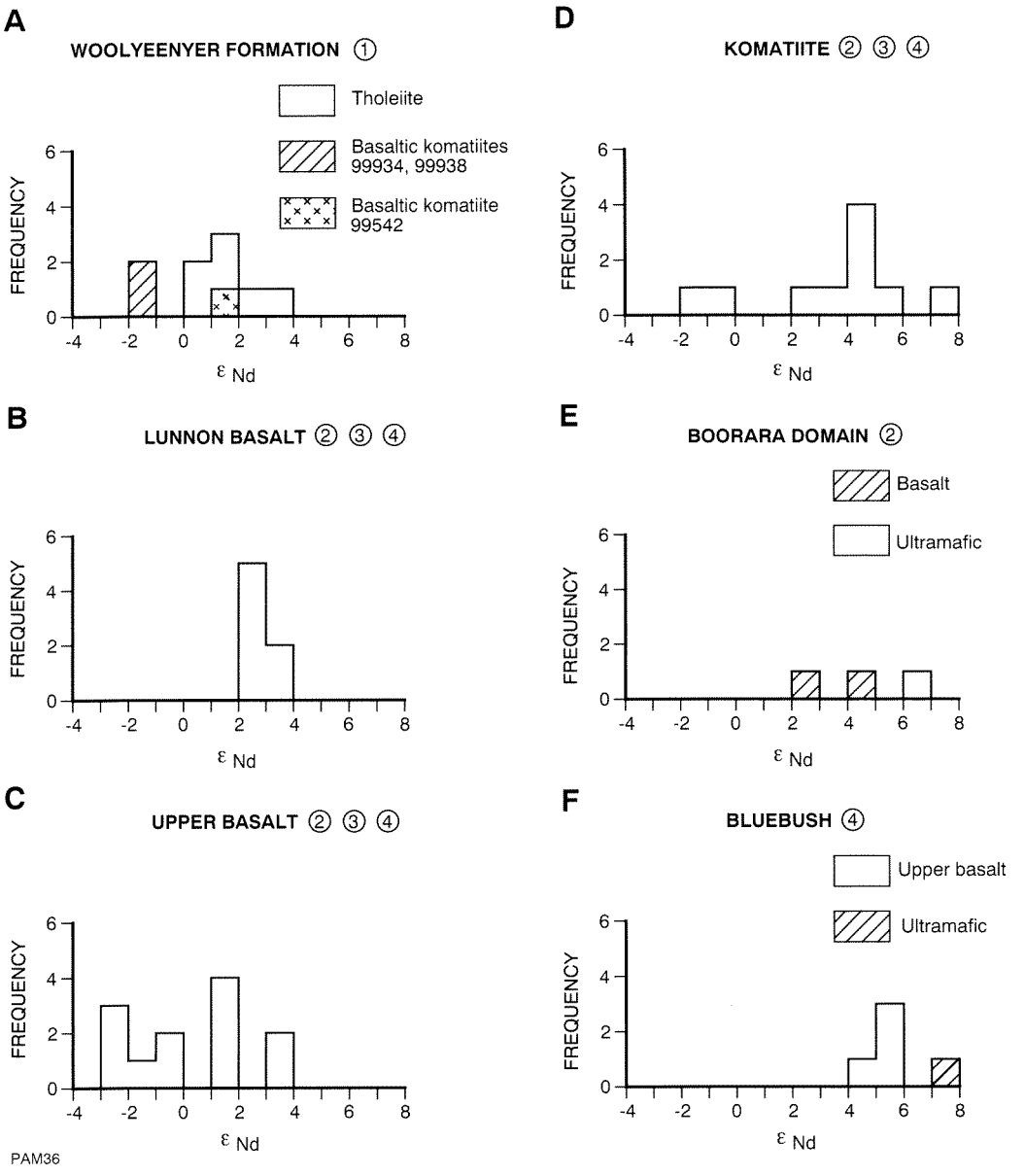

Appendix 3.5 **Summary of available neodymium isotope data for units examined in this study, Kalgoorlie and Norseman Terranes.**

Appendix 3.6 **Jensen Cation Diagrams (Jensen, 1976) for the komatiite fields as in Appendix 3.1.**

A. Kambalda Domain, Kambalda and Kalgoorlie. Closed circles — Kambalda; open traingles — Kalgoorlie.

B. Kambalda Domain, Bluebush–Republican.

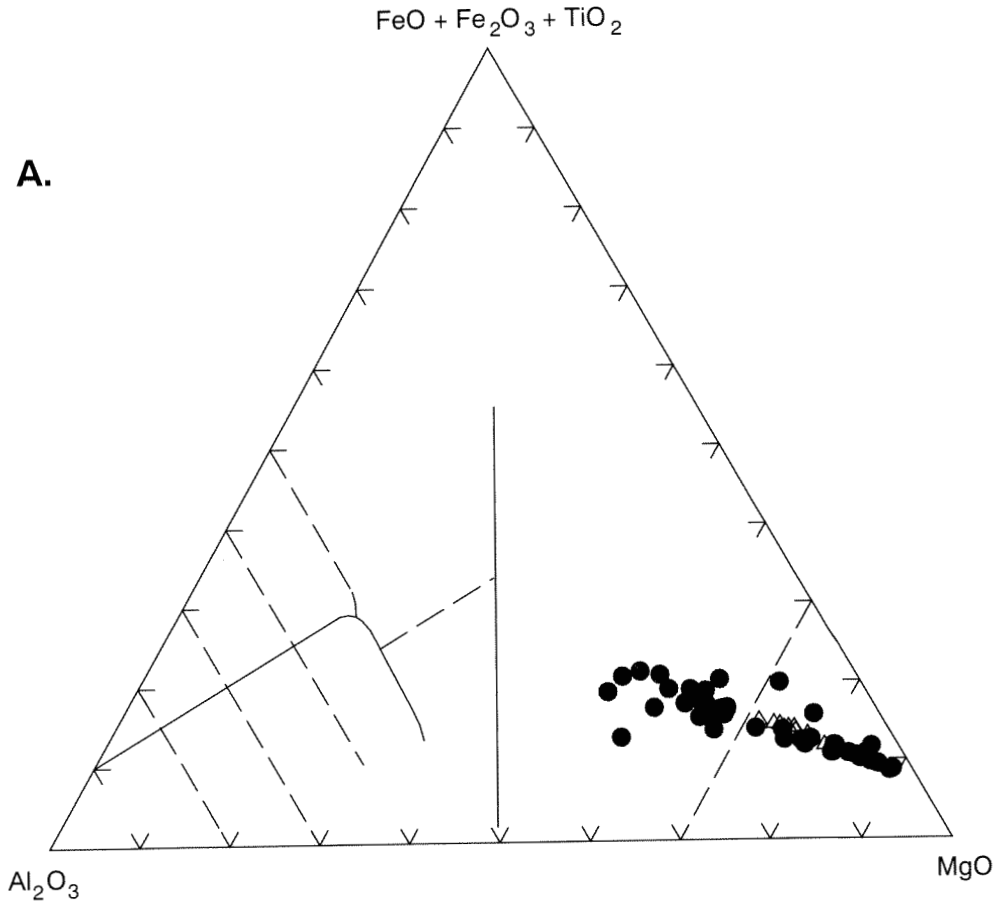

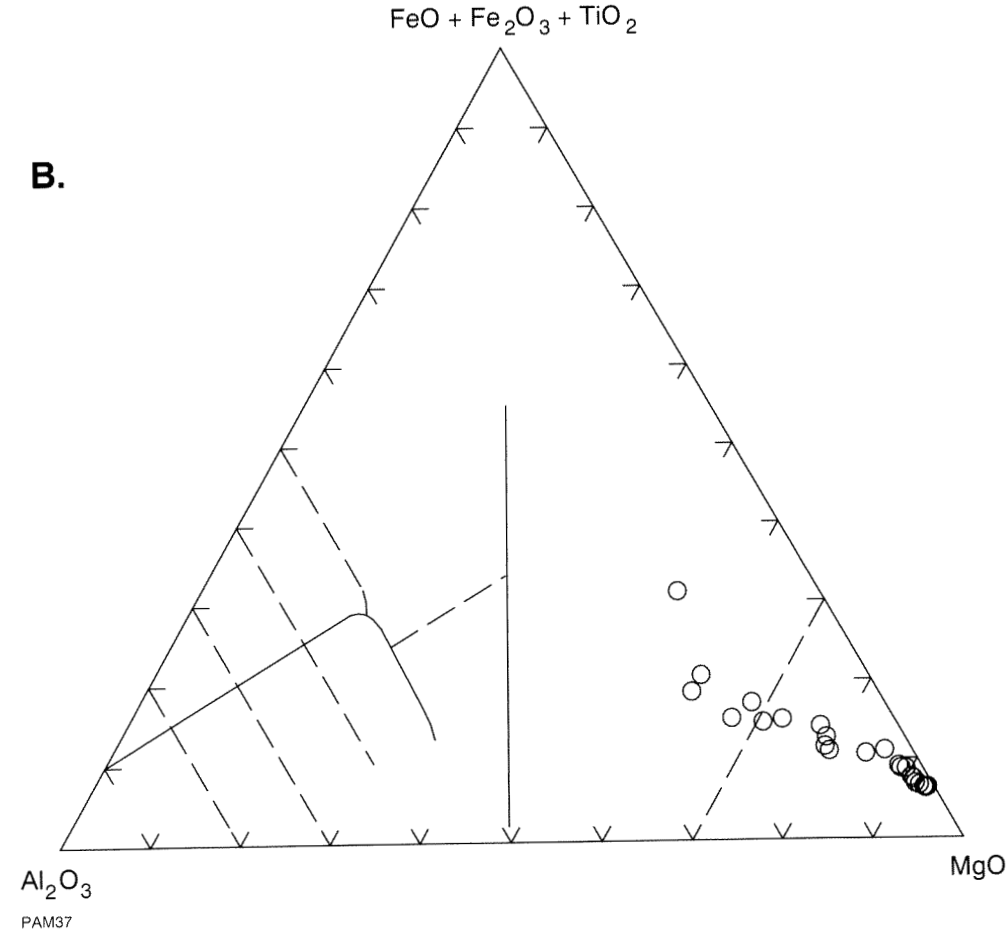

PAM37

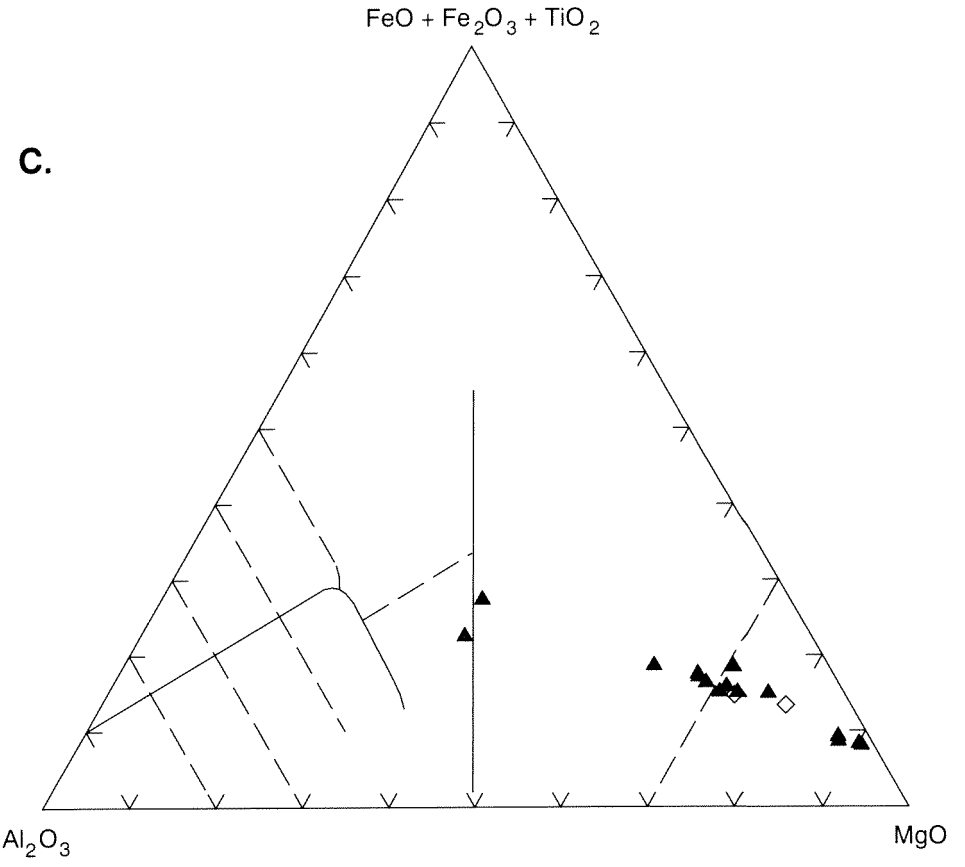

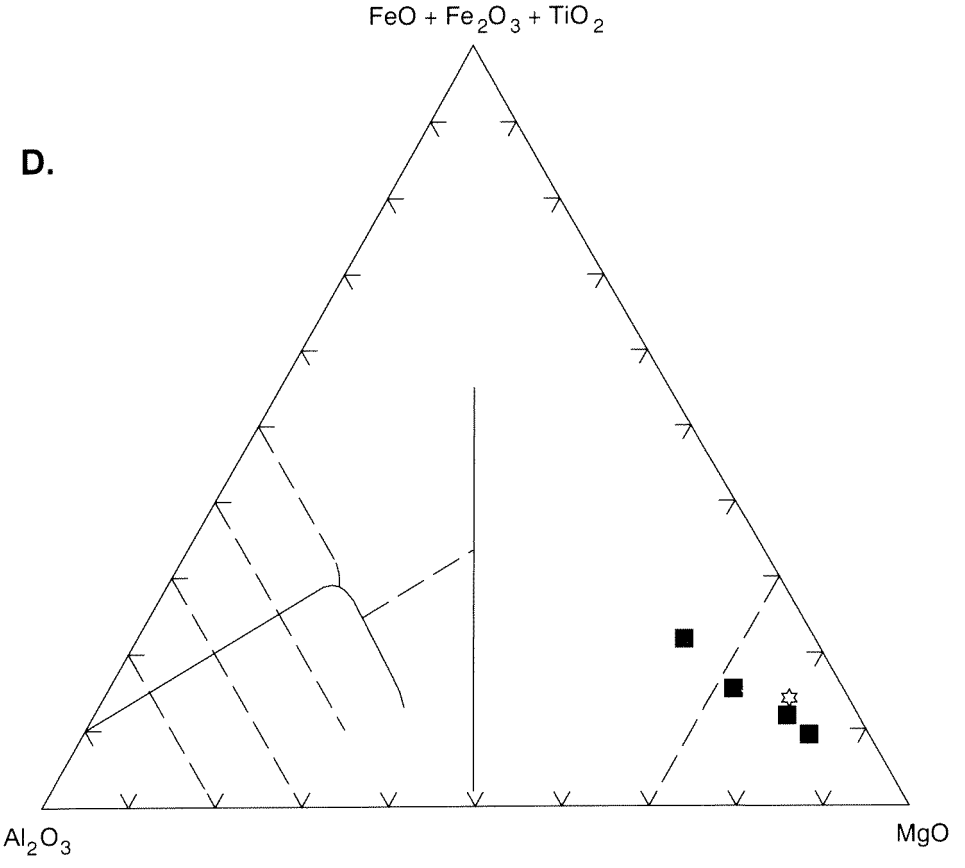

PAM38

C. Coolgardie Domain. Closed triangles — Widgiemooltha–Redross; open diamond — Coolgardie.
D. Boorara Domain. Closed squares — Carnilya Hill; open star — Harper Lagoon.

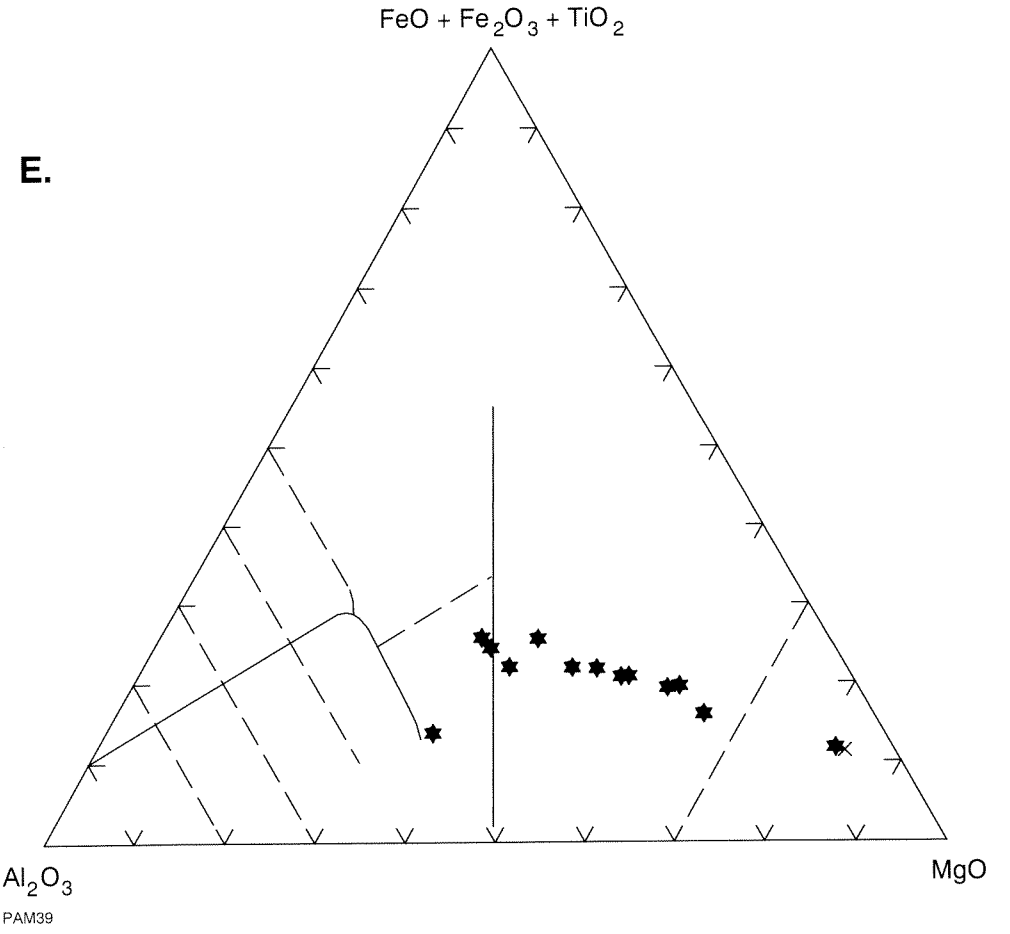

E. Ora Banda Domain. Cross — Walter Williams Formation; closed stars — Siberia Komatiite.

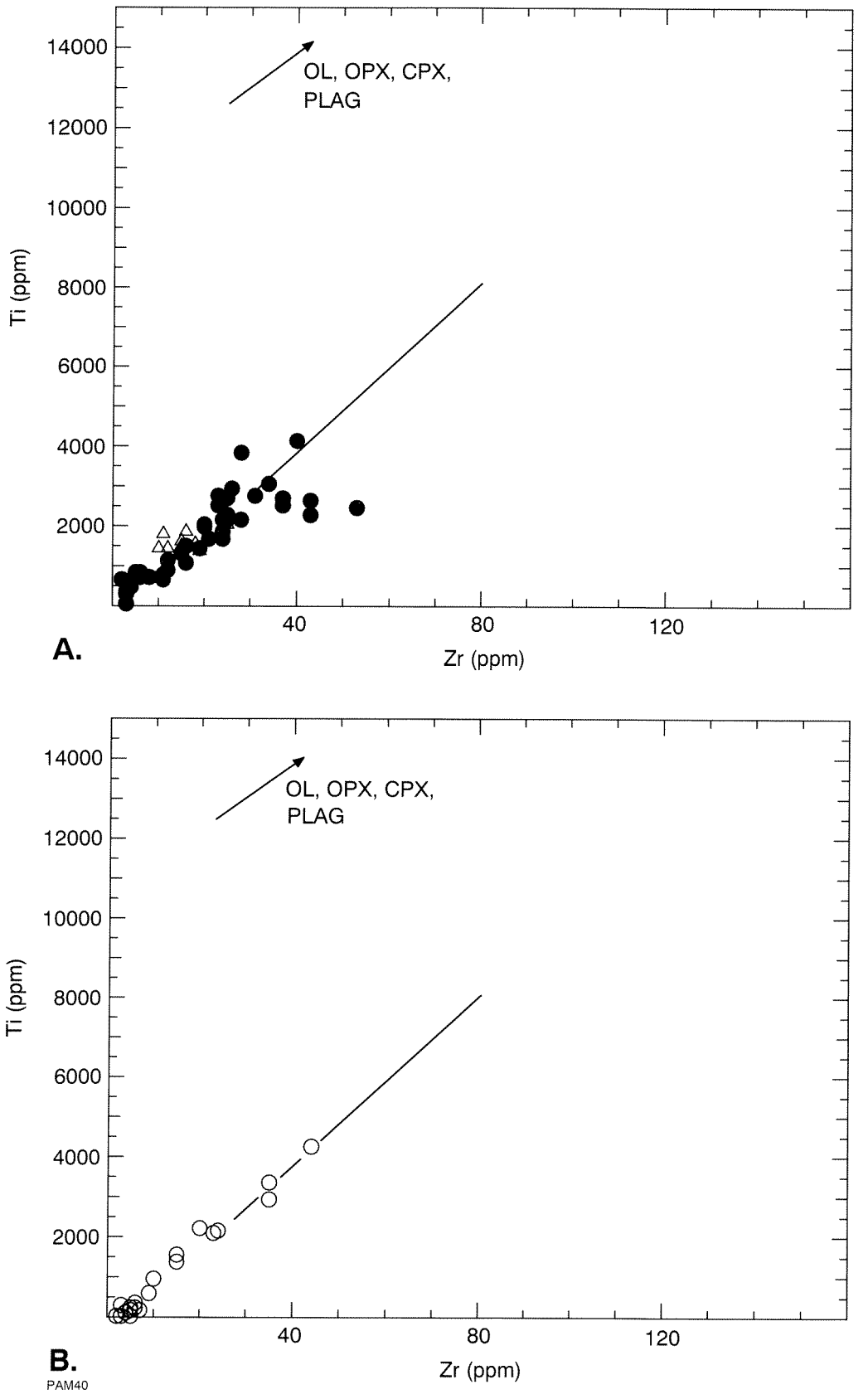

Appendix 3.7 **Ti versus Zr (ppm) for komatiite. See Appendix 3.2 for description of line of best fit, and fractionation vectors.**

A. Kambalda Domain, Kambalda and Kalgoorlie. Symbols as Appendix 3.6.
B. Kambalda Domain, Bluebush–Republican. Symbols as Appendix 3.6.

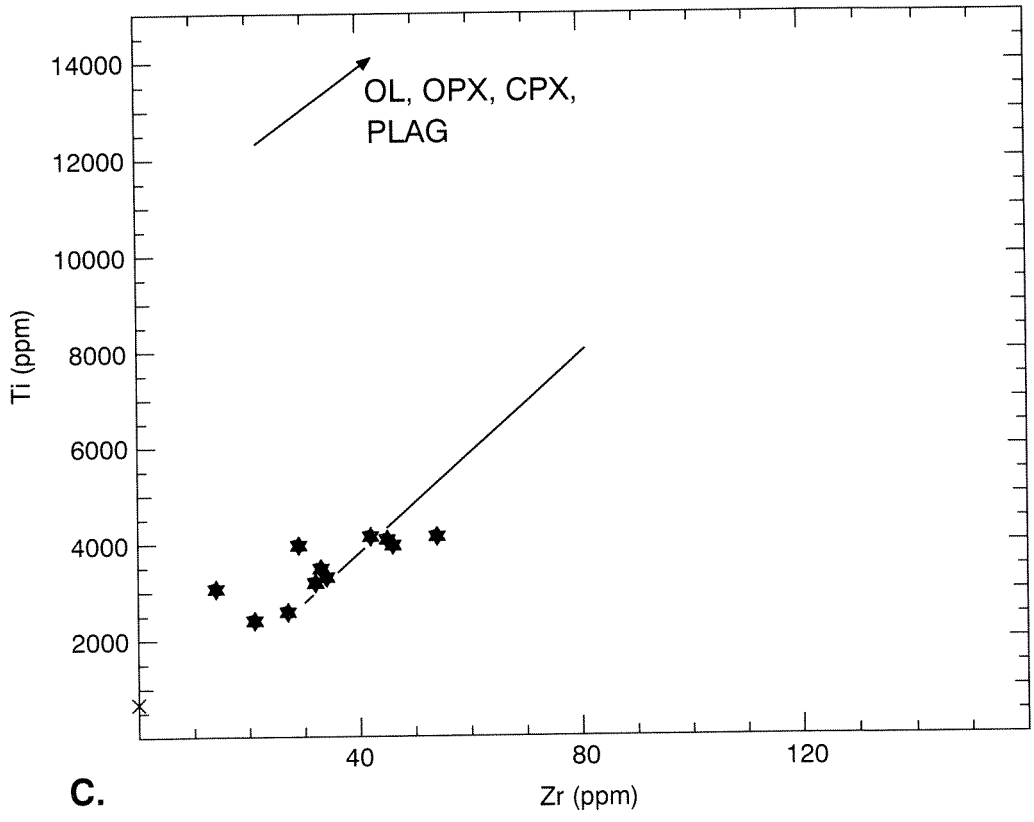

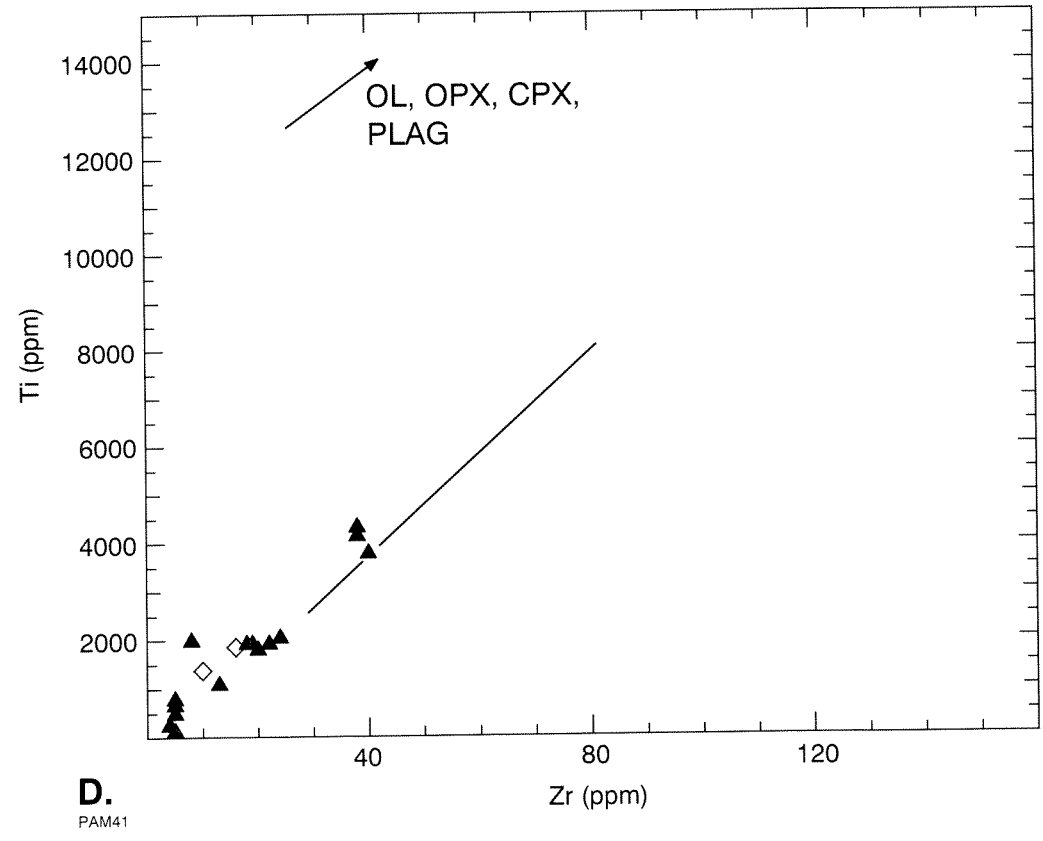

C. Ora Banda Domain. Symbols as Appendix 3.6.
D. Coolgardie Domain. Symbols as Appendix 3.6.

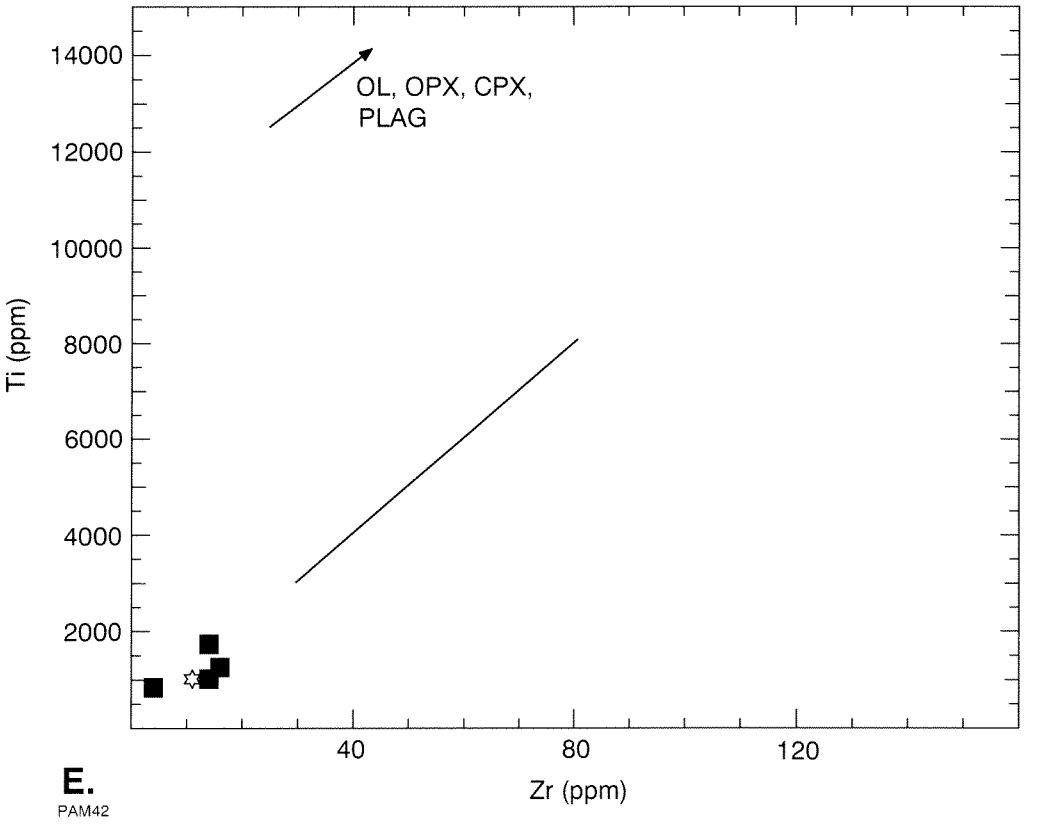

E. Boorara Domain. Symbols as Appendix 3.6.

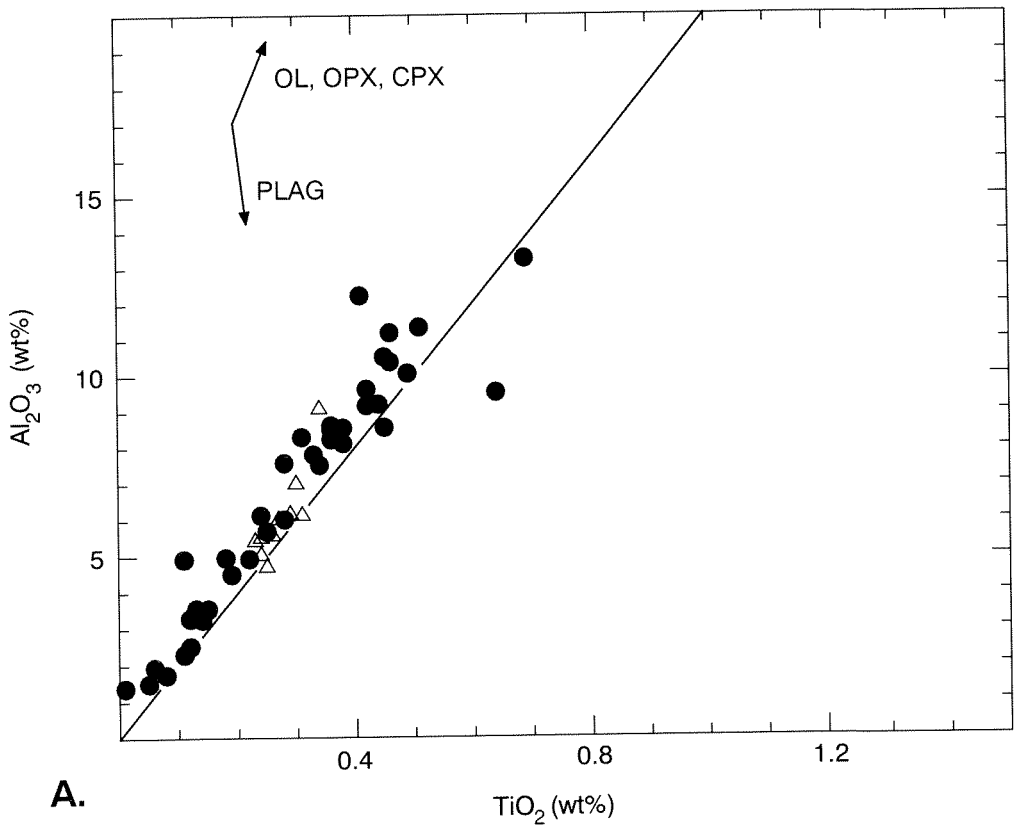

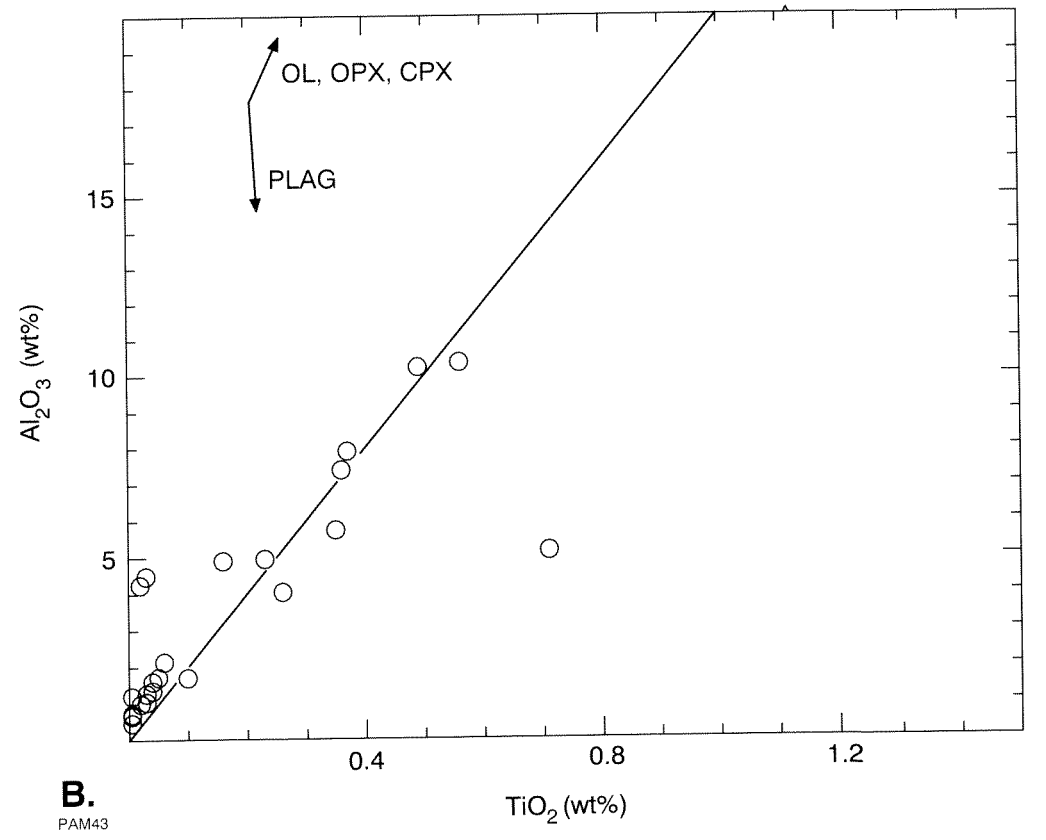

Appendix 3.8 Al_2O_3 versus TiO_2 for komatiite. See Appendix 3.3 for explanation of chondrite line and fractionation vectors.

A. Kambalda Domain, Kambalda and Kalgoorlie. Symbols as Appendix 3.6.
B. Kambalda Domain, Bluebush–Republican. Symbols as Appendix 3.6.

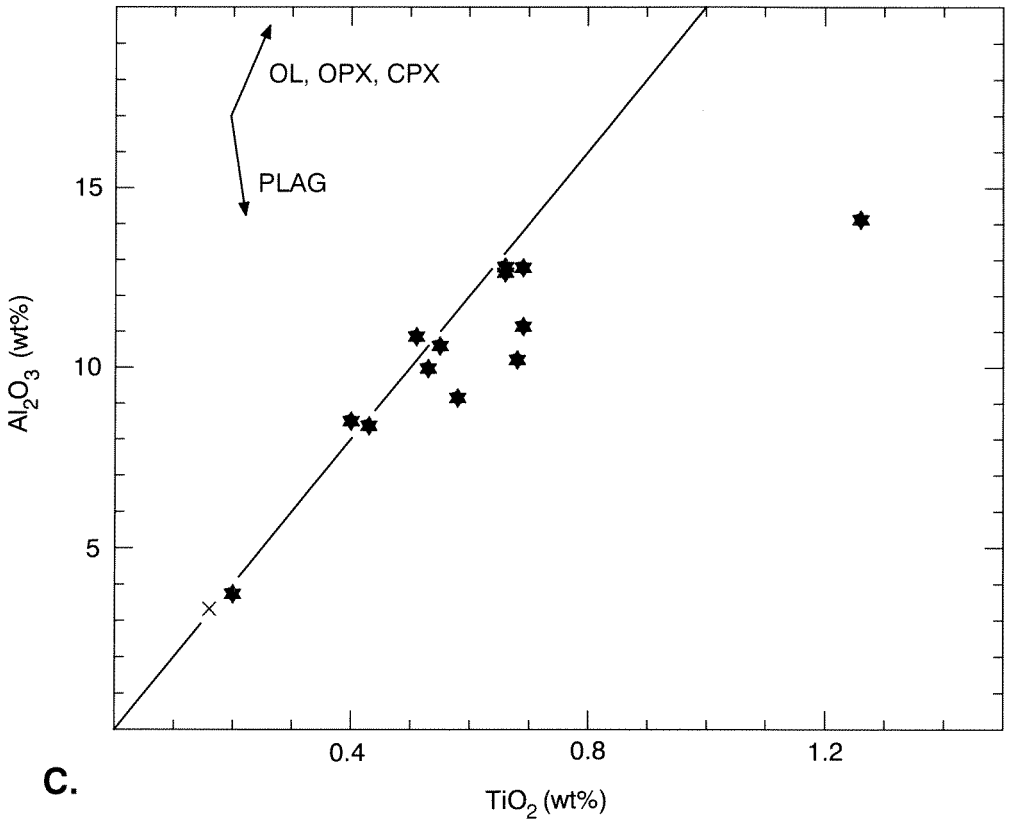

C.

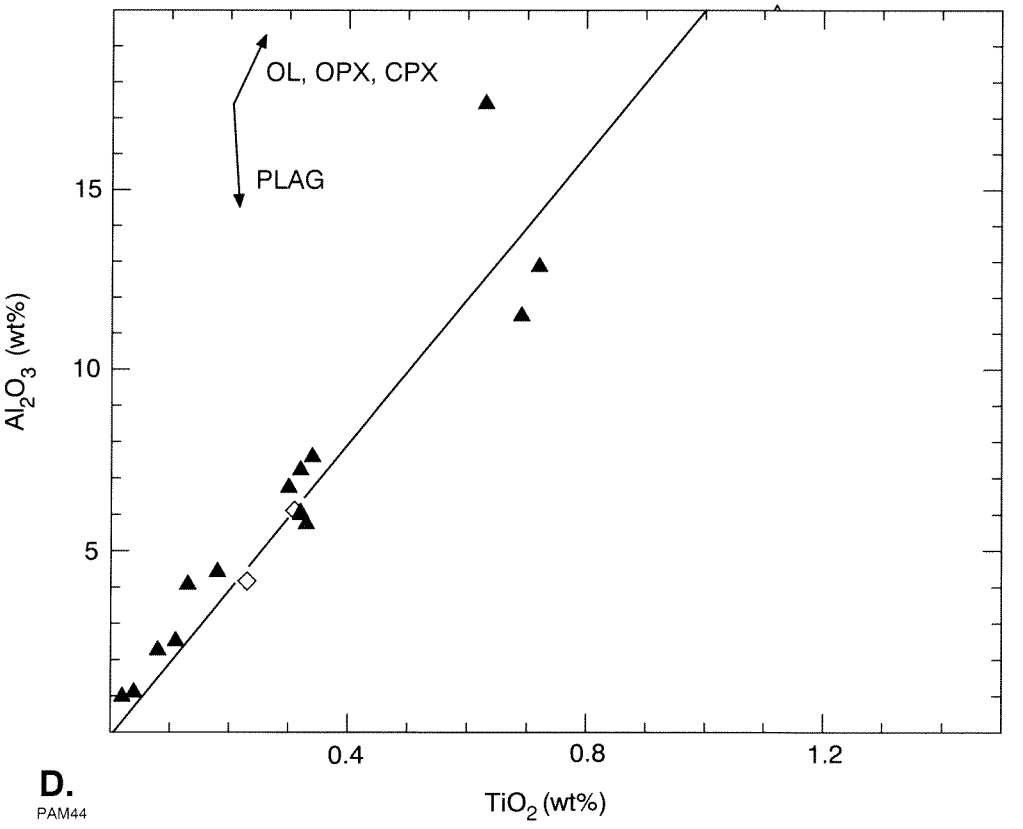

D.

PAM44

C. Ora Banda Domain. Symbols as Appendix 3.6.
D. Coolgardie Domain. Symbols as Appendix 3.6.

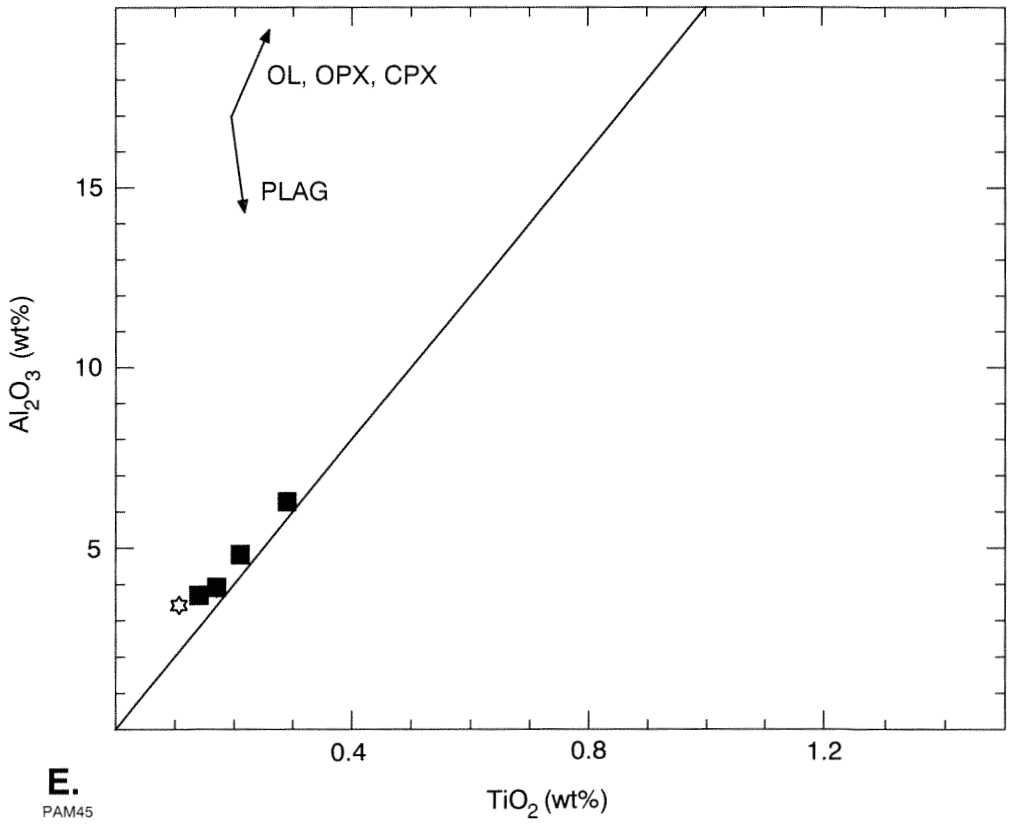

E. Boorara Domain. Symbols as Appendix 3.6.

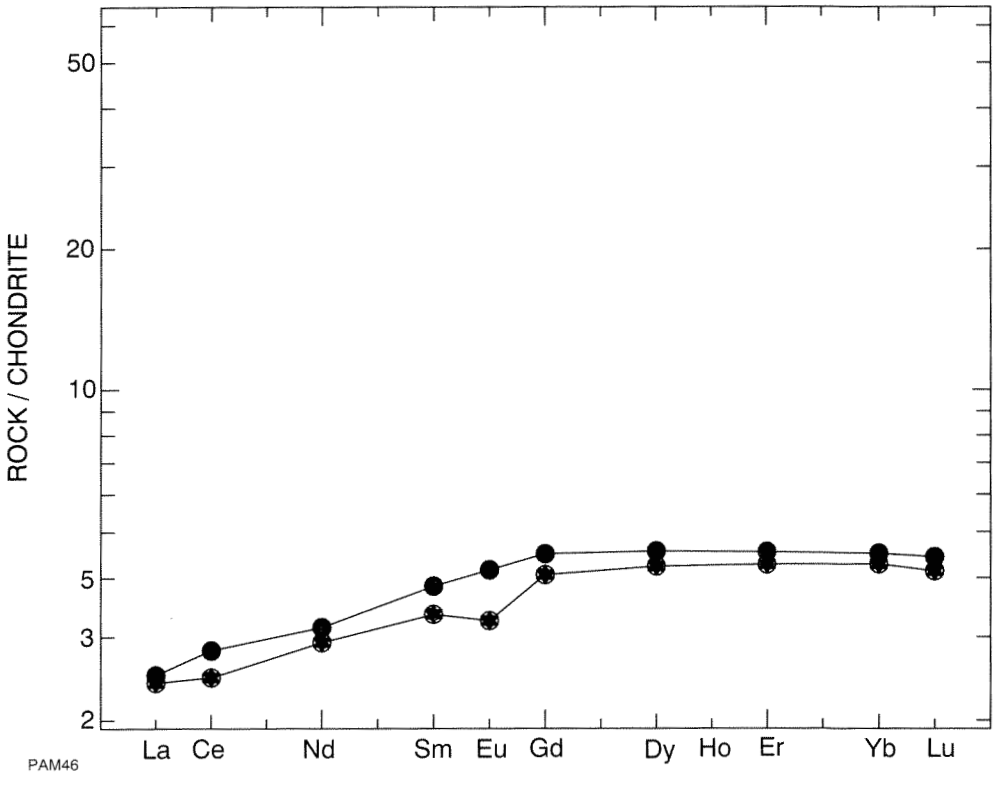

Appendix 3.9 Chondrite normalized rare-earth-element (REE) plots for the komatiite unit of the Kambalda Domain, Kambalda. Data from Arndt and Jenner (1986). Normalization factors from Nakamura (1974), and Evensen et al. (1984).

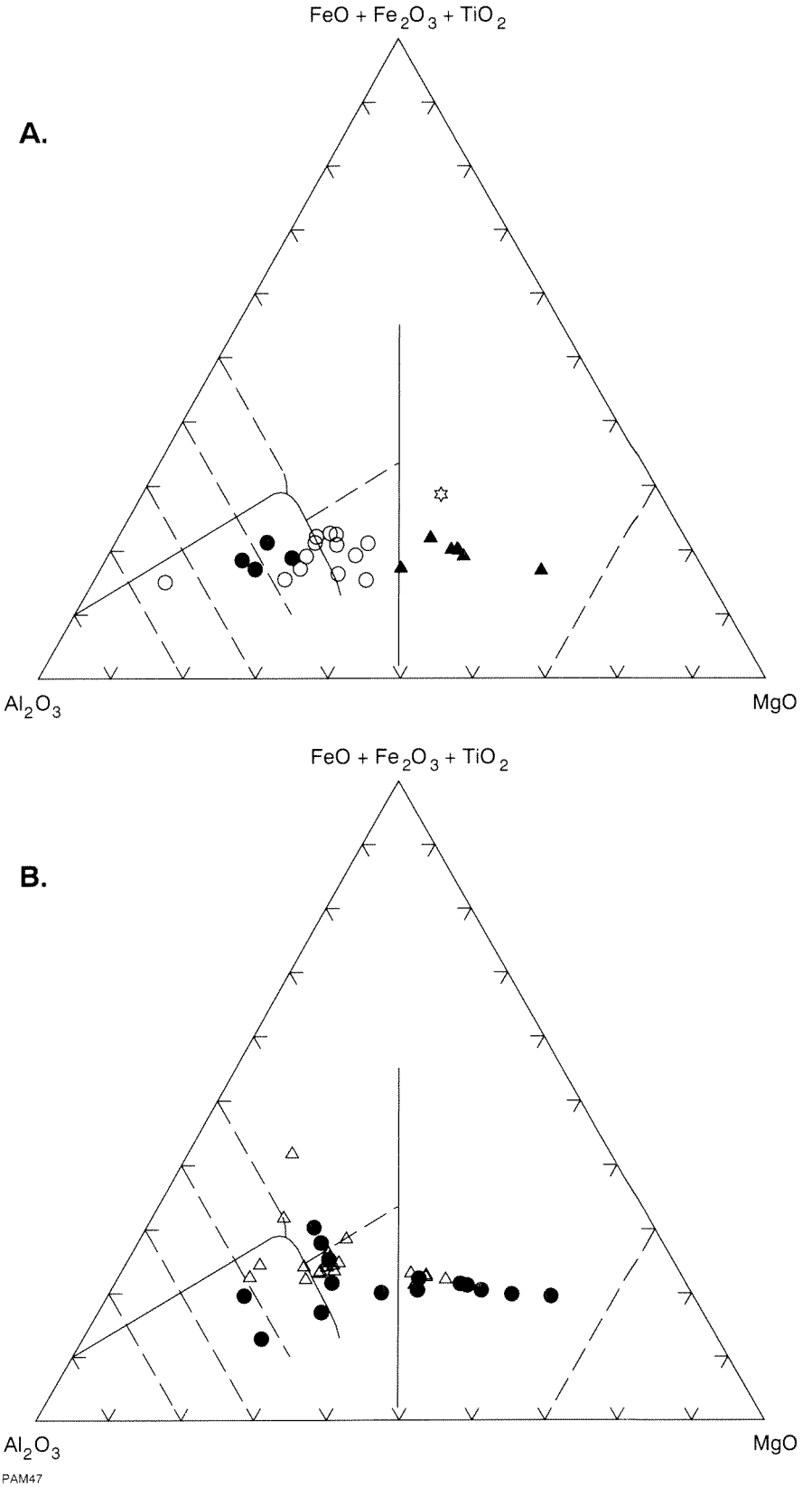

Appendix 3.10 Jensen Cation Diagrams (Jensen, 1976) for the basaltic upper part of the komatiite unit, and the upper basalt unit. Fields as Appendix 3.2.

A. Basaltic upper part of the komatiite unit. Kambalda Domain: Closed circles — Kambalda; open circles — Foster; asterisk — Tramways.
Ora Banda Domain: closed triangles.
Boorara Domain: open star (Harper Lagoon).

B. Upper basalt unit, Kambalda Domain, Kambalda and Kalgoorlie. Closed circles — Kambalda; open triangles — Kalgoorlie.

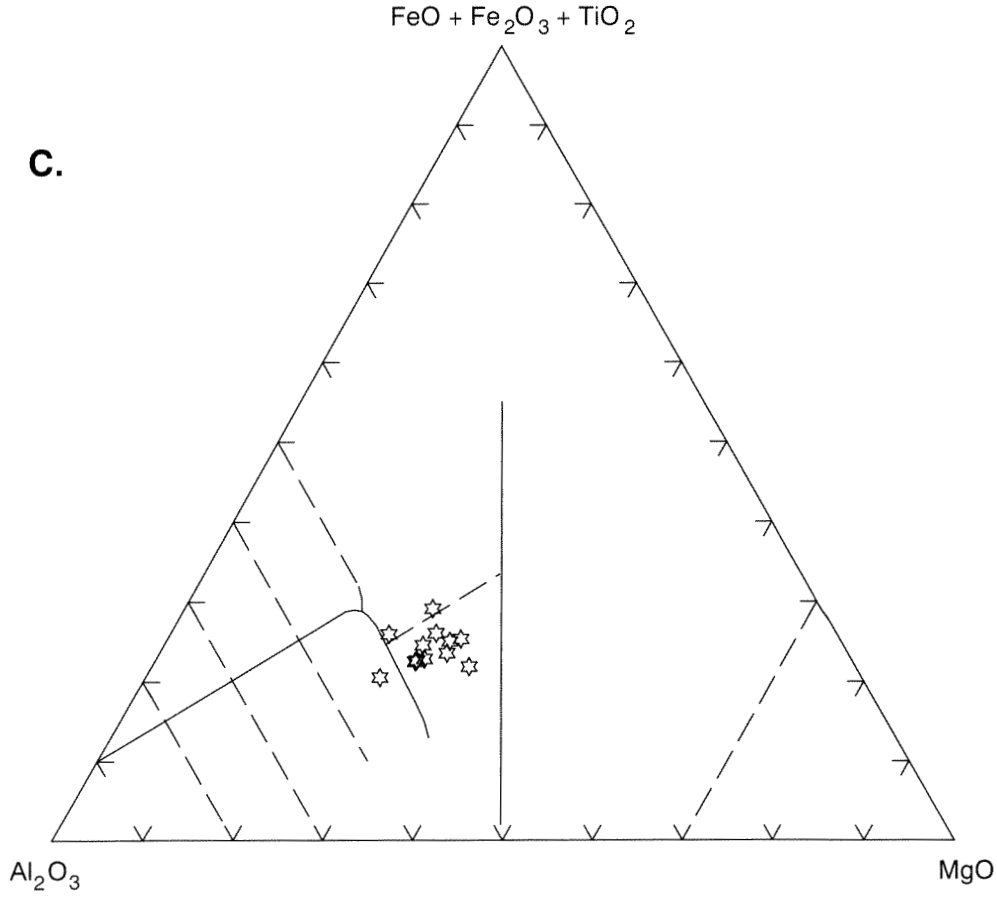

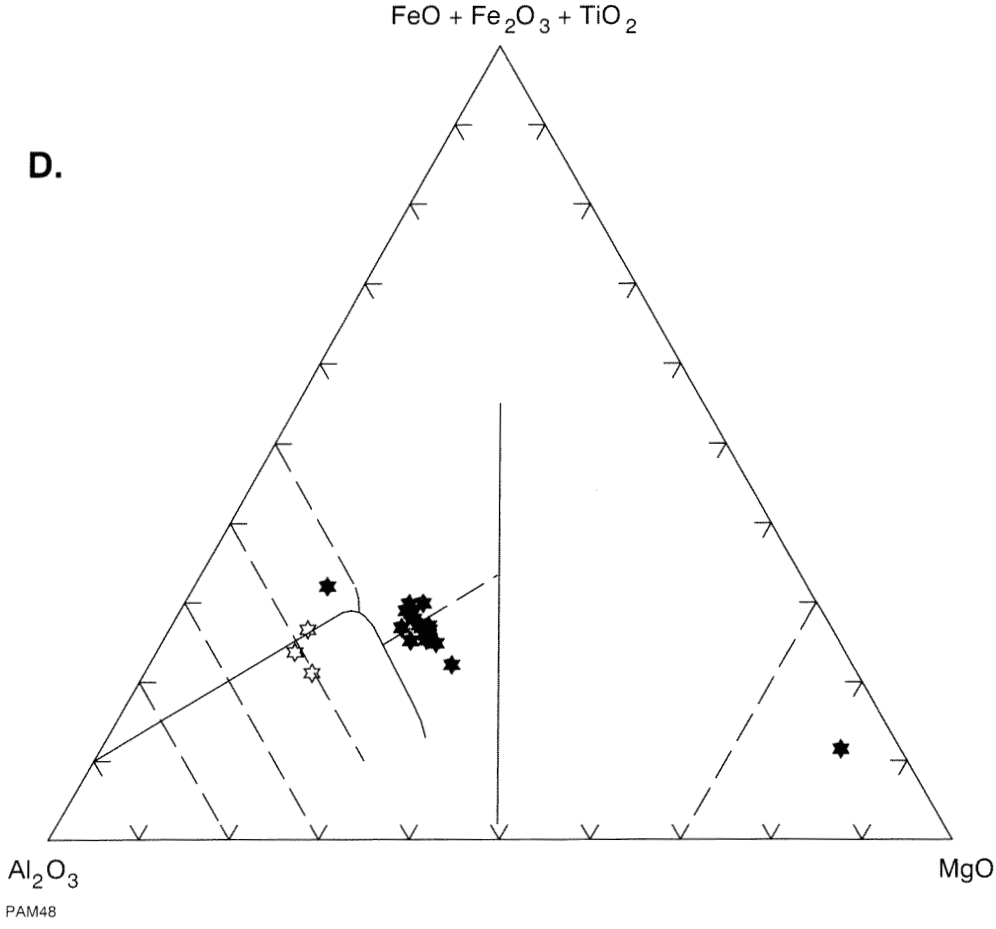

C. Upper basalt unit, Kambalda Domain, Bluebush–Republican.
D. Upper basalt unit, Ora Banda Domain. Closed stars — Bent Tree Basalt; open stars — Victorious Basalt.

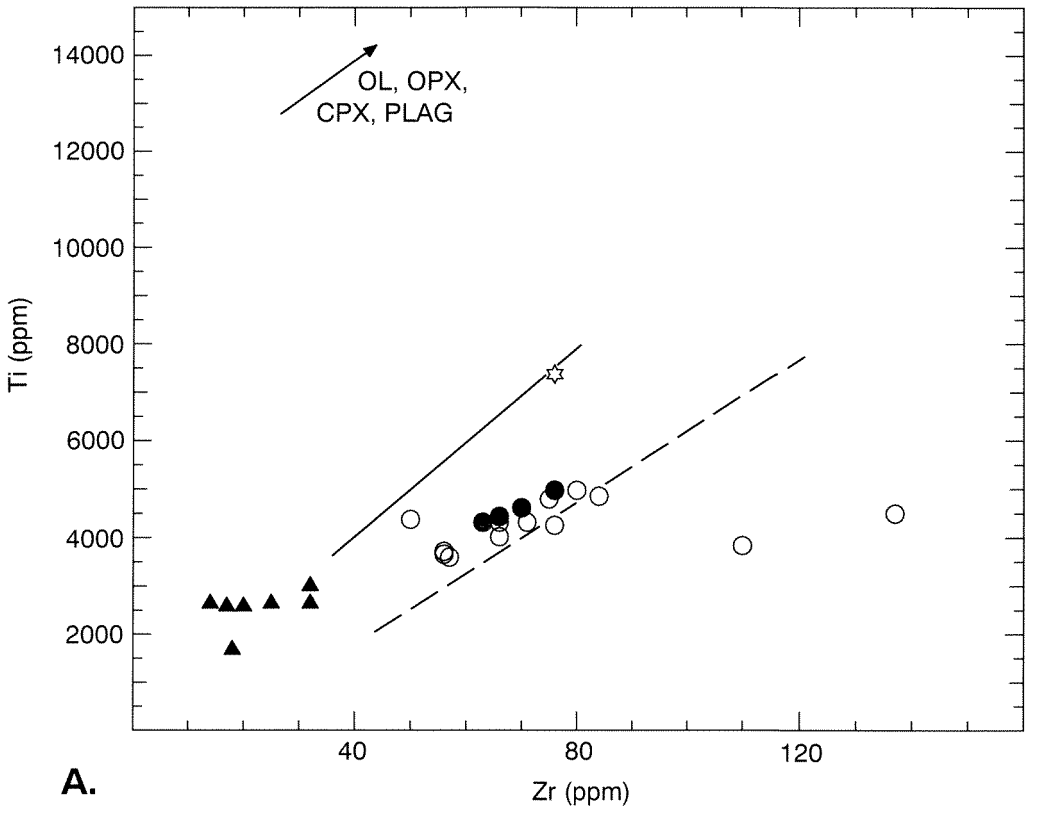

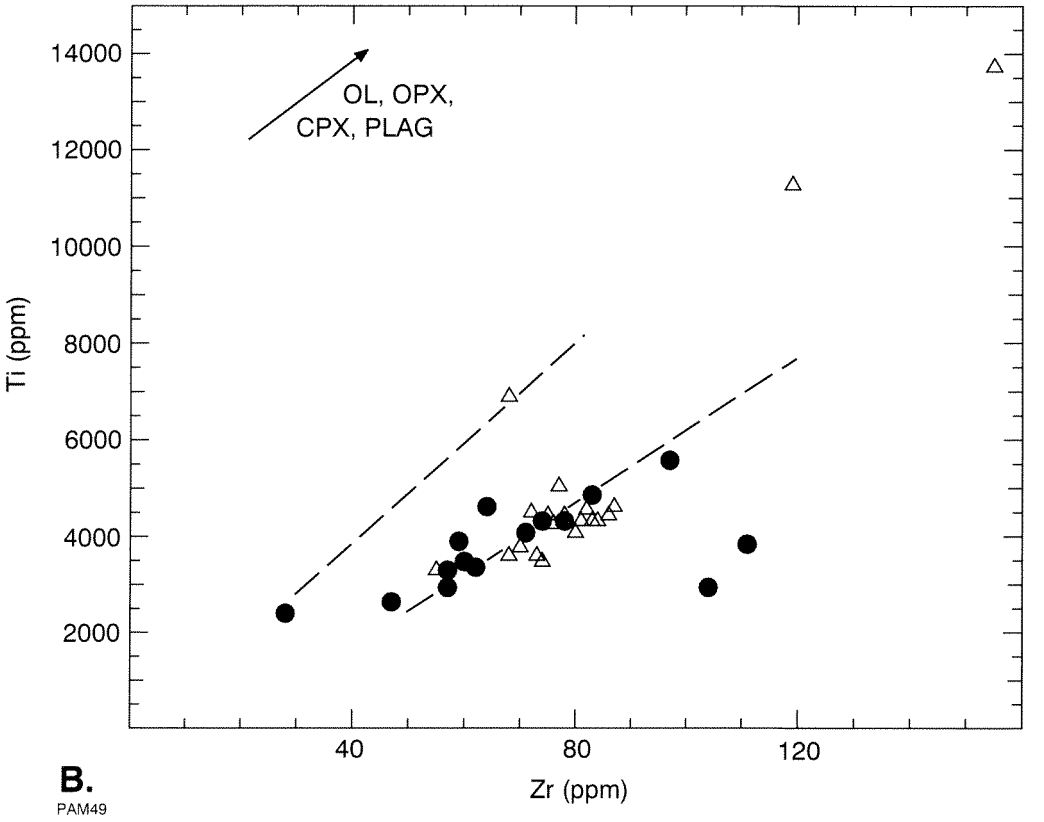

Appendix 3.11 Ti versus Zr (ppm) for basaltic upper part of the komatiite unit, and the upper basalt unit. Line of best fit for Kambalda lower basalt unit and fractionation vectors discussed in Appendix 3.3. Broken line is line of best fit for Kalgoorlie and Kambalda upper basalt unit data (see Appendix 3.11B), which has a slope = 76, intercept = -1303, r = 0.77, n = 36.

A. Basaltic upper part of komatiite unit. Symbols as for Appendix 3.10.
B. Upper basalt unit, Kambalda Domain, Kambalda and Kalgoorlie. Symbols as for Appendix 3.10.

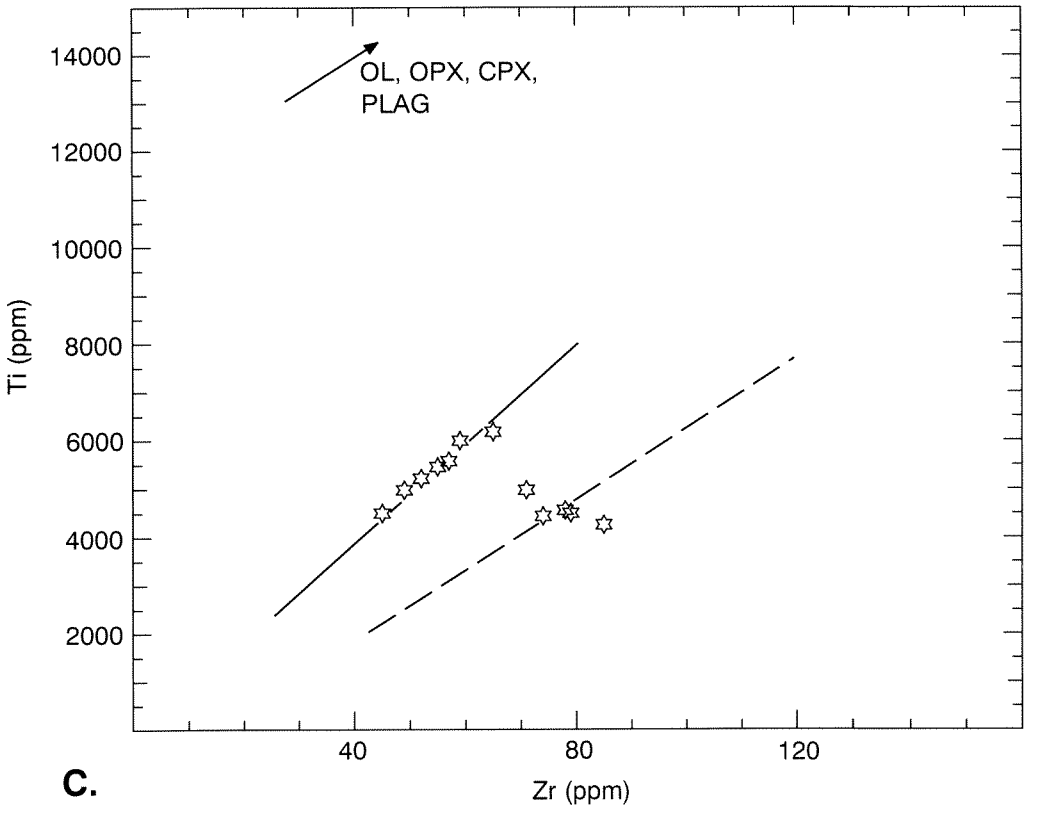

C.

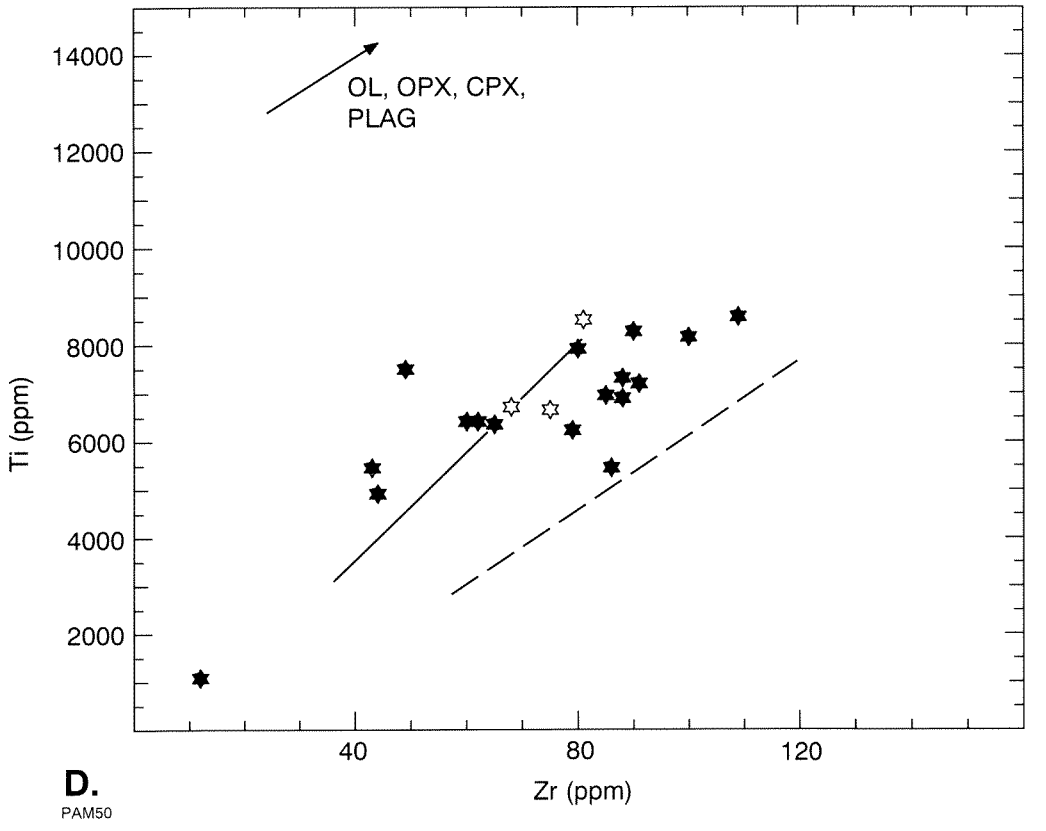

D.

PAM50

C. Upper basalt unit, Kambalda Domain, Bluebush–Republican.
D. Upper basalt unit, Ora Banda Domain. Symbols as for Appendix 3.10.

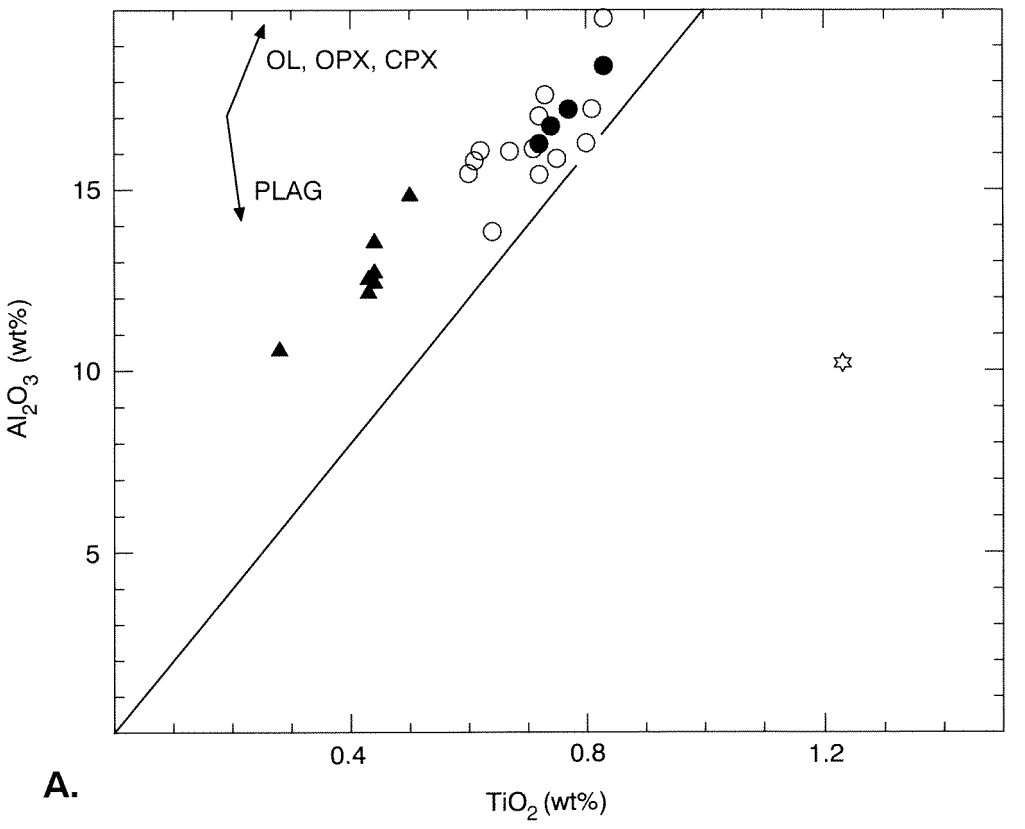

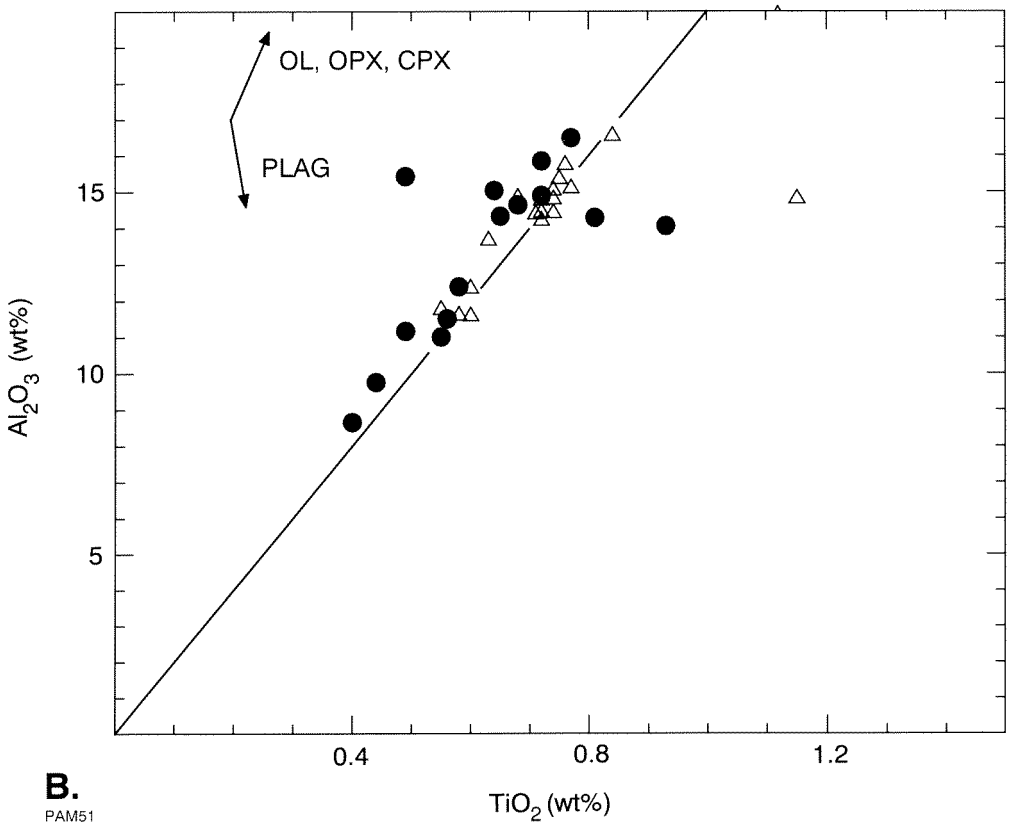

Appendix 3.12 **Al_2O_3 versus TiO_2 (wt%) for basaltic upper part of komatiite unit, and upper basalt unit. See Appendix 3.4 for explanation of chondrite line, and fractionation vectors.**

A. Basaltic upper part of komatiite unit. Symbols as for Appendix 3.10.
B. Upper basalt unit, Kambalda Domain, Kamblada and Kalgoorlie. Symbols as for Appendix 3.10.

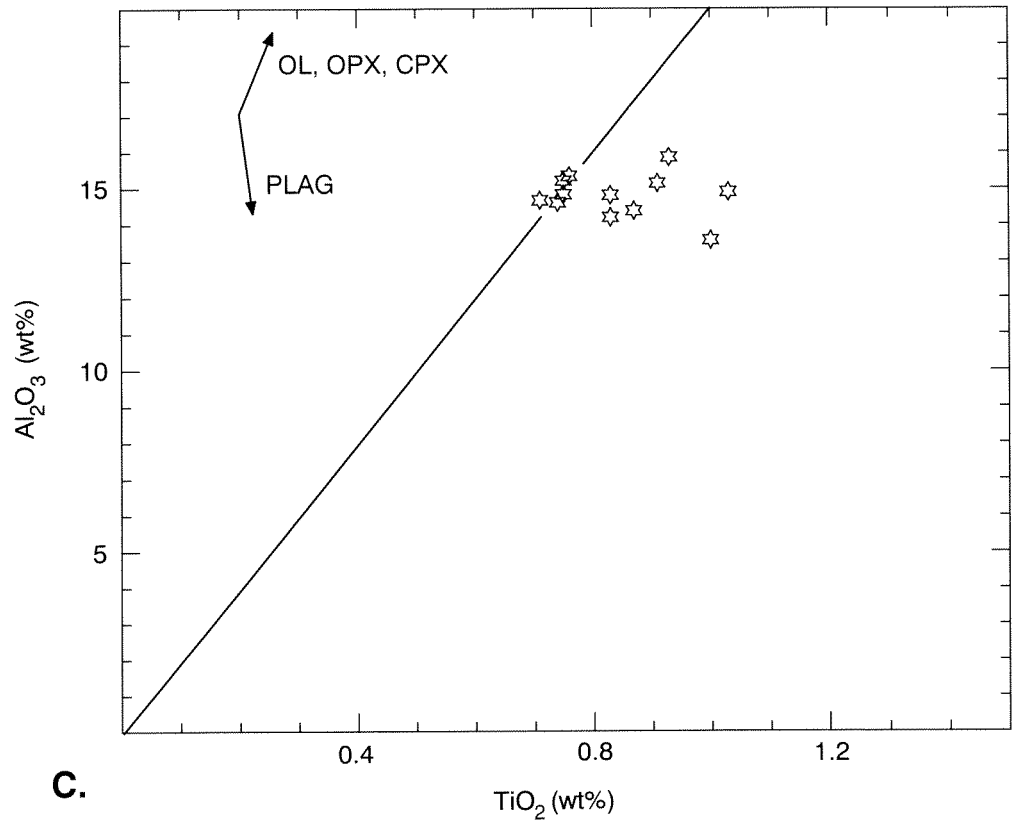

C.

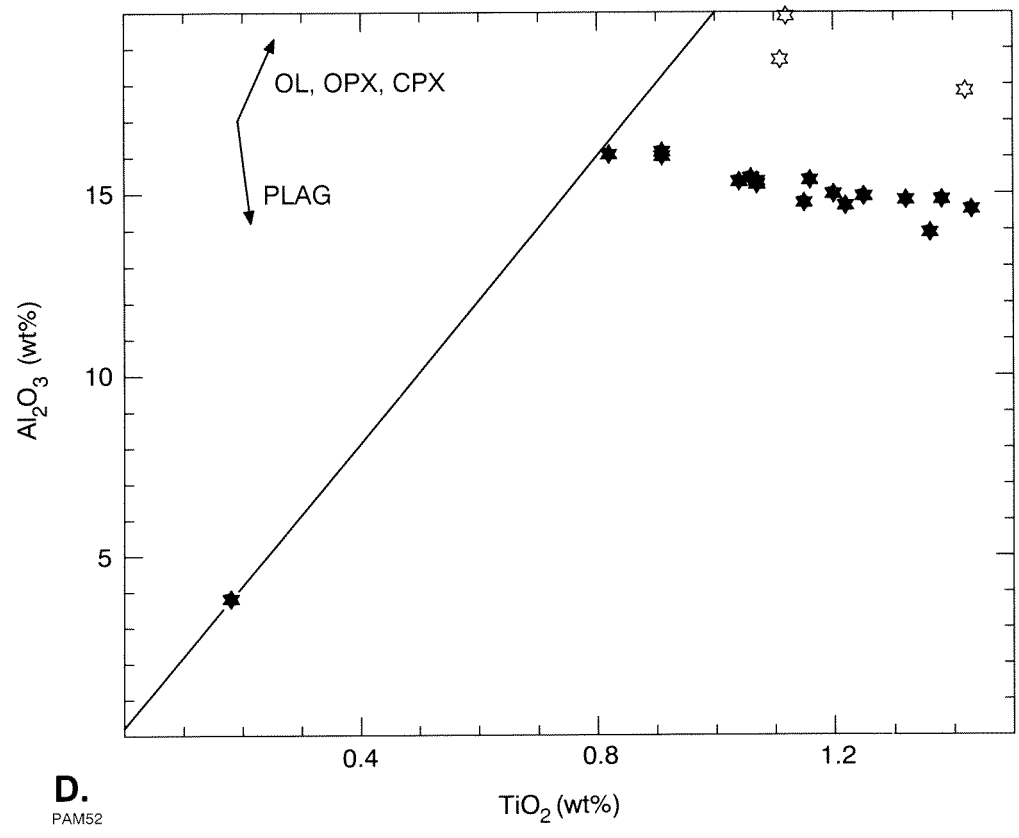

D.

PAM52

C. Upper basalt unit, Kambalda Domain, Bluebush–Republican.
D. Upper basalt unit, Ora Banda Domain. Symbols as for Appendix 3.10.

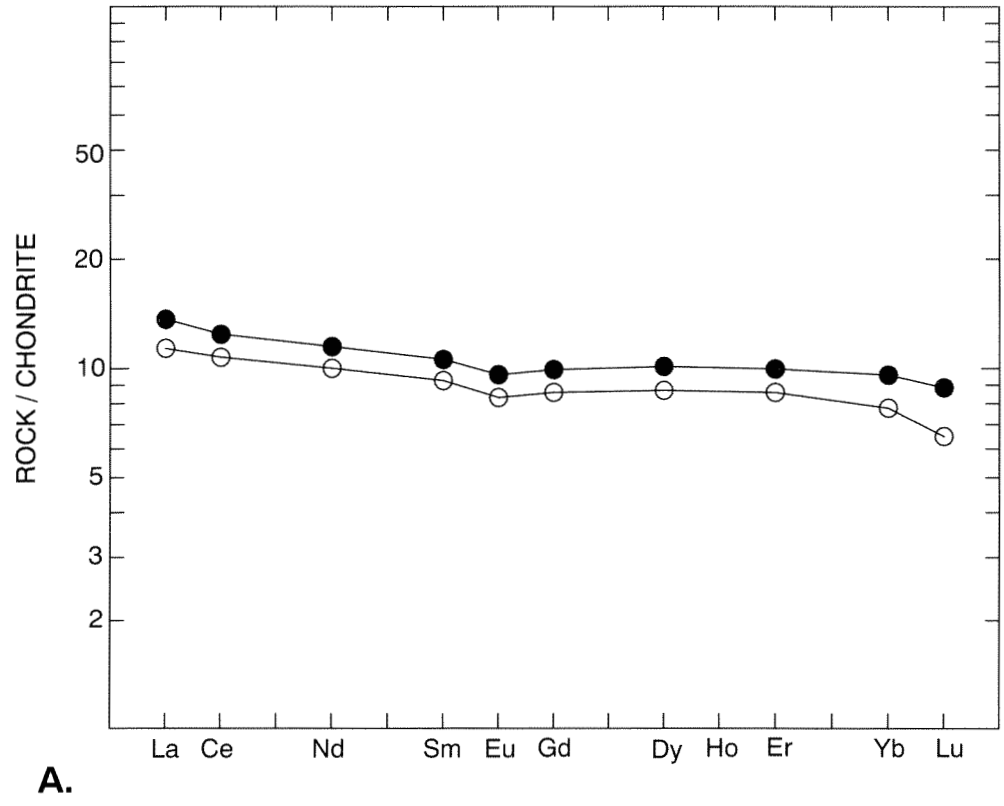

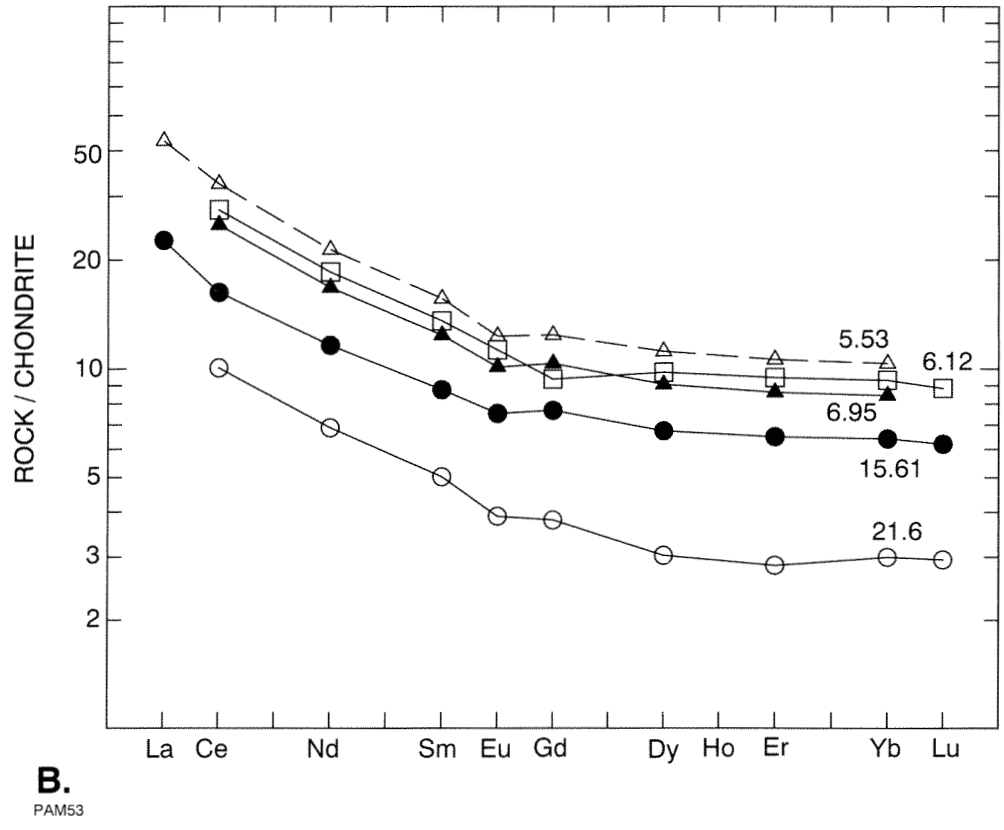

Appendix 3.13 Chondrite normalized rare-earth-element (REE) plots for the basaltic upper part of komatiite unit, and the upper basalt unit. Normalization factors from Nakamura (1974), and Evensen et al. (1984).

A. Basaltic upper part of komatiite unit. Data from Arndt and Jenner (1986). Closed circle — type A; open circle — type B. See text for discussion.

B. Upper basalt unit, Kambalda Domain. Data from Arndt and Jenner (1986). MgO content (wt%) also shown.

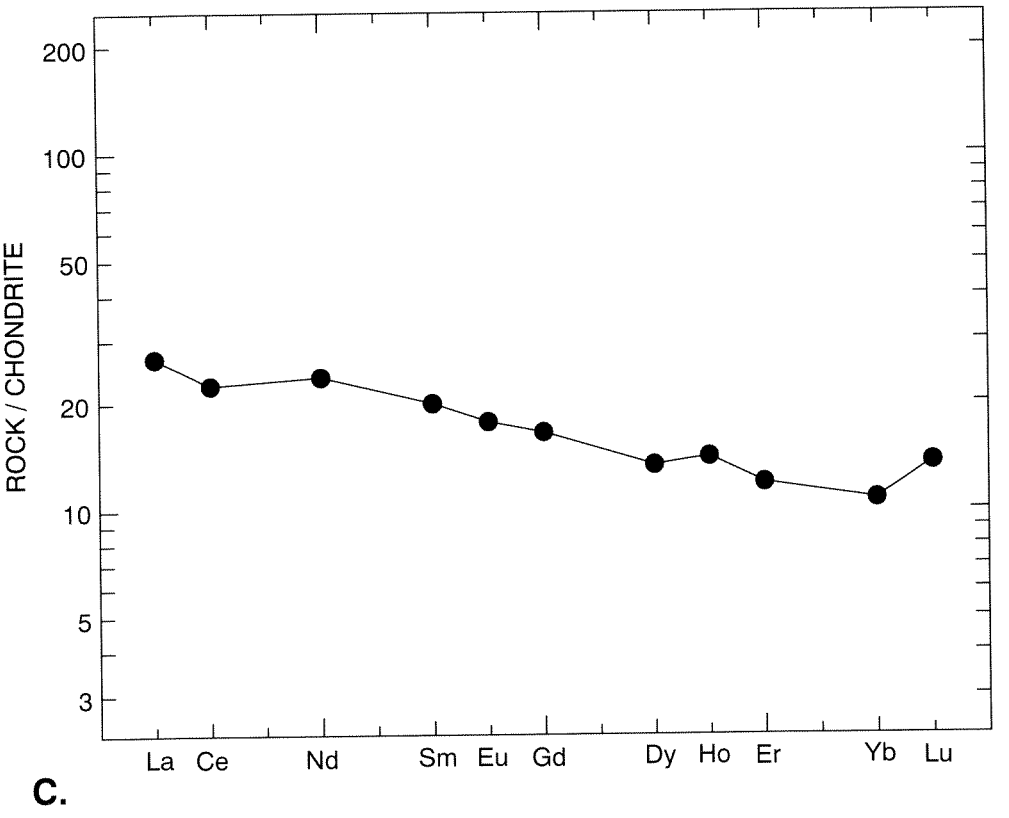

C.

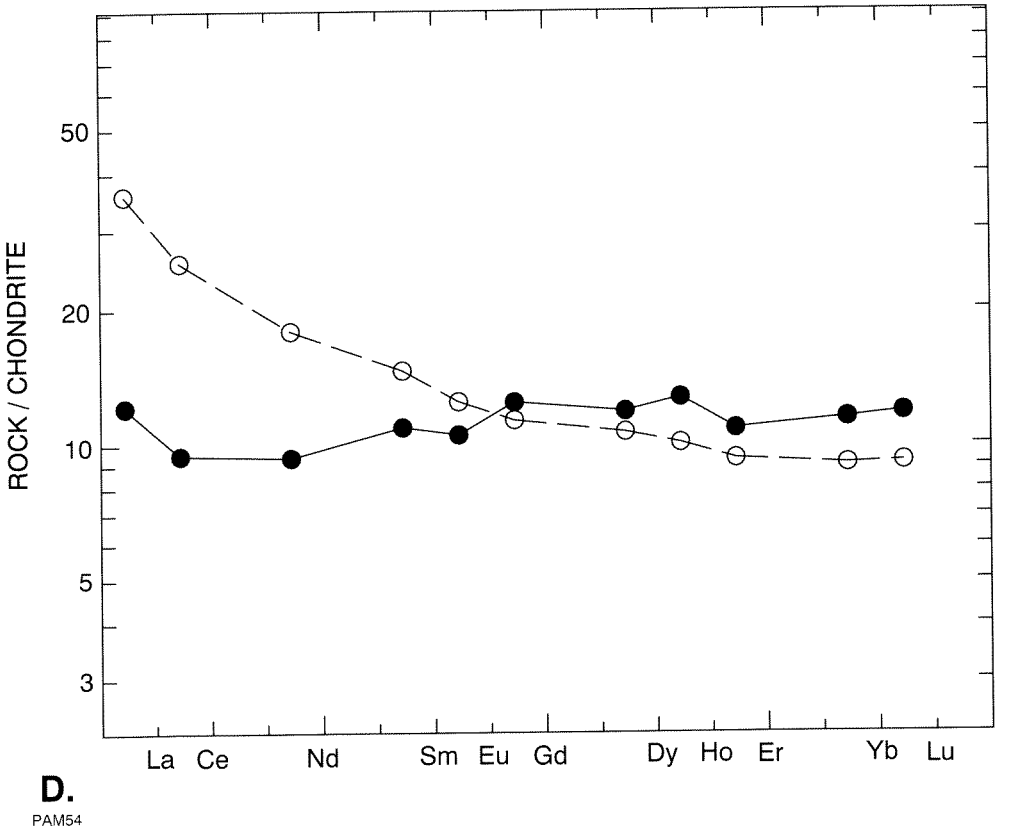

D.

PAM54

C. Basaltic upper part of komatiite unit. Basaltic komatiite 99552, Harper Lagoon.
D. Upper basalt unit, Kambalda Domain, Bluebush–Republican. Closed circle — 99702; open circle — 99683.

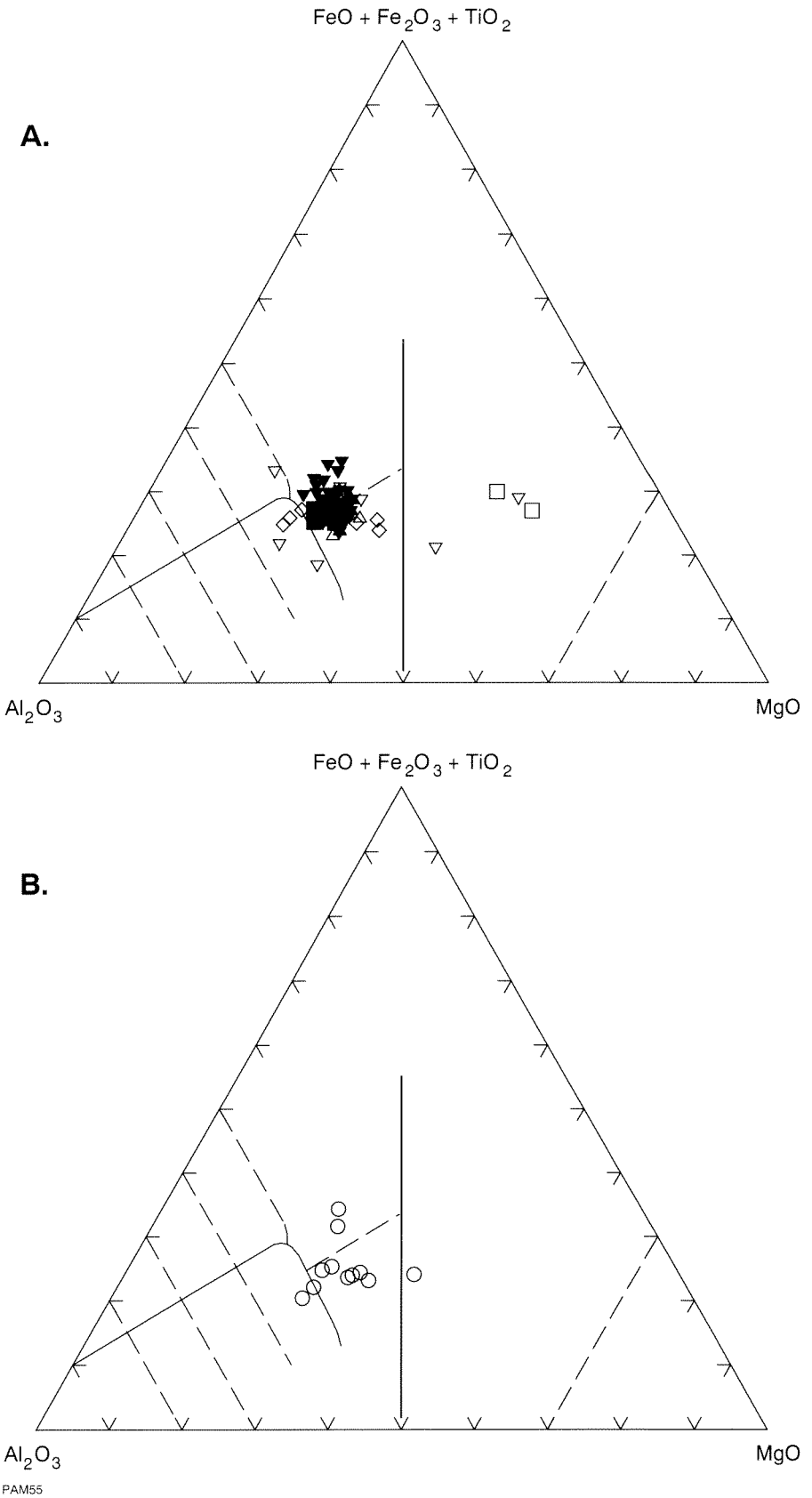

Appendix 3.14 Jensen Cation Diagram (Jensen, 1976) for the Norseman and Menzies Terranes. See Appendix 3.2 for field names.

A. Woolyeenyer Formation, Norseman Terrane. Closed stars — drillhole S169; open diamonds — drillhole C126; closed squares — drillhole S433 (basalt); open squares — drillhole S433 (basaltic komatiite); inverted closed triangles — drillhole S207; open triangle — drillhole S158; inverted open triangle — surface sample.

B. Menzies Terrane.

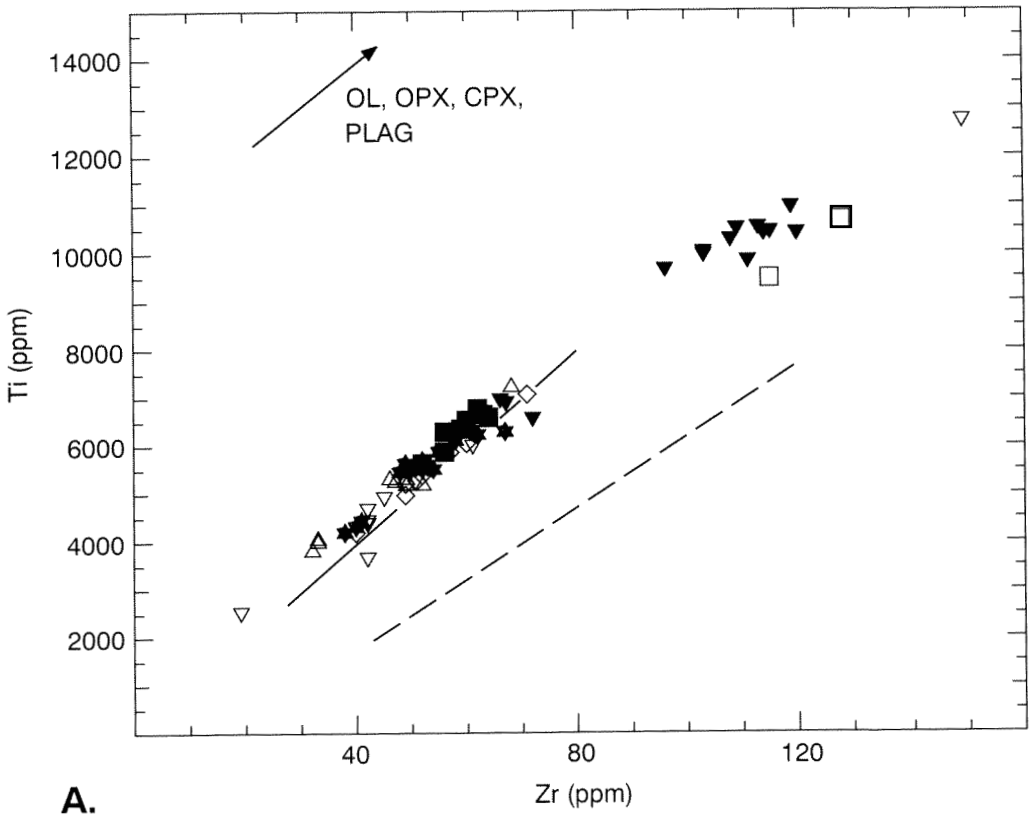

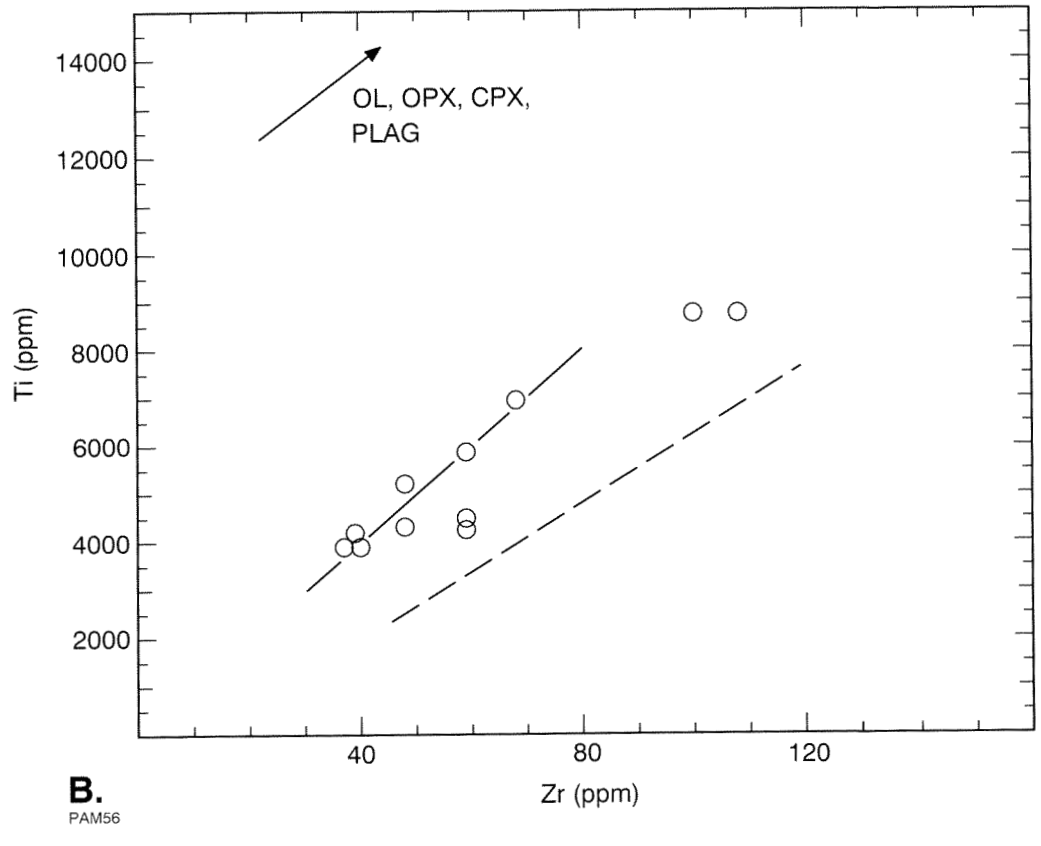

Appendix 3.15 Ti vs Zr (ppm) for the Norseman and Menzies Terranes. See Appendix 3.2 for discussion of fractionation vectors, and Appendix 3.12 for lines of best fit. Symbols as for Appendix 3.14.

A. Norseman Terrane.
B. Menzies Terrane.

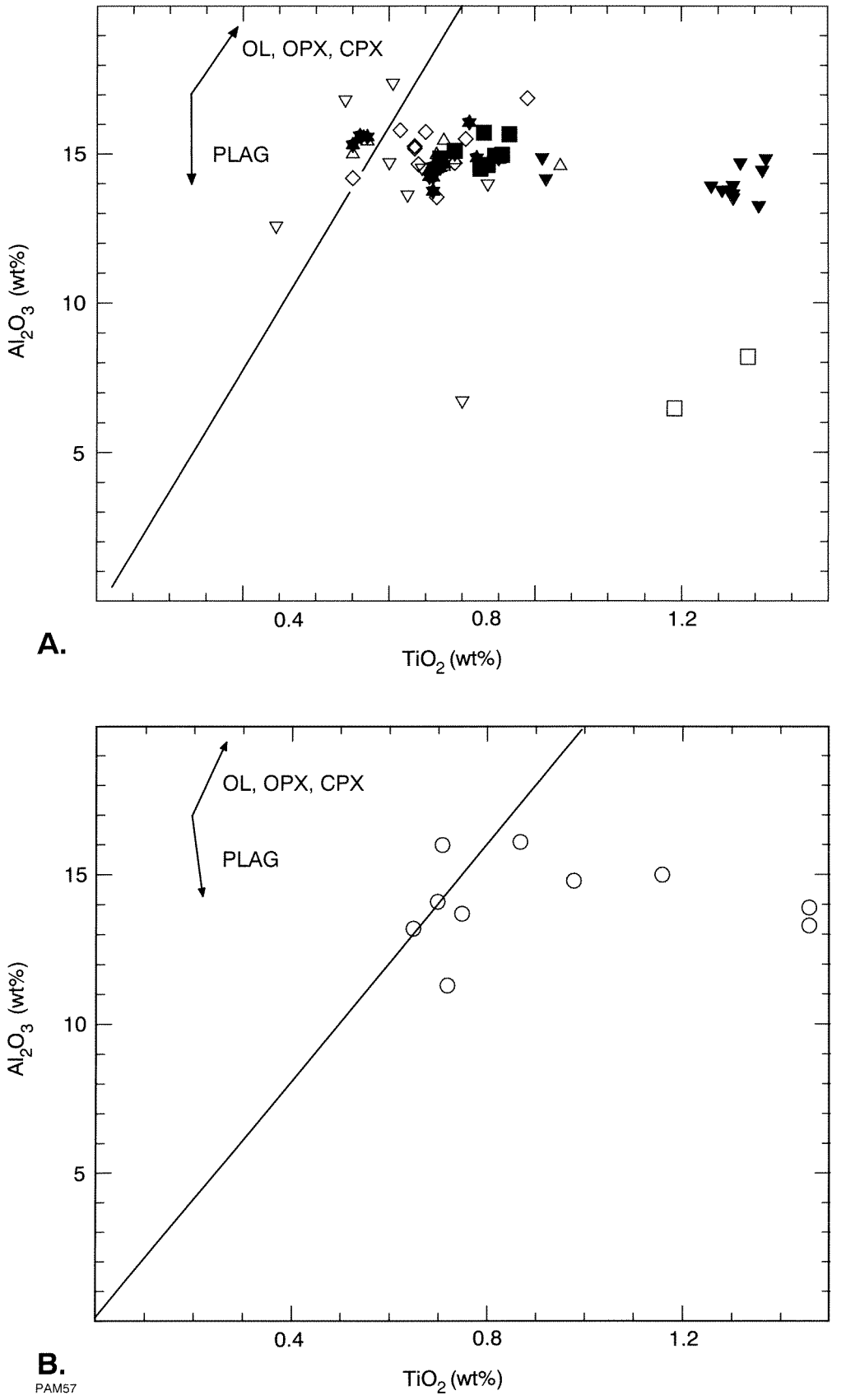

Appendix 3.16 **Al_2O_3 versus TiO_2 (wt%) for the Norseman and Menzies Terranes. Symbols as for Appendix 3.14. See Appendix 3.2 for explanation of fractionation vectors, and Appendix 3.3 for chondrite line.**

A. Norseman Terrane.
B. Menzies Terrane.

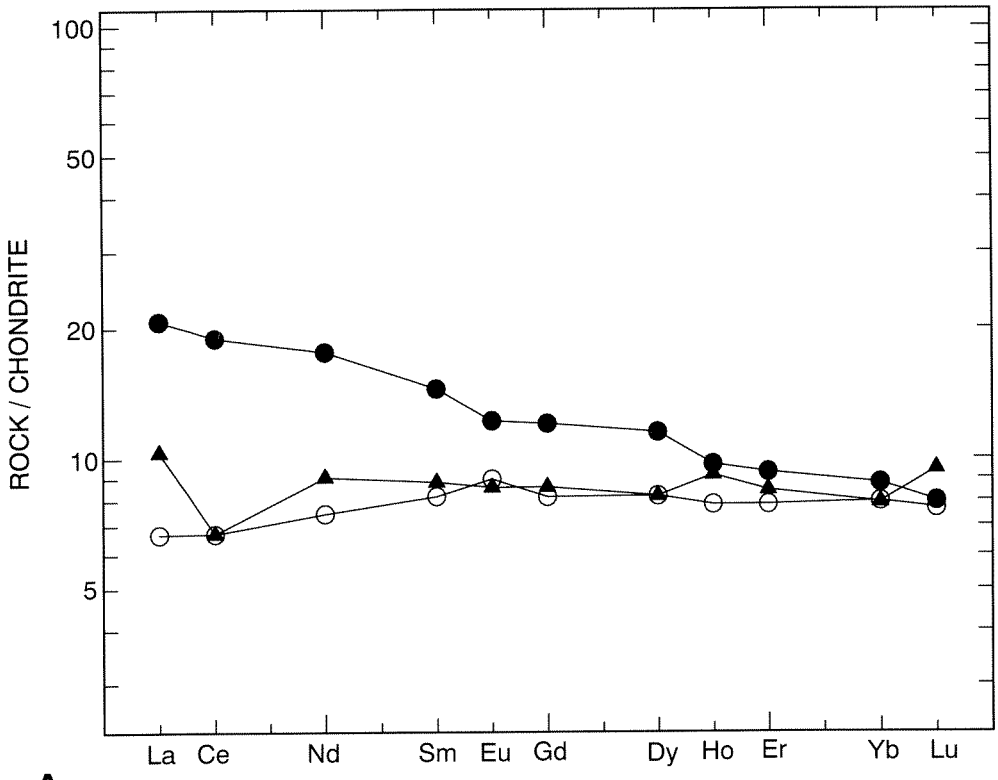

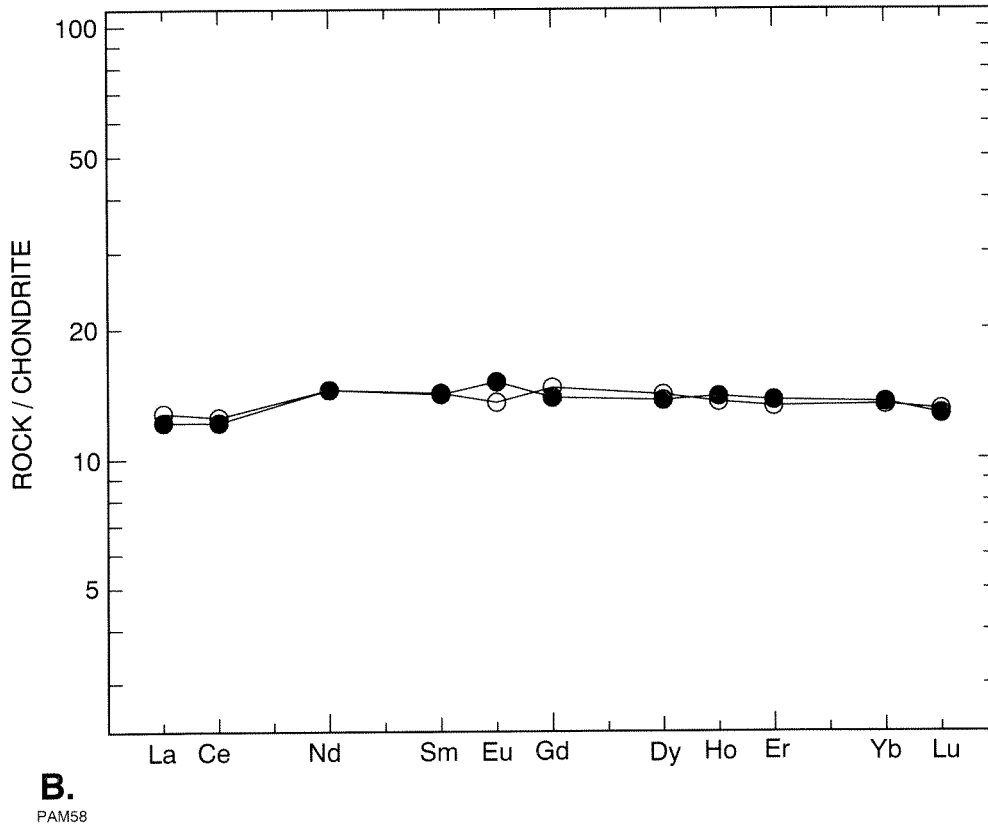

Appendix 3.17 Chondrite normalized rare-earth-element (REE) plots for samples from the Woolyeenyer Formation, Norseman Terrane. Normalization factors from Nakamura (1974) and Evensen et al. (1984). A and B are all basalts; C are basaltic komatiite dikes.

A. closed circle — 99944; open circle — 99912; closed triangle — 99955.
B. closed circle — 99937; open circle — 99903.

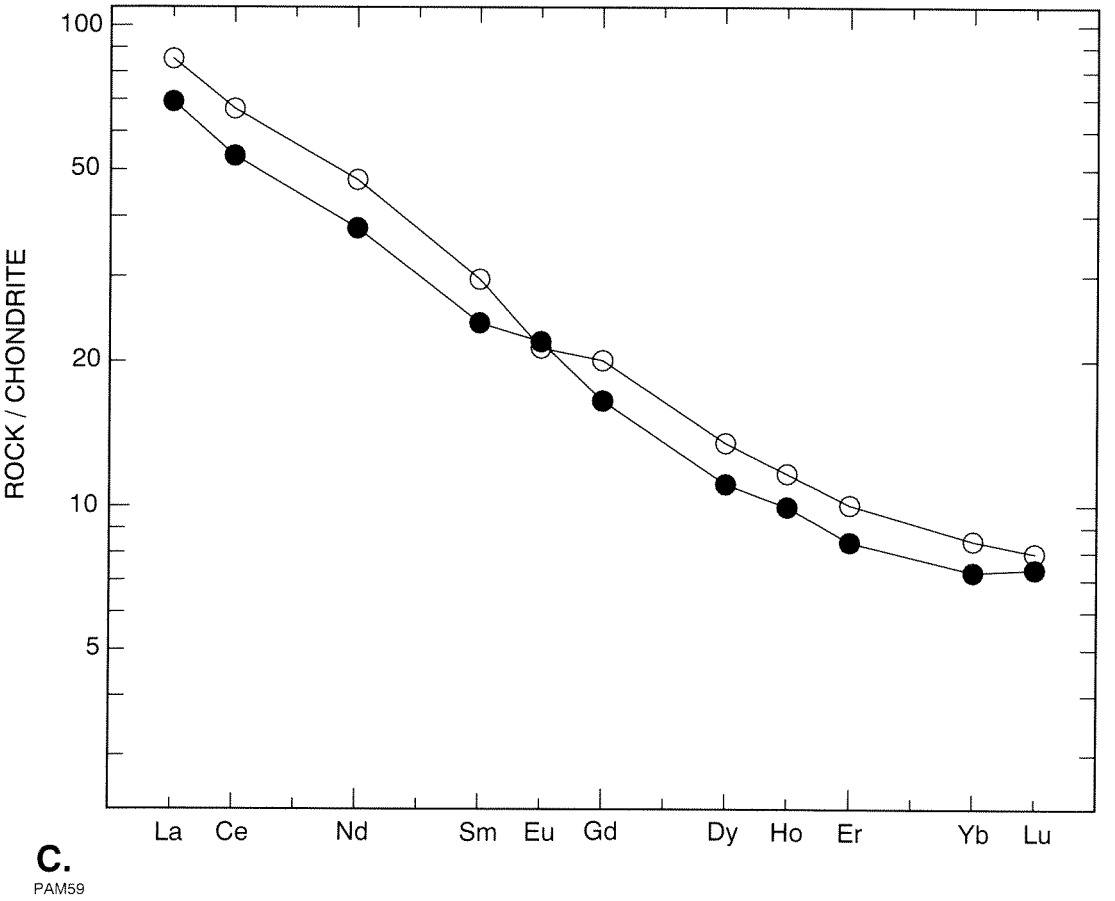

C. closed circle — 99934; open circle — 99938.

GSWA No.	*Sm*	*Nd*	$^{147}Sm/^{144}Nd$	$^{143}Nd/^{144}Nd$	ε_{Nd}
99941	4.09	13.41	0.184285	0.512467	0.95
99944	2.58	9.78	0.159486	0.511996	0.37
99955	1.41	4.15	0.204786	0.512883	1.94
99787	1.39	4.09	0.204624	0.512865	1.65
99932	2.18	6.52	0.202401	0.512915	3.4
99934	3.82	19.07	0.121084	0.511193	-1.96
99938	4.84	24.58	0.118985	0.511190	-1.29
99912	1.41	4.26	0.200364	0.512856	2.96
99542	1.25	3.72	0.202625	0.512823	1.51

$^{143}Nd/^{144}Nd_{MEAS} = {}^{143}Nd/^{144}Nd_{0} - (^{147}Sm/^{144}Nd)_{MEAS}(e^{yt} - 1)$

where:

MEAS = measured ratio
0 = initial ratio
t = age (2.7 Ga)
y = 6.54×10^{-12}

$$\varepsilon_{Nd} = \left[\frac{^{143}Nd/^{144}Nd_{0}}{^{143}Nd/^{144}Nd_{CHUR}} - 1 \right] \times 10^{4}$$

CHUR = chondritic unfractionated reservoir

Appendix 3.18 $^{143}Nd/^{144}Nd$ analyses of basalts and basaltic komatiites from the Woolyeenyer Formation, Norseman Terrane. Analyses carried out at the Institute for Study of the Earth's Interior, Misasa, Japan. Techniques etc. discussed in Morris and Kagami (1989).

14233/12/93—600Bks—L/6253

GARRY L. DUFFIELD, Government Printer, Western Australi